



DESIGN AND REASSESSMENT OF TUBULAR JOINTS
FOR OFFSHORE STRUCTURES

CONFIDENTIAL

AQ

CHAPTER 5: FATIGUE LIFE ASSESSMENT
S-N APPROACH

C6060R09.07 REV B SEPTEMBER 1995

Purpose of Issue	Rev	Date of Issue	Author	Checked	Approved
Subgroup Review	0	August 1994	PAS	/	/
Draft Final Report	A	February 1995	PAS	/	/
Final Report	B	September 1995	PS	PC	/

BILLINGTON OSBORNE-MOSS ENGINEERING LIMITED
Ledger House
Forest Green Road, Fifield
Maidenhead, Berkshire
SL6 2NR

Telephone (01628) 777707
Fax (01628) 777877



REVISION SHEET

REVISION	DETAILS OF REVISION
0	Issued to subgroup on fatigue S-N for review.
A	Final draft issued to participants for comment.
B	Final report incorporating comments from second sub-committee meeting and PSC meeting.



DESIGN AND REASSESSMENT OF TUBULAR JOINTS
FOR OFFSHORE STRUCTURES

CONFIDENTIAL

CHAPTER 5: FATIGUE LIFE ASSESSMENT
S-N APPROACH

CONTENTS

	<u>Page No</u>
NOMENCLATURE	0.8
1. INTRODUCTION	1.1
1.1 General	1.1
1.2 Definitions	1.2
1.2.1 Joint failure	1.2
1.2.2 Hot-spot stress	1.3
1.2.3 Stress range and ratio	1.3
1.2.4 Constant and variable amplitude loading	1.5
1.3 Basic Fatigue Design Approach	1.7
2. METHODS FOR DETERMINING FATIGUE LIFE	2.1
2.1 Experimental Methods	2.1
2.2 Errors in Modelling Fatigue Behaviour	2.1
3. REVIEW OF EXISTING CODES FOR SIMPLE TUBULAR JOINTS	3.1
3.1 DEn T Curve Approach	3.1
3.1.1 UK Health and Safety Executive Guidance Notes	3.3
3.1.2 Det norske Veritas Rules	3.5
3.1.3 Canadian code	3.7
3.1.4 The HSE proposed revisions to Fatigue Guidance (Amended August 1993)	3.8
3.2 API X Curve Approach	3.13
3.2.1 American Petroleum Institute - API RP2A	3.13
3.2.2 American Welding Society Structural Welding Code	3.16
3.2.3 Lloyd's Register of Shipping Rules	3.20
3.3 Comparison of Design Codes	3.20
3.3.1 Summary of design codes	3.20
3.3.2 Illustration of differences in design codes	3.23



CONTENT CONTINUED

	<u>Page No</u>
4. REVIEW OF PUBLISHED DATA AND PARAMETERS AFFECTING FATIGUE LIFE	4.1
4.1 Summary of Parameters Which May Influence Fatigue Life	4.1
4.2 Summary of Main Test Programmes	4.2
4.2.1 United Kingdom Offshore Research Project (UKOSRP)	4.2
4.2.2 European Coal and Steel Community (ECSC)	4.3
4.2.3 Canadian Offshore Research Project (COSRP)	4.4
4.2.4 SERC (Madras)	4.4
4.3 Tubular Joint Fatigue Database and Screening Criteria	4.4
4.4 Basecase S-N Curve	4.5
5. INFLUENCE OF JOINT GEOMETRY	5.1
5.1 The Scale Effect - An Overview	5.1
5.1.1 Gurney	5.2
5.1.2 Bainbridge	5.3
5.1.3 Marshall	5.3
5.1.4 Current views on scale effect	5.4
5.1.5 Summary	5.5
5.2 Joint Configuration	5.6
5.3 Chord Size and Dimensions	5.7
5.3.1 Chord thickness (T)	5.7
5.3.2 Chord diameter (D) and radius/thickness ratio (γ)	5.8
5.3.3 Chord length (L_s) and length/diameter ratio (α)	5.8
5.3.4 Chord end condition	5.10
5.4 Brace Size and Dimensions	5.10
5.4.1 Brace thickness (t) and brace/chord thickness ratio (τ)	5.10
5.4.2 Brace diameter (d) and brace/chord diameter ratio (β)	5.12
5.4.3 Brace inclination (θ)	5.12
5.4.4 Brace separation (ζ)	5.12
5.5 Weld Size and Profile	5.12
5.5.1 Attachment length (l)	5.13
5.5.2 Weld profile	5.14
5.6 Failure Location	5.15
5.7 Summary of Joint Geometry and Weld Effects	5.16
6. INFLUENCE OF LOADING	6.1
6.1 Loading Mode	6.1
6.1.1 Single loading applied to brace	6.1
6.1.2 Single loading applied to brace with compressive chord end loading	6.2
6.1.3 Combined loading applied to brace	6.2



CONTENTS CONTINUED

	<u>Page No</u>
6.2 Constant Amplitude Loading	6.3
6.2.1 Mean and maximum load	6.3
6.2.2 Stress ratio (R)	6.3
6.2.3 Capacity limit (high stress - low cycle)	6.4
6.2.4 Endurance limit (low stress - high cycle)	6.8
6.2.5 Cyclic frequency	6.10
6.3 Variable Amplitude Loading	6.12
6.3.1 Runners retested at increased load range (single loading mode)	6.12
6.3.2 Narrow band random load history	6.14
6.3.3 Broad band random load history	6.16
6.3.4 Palmgren-Miner rule	6.17
6.4 Summary of Joint Loading Effects	6.18
 7. FATIGUE LIFE OF SIMPLE, AS-WELDED TUBULAR JOINTS IN-AIR	 7.1
7.1 In-Air S-N Curve and Thickness Exponent	7.2
7.2 Poor Weld Profile	7.8
7.3 Endurance Limits and Variable Amplitude Loading	7.11
7.4 Highly Stresses Tubular Joints	7.14
7.5 Chord Axial Loading	7.15
7.6 Summary	7.16
 8. INFLUENCE OF ENVIRONMENT	 8.1
8.1 Design Codes	8.1
8.2 Review of Published Data	8.2
8.2.1 Cole	8.2
8.2.2 Tubby	8.3
8.2.3 Ramachandra Murthy	8.4
8.2.4 Dover	8.4
8.2.5 Hara	8.4
8.2.6 Gerald	8.5
8.2.7 Wylde	8.5
8.2.8 UKOSRP II	8.5
8.2.9 Dijkstra and de Back	8.5
8.2.10 COSRP	8.5
8.3 Appraisal of Test Data	8.6
8.3.1 In-seawater with corrosion protection	8.6
8.3.2 In-seawater under free corrosion	8.7
8.3.3 In-splash zone with coating	8.9



CONTENTS CONTINUED

	<u>Page No</u>
9. INFLUENCE OF MATERIALS AND POST-FABRICATION TREATMENTS	9.1
9.1 High Strength Steels	9.1
9.2 Post Fabrication Treatment	9.3
9.2.1 Post weld heat treatment	9.3
9.2.2 Grinding	9.7
9.2.3 Hammer peening	9.11
9.2.4 Shot peening	9.13
9.2.5 TIG dressing	9.14
10. FATIGUE LIFE OF COMPLEX TUBULAR JOINTS AND GIRTH WELDS	10.1
10.1 Overlapping Braces	10.1
10.1.1 Design codes	10.1
10.1.2 Review of published data	10.1
10.1.3 Appraisal of test data	10.2
10.1.4 Recommendations	10.2
10.2 Multiplanar Braces	10.4
10.2.1 Design codes	10.4
10.2.2 Review of published data	10.4
10.2.3 Appraisal of test data	10.5
10.2.4 Recommendations	10.6
10.3 Internally Ring-stiffened Tubular Joints	10.7
10.3.1 Design codes	10.7
10.3.2 Review of published data	10.7
10.3.3 Appraisal of test data	10.10
10.3.4 Recommendations	10.14
10.4 Internally Grouted Tubular Joints	10.16
10.4.1 Design codes	10.16
10.4.2 Review of published data	10.16
10.4.3 Appraisal of test data	10.18
10.4.4 Recommendations	10.18
10.5 Cast and Forged Steel Joints	10.20
10.5.1 Design codes	10.20
10.5.2 Review of published data	10.24
10.5.3 Appraisal of test data	10.27
10.5.4 Recommendations	10.30
10.6 Tubular Girth Welds	10.31
10.6.1 Design codes	10.31
10.6.2 Single sided closure welds	10.31
10.6.3 Backing strips	10.33

CONTENTS CONTINUED

	<u>Page No</u>
11. SUMMARY OF MEAN AND DESIGN S-N CURVES FOR TUBULAR JOINTS	11.1
11.1 Mean Fit S-N Curves	11.1
11.2 Design S-N Curves	11.1
11.3 Factors on Fatigue Life	11.2
12. REFERENCES FOR CHAPTER 5	12.1

APPENDICES

- A TUBULAR JOINT CLASSIFICATIONS
- B INITIAL SCREENED DATABASE OF SIMPLE TUBULAR JOINTS
- C BASECASE DATABASE OF SIMPLE TUBULAR JOINTS
- D DATABASE OF TUBULAR JOINTS IN-SEAWATER
- E DATABASE OF TUBULAR JOINTS WITH POST FABRICATION TREATMENT
- F COMPLEX TUBULAR JOINTS



NOMENCLATURE

CA	Constant amplitude loading
D	Chord outside diameter
D_s	Cumulative damage summation
DAF	Dynamic amplification factor
d	Brace outside diameter
f	Cyclic frequency
K	Constant in S-N relationship
L_s	Length of chord specimen
L_s'	Modified length of chord specimen
l	Weld attachment leg length
m	Slope in S-N relationship
N	Number of cycles
N1	Number of cycles to first detectable surface cracking
N2	Number of cycles to visible surface cracking
N3	Number of cycles to first through thickness cracking (failure)
$N3'$	Predicted number of cycles to first through thickness cracking (failure)
N4	Number of cycles to the end of fatigue test
n	Exponent in scale effect factor
P	Load
P_k	Characteristic static capacity of joint
P_u	Mean static capacity of joint
Q'_β	Beta modification factor
R	Stress ratio
rms	Root mean squared
S	Stress (see also σ)
S_B	Stress related to the basic S-N curve



NOMENCLATURE (cont.)

S_m	Mean stress
S_o	Stress range endurance limit
S_p	Peak stress
S_r	Stress range
S_2	rms stress for peaks
S^*	rms stress for process
T	Chord thickness
t	Brace thickness (or unspecified member thickness)
t_o	Member thickness of nominal S-N curve
VA	Variable amplitude loading
X	Stress amplitude
α	$2L_s/D$
α'	$2L_s'/D$
β	d/D
γ	$D/2T$
ξ_m	Damping ratio
ζ	Brace separation
ϕ	Wave direction
σ	Stress (see also S)
σ_b	Maximum braceside stress
σ_c	Maximum chordsides stress
σ_{LT}	Long term root mean squared stress
σ_r	Stress range
σ_y	Steel yield stress
τ	t/T
θ	Brace inclination



1. INTRODUCTION

1.1 General

Steel offshore jacket structures consist primarily of tubular joints which are formed by the intersection of brace and chord members, with the outside diameter of the brace less than or equal to the outside diameter of the chord. The complex intersection of tubular members gives rise to severe stress concentrations which have been discussed in detail in Chapter 4. Ocean waves loading such a tubular structure cause fluctuations in the stress levels at the joint, leading to fatigue crack growth and eventual failure. Fatigue failure is defined as the number of stress cycles (and hence the time) taken to reach a pre-determined failure criterion.

Fatigue failure analysis is by no means a rigorous science and the idealisations and approximations inherent in it prevent the calculation of absolute fatigue life (time to failure) for even the simplest joint. Any fatigue analysis approach encounters at least four areas of considerable uncertainty:

1. The operational environment of a structure and the relationship between the environment and the actual forces in a structure.
2. The internal stresses at a critical point in the structure (around the intersection of the tubular joint, for example) induced by external forces acting on the structure.
3. The time to failure due to the accumulated stress history at the critical point.
4. The definition of 'failure' used in design.

The potential for error in the above predictions clearly precludes the exact calculations of absolute time to failure. Nevertheless, fatigue analysis is an important design tool for the prediction of the relative magnitudes of fatigue lives at potentially critical points. The calculated lives will enable critical parts to be ranked in terms of fatigue sensitivity and may be used:

- a) to select joints to be used in studies on the consequences of joint failure.
- b) to establish a priority basis for developing a selective inspection programme to be followed during the service life of the installation.

Two basic approaches are available for fatigue life assessment of structural components. The first method which is currently in more general use relies on empirically derived relationships between applied stress ranges and fatigue life (S-N approach). This approach is discussed in this Chapter of the Design Guide. The second method, described in Chapter 6, is based on linear elastic fracture mechanics, which considers the growth rate of



an existing defect at each stage in its propagation. Current practice is to use the S-N approach for design and general assessment, and the fracture mechanics approach for the appraisal of existing joints with known defects.

1.2 Definitions

The S-N approach relates the number of cycles to 'failure' of the steel section (N) to the critical 'hot-spot' stress (S). It has been found that in the range of stress where most damage occurs under ocean wave loading, there is an approximately linear relationship between $\log(S)$ and $\log(N)$. It should be noted, however, that this linear relationship is not constant for all steel attachments, but varies with the joint classification (eg. brace/chord intersection, girth welds, plate stiffener to member attachment, etc); environment (eg. air, seawater); post-welding treatment (eg. grinding, post weld heat treatment, etc); and member size.

1.2.1 Joint failure

The term 'joint failure' is, in general, not taken to be the complete separation of two sections, since this would be a function of the load applied and in most test situations is difficult to achieve without varying the frequency and directionality of loading. Furthermore, from a structural viewpoint complete separation represents loss of load path and presents a connection that will be both difficult and expensive to repair.

The four most commonly reported milestones in the life of a tubular joint are:

- N1 - Number of cycles to first detectable surface cracking by whatever method employed.
- N2 - Number of cycles to visible surface cracking.
- N3 - Number of cycles to first through thickness cracking.
- N4 - Number of cycles to end of fatigue test either due to complete severance of the welded joint or large loss of stiffness.

Of these milestones N3, the number of cycles to first through thickness cracking, has least dependence upon the experimental monitoring equipment, the operator skill or test rig capacity. In addition, there will probably be little loss of strength at N3 and repair can be more easily determined and performed.

In most codes and in this Guide, N3 is taken to be the definition of joint failure.



1.2.2 Hot-spot stress

The stress at any location on the joint (σ) is defined as the nominal stress (σ_{nom}) factored by the stress concentration factor (SCF) at that location, ie.

$$\sigma = \sigma_{nom} \times SCF$$

The hot-spot is defined as the location (or locations) where fatigue cracking is most likely to initiate. The term hot-spot stress is often misused, in particular it is confused with the location of maximum stress on the joint or member.

For a simple tubular joint, the hot-spot stress is generally the greatest value around the brace/chord intersection of the extrapolation to the weld toe of the geometric stress distribution near the weld toe. However, in more complex joints where more than one fatigue classification may apply (eg. a tubular joint with internal ring-stiffeners) the hot-spot may not be the location of largest stress concentration. Therefore, the maximum stress for each component within a joint or node must be calculated and assessed separately.

The hot-spot stress definition favoured in this Guide incorporates the effects of overall joint geometry (ie. the relative sizes of brace and chord) but omits the stress concentrating influence of the weld itself which results in a local stress distribution. Hence, the hot-spot stress is considerably lower than the peak stress but provides a consistent definition of stress range for the design S-N curve. In other definitions (eg. Marshall 1993) the SCF is defined to include some of the local notch effects near the weld toe.

Further details of the definition and estimation of SCFs are given in Chapter 4. While no one SCF definition is all encompassing and therefore 'correct', it is very important to note that there must be consistency between the SCF definition and the S-N curve to which it is applied. For example, a stress determined by the API method (API 1993) should only be applied to the API (or similarly defined) S-N curve and not to other S-N curves (eg. HSE (1993a), DnV (1992), etc).

1.2.3 Stress range and ratio

The load range is defined as the peak-to-trough magnitude of the applied loading, ie $P_{max} - P_{min}$ (where compressive load is defined as a negative load), see Figure 1.1. Similarly, the stress range, $\sigma_{range} = \sigma_{max} - \sigma_{min}$.

For constant amplitude loading, the stress ratio, R, is defined in this Guide as the minimum (trough) stress (or load) divided by the maximum (peak) stress (or load).

$$\text{ie } R = P_{min}/P_{max} = \sigma_{min}/\sigma_{max} \quad (-1 \leq R \leq 1)$$



The most common values for the stress ratio, R , are either $R = -1$ which describes cyclic tensile/compressive load of equal magnitude, or $R \approx 0$ where the applied load/stress range is always in either the tensile or compressive mode.

For variable amplitude loading this definition is often quoted to describe the range within which the stress is varying.

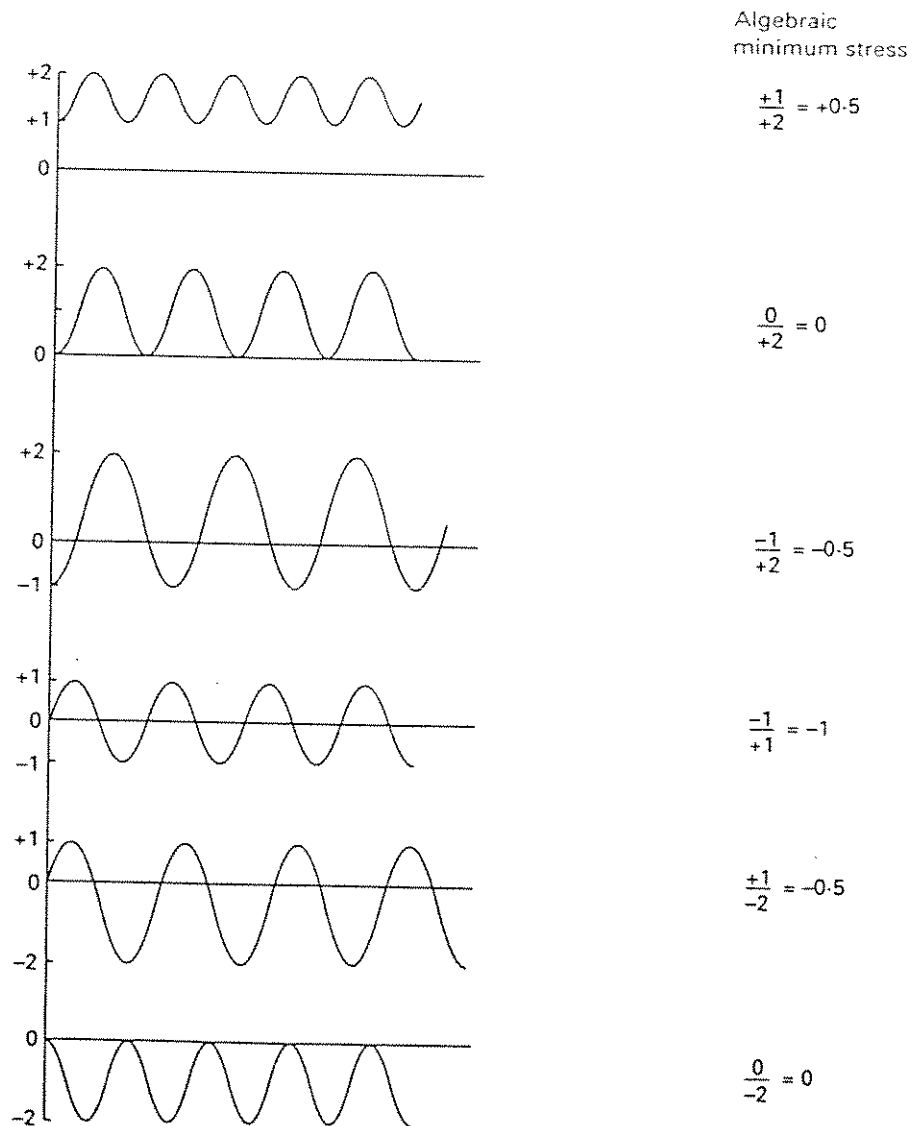
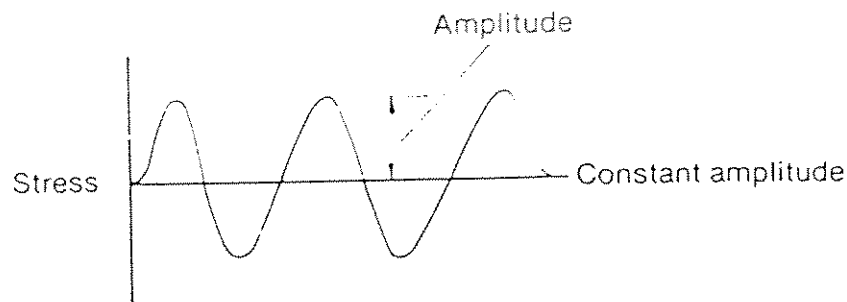


Figure 1.1 Examples of various load range and ratio definitions from Maddox (1991a)

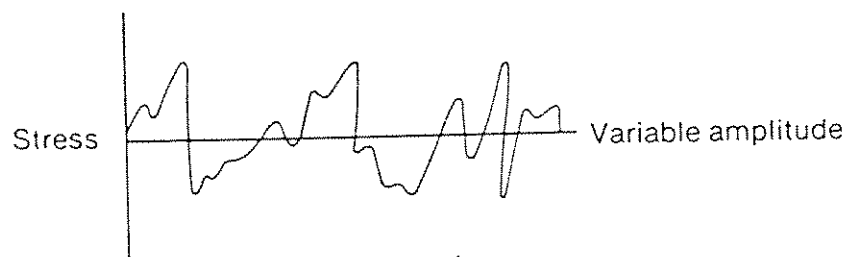


1.2.4 Constant and variable amplitude loading

A loading process has constant amplitude (CA) when the distances between successive peaks and troughs in the loading spectrum are equal, as illustrated in Figure 1.2(a), while a loading process has variable amplitude (VA) when the distances between successive peaks and troughs in the loading spectrum are not equal, as illustrated in Figure 1.2(b).



(a) Constant amplitude loading



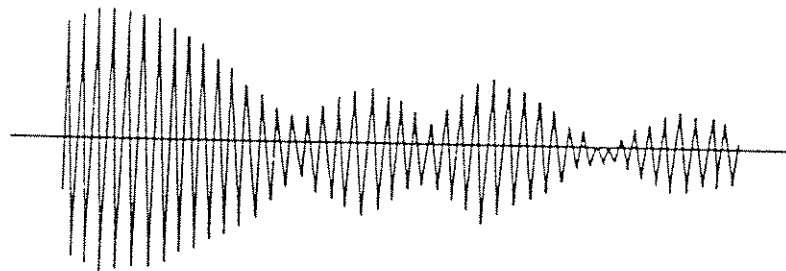
(b) Variable amplitude loading

Figure 1.2 Examples of constant and variable amplitude loading

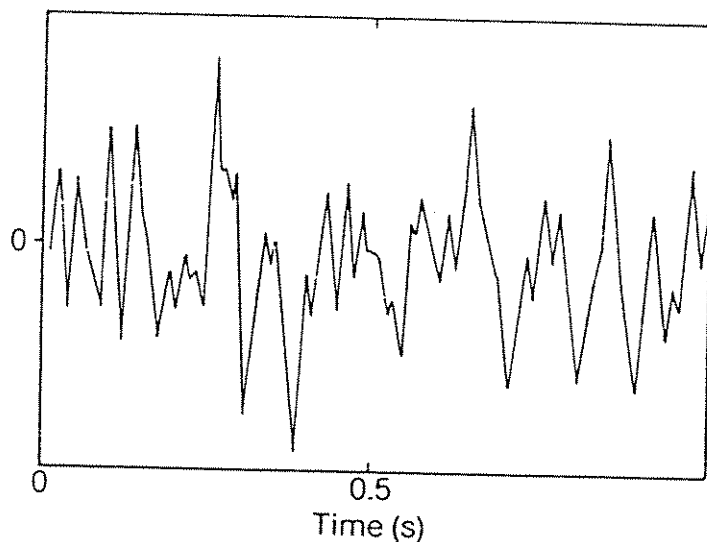
A number of different approaches have been developed for VA loading with the aim of generating a cyclic stress which is equivalent to a CA stress in terms of fatigue (eg. rainflow, range-pair, reservoir, etc. see Maddox 1991a). In this Guide, the root mean square (rms) amplitude of the stress process has been used to characterise the random load spectra investigated, as described in UKOSRP I (1988). This approach is simple to describe and is independent of both the outcome of the experiment and the slope of the S-N curve, but does not generally equate to the CA S-N approach. Only the rms value of the cyclic part of the curve is taken and thus the mean stress, S_m , does not enter. For further details and an assessment of this approach, see Section 6.3.



Random loading patterns can be classed as broad-banded if the energy is spread over a wide range of frequencies, or narrow-banded if the energy is concentrated close to a single frequency. If the spectrum of a time record is broad-banded then individual cycles in the record cannot be distinguished, and some peaks of the record have negative values. If a spectrum is narrow-banded then the record has the form of a slowly modulated sinusoid, see Figure 1.3. The irregularity factor can be used to categorise the loading band. This factor is defined as the number of positive-going zero crossing points divided by the number of maxima, as illustrated in Figure 1.3.



Narrow-band random load record from test machine
(Irregularity factor 0.99)



Computer generated broad-band random signal
(Irregularity factor 0.6)

Figure 1.3 Narrow band loading, broad band loading and irregularity factor



1.3 Basic Fatigue Design Approach

To perform a fatigue life estimation for a given tubular joint, a fatigue damage model is used in conjunction with an appropriate design S-N curve, where S is the total cyclic stress range and N is the design life.

An example S-N curve is presented in Figure 1.4. It can be seen that a linear relationship is generally assumed between the natural logarithm of both the stress range and design life parameters. The design S-N curves presented in guidance documents are typically based on a mean fit to fatigue test data generated under constant amplitude loading conditions with a safety factor applied to give a characteristic S-N equation. The characteristic equation is generally taken to be the mean equation less two standard deviations, thereby implying that approximately 2.3% of test data will fall below this line provided that the database is sufficiently large and unbiased.

Therefore, for a tubular joint under constant amplitude loading, estimating the design fatigue life of the joint is simply a matter of accurately determining the hot-spot stress range and applying this value to the design S-N curve. It should be noted that relatively small errors in determining the stress range can lead to significant errors in the estimated life, eg for an S-N curve with an inverse slope of $m = 3$ the error in the life is the cube of the error in the stress range.

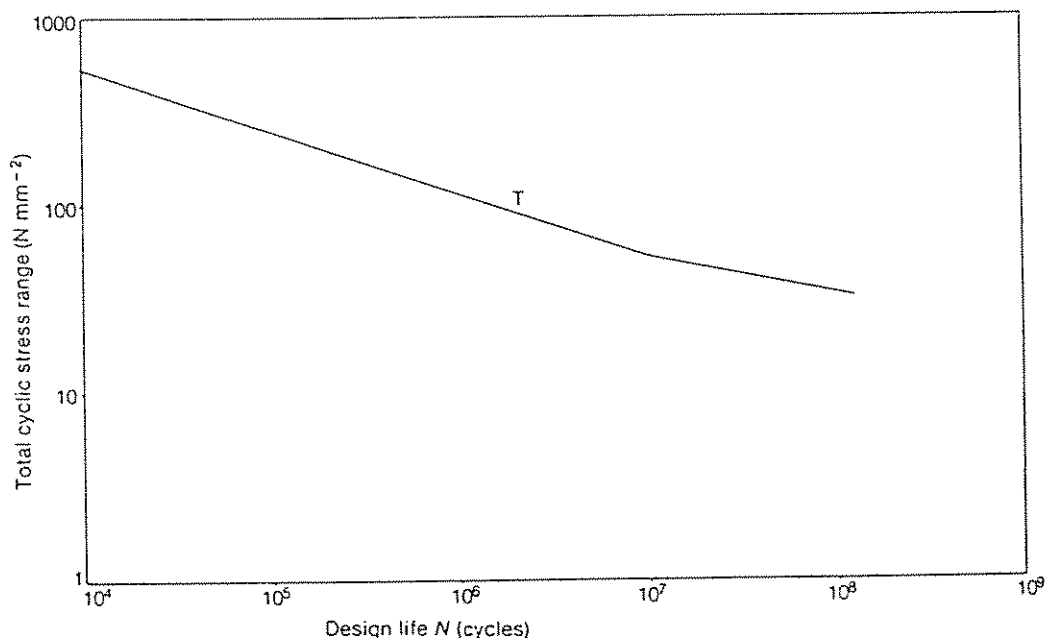


Figure 1.4 Example of S-N curve



However, in-service loading, and thus the stress range on the tubular joint, will be highly variable in magnitude and random in occurrence and therefore a fatigue damage model must be adopted. The favoured fatigue damage model within the fatigue S-N approach is that proposed by Palmgren-Miner's linear cumulative damage rule (abbreviated to Miner's rule), which, in essence, assumes that irreversible damage occurs with each stress cycle and that damage accumulates linearly to a fixed level at which point failure occurs (Palmgren (1924) and Miner (1945)). This approach is adopted in this Guide although its validity is critically appraised in Section 6.3.4 of this Chapter.

Initially, the distribution of stress ranges applied to the joint must be accurately (or conservatively) estimated using a cycle counting approach, as described in the following Section. From this a histogram can be derived, yielding the number of occurrences within a given stress range. For a particular stress range, S_1 , the constant amplitude endurance, N_1 , is a measure of the available damage at that stress level. Therefore, if n_1 stress cycles are applied at a stress range of S_1 then $n_1/N_1 \times 100\%$ of the joint life has been used up.

Fatigue failure occurs once the linear cumulative damage of cycles in the variable amplitude loading sequence has reached a fixed level,

$$\text{ie } \frac{n_1}{N_1} + \frac{n_2}{N_2} + \frac{n_3}{N_3} + \dots + \frac{n_i}{N_i} = D_s$$

where D_s is the damage accumulation limit, which should be taken to be $D_s = 1$ if Miner's law holds true. However, it should be noted that the value of D_s is sometimes chosen to reflect the safety level for a particular joint, for example where inspection of the joint may be difficult or impossible to perform.



2. METHODS FOR DETERMINING FATIGUE LIFE

2.1 Experimental Methods

Prior to the cyclic testing of tubular connections, a static test will generally be performed to determine the hot-spot stress(es) and its (their) location on the joint. Using an appropriate mean S-N curve whenever possible, the joint fatigue life for a given load range, or the load range required for a given fatigue life, should be estimated using the measured hot-spot stress range. This exercise is of particular value for low stress - high cycle tests where test durations in excess of one year have been required to achieve failure. The test can then be designed to suit inspection intervals with cycling frequency determined accordingly. Once under way, the output from the strain gauges can be monitored to ensure that the stress range is in accordance with that determined from the static test.

Initial crack detection (N1) may be electronically detected by the use of potential drop methods, time of flight diffraction techniques or a similarly proven method; or visually (N2), generally with the aid of a soap solution applied in the region of hot-spot stresses while cyclic loading is being applied. These inspection methods are described in detail in Chapter 2 of this Guide, Non-Destructive Examination (NDE).

Through thickness member cracking (N3) may be determined via visual inspection, the use of compressed air (within a sealed member), or one of the alternative techniques described in Chapter 2.

The end of test (N4) varies between test programmes and sometimes between individual tests within a single test programme. Generally, the end of the test will represent either complete separation of chord and brace members or, at least deflections that become too large to maintain the actuator stroke at the appropriate load frequency. However, in some cases, through thickness cracking may yield sufficient information to halt the test, particularly on joints with long lives.

2.2 Errors in Modelling Fatigue Behaviour

In S-N fatigue design, conservative assumptions tend to be made for both the loading and resistance parameters. To date, few studies have addressed the reliability of tubular joints to fatigue loading due to the complexity of the problem and the number of variables that need to be considered.

The typical log-log relationship between the stress range and the number of loading cycles to failure implies that errors in the measured stress range have a significant effect on estimated life, but error in a given fatigue life will have relatively little effect upon the estimated stress range. The following checklist describes good practice in performing fatigue tests and post-processing test data.



- a) SCFs should be measured on each joint rather than basing the hot-spot SCF on one control specimen, or on an empirical estimate of SCF. Gross errors can result by failing to identify the hot-spot location and the maximum stress prior to the fatigue test.

In Chapter 4 it was reported that differences in SCFs of $\pm 10\%$ could be anticipated in steel joint tests.

- b) The dimensions of all members should be measured on each specimen since their values are required in determining the stress range and scale effect. In addition, weld profile models should be given at the hot-spot and other key locations on the joint.

The error in basing the joint on nominal dimensions will largely be a function of the specimen size, with larger percentage errors associated with small scale tests. For a brace of dimensions: $d = 457 \pm 9\text{mm}$ and $t = 16 \pm 1.6\text{mm}$, the error in cross sectional area and section modulus would be around $\pm 10\%$ and $\pm 14\%$ respectively.

- c) The linearity of the load and strain should be checked prior to the test, although it should be noted that for reversible load ($R < 0$) there will tend to be some discontinuity at the tension-compression changeover due to play in the bearings.

The loading rig should be calibrated at the beginning of any test programme thereby enhancing the accuracy of the recorded load. Inaccuracies in the load and brace area or section modulus should be significantly reduced by measuring the nominal stress on the brace prior to the fatigue test.

- d) In general, fatigue lives are only expressed to three significant figures since any further level of accuracy implies a consistency in fatigue results that cannot be achieved. Therefore, inspection intervals should be set to achieve this level of accuracy.

- e) Key events in the joint fatigue life should be identified at the periodic inspections. However, the probability of detection of such events will depend upon factors such as technician experience, joint complexity and environmental conditions (eg. fully submerged in seawater). Furthermore, failure to correctly identify the hot-spot location in the static test will encourage inspection in the wrong location, thus emphasising the need to comprehensively strain gauge the specimen prior to testing.

- f) In presenting the data, it is typical to plot the stress on the Y-axis and the life on X-axis, since time dependent variables are traditionally drawn along the horizontal axis.



This would imply a relationship of the form:

$$\log_{10}(S) = a - b \log_{10}(N) + \epsilon_s$$

where ϵ_s is the difference between the estimated stress and that measured, Figure 2.1(a).

However, joint life is the dependent variable (ie. is a function of stress range) and therefore the correct form of the S-N equation, as expressed in the design codes, is:

$$\log_{10}(N) = K - m \log_{10}(S) + \epsilon_N$$

where ϵ_N is the difference between the estimated fatigue life and the measured fatigue life, Figure 2.1(b).

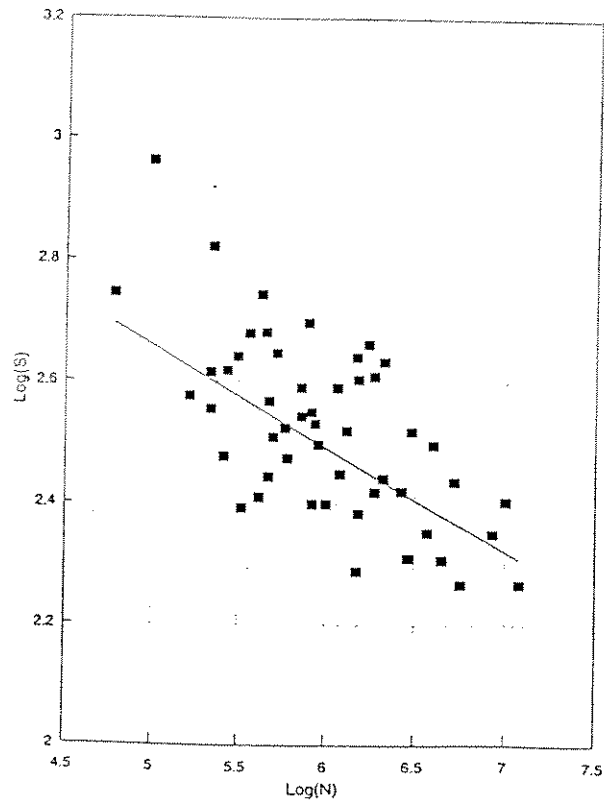
Performing a linear regression curve fit to these two expression will yield different curves, different coefficients and different estimates of scatter (unless $\epsilon_s = \epsilon_N = 0$).

No studies have been published on the experimental errors associated with fatigue tests, although the acknowledged level of uncertainty in fatigue testing generally requires several tests on identical configurations to be performed at either the same stress range or over a series of stress ranges.

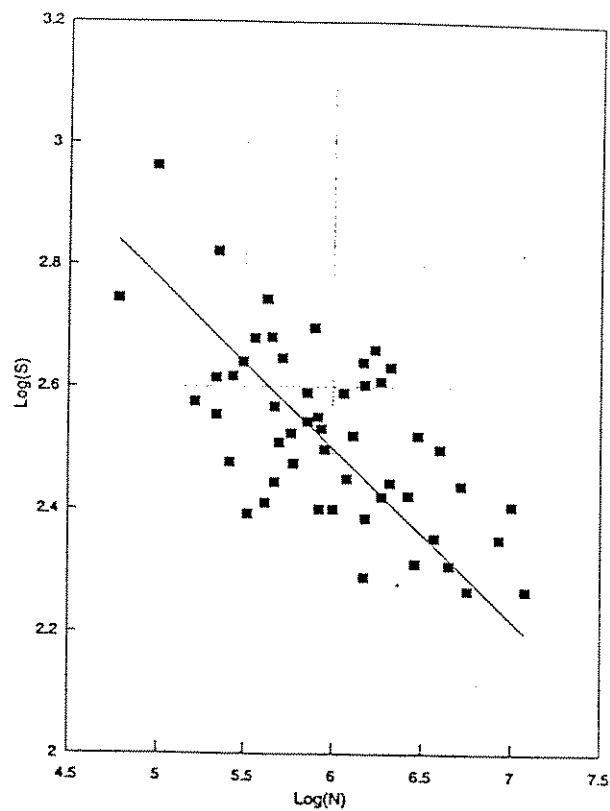
If the above uncertainties are combined to give an overall inaccuracy in the measured stress range throughout the test of $\pm 20\%$, then the spread of fatigue lives (assuming perfect material behaviour and crack detection) would be around $\pm 70\%$ for typical stress ranges considered. Such a spread within one programme of fatigue tests is not untypical.



$$\log(S) = \log(N) + C$$



(a) $\log(S)$ is the dependent variable
 $\log(N) = \log(S) + C$



(b) $\log(N)$ is the dependent variable

Figure 2.1 Comparison of statistical regression analyses with either $\log(S)$ or $\log(N)$ as the dependent variable



3. REVIEW OF EXISTING CODES FOR SIMPLE TUBULAR JOINTS

This Section refers to fatigue S-N curves for simple tubular brace-chord connections. Reference should be made to Section 10 for complex joints and circumferential girth welds.

The fatigue strength of tubular joints cannot, by the complex nature of crack propagation, be defined by theoretical means. To derive a quantitative approach for use in design it is necessary to conduct experiments, and to date all design codes have been based on such an empirical approach.

The 1972 editions of API and AWS gave the first recommendations for the design of tubular joints against fatigue based on the use of S-N curves. The curves were developed on the basis of two concepts. The first was an attempt to define a brace nominal stress to correlate with failure, while the second concept successfully correlated fatigue data with the hot-spot stress of the joint. The data used to obtain the S-N curve (called the X curve in the two documents) was obtained from small specimens tested in air under constant amplitude loading. In the 1970s this curve became the most widely used S-N curve despite the caution expressed by the AWS code at that time that 'calculated fatigue lives based on the proposed curves should be viewed with a healthy amount of scepticism and should be used more as design guidance than as an absolute requirement.'

In 1984, following the completion of a large European fatigue test programme the UK Department of Energy (DnV 1984a), published a more comprehensive set of S-N curves and factors covering environment, post-fabrication treatment and stress range. (nb. the UK Health and Safety Executive, HSE, is now responsible for offshore safety in the UK). The T curve was derived specifically for tubular joints based on these data with both mean and design curves specified. These curves were based on a slightly different definition of SCF to that for the X curve, which aimed at removing any notch stress from the SCF rather than providing for these effects in the S-N curves themselves. The T curve is currently the most widely used fatigue curve and is the one given prominence in this Guide as it is based on the definition of SCF recommended in Chapter 4 (nb. this SCF definition was preferred primarily because most published fatigue data follows this approach).

These two approaches and the main national codes that follow these approaches are discussed in the following Section. It should be noted that both these sets of S-N curves are largely based on small-scale specimens tested in-air under constant amplitude loading.

3.1 DnV T Curve Approach

The DnV T curve (DnV 1984) was primarily based on results from European research programmes performed in the early 1980's, and forms the basis of the recently superseded UK HSE (1993), the DnV (1992) and the Canadian codes (CAN/CSA 1992) for tubular joints fatigue life assessment at the brace/chord intersection. For non-tubular components, such as welded stiffeners or attachments, a series of S-N curves is given under the classifications: B, C, D, E, F, F2, G and W. The classifications applicable to tubular connections are given in Appendix A.



The basic design S-N curves ($N < 10^7$) are all described by the form:

$$\log_{10}(N) = K - d\sigma - m \log_{10}(S_B)$$

where K is the constant
 m is the inverse slope of the S-N curve
 d is the number of standard deviations below the mean
 thus typically $d=0:d=2$ are the mean:design curves
 and σ is the standard deviation of $\log(N)$

For the quoted joint classifications the parameters K , m and σ are specified as follows:

CLASS	K	σ	m
T	12.6606	0.2484	3.0
B	15.3697	0.1821	4.0
C	14.0342	0.2041	3.5
D	12.6007	0.2095	3.0
E	12.5169	0.2509	3.0
F	12.2370	0.2183	3.0
F2	12.0900	0.2279	3.0
G	11.7525	0.1793	3.0
W	11.5662	0.1846	3.0

For full details on the strategy and development of the tubular T S-N curve, reference should be made to the 'Background to new fatigue design guidance for steel welded joints in offshore structures' (DEn 1984b).

The HSE have recently proposed amendments to their Guidance Notes including modifying the tubular S-N curve to the T' curve and combining the various plate curves into a single P curve with factors applied depending upon the fatigue classification (HSE 1995). Details of the derivation of the T' curve are given in a 'fatigue background guidance document' (MaTSU 1992).

CLASS	K	σ	m
T'	12.9420	0.2330	3.0
P	12.6007	0.2095	3.0

CLASS	CLASSIFICATION FACTOR (stress range modifiers)
B ^{*1}	0.64P
C ^{*1}	0.76P
D	1.00P
E	1.14P
F	1.34P
F2	1.52P
G	1.83P
W ^{*2}	2.54P

*1 The former B and C class S-N curves now have a slope of $m = 3$ and thus the classification factors are approximations in these cases. *2 The W curve has been modified and therefore this factor does not correlate with the current W curve.



3.1.1 UK Health and Safety Executive Guidance Notes (HSE 1993)

The current HSE Guidance Notes (HSE 1993) represent the latest version of the original DEn Guidance Notes (DEn 1984a) and their background (DEn 1984b).

General considerations

The HSE state that 'Stresses may also be reduced by increasing the thickness of parent metal; this should improve fatigue life but it should be remembered that fatigue strength tends to decrease with increasing thickness. The effectiveness of cathodic protection is also an important factor influencing the fatigue behaviour of structural steels in sea water but it should be noted that over-protection may be detrimental.'

The HSE note that every welded joint or other form of stress concentration is potentially a source of fatigue cracking and each should be individually considered. In assessing fatigue performance all types of cyclic loading should be considered, with cyclic loading from different sources potentially significant at different phases of the life of a structure (eg. construction, transportation, installation, in-service, etc).

Unless otherwise agreed, the calculated fatigue life should be the required service life (at least 20 years). Normally dynamic amplification should be considered when the natural period of the structure is greater than three seconds.

An additional factor on life should be considered for cases of inadequate structural redundancy, and account should be taken of the accessibility of the joint and the proposed degree of inspection as well as the consequences of failure. However, no specific factors are recommended in the Guidance Notes.

Stresses to be considered

It is assumed that it is only necessary to consider ranges of cyclic stress in determining the endurance (ie. mean stresses are neglected). The hot-spot stress is defined by the HSE as the greatest value around the brace/chord intersection of the extrapolation to the weld toe of the geometric stress distribution near the weld toe.

Stress ranges for post-weld heat treated joints should be assumed the same as for as-welded joints. The use of full penetration welds is recommended for all nodal joints.

Basic design S-N curves

The design T S-N curve is applied for tubular joints which are either in-air or exposed to seawater but adequately protected from corrosion. For unprotected joints exposed to seawater the basic S-N curve is reduced by a factor of two on life.

A number of factors should be considered in using the basic HSE T design S-N curve:



- Treatment of low stress cycles

While an endurance limit is noted for CA loading at around $N = 10^7$ cycles, it is felt that under VA loading the endurance limit may vary. HSE represent this uncertainty by a change of slope from $m = 3$ to $m = 5$ at $N = 10^7$.

This correction does not apply in the case of unprotected joints in seawater.

- Treatment of high stress cycles

For high stress cycles the design S-N curve should be limited to a stress range equal to twice the material yield stress ($2\sigma_y$), where $\sigma_y \leq 400 \text{ N/mm}^2$.

- Effect of plate thickness

The basic S-N T curve relates to 32mm thick members. For tubular joints of other thicknesses correction factors on life or stress have to be applied to produce a relevant S-N curve. The correction on stress range is of the form:

$$S = S_B(32/t)^{0.25}$$

where

S is the fatigue strength of the joint,

S_B is the fatigue strength of the joint using the basic S-N curve,

t is the actual thickness of the member under consideration (nb. $t_{\min} = 22\text{mm}$).

- Weld improvement

For welded joints involving potential fatigue cracking from the weld toe an improvement in strength by at least 30%, equivalent to a factor of 2.2 on life, can be obtained by controlled local machining or grinding of the weld toe. However, it is recommended that no advantage for toe grinding should be taken at the initial design stage and only joints adequately protected from corrosion can receive this benefit.

This is normally carried out either with a rotary burr or by disc grinding. The treatment should produce a smooth concave profile at the weld toe with the depth of the depression penetrating into the plate surface to at least 0.5mm below the bottom of any visible undercut and ensuring that no exposed defects remain. The maximum depth of local machining or grinding should not exceed 2mm or 5% of the plate thickness.

Damage calculation

For each potential crack location the long term distribution of relevant stress ranges should be established and the calculated fatigue life estimated by consideration of cumulative damage.



3.1.2 Det norske Veritas Rules (DnV 1992)

The DnV Rules for Classification make brief direct reference to fatigue of tubular joints. Sections B400 and C400 cover the Fatigue Limit State (FLS) for design by partial coefficient and allowable stress methods respectively. The fatigue criteria is based on the Palmgren-Miner rule such that $\Sigma(n/N) \leq D_s$, where the cumulative damage ratio to be used in the design is dependent upon the access for inspection and repair as specified below.

Cumulative Damage Ratios (D_s)		
No access for inspection and repair	Below or in the splash zone *	Above the splash zone
0.33	0.5	1.0
* In typically harsh environments (eg. the North Sea) structural details exposed to seawater in the splash zone are normally to be considered to have no access for inspection and repair.		

If failure of a member or joint caused by fatigue may result in progressive collapse, a reduction of the cumulative damage ratios beyond these values is to be considered. Such reduced cumulative damage ratios are to be approved by the Society.

Section E600 addresses the fatigue strength of tubular joints. This section gives general guidance on designs to be avoided and methods for increasing fatigue life in-service via grinding. DnV note that designs which are sensitive to the quality and accuracy of workmanship are to be avoided.

The following measures may be considered to improve the fatigue design life of tubular joints:

- Avoiding gussets and stiffeners creating local points of high rigidity.
- To grout reinforce the chord.
- To grind the weld toe including the adjacent parent material to remove the surface defects created by welding. Such grinding is to be carried out according to a recognised standard.

(Note: Increase in fatigue life due to grinding is not normally accounted for at the design stage. In-service, grinding carried out according to a recognised standard may be accepted in order to increase fatigue life).

- To locate the welded joints outside the areas of high stress concentration. This may be achieved by incorporating forgings or castings.



The user is referred to Classification Note No. 30.2 for further guidance, DnV (1984). The introduction states that the fatigue test analyses are based on the DEn Guidance (DnV 1984a), and therefore the basic design T curves in-air and in-seawater with adequate CP are identical to that specified by the HSE. For unprotected joints in seawater the S-N curve is reduced by a factor of two on life.

- Treatment of low stress cycles

For joints exposed to seawater with adequate cathodic protection (CP), an endurance limit (S_0) at $N = 2 \times 10^8$ cycles is proposed so that stress range levels below S_0 do not contribute to fatigue damage.

For joints in-air, a change of slope from $m = 3$ to $m = 5$ is recommended.

No change in slope is described for joints exposed to seawater with inadequate cathodic protection.

- Treatment of high stress cycles

It is stated that the yield stress of the material should not exceed 400 N/mm^2 . However, no specific guidance on an upper stress range is given.

- Effect of plate thickness

For thicknesses of tubular joints other than that included in the basic S-N curve, a modification on stress is carried out such in the same manner as for the HSE code (HSE 1993), ie.

$$S = S_B(32/t)^{0.25}$$

In the DnV code, there does not appear to be a minimum thickness specification.

- Weld improvement

With regard to weld profiling, DnV note that the effect of weld profiling giving the weld a smooth concave profile compared to the typical triangular or convex shape may increase the fatigue life. Thus, provided weld profiling is carried out, an X curve in line with API RP2A (API 1993) may be accepted instead of the T curve.

For joints in seawater with adequate CP grinding may be used, once in-service, to enhance the joint life. A factor of two on life can be obtained by controlled local machining or grinding of the weld toe. This is normally carried out by a rotary burr. The treatment should produce a smooth concave profile at the weld toe with the depth of depression penetrating into the plate surface to at least 0.5mm below the bottom of any visible undercut. The maximum grinding depth should not exceed 2mm or 5% of the plate thickness, whichever is smaller.



3.1.3 Canadian code (CAN/CSA 1992)

The Canadian code largely follows the requirements of the UK HSE Guidance Notes (HSE 1993). Under the 'General' heading it is noted that members and connections subjected to fatigue loading shall be designed, detailed and fabricated so as to minimise stress concentrations and abrupt changes in cross-section.

The design life shall be the greater of 20 years or the required service life.

It is noted that the limit damage ratio, D_s , depends upon:

- a) the safety class of the structure,
- b) the consequence of failure,
- c) the importance of a particular construction detail,
- d) the access for inspection and repair.

The limit damage ratio is given by $D_s = \alpha' \beta'$, where α' is a factor that depends on the safety class of the structure and the importance of the particular construction detail analysed, and β' is a factor depending upon access for inspection and repair.

Safety class of structure	Damage factor, α'	
	Importance of structural detail	
	Minor	Major
1	1.0	0.5
2	1.0	0.5

Damage factor, β'		
Access for inspection and repair		
No access 0.2	Poor access 0.6	Good access 1.0

Dynamic amplification shall be considered in the calculation of the fatigue stress spectrum when considered significant.

Joint classification and stresses to be considered

All full penetration tubular joints are classified in accordance with the T curve.

Stress ranges for post-weld heat treated joints are taken to be the same as for as-welded joints.



- Treatment of low stress cycles

For joints in-air, a change of slope from $m = 3$ to $m = 5$ is recommended at $N = 10^7$ cycles.

For joints exposed to seawater without corrosion protection, no change in slope is taken. With cathodic protection the change of slope is at $S_0 = 53 \text{ N/mm}^2$, $N = 10^7$ cycles.

- Treatment of high stress cycles

No specific guidance on an upper stress range is given.

- Effect of plate thickness

For thicknesses of tubular joints other than that included in the basic S-N curve, a modification on stress is carried out in the same manner as for the HSE code, ie.

$$S = S_B(32/t)^{0.25}$$

- Weld improvement

Credit for beneficial treatment of welds may be taken, subject to satisfactory documentation of the proposed procedure and the change in damage ratio.

3.1.4 The HSE Proposed Revisions to Fatigue Guidance (HSE 1995)

The UK HSE is currently revising some sections of its Guidance Notes, summarised in Section 3.1.1 (HSE 1993).

This new document has recently been published (February 1995) and will supersede the 1993 Guidance Notes. Significant revisions have been made to the 1993 HSE Guidance and new clauses are proposed for high strength steels, bolts and threaded connectors, moorings, fatigue performance of repaired joints and fracture mechanics. Justification for changes is detailed in a background document (MATSU, 1992).

Stresses to be considered

Proposed Guidance (HSE 1995) adds a clause regarding mean stresses and PWHT. For PWHT joints the fatigue performance may improve as the load applied becomes more compressive. However, under purely tensile loading the fatigue performance should be regarded as that for as-welded joints. It is recommended that for PWHT joints, no advantage in terms of fatigue performance should be taken at the design stage.

In addition to the clause stating that the stress range for PWHT should be the same as the as-welded case, the Proposed Guidance states: 'However, in the event that it can be demonstrated using validated techniques that a compressive component of the combined applied and residual stresses exists and can be quantified, it would be permissible to assume a stress range for



fatigue of the tensile component plus 60% of the compressive component. To ensure the effectiveness of post-weld heat treatment, the process should be carried out in accordance with accepted standards (eg. BS 5500).

In addition to the statement on full penetration welds: 'In load-carrying partial penetration or fillet-welded joints, where cracking could occur in the weld throat, the relevant stress range is the maximum range of shear stress in the weld metal.'

In the current HSE Guidance Document (HSE 1993) nodal joints are specifically covered, although this section only really covers simple and overlapping joints, given the data available. The Proposed Guidance (HSE 1995) gives more in-depth coverage: Simple nodal joints are defined as being non-overlapped, unstiffened, ungrouted and uniplanar. Complex nodal joints incorporate overlapping braces, stiffening or grout in the chord and may have braces in several planes (ie. multiplanar).

The recommended SCFs for simple joints, and the effect upon the hot-spot stress of overlapping braces, ring-stiffening, grouting and cast joints is addressed. Reference is made to either an Appendix of SCF equations or to the Background Document to Fatigue Guidance (MaTSU 1992), see Chapter 4.

Joint classification

For the purpose of fatigue design, welded joints are divided into several classes, as illustrated in Appendix A.

All tubular joints are assumed to be in Class T'. Other types of joint, including tube to plate, may fall in one of several classes depending upon:

- a) the geometrical arrangement of the detail
- b) the direction of the fluctuating stress relative to the detail
- c) the method of manufacture and inspection of the detail.

Basic design S-N curves

The proposed design S-N T' curves for tubular joints in-air is:

$$\log_{10}(N) = 12.476 - 3.0 \log_{10}(S_B) \quad (S_B \text{ in N/mm}^2)$$

For plate and tubular joints exposed to seawater but protected from corrosion, fatigue lives are reduced by a factor of two (except at low stress ranges).

For tubular joints exposed to seawater but without adequate corrosion protection, fatigue lives reduced by a factor of three from the in-air curve.

A number of factors should be considered when using the basic design T' S-N curves for welded joints.



- Treatment of low stress cycles

HSE propose a change of slope on the S-N curves from $m = 3$ to $m = 5$, for in-air and in-seawater with adequate cathodic protection. However, unlike previous guidance, this change of slope is a function of the stress range rather than the number of cycles.

In-air the change of slope occurs at a stress range of 67 N/mm^2 ($T = 16\text{mm}$), while in seawater with adequate cathodic protection the change of slope occurs at a stress range of 95 N/mm^2 ($T = 16\text{mm}$).

This correction does not apply in the case of unprotected joints in seawater.

- Treatment of high stress cycles

'For welded plates and tubular joints in air or seawater (with or without CP) values of the stress range greater than twice the yield stress need special consideration. Further information is given in the background document (MaTSU, 1992).'

'The limits from static strength should be considered. The design tensile stress will be governed by a fracture criterion or by the tensile limitations on normal member stress. For compressive loading, buckling considerations may be critical and should be included in the analysis.'

- Effect of plate thickness

The basic design S-N curves are applicable to thicknesses less than the basic thickness, which for the T' S-N curve is 16 mm .

For members of greater thickness, a modified S-N relationship applies as follows:

$$S = S_B(16/t)^{0.30}$$

where

S is the fatigue strength of the joint,

S_B is the fatigue strength of the joint using the basic S-N curve,

t is the actual thickness of the member under consideration (nb. $t_{\min} = 16\text{mm}$).

Other thickness correction relationships may be used if they can be justified by data from a validated test programme or by fracture mechanics analysis.



- Weld toe improvement

'For welded joints an improvement of 2.2 on life can be obtained by controlled local machining or grinding to produce a smooth concave profile at the weld toe which blends smoothly with the parent material. This benefit may be claimed for welded joints in air and for joints in seawater with adequate protection against corrosion. However, it is recommended that this advantage should not be utilised at the initial design stage'.

'Care should be taken to remove all defects in the critical region, by grinding to the weld toe to a depth of not less than 0.5mm', see Figure 3.1. 'The maximum depth of local grinding should not exceed 2 mm or 5% of the plate thickness, whichever is less. It is recommended that the final grinding operation should be carried out using a rotary burr to provide a generous radius to blend with the surrounding material. An appropriate NDE technique eg. BS 6072 should be used to ensure that no significant defects remain after grinding. Where appropriate, the final ground surface should be suitably protected in order to avoid local corrosion pitting prior to the application of cathodic protection'.

'Where toe grinding is used to improve the fatigue life of fillet welded connections, care should be taken to ensure that the required throat size is maintained. It should also be noted that grinding of the weld toe will not give an increase in life in other fatigue sensitive regions such as the weld root. It is known from laboratory tests that other weld improvement techniques such as hammer or shot peening can also enhance fatigue life. Any advantage in terms of improved fatigue performance as a result of using these techniques should be justified by evidence obtained from a validated test programme'.

It should be noted that no benefit from toe grinding or other weld improvement techniques should be assumed for unprotected joints in seawater.

Stress Concentration Factors

For simple tubular joints, either the Efthymiou (1988) or the Smedley/Fisher (1991a) SCF equations may be employed, although there are specific configurations/loadcases that a given equation may not be acceptable.

Factor of Safety

A pilot study of uncertainties in fatigue design (Thorpe and Sharp, 1990) showed that a safety factor of ten for critical, non-inspectable joints reduces the probability of failure to less than 10^{-4} which is in-line with other offshore levels of structural reliability. Therefore, it is proposed (MaTSU, 1992) that this value be applied to all critical, non-inspectable joints.

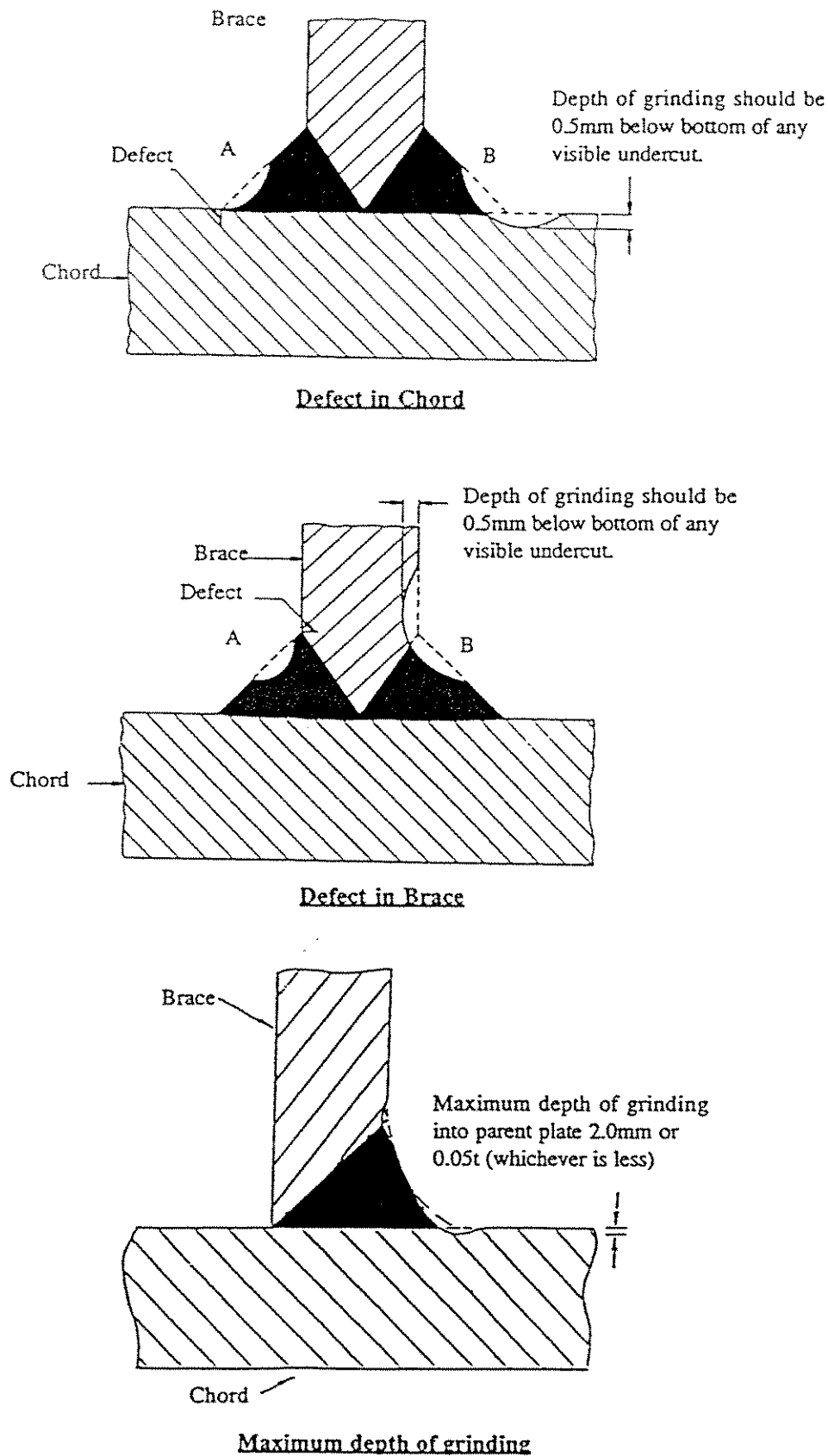


Figure 3.1 Weld toe improvement (HSE 1995)



Fatigue performance of repaired joints

A detailed appraisal of repairs to tubular joints damaged by cyclic loading is given in Chapter 7 of this Guide.

It should be noted that repair to original standards may not be sufficient to achieve an adequate level of structural safety. The discovery of fatigue damage, particularly if it has occurred rapidly or unexpectedly, may indicate the need for a wider reappraisal of the fatigue performance of the structure.

Welded joints may be repaired by either: repair welding, repair welding and grinding, or bolted clamps.

3.2 API X Curve Approach

The X and X' curves (API 1993) are based on a lower bound to a database of tubular joint results. These data cover all joint types and environmental conditions. The only difference, and hence the two S-N curves, being the weld treatment.

The X-curve is applicable for welds with profile control and having a brace thickness less than 1 in. (25mm).

$$X: \log_{10}(N) = 15.063 - 4.38 \log_{10}(S_B) \quad (S_B \text{ in N/mm}^2)$$

The X' curve is applicable for welds without profile control, but conforming to a basic standard flat profile, AWS (1992).

$$X': \log_{10}(N) = 13.396 - 3.74 \log_{10}(S_B) \quad (S_B \text{ in N/mm}^2)$$

The forerunner of the X curve was the Q curve which is still accepted by Lloyd's Register (Lloyds 1989).

3.2.1 American Petroleum Institute - API RP2A (API 1993)

In 1993, revised S-N curves were published for tubular connection design, including both size and profile corrections. These provisions are included in both the working stress and LRFD versions of the API RP2A code and essentially follow the 1986 AWS provisions (AWS 1992), with implementation by API delayed until 1993 while confirmation tests were performed.

Section 5, Fatigue, of API RP2A covers: fatigue design, fatigue analysis, S-N curves for all members and connections, except tubular connections, S-N curves for tubular connections, stress concentration factors.

A detailed commentary on fatigue is incorporated at the back of the API RP2A document and gives an overview of the development of API Guidance on fatigue, defines terms relating to fatigue and gives background details to the five fatigue sub-sections. Those parts relating to tubular joint fatigue design and analysis are reproduced in summary form.



Fatigue design

API RP2A states that a detailed fatigue analysis should be performed for template type structures with a spectral analysis technique recommended, although other rational methods may be used provided adequate representation of the forces and member responses can be shown.

In lieu of detailed fatigue analysis, simplified fatigue analyses, which have been calibrated for the design wave climate, may be applied to tubular joints in template type platforms that:

- 1) Are in less than 400 feet (122 m) of water.
- 2) Are constructed of ductile steels.
- 3) Have redundant structural framing.
- 4) Have natural periods less than 3 seconds.

Fatigue analysis

A detailed analysis of cumulative fatigue damage should be performed as follows:

- a) The wave climate should be derived as the aggregate of all sea states to be expected over the long term.
- b) A space frame analysis should be performed to obtain the structural response in terms of nominal member stress for given wave forces applied to the structure. A general wave force calculation procedure is then described in API RP2A.
- c) A spectral analysis technique should be used to determine the stress response for each sea state. Dynamic effects should be considered for sea states having significant energy near a platform's natural period.
- d) Local stresses should be considered in terms of hot-spot stresses located immediately adjacent to the joint intersection using suitable SCFs. The microscale effects occurring at the toe of the weld are reflected in the appropriate choice of the S-N curve.
- e) For each location around each member intersection of interest in the structure, the stress response for each sea state should be computed, giving adequate consideration to both global and local stress effects.
- f) The stress responses should be combined into the long term stress distribution, which should then be used to calculate the cumulative fatigue damage ratio, $D_s = \sum (n/N)$.

In general the design fatigue life of each joint and member should be at least twice the intended service life of the structure (ie. Safety Factor = 2.0). For the design fatigue life, D_s should not exceed unity. For critical elements whose sole failure could be catastrophic, use of a larger safety factor should be considered.



S-N curves for tubular connections

API states that for tubular connections exposed to variations of stress due to environmental or operational loads, the X and X' curves should be used. These curves are applicable to random loading and presume effective cathodic protection in seawater. (Connections in the splash zone should generally be avoided.)

The X-curve is applicable for welds with profile control and having a brace thickness less than 1 in. (25mm). For the same controlled profile at greater wall thicknesses, the recommended scale effect correction should be used unless grinding is performed. However, scale effect reductions below the X' curve are not required.

The X' curve is applicable for welds without profile control, but conforming to a basic standard flat profile (AWS 1992) and having a brace thickness less than 0.625 in. (16mm). For the same flat profile at greater wall thicknesses the scale effect correction below should be used. However, the X' curve may be used for unlimited branch thicknesses provided the profile control requirements are satisfied.

- Treatment of low stress cycles

The endurance limit for the basic X and X' S-N curves occurs at 2×10^8 cycles. However, for tubular connections in-air, the endurance limit for the X curve may be assumed to be at 10^7 cycles. For splash zone, free corrosion, or excessive corrosion conditions no endurance limit should be considered.

- Treatment of high stress cycles

The allowable peak hot-spot stress, S_p , is determined as a function of water depth, member location, S-N curve and design fatigue life. Figure 3.2 illustrates the maximum allowable hot-spot stress for 40 year and 100 year design life (at least twice service life), for waterline members and other members, for the X curve, Figure 3.2(a), and the X' curve, Figure 3.2(b).

The allowable hot-spot stress range $S_r = S_p (1-R)$, where R is the stress cycle ratio. Typical values of R range from -0.15 to -0.50 and are dependent upon the water depth.

- Effect of plate thickness

The scale effect correction is:

$$\text{allowable stress} = S_o(t/t_o)^{-0.25}$$

S_o is the allowable stress from the S-N curve,
 t is the brace member thickness ($\geq t_o$),
 t_o is the limiting brace thickness
 (25mm for the X curve and 16mm for the X' curve).



- Weld improvement

For branch thicknesses greater than 1 in. (25mm), the X-curve may be used without scale effect provided the profile is ground smooth to a radius greater than or equal to half the branch thickness. Final grinding marks should be transverse to the weld axis and the entire finished profile should pass magnetic particle inspection.

Stress concentration factors

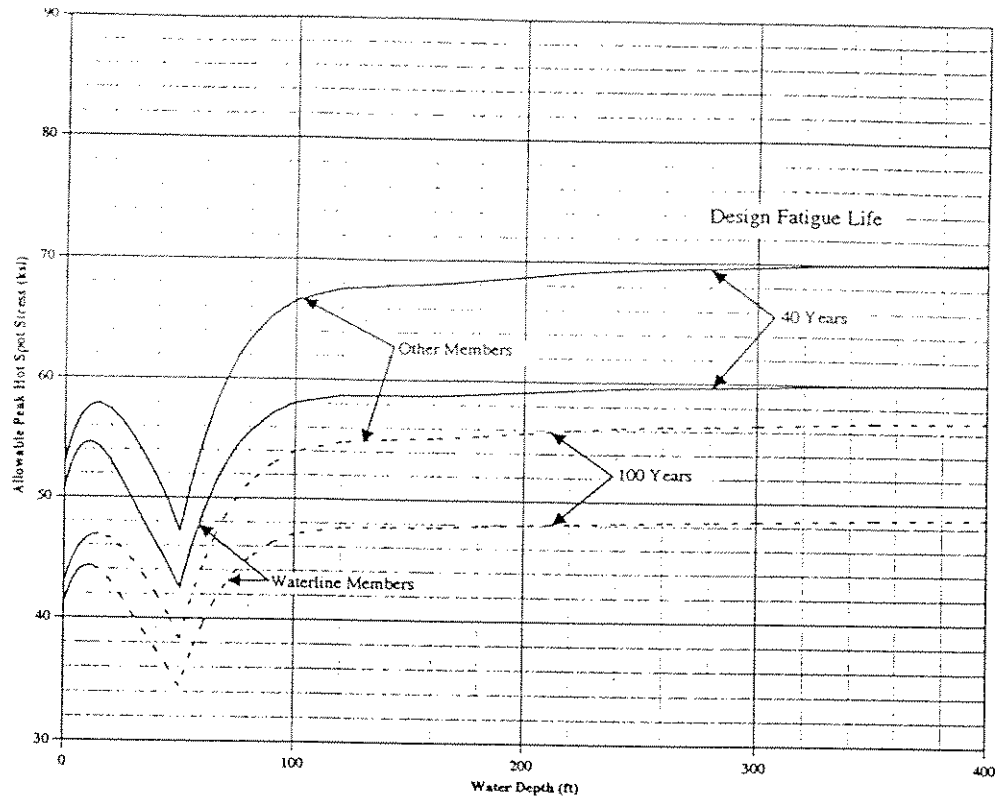
The X and X' curves should be used with hot-spot stress ranges based on suitable SCFs. SCFs may be derived from finite element analyses, model tests or empirical equations based on such methods. In API RP2A, the Kellogg (1956) SCF expressions are favoured, with stresses sampled $0.1(rt)^{0.5}$ from the weld toe. Therefore, this definition of SCF differs from that recommended in Chapter 4 of this design guide.

3.2.2 American Welding Society Structural Welding Code (AWS 1992)

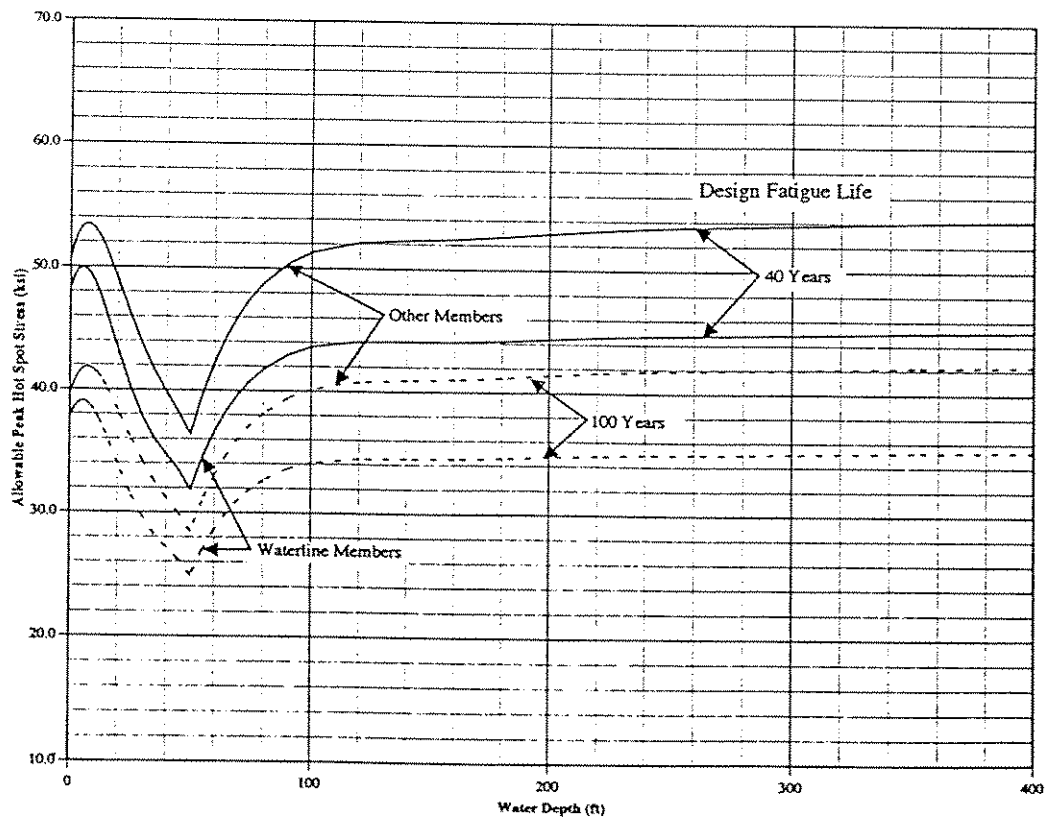
The fatigue behaviour of tubular structures is addressed in Section 10.7 of the ANSI/AWS D1.1-90 structural welding code and substantiated in Commentary C10.7 (AWS 1992). Several S-N curves are defined for tubular T, Y or K connections based on data from circular sections originating from work by Marshall and Toprac (1974).

In defining fatigue, this code states that 'Fatigue, as used herein, is defined as the damage that may result in fracture after a sufficient number of stress fluctuations. Stress range is defined as the peak-to-trough magnitude of these fluctuations. In the case of stress reversal, stress range shall be computed as the numerical sum (algebraic difference) of maximum repeated tensile and compressive stresses, or the sum of shearing stresses of opposite direction at a given point, resulting from changing conditions of load. In the design of members and connections subject to repeated variations in live load stress, consideration shall be given to the number of stress cycles, the expected range of stress, and type and location of member or detail.'

For the fatigue summation model, AWS state that: *'Where the fatigue environment involves stress ranges of varying magnitude and varying numbers of applications, the cumulative fatigue damage ratio, D_s , summed over all the various loads, shall not exceed unity, where $D_s = \sum (n/N)$. For critical members whose sole failure mode would be catastrophic, D shall be limited to a fractional value of 1/3.'*



(a) X S-N curve



(b) X' S-N curve

Figure 3.2 Allowable peak hot-spot stress (API 1993)



AWS provides a series of stress categories related to particular S-N curves. The S-N curves for simple welded joints are the X_1 (X) and X_2 (X') curves. It is recommended that curve X_1 should be used where hot-spot stresses are known and welds are profiled so as to merge smoothly with the adjoining base metal. The lower X_2 curve applies to joints where hot-spot stresses are known but without smoothly profiled welds. Curves X_1 and X_2 equate to the API X and X' S-N curves, although AWS specify that the API adopted cut-off of 200 million cycles need not be applied to AWS.

The other S-N curves are classified as follows:

- K_1 Simple T, Y, and K connections in which $\gamma \leq 24$. Punching shear for main members; for chord members ($\gamma > 24$) reduce allowable stress in proportion to $(24/\gamma)^{0.7}$. Where actual SCFs or hot-spot strains are known, use of curve X_1 or X_2 is preferred.
- K_2 As for K_1 , except no improved weld profile.
- DT Connections designed as simple T, Y, or K connections with complete joint penetration groove welds. If actual SCFs or hot-spot strains are known, use of curve X_1 or X_2 is preferred. (nb. main member must be checked separately per category K_1 or K_2 .)
- ET Simple T, Y, and K connections with partial penetration groove welds or fillet welds. If actual SCFs or hot-spot strains are known, use of curve X_1 or X_2 is preferred.
- FT Simple T-, Y-, or K-connections loaded in tension or bending, having fillet or partial joint penetration groove welds. Shear in weld (regardless of direction of loading).

- Treatment of low stress cycles

AWS specifies endurance limits for all the above S-N curves between 10^7 and 5×10^7 cycles. For the X curve this is at 10^7 , while for the X' curve this endurance limit is at 2×10^7 .

- Treatment of high stress cycles

The maximum stress shall not exceed the basic allowable stress provided in the AWS Code, and the range of stress shall not exceed 100 ksi (= 690 N/mm²).

- Effect of plate thickness

The fatigue strength should be reduced in proportion to:

$$(\text{size/size limit})^{-0.25}$$

where the following size limits are specified for the X_1 and X_2 curves:



- X_1 = 9.5mm (Standard flat weld profile)
= 15.9mm (Profile with toe fillet)
= 25.4mm (Concave profile, as-welded, with disk test)
= unlimited (Concave smooth profile fully ground)
- X_2 = 15.9mm (Standard flat weld profile)
= 38.1mm (Profile with toe fillet)
= unlimited (Concave profile, as welded, with disk test)

- Weld improvement

AWS gives guidance on obtaining the required weld profile to allow use of the curves X_1 and K_1 . The recommended weld profile is similar to that given in API RP2A. The Code states that *'For the purpose of enhanced fatigue behaviour, and where specified in contract documents, the following profile improvements may be undertaken:*

1. *A capping layer may be applied so that the as-welded surface merges smoothly with the adjoining base metal, and approximates the profile specified. Notches in the profile shall be no deeper than 1.0mm relative to a disc having a diameter equal to or greater than the brace member thickness.*
2. *The weld surface may be ground to the profile specified. Final grinding marks shall be transverse to the weld axis.*
3. *The toe of the weld may be peened with a blunt instrument, so as to produce local plastic deformation which smooths the transition between weld and base metal, while inducing a compressive residual stress. Such peening shall always be done after visual inspection, and be followed by magnetic particle inspection (as described).*

Consideration should be given to the possibility of locally degraded notch toughness due to peening.

In order to qualify for fatigue categories X_1 and K_1 , representative welds (all welds for non-redundant structures or where peening has been applied) shall receive magnetic particle inspection for surface and near-surface discontinuities. Any indications which cannot be resolved by light grinding shall be repaired.'

AWS also state that the smooth surface profile of fully ground welds exhibit no size effects. Since peening only improves a relatively limited volume of welded joint, the size effect would be expected to show up fairly soon if peening is the only measure taken; however, peening should not incur a size effect penalty where it is done in addition to profile control.



3.2.3 Lloyd's Register of Shipping (Lloyds 1989)

Fatigue requirements for tubular joints in offshore fixed steel jackets are given in Sections 5 and 7 of Part 4, Chapter 1 of the Rules and Regulations. These rules employ the Q design S-N curve specified.

The S-N Q curve as employed by Lloyd's Register assumes that CP and PWHT has been performed in accordance with requirements in Part 6 and Part 2 respectively (Lloyds 1989).

$$Q: \log_{10}(N) = 14.624 - 4.132 \log_{10}(S) \quad (S \text{ in } N/mm^2)$$

At long-life, no change in slope or endurance limit on the S-N curve is taken without supporting evidence. No limit on high stress joints is specified and no scale correction is taken. It is assumed that residual stresses are built in to the S-N curve.

SCF expressions are recommended for simple tubular joints:

- i) T/Y joints - Wordsworth/Smedley (1978)
- ii) X joints - Wordsworth/Smedley (1978)
- iii) K/KT joints - Kuang (1975, 1977) for axial load and IPB, and Wordsworth (1981) for OPB.

3.3 Comparison of Design Codes

Several offshore design codes have been reviewed in this Section and the fatigue provisions in each code have been summarised. The following notable differences between the fatigue guidance recommendations are summarised in Section 3.3.1 while a comparison of the codes is given in Section 3.3.2 for the case of a joint in seawater below the splash zone with adequate CP.

3.3.1 Summary of design codes

Joint classification

The T curve employs a different definition of SCF, and therefore hot-spot stress, to the X/X' curves. Since the X/X' curves are based on stresses measured closer to the weld toe, larger SCFs would generally be expected and therefore S-N curves above the design T curve may be anticipated. However, this is not the case, probably due to the preference for a lower bound curves rather than 97.5% probability design curve.

API	X based on $t \leq 25.4\text{mm}$
AWS	X based on $t \leq \text{variable}$ (subject to condition)
CSA	T based on $T = 32\text{mm}$
DnV	T based on $T = 32\text{mm}$
HSE	T based on $T = 32\text{mm}$
HSE (prop)	T' based to $T = 16\text{mm}$
Lloyds	Q based on all T



Scale effect factor

API	$n = 0.25$ for $t > 25.4\text{mm}$
AWS	$n = 0.25$ for $t > \text{variable}$ (subject to condition)
CSA	$n = 0.25$ for $T > 22\text{mm}$ (based on $T = 32\text{mm}$)
DnV	$n = 0.25$ for $T \neq 32\text{mm}$
HSE	$n = 0.25$ for $T > 22\text{mm}$ (based on $T = 32\text{mm}$)
HSE (prop)	$n = 0.30$ for $T > 16\text{mm}$
Lloyds	No scale effect provided PWHT applied

Effect of being in-seawater with adequate CP

API	X curve (lower endurance limit)
AWS	X curve
CSA	0.5T curve
DnV	0.5T curve (access factor, lower endurance limit)
HSE	T curve
HSE (prop)	0.5T' curve (at high stresses)
	1.0T' curve (at low stresses)
Lloyds	Q curve

Effect of being in-seawater with inadequate CP

API	X curve (no endurance limit)
AWS	X curve
CSA	0.5T curve (no endurance limit)
DnV	0.25T curve (nb. $D_s = 0.5$, no endurance limit)
HSE	0.5T curve (no endurance limit)
HSE (prop)	0.33T' curve (no endurance limit)
Lloyds	Not applicable

High stress cycles (maximum allowable stress)

API	S_{\max} function of water depth, member location, S-N curve and design life and stress ratio.
AWS	$S_{\max} \leq 690 \text{ N/mm}^2$
CSA	$S_{\max} \leq \text{static strength}$
DnV	$S_{\max} \leq \text{static strength}$
HSE	$S_{\max} \leq 2\sigma_y (\leq 800 \text{ N/mm}^2)$
HSE (prop)	$S_{\max} \leq 2\sigma_y$ or maybe related to ultimate strength
Lloyds	$S_{\max} \leq \text{static strength}$

Low stress cycles

API	in-air : 1×10^7 limit
	sw + CP: 2×10^8 limit (except splash zone)
	sw - CP: none
AWS	Unspecified: 1×10^7 (X) and 2×10^7 (X') limit
CSA	in-air : 1×10^7 (m+2)
	sw + CP: 1×10^7 (m+2)
	sw - CP: none
DnV	in-air : 1×10^7 (m+2)
	sw + CP: 2×10^8 (m+2)
	sw - CP: none



HSE in-air : 1×10^7 (m+2)
 sw + CP: 1×10^7 (m+2)
 sw - CP: none

HSE (prop) in-air : 1×10^7 (m+2)
 sw + CP: $< 10^7$ (m+2)
 sw - CP: none

Lloyds None unless justified

Recommended empirical SCF equations

API Kellogg (1956)

AWS None

CSA None

DnV Wordsworth and Smedley (1978), Kuang (1975, 1977) and
 Gibstein (1978)

HSE None

HSE (prop) Efthymiou (1988) or Smedley and Fisher (1991a)

Lloyds Wordsworth and Smedley (1978), Wordsworth (1981),
 Kuang (1975, 1977) and Efthymiou (1988)

Weld profile or ground weld toe

API Use of X rather than X' curve

AWS Use of X rather than X' curve

CSA Credited if evidence provided

DnV Factor of two on life or use of X curve

HSE Factor of 2.2 on life

HSE (prop) Factor of 2.2 on life

Lloyds Not specified

Non-inspectability

API Not specified

AWS Not specified

CSA 0.2T (no access); 0.6T (poor access)

DnV 0.33T (cf. in-air); 0.66T (cf. in-seawater)

HSE Required but not specified

HSE (prop) 0.1T' for critical joints

Lloyds Not specified

Other factors

AWS 0.33T for critical joints

CSA 0.5T safety class 1 and major importance detail



3.3.2 Illustration of differences in design codes

The design S-N curves described in Section 3.1 and 3.2 are compared in Figure 3.3 for joints in seawater with adequate cathodic protection, $T = 40\text{mm}$ and $t = 40\text{mm}$.

It has been assumed that the joints can be easily inspected and therefore, no factors for inspectability have been taken with the codes. The joint is not defined to be a significant structural component. The weld profile is in accordance with the controlled requirement but has not been ground.

Therefore, the basic curves are:

API	1.0X
AWS	1.0X
CSA	0.5T (0.5 for in seawater+CP)
DnV	1.0T
HSE	1.0T
HSE (prop)	0.5T' (0.5 for in seawater+CP)
Lloyds	1.0Q

It can be seen in Figure 3.3 that, even for the simple case of an inspectable joint in seawater with CP, there are significant differences between the Codes, with the most similar S-N estimates occurring around $N = 10^5$ cycles.

The API X curve is identical to the AWS X_1 curve for $N < 10^7$, however, while AWS takes the endurance limit at this value API recommends an endurance limit at 2×10^8 cycles. The Lloyd's Q curve estimates longer lives for $N < 3 \times 10^8$.

For $T = t = 40\text{mm}$, the proposed HSE Guidance yields an S-N curve that is nearly identical to the current T curve for $N > 10^7$ cycles. Above $S = 69 \text{ N/mm}^2$ ($N < 2 \times 10^6$ cycles), the proposed Guidance reduces the in-air life by a factor of two while the current Guidance states that of joints in-seawater with CP is the same as in-air.

The DnV S-N curve is the same as the replaced HSE T curve, except at high stresses in excess of $2\sigma_y$, where no stress range limit is imposed. For $S < 69 \text{ N/mm}^2$ the DnV T curve is more pessimistic with no change of slope up to the endurance limit at $N = 2 \times 10^8$ cycles.

The CSA curve lies parallel to the current HSE curve except for the reduction factor of two on life. The change of slope from $m = 3$ to $m = 5$ is effected at $N = 10^7$.

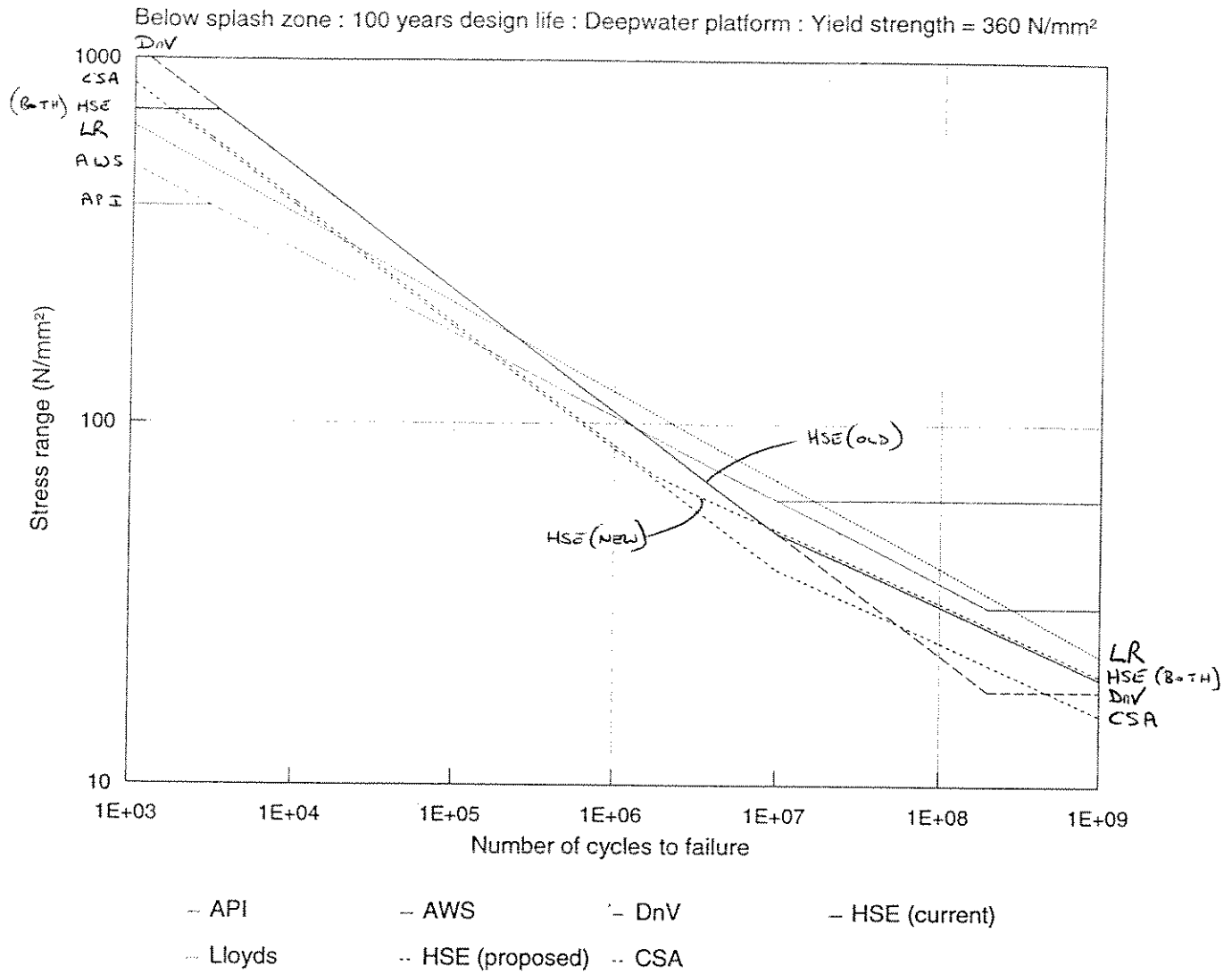


Figure 3.3 Comparison of design S-N curves in seawater with adequate cathodic protection



4. REVIEW OF PUBLISHED DATA AND PARAMETERS AFFECTING FATIGUE LIFE

The hot-spot is defined as the location of maximum stress where fatigue cracking is most likely to occur.

It should be noted that several definitions of SCF are employed, as discussed in Chapter 4, and that the measured stress will be a function of the definition of SCF adopted. It is important to note that while no one definition of SCF is correct, S-N curves should not be derived or compared to test results based on inconsistently derived hot-spot stress data. In this Guide, the UK HSE SCF definition has been adopted (DEN 1984b), primarily because the majority of SCF and fatigue S-N data has been based on this approach. Therefore, in the screened S-N database, contained in this Chapter, only data sampled in accordance with the HSE recommended method is employed in the derivation and comparison of S-N curves (see Chapter 4 for details of this approach). However, where there is a lack of data for a given effect (eg influence of seawater, post weld heat treatment, etc), direct comparisons between data using an alternative SCF definition may be employed to estimate the percentage gain or reduction on the joint fatigue life due to the variable considered.

4.1 Summary of Parameters Which May Influence Fatigue Life

In the design codes and published literature many parameters have been investigated and their influence on fatigue life considered. Some of these, for example the scale effect and the effect of environment, have been the focus of extensive test programmes, while other parameters are believed to have either no effect or an insignificant effect.

In summarising the list of parameters that are considered in this Guide it should be remembered that, while on most offshore structures fatigue failures occur on complex nodes at least partially submerged in seawater under complex loading patterns, most test results relate to simple T joints in dry air under constant amplitude single mode loading.

- The geometry of the tubular joint and weld

The geometry governs the size and location of the hot-spot stress where fatigue cracking is most likely to occur.

- The method of loading

The type, amplitude, mean/maximum level, range and distribution of the applied load directly governs the fatigue life.

- The fabrication method and materials

The process adopted during fabrication will determine the local material properties, residual stress pattern and distribution of defects. These factors tend to control the crack initiation period of the joint fatigue life.



- The environment in which fatigue cracks initiate and grow

Three areas are relevant:

- i) Air - well above the splash zone, although such air could have a high water vapour and salt content.
 - ii) Mixed air and seawater - splash zone where immersion is controlled by wave height and tide.
 - iii) Seawater - complete immersion in seawater with the fatigue behaviour possibly a function seawater temperature, salinity and alkalinity.
- Post-fabrication processes applied to the tubular joint in order to improve fatigue life or some other aspect of performance

These topics include:

- i) Corrosion protection (CP)
- ii) Post-weld heat treatment (PWHT)
- iii) Weld toe grinding, hammer peening, TIG dressing, overall profiling, etc.

4.2 Summary of Main Test Programmes

Fatigue testing of tubular joints is expensive and time consuming and, due to the inherent variability in fatigue tests, generally requires several tests to be performed at one, or over a range of, stress levels to develop a sufficient understanding of fatigue behaviour for a given configuration. Therefore, most tubular joint data tends to be the result of a relatively large joint industry funded test programme of which there are relatively few. This number is further reduced in the screened database since alternative definitions of SCF to that adopted in this Guide tend to be used in the USA, Japan and Norway. In fact of the screened database of 157 simple tubular joints, nearly 90% come from the following four international studies.

4.2.1 United Kingdom Offshore Research Project (UKOSRP)

This project was performed in two distinct phases. UKOSRP I (between 1975 and 1981) and UKOSRP II (between 1982 and 1986).

UKOSRP I (1988, 1989) was a programme of research into the fatigue and fracture strength of tubular joints used in offshore steel structures. In 1975, the UKOSRP I project was set up under the auspices of the UK Department of Energy (now HSE) in response to the perceived sparsity of data relevant to fatigue endurance in the North Sea. Subsequently, in September 1976, the European Coal and Steel Community (ECSC) entered into collaboration in the project contributing £0.8m towards the overall cost of £4.5m.



The main emphasis of the project was on providing experimental data to significantly enlarge the set of constant amplitude data on which the design S-N curves were based. Thus 175 tubular joint tests and over 375 plate joint tests were performed in this phase of the project. The effects of variations in the environment, stress range and weld treatment were examined using the welded plate joints and pre-cracked plate specimens. To simulate real marine loadings, variable amplitude tests were performed on both welded plates and tubular joints. Beside their intrinsic value, these tests enabled the linear Palmgren-Miner damage accumulation rule to be assessed in prescribed experimental conditions. Fatigue tests were carried out in the UK on tubular joints with chord diameters varying from $D = 168\text{mm}$ to 1830mm and chord thicknesses varying from $T = 6.3\text{mm}$ to 76.0mm . The configurations of the tubular joints were T, K and KT both with and without overlaps under axial, in-plane and out-of-plane loading applied to the brace member.

UKOSRP II (1987, 1989a, 1989b) was designed to cover uncertainties and areas not addressed in the UKOSRP I programme. This project was funded by 26 offshore energy companies, with interests around the world, at a total cost of £3.25m.

A total of 25 tasks were addressed under six topic areas: thickness effect, corrosion effects, PWHT, weld improvement techniques, effect of joint geometry and variable amplitude testing. To meet these tasks, 92 tubular joint tests (46 fatigue tested) and over 330 plate joint tests were performed in this second phase of the project. Fatigue tests were carried out on T joints and K joints with varying degrees of gap/overlap between braces, and T joints with internal stiffening under axial load.

4.2.2 European Coal and Steel Community (ECSC)

The ECSC funded research into the fatigue behaviour of tubular joints in 1976 to supplement the programme of work on both plate and tubular joints planned in UKOSRP I. In addition to funding some work in UKOSRP I, further tests were funded in the Netherlands, France, Italy and Norway.

In the Netherlands, Dijkstra and de Back (1981), 26 simple T joints and fourteen simple X joints were funded, with variations in scale, load ratio, test frequency, loading mode and environment.

In France, Lieurade (1981a, 1981b), ten simple X joints were funded, with variations in scale, test frequency and loading mode.

In Italy, Brandi (1981) and Damilano (1981), eight static and twelve fatigue tests on simple, ring-stiffened and stiffened/grouted joints were tested, with variations in the number of ring-stiffeners.

In Norway, Gibstein (1981), eight simple T joints, one simple Y joint and two simple K joints were funded, with variations in overlap of braces, test frequency and environment.



4.2.3 Canadian Offshore Research Project (COSRP)

In 1981, the Canadian Department of Energy, Mines and Resources, Thomson and Tyson (1987), initiated a programme of work with the twin objectives of 'ensuring that appropriate regulations, standards and design data are generated to govern the selection and performance of welded steel structures; and simultaneously equipping Canadian Industry with the technology base needed to maximise its share of the material supply aspects of offshore resource development.'

This programme covered welding technology, particularly at cold temperatures; and fatigue analyses of plate T joints, pipe-to-pipe joints and large scale tubular joints. The testing of stiffened tubular joints was undertaken in a manner that would compliment the work previously undertaken in UKOSRP II (1987).

In total, twelve tubular joints were tested of which ten had internal ring-stiffening via plate type stiffeners, COSRP (1989, 1991). The effect of the stiffening on stress distribution and fatigue crack development was documented for tests in-air under all modes of loading and in-seawater using optimum CP under axial load alone.

4.2.4 SERC (Madras)

In 1988, the Council of Scientific and Industrial Research, India, funded the Structural Engineering Research Centre (SERC) in Madras the sum of around £0.24m to study fatigue in offshore structures and formulate guidelines for Indian waters.

Early work, for example Ramachandra Murthy (1990), considered the experimental and analytical behaviour of simple T and Y joints, although most of the work has been aimed at the influence of internal ring-stiffening. Fatigue and fracture behaviour of ring-stiffened joints under axial load, IPB and OPB has been studied both in-air and in-seawater under free corrosion conditions.

4.3 Tubular Joint Fatigue Database and Screening Criteria

The full initially screened database of fatigue S-N data for simple tubular joints are listed in Appendix B, with the data arranged by test programme. For all data, the following factors have been reported:

- Geometric dimensions for the chord, brace and weld
- Strain gauging and stress extrapolation methodology
- Loading mode and nominal brace stress
- For each member: maximum SCF and location, steel grade and yield strength and maximum stress range
- Hot-spot stress, failure location and N1 - N4



- Data for PWHT, grinding, environment, stiffening, etc.

The initial screening criteria were specified as

- i) Only data based on ECSC hot-spot stress definition (HSE 1984b)
- ii) All geometric details of chord and brace required
- iii) Loading mode must be specified
- iv) SCF at the failure location must be given
- v) The nominal brace stress must be given, or must be calculated from the applied loading and joint area or section modulus, as applicable.
- vi) The location of failure must be given
- vii) The number of cycles to through thickness cracking must be given.

In total, 157 joints passed the initial screening:

120 T joints
16 X joints
7 K joints
2 KT joints
8 TT joints
4 H joints

4.4 Basecase S-N Curve

Ideally, a basecase S-N curve for tubular joints would be derived from a sufficiently large database where the only variable is the applied stress range. Subsequently, each parameter would be assessed against this S-N curve and its influence considered independently. However, given that at the very least 20 test results would be required to establish a sufficiently large database this approach is not possible.

In Section 4.1 of this Chapter, several parameters were listed that could have an influence on the tubular joint fatigue life. Previous studies into the effect of many of these parameters suggests that their influence may be insignificant or they may have no effect at all on tubular joint life. Therefore, it is proposed that these potentially insignificant effects are initially ignored, thus enabling a basic S-N curve to be derived. The recognition of a scale effect for non-PWHT joints, as evidenced by a reduction in fatigue life for an increase in member thickness, led to the basecase S-N curve being derived from T = 16mm data alone.

Following the derivation of this S-N curve, the effect of variations in all parameters can be considered and their significance quantified.



In this Guide, it is proposed to derive the basecase S-N curve on:

- i) Simple non-overlapped, single planar, unreinforced, as-welded tubular joints.
- ii) Chord thickness of $T = 16\text{mm}$ ($\pm 10\%$), with failure occurring due to through thickness cracking of the chord member (N3), with failure occurring between 10^4 and 10^7 cycles.
- iii) Single mode, constant amplitude loading, with no chord end loading applied.
- iv) Tests performed in-air with no post-fabrication treatment, eg. PWHT, weld toe grinding, etc.

Thus there is an underlying assumption that joint geometric parameters, weld attachment length, loading mode, frequency and range have minimal effect on the joint fatigue life. This assumption will be appraised in Section 5 along with the other variables that are considered to have a more significant influence on joint fatigue life.

The screened basecase database contains 36 fatigue results. The choice of 16mm for the chord thickness was based on the amount and quality of data at this thickness. For $T = 32\text{mm}$, only twelve data points met the screening criteria, while data for thinner chord walls was considered to be too inconsistent to be adopted as the basecase.

The 36 S-N data points are listed in Appendix C and it can be seen that the data covers relatively large ranges of θ , β , weld leg length, loading mode and stress range to yield stress ratio. However, within this dataset there is little variation in joint configuration, chord end fixity, α , γ and brace inclination.

Applying a linear regression least squares error minimisation technique to this $\log(S):\log(N3)$ dataset yields the following relationship:

$$\log(N3) = 12.07 - 2.64 \log(S)$$

The standard error, S_E , of this estimate is 0.213.

Simplifying the expression by forcing the gradient of the slope to be equal to three gives an expression of not dissimilar accuracy:

$$\log(N3) = 12.90 - 3 \log(S)$$

The standard error, S_E , of this estimate is 0.222.

This simplified expression is taken to be the basecase relationship between the joint through thickness failure and applied hot-spot stress range and is illustrated in Figure 4.1.

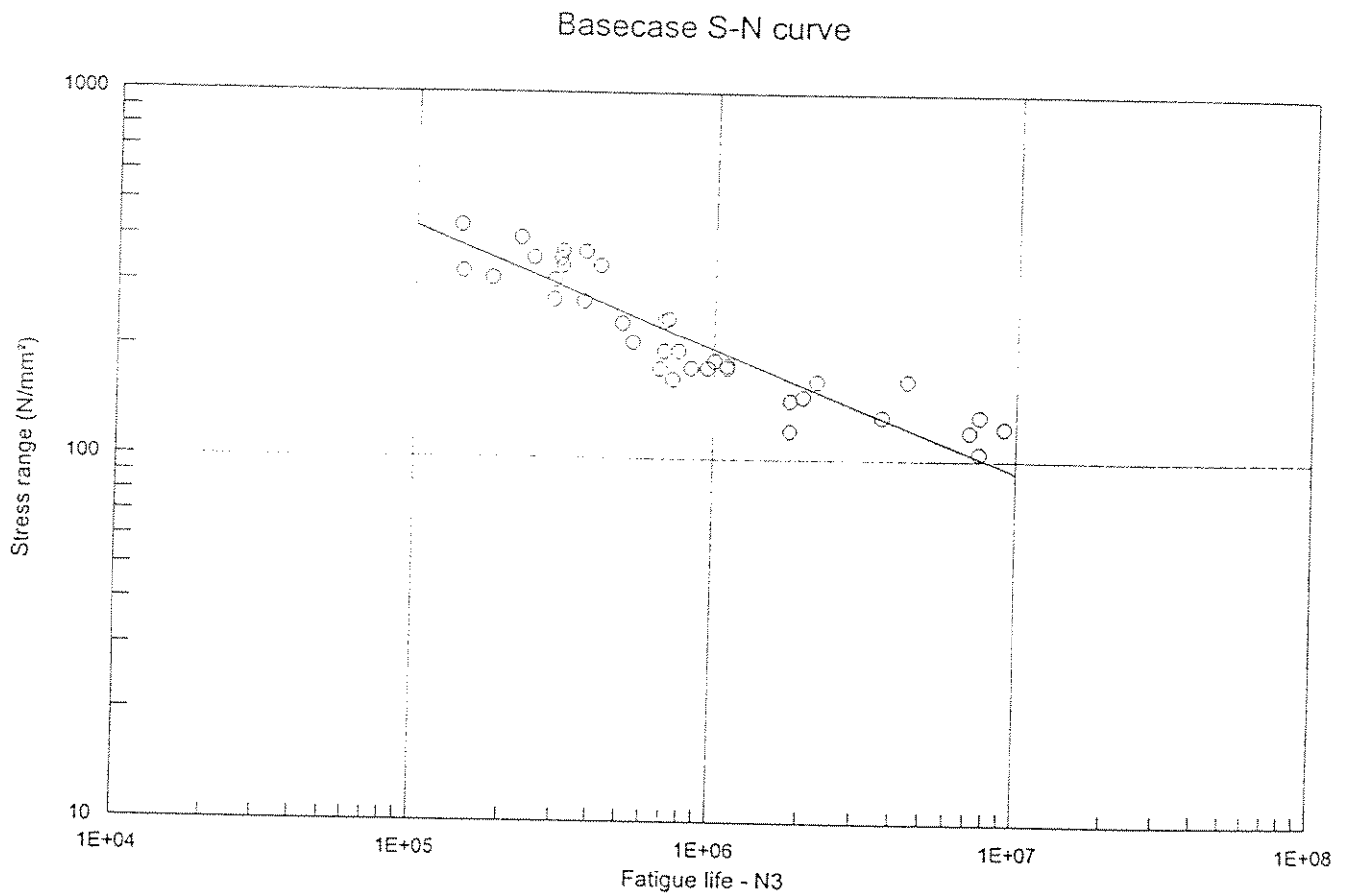


Figure 4.1 Basecase S-N curve and supporting test data



5. INFLUENCE OF JOINT GEOMETRY

In recent years there has been much debate over the specification of a 'scale', 'size' or 'thickness' effect, whereby fatigue life reduces as joint size increases.

This effect is generally expressed by modifying the stress range in the basic 'nominal' S-N curve (S_0), in proportion to the ratio of thickness of a specified member (t) to the nominal member thickness (t_0):

$$S = S_0 (t_0/t)^n$$

where n is a scale effect exponent.

In Section 5.1, a brief review of the development and current views on the scale effect is given.

In Sections 5.2 - 5.7, all the geometric parameters that describe the fatigue behaviour of simple tubular joints in-air are assessed against the full screened in-air simple tubular joint database of 157 results, as presented in Section 4.3. Only data from simple joints under constant amplitude loading are considered at this stage, although other potential loading variables such as loadcase, chord end loading and stress range are also included. In addition, where sufficient variation permits, the basecase database of 36 results, presented in Section 4.4, is also referenced.

5.1 The Scale Effect - An Overview

In the 1970's and 1980's many fatigue and fracture assessments were performed, on both plate joints and tubular joints, in an attempt to understand and quantify scale effects that were evident in test specimens. However, the range, and sometimes strong divergence, of opinions often left the designer with the feeling that each new test programme led to a new interpretation of the scale effect.

The discrepancies in the interpretation of scale effect were, in part, due to the differing definitions of the hot-spot stress concept adopted in Europe and in the USA. These differences may be simply described as:

- In Europe the perception of a tubular joint has tended to be from a wider viewpoint as the connection of two members. Stresses are measured well away from the notch zone and therefore local weld effects are removed. It is then assumed that the local notch effect will be accounted for in the T S-N curve.
- In the USA the perception of a tubular joint has tended to be from a more local viewpoint as a welded connection. Stresses are measured nearer to the weld within the notch zone and some weld size and profile effects are included in the X S-N curve.



Recently there appears to be more of a consensus on the cause of the scale effects and a recognition that design guidance needs to reflect this effect in a simple yet not overly conservative manner.

A synopsis of three of the more predominant views of scale effect that have influenced scale factors in design codes is given below, followed by a summary of the more recent thinking on scale effect and how it should be allowed for in design.

5.1.1 Gurney (1979)

In 1979, Gurney of TWI reported a thickness effect based on a fracture mechanics assessment of axially loaded welded joints. The existence of this thickness effect was confirmed in the first phase of the UKOSRP project which yielded a series of S-N curves (UKOSRP I 1988), each dependent upon the thickness of the failed specimen, Figure 5.1.

This effect was attributed to the thickness of the member in which cracking occurred, although it should be noted that for tubular joints nearly all joint failures occurred in the chord member. In 1984, this thickness effect was incorporated in the UK DEn Guidance Notes (Dn 1984a) and a thickness exponent $n = 0.25$ was recommended. Subsequently, this thickness correction factor was adopted in the DnV fatigue guidance notes (DnV 1984).

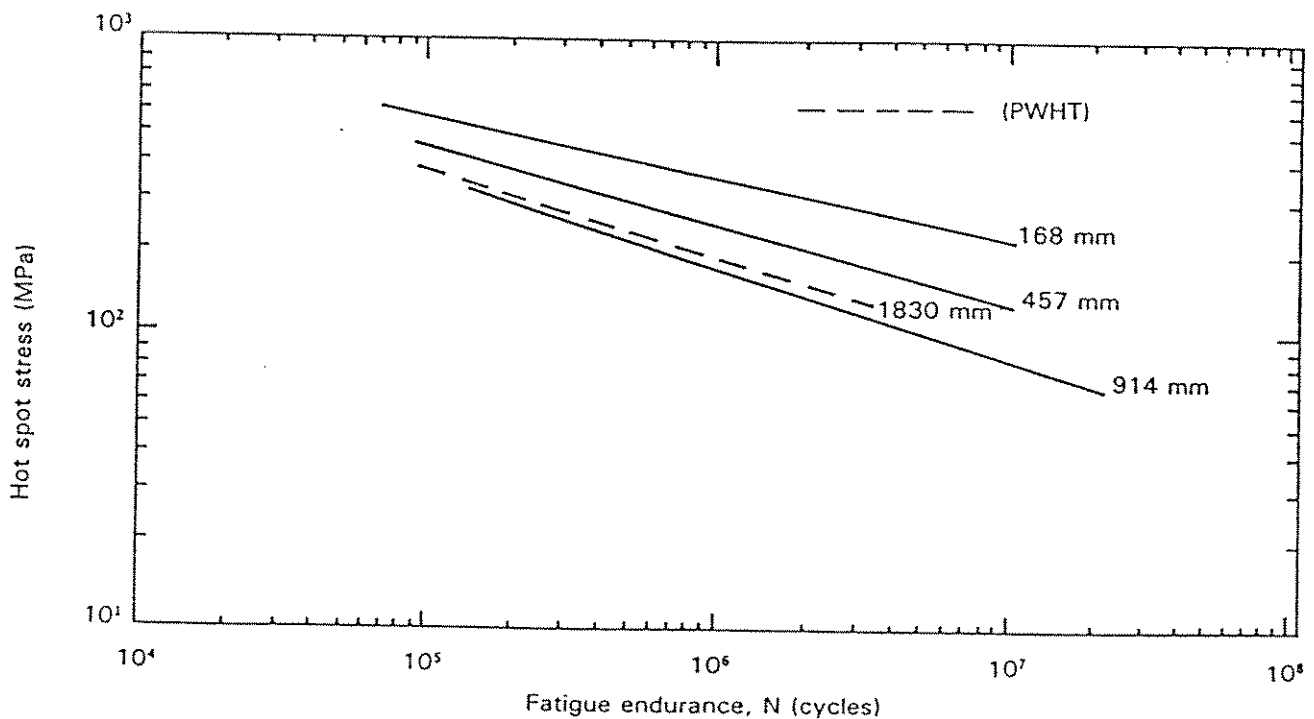


Figure 5.1 Mean S-N curves for T joint specimens, from UKOSRP I (1988)



5.1.2 Bainbridge (1985)

Bainbridge of Lloyd's Register, in an overview of North Sea joint design, noted the apparent clockwise rotation in the S-N curves, with the curves relating to thicker members having more significant slope (ie. lower value of m). see Figure 5.1. This relationship was attributed to tensile residual stresses at the weld toe which increase the rate of fatigue crack propagation and accentuate the observed size effect. Therefore, any method of reducing these residual stresses would reduce the variation between slopes on the S-N curves.

Bainbridge noted that the benefit of PWHT is dependent upon the level of the mean stress and that, in general, PWHT produces an apparent negative thickness effect. Furthermore, it was reported that most fatigue damage occurs in the low stress/high cycle region, where PWHT is likely to produce a significant improvement in joint life. Bainbridge concluded that the benefit of PWHT is at least of the same order as that imposed by a thickness correction. Therefore, in the Lloyd's Register rules there is no provision for scale effect on the basis that all joints are post weld heat treated.

5.1.3 Marshall (1983, 1993)

Marshall, formally with Shell Oil, spent many years investigating the fatigue behaviour of welded joints and acted as an advisor to API and AWS Code committees.

In 1983, Marshall considered size effects in welded joints in the light of the findings by Gurney and the test results from the UKOSRP I study. Marshall (1983) noted the differing hot-spot stress definitions employed in Europe and the USA, and re-emphasised the importance placed on weld profile control in AWS (1992). With reference to results from three cruciform joints from the UKOSRP I study (UKOSRP I 1989), Figure 5.2, Marshall also noted that there was a significant reduction in fatigue life for a larger scaled specimen (B), yet only a relatively small reduction in fatigue life for a thicker plate with the same thickness of fillet and attachment length (C) as the original specimen.

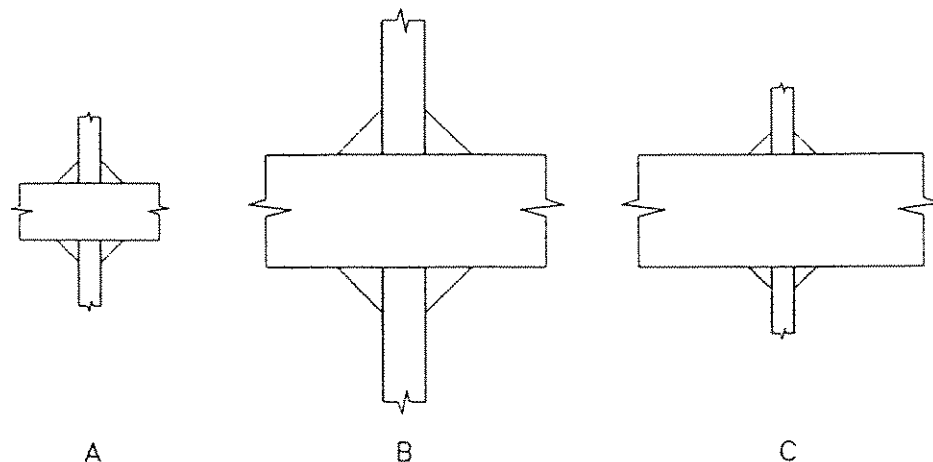


Figure 5.2 Three cruciform joints considered by Marshall (1983)



For tubular joints, Marshall likened these three specimens to small scale joint tests (A), large scale joints (B) and typical in-service joints (C), and in addition noted the uncontrolled profile in the 76mm tubular joint tests in the UKOSRP I study which would accentuate any scale effects.

In conclusion, Marshall stated that the scale effect noted in the UKOSRP study was likely to be due to both a thickness effect and to a weld profile effect.

Ten years later, Marshall (1993) described the API provisions for SCF, S-N and size-profile effects. This Code now includes a scale effect which is always a function of the brace thickness, irrespective of the location of cracking. This paper reiterates Marshall's earlier conclusions, although now with the benefit of supporting confirmation test results. Marshall also reported notch stress theory developed by Lawrence et al (1978). These curves not only show the progressively reduced fatigue performance as the notch angle increases, but illustrate a thickness effect with $n = 0$ for the ground smooth weld, $n = 0.25$ for a 10° reinforcement (typical of offshore design), up to $n = 0.40$ for a 90° notch.

5.1.4 Current views on scale effect

A consensus view that the observed scale effect is a function of more than one factor is increasing, with both Marshall (1993) and Haagenzen (1990) attributing the scale effect to three factors:

- Technological effect - caused by variations between material properties. Thicker plate tends to have: larger, coarser grain size, with more unfavourably shaped inclusions than the more heavily deformed thinner plate, leading to a lower yield strength; higher residual stresses and likelihood of pop-ins; increased risk of hydrogen cracking during fabrication; plain strain vs plane stress and lower notch toughness.
- Statistical effect - caused by the higher probability of having a significant initial defect in the larger volume of stressed material, cf. castings, forgings, etc.
- Geometrical effect - caused by the stress gradient at the notch root affecting crack initiation as well as crack propagation. The stress gradient in the thinner part is steeper and a surface grain experiences a lower average strain than a grain at the surface of a thick part.

With regard to design, at present a simple scale exponent is applied to the ratio of actual thickness to nominal thickness, although the scale exponent and relevant thickness is dependent upon the S-N curve favoured.

Maddox (1991a) of TWI has suggested a scale correction factor based on the attachment toe-to-toe weld leg length for plate connections, although the paucity of data from tubular tests prevented extending this theory to tubular joints. Maddox



suggests that the scale exponent would be reduced using this method, although Haagensen (1990) argued that the relatively large weld on small scale plate specimens must increase rather than decrease the scale exponent.

Haagensen (1990) suggested that the scale exponent for plate connections should be a function of the attachment thickness to plate thickness ratio (r), the weld profile and the resulting SCF; with lower r and smoother weld profiles giving lower scale exponents. In addition, a relationship between the mode of loading and the scale exponent is suggested, such that the largest exponent will occur under bending, a lower exponent under tensile axial loading and a small exponent for compressive axial loading.

Cole (1993), in a study of thickness effect and the effect of cathodic protection in seawater, noted that the thickness effect should be varied according to the nature of the connection with lower thickness exponents for weld-improved joints. Exponents of $n = 0.25$ and 0.17 were measured on X joints in-air and in-seawater with CP respectively, while significantly higher exponents were measured on similarly tested T-butt joints ($n = 0.35$ and $n = 0.48$). Therefore, the authors concluded that thickness exponents from plate data could not be used to determine behaviour of tubular connections. Furthermore, Cole reiterated the more significant thickness effect at lower stress ranges observed in the UKOSRP I data (Figure 5.1).

5.1.5 Summary

Tests on both plate connections and tubular connections have shown an increase in life for thinner sections. Initially it was argued that this effect was purely due to the thickness of the section, although it is now generally agreed that the weld attachment and profile and the post fabrication treatment of the joint (PWHT, grinding, etc) change the significance of this 'thickness' effect on fatigue life. To avoid confusion in this Guide this effect is referred to as a scale effect and as such encompasses the technological, statistical and geometrical effects specified by Marshall.

While it is not yet possible to specify the contribution of each effect there is a reasonable consensus that:

- a scale exponent of $n = 0.1 - 0.2$ can be justified on joints with smooth ground profiles or castings,
- a scale exponent of $n = 0.2 - 0.3$ appears reasonable for typical tubular joints with controlled weld profiles as seen offshore,
- a scale exponent of $n = 0.3 - 0.4$ may be required on plate specimens or for tubular joints with uncontrolled weld profiles,
- the scale effects may reduce in joints at high stress ranges, with PWHT applied, with large weld attachments and possibly in seawater with adequate cathodic protection.



5.2 Joint Configuration

The relationship between the hot-spot stress and joint fatigue life should be independent of the joint configuration if all other parameters are equal.

In the basecase database, 31 of the 36 data points (86%) have been obtained from simple T joints, while 120 of the 157 data points (76%) in the full in-air database have been obtained from simple T joints.

In Table 5.1 below, the measured fatigue life of each configuration type (N3) is compared to that predicted using the basecase S-N equation (N3') for the full in-air database.

Configuration	No. joints	$\log(N3)/\log(N3')$
T	120	1.07
X	16	0.97
K	7	1.07
KT	2	0.97
H	4	0.95
TT	8	0.88
TOTAL	157	1.04

Note: In this Guide, H joints are defined as two chord members separated by a single brace and TT joints are defined as two parallel braces on a single chord. All joint definitions are fully described in Chapter 1.

Table 5.1 Goodness of fit of basecase S-N curve for each joint configuration type

There is a slight difference between the fatigue data from T and K joints and from X, KT or H joints, although there are too few data and too many other parameters to draw any firm conclusions about the effect of joint configuration. However, the joint lives from the eight TT joints tested by SINTEF/TWI (Tubby 1994) are significantly less than anticipated.

This trend was noted by Tubby (1994) who reported:

- i) The joint geometry adopted in this study had:
 - a relatively uniform hot-spot stress field at the inboard crown positions extending to $\pm 45^\circ$ of the centre line
 - a lower hot-spot stress at the outboard crowns
 - a relatively high membrane stress component in the chord wall at the hot-spot (DOB = 0.65 to 0.69 compared with about 0.7 to 0.8 for other specimen geometries).



- ii) The fatigue strength of the joints under constant amplitude loading in-air was low by comparison with the expected mean S-N curve and was close to the current T design S-N curve for 32mm.
- iii) The high membrane stress component (low DOB) at the hot-spot contributed to the low fatigue strength in-air, although further assessment of DOBs for joint geometries in the database on which the design curve is based is required to quantify this. These results call into question the current fatigue design philosophy for tubular joints, ie. the use of a single stress parameter.

These TT joint test results are considered further in Section 5.3.3 where chord length effects are considered.

5.3 Chord Size and Dimensions

5.3.1 Chord thickness (T)

The possible requirement for a factor to be incorporated in the S-N curves to account for thickness effect is outlined at the beginning of this Section. For the more common chordside failures, HSE and DnV specify that the scale effect factor should be based on the chord thickness.

For the full in-air database, chord thickness data has been recorded for $T = 5.1\text{mm} - 76.7\text{mm}$. It can be seen in Figure 5.3 that joints with $T < 30\text{mm}$ exhibit significantly longer life (measured life $N_3 >$ basecase predicted life N_3') than data from joints with $T > 30\text{mm}$. In this initial review where other potentially significant parameters are included in the database, there does not appear to be a significant change in fatigue life with an increase in chord thickness above 30mm. Although it should be noted that there are few data with $T > 32\text{mm}$ and that other factors may affect joint fatigue life.

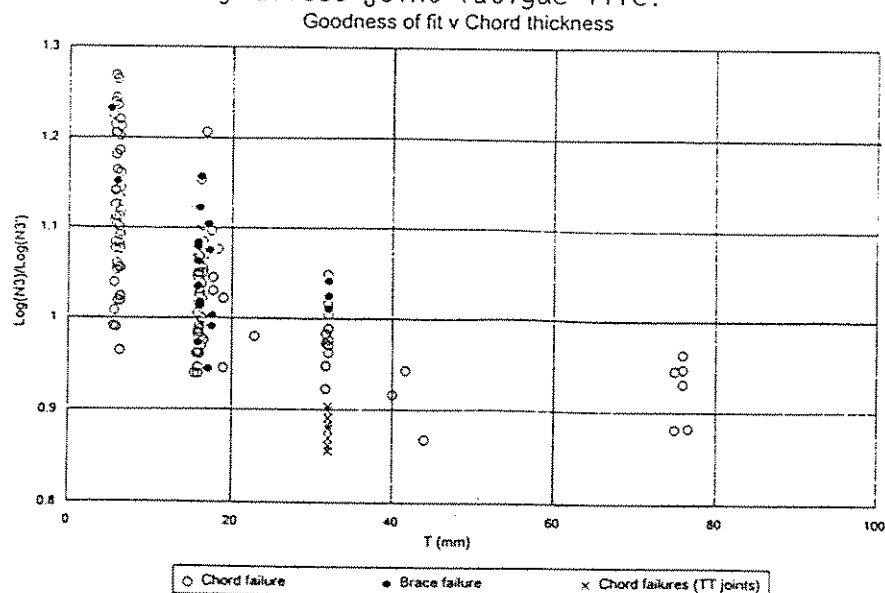


Figure 5.3 Goodness of fit of basecase S-N curve with variation in chord thickness



5.3.2 Chord diameter (D) and radius/thickness ratio (γ)

Chord diameter values in the full database have been recorded in the range $D = 168.3\text{mm} - 1830.0\text{mm}$. As stated above, the variation in joint fatigue life with scale is generally attributed to, and estimated by, variations in member thickness. However, for the database compiled in this Guide there is a strong correlation ($\rho = 0.96$) between the chord thickness and the chord diameter. Therefore, a very similar distribution relating the goodness of fit of the basecase S-N relationship is obtained for chord diameter and chord thickness.

In accordance with the distribution for the chord thickness, in this initial appraisal there does not appear to be a significant reduction in life for joints with $D > 900\text{mm}$.

Chord radius to thickness values (γ) have been recorded in the range $\gamma = 8.3 - 24.1$, although nearly 90% of simple joint in-air data has been obtained from joints with $\gamma = 13.0 - 15.5$. Therefore, it is very difficult to draw conclusions about the effect of the γ parameter. However, for the limited data at the extremes of the γ range there does not appear to be any notable trend.

5.3.3 Chord length (L_s) and length/diameter ratio (α)

Recent investigations identified the importance of the chord length and chord end fixity in determining the SCF (Efthymiou and Durkin 1985) and ultimate static strength (Bolt 1992) of tubular joints. The importance of chord length and end fixity becomes increasingly significant as the distance between the brace and the chord end diaphragms reduces. The reduction in this distance leads to reduced SCFs at saddle locations and increases strength for most failure modes. However, in current guidance, chord length is not considered to affect fatigue crack growth rate or joint fatigue life.

Comparing the goodness of fit of the basecase S-N curve against $\alpha = 2L_s/D$, where L_s is the physical specimen length, shows a trend for fatigue life to reduce as α reduces. Although it must be remembered that again there is some degree of correlation between α and chord thickness (and therefore chord diameter), $\rho = -0.66$, ie. large scale, thick chords tend to be relatively short in length.

In one series of tests on TT joints performed by SINTEF/TWI (Tubby 1994), the distance between the braces and the ends of the chord specimen may have been one parameter leading to the relatively low joint fatigue life, as described in Section 5.2. The specimens tested were 4000mm in length ($\alpha = 8.75$), although there was only 534.5mm between the end of the specimen and the nearest brace crown.

In Figure 5.4, the relationship between the measured and estimated fatigue life is considered in relation to $\alpha' = 2L_s'/D$, where L_s' is twice the distance from the end of the specimen to the mid-point of the nearest brace. It can be seen that



performing a comparison in this manner indicates a clear trend between the goodness of fit of the basecase S-N relationship and the modified chord length to diameter ratio. However, it should be reemphasised that the chord 'length', by whichever definition, is correlated to the chord thickness to some degree.

Goodness of fit v Alpha' ($=2L_s/D$)

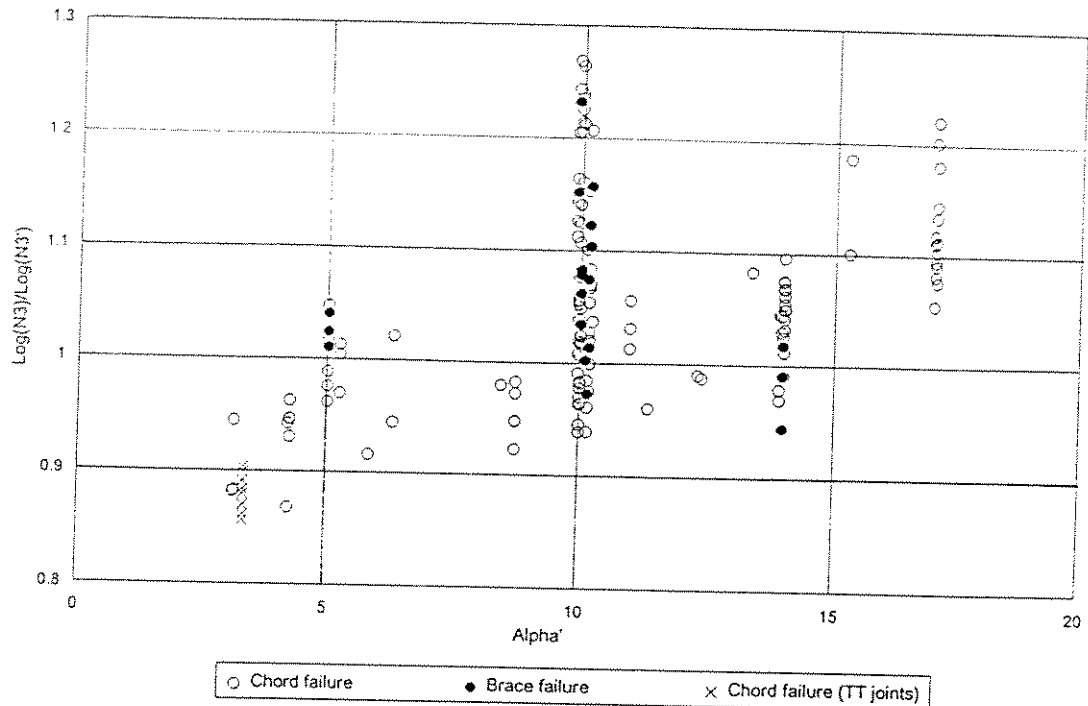


Figure 5.4 Goodness of fit of basecase S-N curve with variation in $\alpha' = 2L_s/D$

The potential for fatigue life to be influenced by the distance between the chord ends and brace member may be partially explained by the fracture mechanics FE analysis of these TT joint configurations, reported by Berge (1994).

Tubular TT joints under in-plane bending were modelled with two methods of analysis employed: 3-D shell analysis with Y compliance calibration based on line spring model computations, and a simplified two-dimensional analysis with a load shedding model, characterised by a degree of bending (DOB) parameter.

The following conclusions were obtained:

- DOB may significantly affect the fatigue strength of a tubular joint. For a given hot-spot stress, the fatigue life may vary considerably, due to different through thickness distributions of stress. The hot-spot stress approach may in some cases lead to unconservative predictions of fatigue life.
- DOB effects may be understood as effects of load shedding. Bending stresses in the hot-spot region are more strongly affected by the presence of a crack relative to membrane stresses.



- With parametric equations for DOB becoming available, the effect may be implemented in design procedures for tubular joints.

While the DOB for these joints differ from typical tubular joint configurations, it would have been a useful exercise to vary the distance between the chord end restraints and the loaded braces to see if the reduced DOB was a function of either joint configuration or boundary conditions.

5.3.4 Chord end condition

In accordance with FE appraisals of chord end length on SCF by Efthymiou and Durkin (1985) and static strength by Bolt (1992), the influence of tubular joint chord end fixity was considered. If the chord end is fully fixed then a lower SCF at all locations and a larger ultimate static strength would be anticipated for relatively short chord lengths ($\alpha < 12$).

In the basecase database, only two data points are based on tests with pinned chord ends and therefore no conclusions can be made regarding end fixity.

In the full in-air database, ten results are based on pinned ends, 128 results are based on fully fixed chord ends and the remaining nineteen results have either open chord ends (X joints under balanced axial load) or are unspecified. The average measured to predicted fatigue life ratio is 1.063 for the fixed chord ends, yet 0.982 for the pinned chord ends. This gives a statistically significant difference between the mean values of fatigue life and suggests that the pinned chord end condition will lead to a lower fatigue life. Once again there is a significant degree of correlation between the end fixity and joint geometry which makes it difficult to isolate causes and effect. Furthermore, given the findings of Section 5.3.3 on chord length, it would be expected that if short chord lengths do detrimentally affect joint life then it would be the fixed rather than the pinned end condition that would reduce joint fatigue life.

5.4 Brace Size and Dimensions

5.4.1 Brace thickness (t) and brace/chord thickness ratio (τ)

API and AWS now specify a scale effect, with this scale effect dependent upon the brace thickness, irrespective of the location of the hot-spot.

In Figure 5.5, the full in-air database goodness of fit is expressed in terms of the brace thickness, in the range $t = 3.2\text{mm} - 43.5\text{mm}$. In a similar manner to the chord thickness, there is a reduction in life with brace thickness, with most recorded failures occurring on the chordside of the joint. If the relatively early joint failures noted in the SINTEF/TWI test programme (Tubby 1994) are ignored ($t = 16\text{mm}$) then there is a trend for fatigue life to reduce as brace thickness increases, even for relatively thick joints.



In Figure 5.6 the goodness of fit of the measured to predicted joint fatigue life is related to the ratio of the brace to chord thickness (τ). It can be seen that there is a wide coverage of the τ range, with τ values recorded from $\tau = 0.25 - 1.14$. Across the range of τ there does not appear to be any significant trend for fatigue life to either increase or decrease with variations in τ .

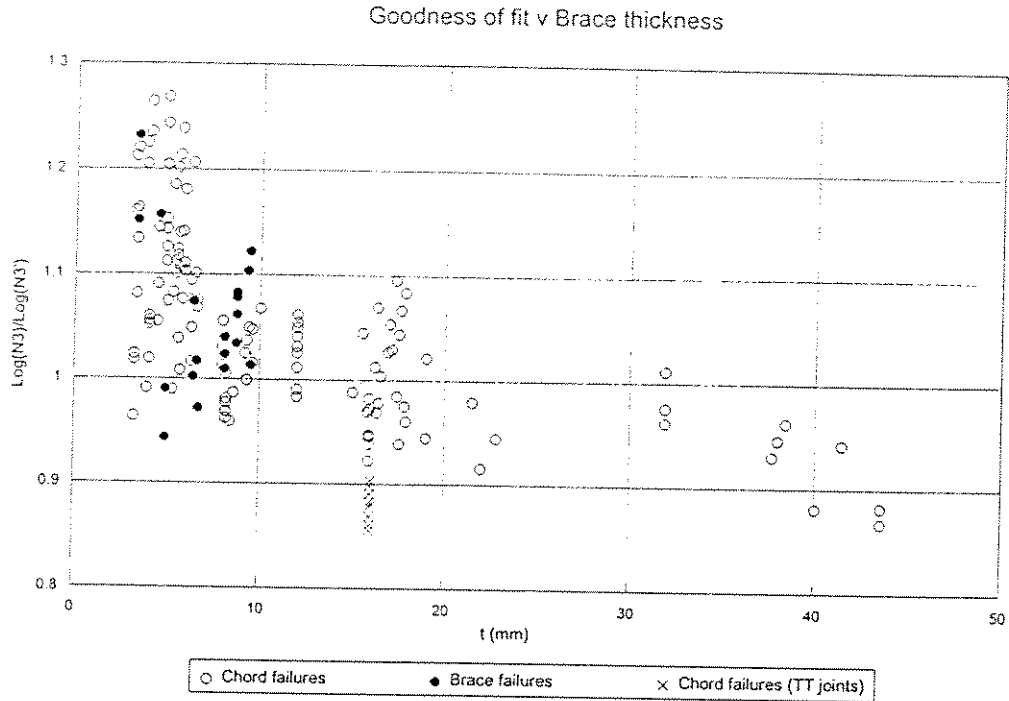


Figure 5.5 Goodness of fit of basecase S-N curve with variation in brace thickness

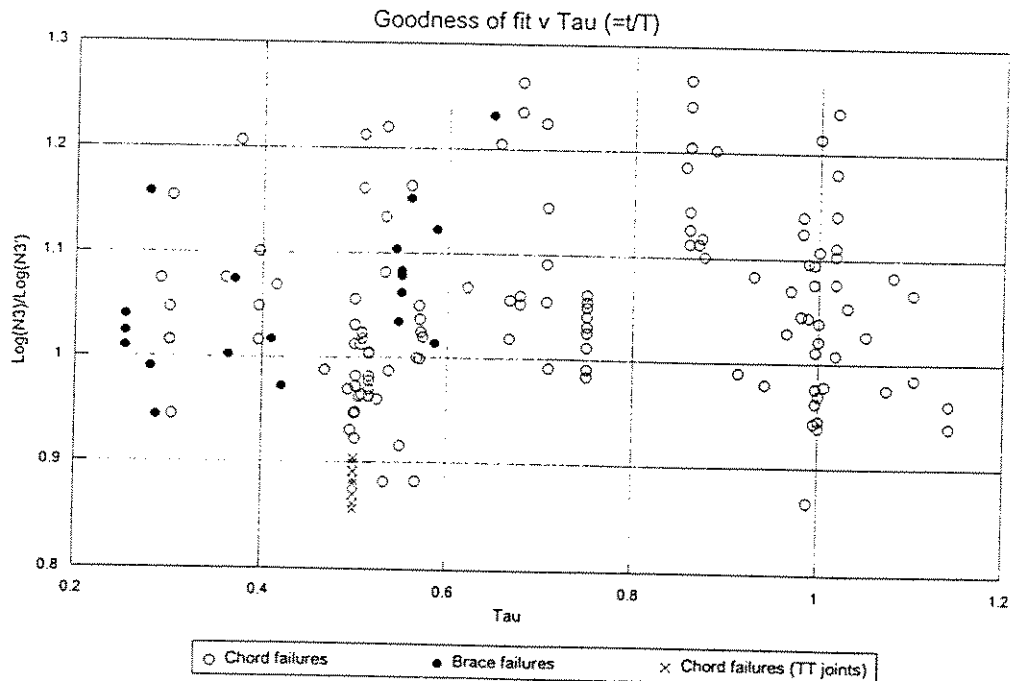


Figure 5.6 Goodness of fit of basecase S-N curve with variation in τ



5.4.2 Brace diameter (d) and brace/chord diameter ratio (β)

In the full in-air database, brace diameter (d) is recorded in the range $d = 88.9\text{mm} - 914.0\text{mm}$. In accordance with the findings for the relationship between the chord thickness and chord diameter, there is a strong correlation between the brace thickness and brace diameter, $\rho = 0.85$. Therefore, again there is a strong similarity between the brace diameter and the brace thickness shown in Figure 5.5.

The ratio of brace to chord diameter, β , has been recorded over a wide range with $\beta = 0.24 - 1.01$. However, most data has been obtained from joints with $\beta = 0.25$, $\beta = 0.50 - 0.55$ and $\beta = 1.00$. There is no significant variation of the goodness of fit of the ratio of measured to predicted fatigue life for variations in β .

Due to the more complex geometry of $\beta = 1.0$ joints at the saddle, there is often an increased scatter associated with these joints when the joint hot-spot SCF or strength is considered. However, an initial assessment of the $\beta = 1.0$ joints in the basecase database does not indicate any increased uncertainty in the measured fatigue life of $\beta = 1.0$ joints. Although, the estimated fatigue life of $\beta = 1.0$ joints is likely to exhibit more scatter due to the relatively poor estimate of SCFs in $\beta = 1.0$ joints.

5.4.3 Brace inclination (θ)

In the full in-air database, 94% of critical brace connections are perpendicular to the chord (ie. $\theta = 90^\circ$). In these 90° joints the maximum principal stress tends to lie perpendicular to the weld fillet. On joints with increasing angle of inclination, the maximum principal stress may be $30^\circ - 40^\circ$ away from the perpendicular to the weld fillet. The direction of maximum principal stress may have an effect on the joint fatigue life, although there is insufficient data to investigate this potential effect further.

5.4.4 Brace separation (ζ)

Of the nine K/KT joints in the full in-air database, the brace separation (ζ) lies in the narrow range $\zeta = 0.11$ to 0.13 , therefore, no conclusions can be drawn on the effect of varying the gap between braces. However, the effect of brace separation is investigated further in Section 10.1 where the fatigue behaviour of overlapping braces is considered.

5.5 Weld Size and Profile

TWI have recently completed a comprehensive study on the effect of weld profile and attachment leg length on fatigue life (Maddox 1991b). This study investigated five different weld profiles from 'poor' through 'normal' to 'improved' to meet the AWS specification (in 1984). A sixth test series involved welds that had been toe ground.



5.5.1 Attachment length (l)

Maddox (1991a) suggested that a better scale effect factor for plate connections may be obtained by taking the ratio of the toe-to-toe weld attachment leg length to a nominal length, rather than considering the brace or chord member thickness.

In the TWI study of tubular T joints (Maddox 1991b) it was concluded that increasing the weld leg length moved the weld toe away from the theoretical point of maximum stress into a lower stress region and, therefore, the reduced SCF on the chord side led to improved fatigue life.

In the S-N databases developed for this Guide the weld toe-to-toe attachment has been recorded for the location of failure in those cases that this value has been reported. In most cases, this value has been obtained by measuring the attachment length and chord thickness off weld profile plots and scaling the attachment length accordingly. Although the values reported for the attachment length at the failure location are only approximate it is possible to investigate possible trends.

The full in-air database has recorded attachment thicknesses, in the range $l = 9\text{mm} - 100\text{mm}$. In a similar manner to the chord and brace thicknesses, there is trend for reduced life with increase thickness (or length) for a given stress range. However, the trend is less marked for this attachment length, with only attachments $< 20\text{mm}$ showing a clear extension in life above the basecase prediction. Again there is a significant correlation between chord thickness and attachment thickness.

In Figure 5.7 the goodness of fit of the measured to predicted joint fatigue life is related to the non-dimensional ratio of attachment length to chord thickness (l/T). It can be seen that there is a wide range of l/T values, with l/T varying between $0.44 - 6.17$. Across the range of l/T there does not appear to be any consistent trend for variation in fatigue life, although measured life generally exceeds the basecase predicted life for attachments that are two to four times the chord thickness.

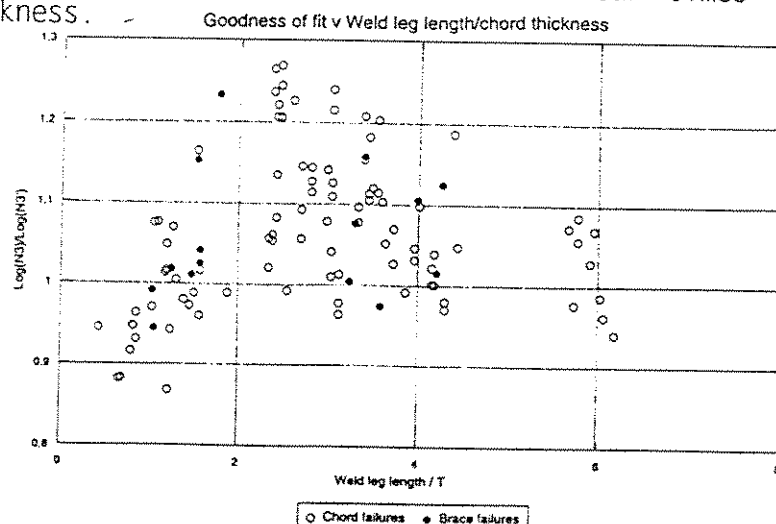


Figure 5.7 Goodness of fit of basecase S-N curve with variation in attachment thickness to chord thickness ratio (l/T)



5.5.2 Weld profile

In API guidance (API 1993), the weld profile is considered to be a significant factor in fatigue life estimation. The X curve is applicable for welds with profile control while the X' curve is specified for welds without profile control but conforming to the basic standard flat profile (AWS 1992). The UK DEn were also concerned about weld profile effects in 1984 with an appraisal of the ECSC database (Dn 1984b). In this document it was noted that the French joints tested (Lieurade 1981a, 1981b) and most of the Dutch joints tested (Dijkstra and de Back 1981) had poor weld profiles.

In the S-N database, the weld profile has been recorded for most specimens or test series. The weld leg length was measured as stated in Section 5.5.1, along with a subjective classification of the weld as either 'concave', 'flat', 'convex' or 'poor'. These are illustrated in Figure 5.8. The 'poor' classification covers welds that have particularly sharp notches at the weld toe. Furthermore, the weld angle was recorded on both the chordside and braceside at the failure location as illustrated in Figure 5.8. It should be noted that in many cases only one 'typical' profile was reported and consequently, in these cases it was assumed that this profile was applicable to all joints in the series that failed at the same location.

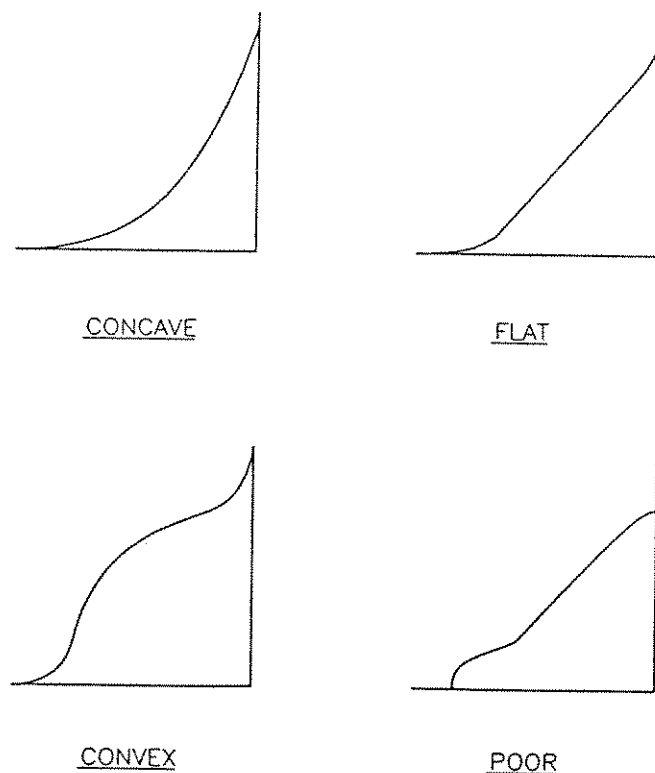


Figure 5.8 Weld profile classification

Welds with angles of 60° or less at the failure location (chordside or braceside as applicable) and having concave or flat profile were classified as 'controlled', while welds in excess of 60° or having a convex or poor profile were classed as 'uncontrolled'.



In the full initially screened database 103 joints were classified as controlled and 46 joints as uncontrolled. The SINTEF/TWI joints were excluded in this study (Tubby 1994). Of the 46 uncontrolled weld specimens, eight had concave weld profile, 31 had a poor profile and seven had weld angles in excess of 60°.

For the full database points that meet the initial screening criteria it was found that on average the uncontrolled weld data had slightly lower lives than the controlled weld data. This was in contradiction to the findings of Maddox (1991b) who concluded that apart from the beneficial effect of any increase in weld leg length, control of overall weld shape and weld surface finish according to the AWS D1.1 specification (AWS 1992) for improved weld profile had no significant influence on the fatigue strength of tubular joints.

In Section 7 of this Guide, the database was further screened based on the findings of this Section and Section 6. Following this more rigorous screening, it was found that there was no significant difference in fatigue life due to weld profile, although there was significantly more scatter in the data from joints with poor weld profiles.

5.6 Failure Location

There is currently an inconsistency between the current Codes of Practice in the way that the scale effect factor is determined. The European Codes base this factor on the thickness of the member under consideration, (ie. chord thickness for chordside life and brace thickness for braceside life), while the American Codes always relate the life to the brace member thickness. In Figure 5.9, the ratio of the maximum brace stress to the maximum chord stress is plotted against the brace thickness to chord thickness ratio (τ), with the failure location(s) specified.

Following the American Codes, it would be expected that once the braceside stress (σ_b) exceeds the chordside stress (σ_c), failure would occur on the brace. There are 36 joints where $\sigma_b > \sigma_c$, 55% chord failures, 36% brace failures, 6% weld failures and 3% both chord and brace failures. For the 67 joints with $\sigma_b < \sigma_c$, there are 97% chord or weld failures and 3% brace (or brace and chord) failures. (nb. there are 54 joints where the stress on the member that did not fail was not reported).

In the European Codes this relationship is more complex due to the fact that the brace member is generally thinner than the chord and therefore a larger stress is required for the brace to fail. If a scale exponent of $n = 0.25$ is defined, then on a joint with $\tau = 0.5$ the braceside stress will need to be at least $(0.5)^{(-0.25)} = 19\%$ larger than the chordside stress to yield a braceside failure. This is illustrated in Figure 5.9 by the solid curve reducing from 1.5 at $\tau = 0.2$ to 1.0 at $\tau = 1.0$. It can be seen that while some chord failures around $\tau = 0.5$ would be predicted there are several braceside failures at $\tau < 0.4$ which are unexpected.



Therefore, neither the American nor the European approach appears to fully define the location of failure satisfactorily. A possible explanation for the trends noted could lie in the differing weld profiles at the chord weld toe and brace weld toe, as discussed in Section 5.5. Most of the test specimens have greater weld angles and shorter attachment lengths at the chordside weld toe than the braceside weld toe, which may explain why joints with twice the stress in the brace still fail in the chord.

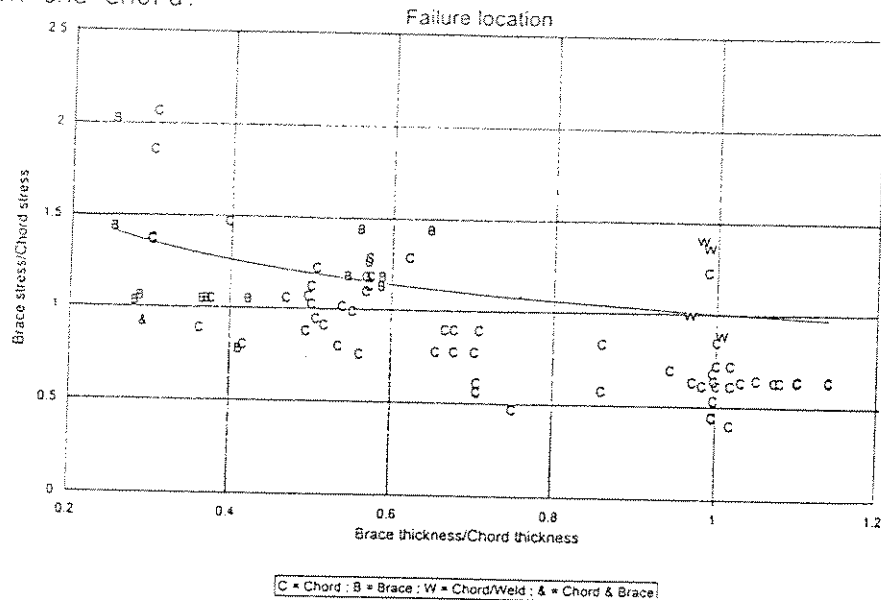


Figure 5.9 Predicted and observed failure location

5.7 Summary of Joint Geometry and Weld Effects

In this Section, an appraisal of each geometric or parametric variable has been performed with regard to fatigue life, N3. The main problem with this assessment is the significant correlation between key variables thereby making it difficult, if not impossible, to identify the variables that influence fatigue life. A summary of linear correlation (ρ) between the basic variables is given in Table 5.2.

	T	D	Ls	t	d	γ	α	r	β
T	X	0.96	0.57	0.84	0.77	-0.45	-0.67	-0.33	-0.33
D	0.96	X	0.68	0.81	0.80	-0.22	-0.68	-0.34	-0.36
Ls	0.57	0.68	X	0.48	0.60	-0.04	-0.12	-0.32	-0.29
t	0.84	0.81	0.48	X	0.85	-0.34	-0.58	0.14	-0.06
d	0.77	0.80	0.60	0.85	X	-0.19	-0.53	0.04	0.20
γ	-0.45	-0.22	-0.04	-0.34	-0.19	X	0.10	0.22	0.07
α	-0.67	-0.68	-0.12	-0.58	-0.53	0.10	X	0.24	0.22
r	-0.33	-0.34	-0.32	0.14	0.04	0.22	0.24	X	0.62
β	-0.33	-0.36	-0.29	-0.06	0.20	0.07	0.22	0.62	X

Table 5.2 Correlation coefficients for main joint parameters



From Table 5.2 it can be seen that the five relationships with the highest degree of linear correlation are:

1. D : T ($\rho = 0.96$)
2. d : t ($\rho = 0.85$)
3. T : t ($\rho = 0.84$)
4. D : t ($\rho = 0.81$)
5. D : d ($\rho = 0.80$)

Following this initial appraisal of the in-air database for simple joints, it is clear that there is a scale effect associated with tubular joints. This effect is probably due to a number of causes, with the ability to separate the influence of each individual cause still only a long term objective. A reduction in fatigue life is evident in tubular joints with large diameters, thick members and short chords, and while there is a high correlation between member thickness and diameter in particular, evidence from both fracture mechanics and plate test data suggest that it is the member thickness rather than diameter or chord length that leads to this apparent reduction in fatigue life.

It has been noted that joint configuration appears to have a small effect on fatigue life, with T and K joints tending to have slightly longer lives, on average, than X, KT and H joints, although this is probably a function of other variables in the database. However, results from TT joints tested under IPB by SINTEF/TWI exhibit significantly lower fatigue lives (Tubby 1994). FE modelling of these joints (Berge 1994) suggests that there is an untypically low DOB in these particular joint configurations. It has been further noted that joints with braces near to the chord ends tend to fail earlier than joints with braces a significant distance from the chord ends. The effect of chord length, chord end fixity and degree of bending variations need to be considered further before the results from these tests can be fully understood.

With regard to the weld fillet, it is recognised that an enlarged weld attachment leg length can reduce the SCF and therefore improve the fatigue resistance of the joint. This is due to the fact that the stress sampling points are moved away from the joint and that there is some additional local stiffening at the junction. It was found that the weld profile has little, or no, effect on fatigue life unless the weld toe is ground smooth.

Current Codes of Practice modify joint fatigue life with respect to either the brace thickness, irrespective of the failure location, or to the thickness of the member being considered. It has also been proposed that the attachment length may give a more consistent basis for applying a scale effect. In Section 7, following the final screening of the S-N database, recommendations for applying scale effects are given, mean and design S-N curve are calculated, and scale effect exponents are recommended.



6. INFLUENCE OF LOADING

In-service, tubular joints within a complex structural frame experience a loading sequence that is essentially random over the platform life; in the laboratory, most individual tests are performed under one mode of loading applied to one brace over a constant stress range at regular cyclic frequency. This simplification of the in-service condition has allowed the fatigue behaviour of simple tubular connections to be well understood and, along with simplifications in the design approach, allow the designer to safely estimate in-service joint fatigue lives.

In this Section, differences between loading modes are addressed along with variations in the load range applied to the test specimen. Load is generally applied in a constant cyclic manner, although variable amplitude loading over a wide range of irregularity functions has also been investigated. All of these loading parameters are assessed against the full screened in-air simple tubular joint database of 157 results, as presented in Section 4.3. In addition, where sufficient variation permits, the basecase database of 36 results, presented in Section 4.4, is also referenced.

6.1 Loading Mode

6.1.1 Single loading applied to brace

For most fatigue tests either axial, in-plane or out-of-plane loading is applied throughout the duration of the test. In the fatigue S-N approach, it is assumed that the fatigue life is independent of loading mode.

In Table 6.1, the ratio of the measured life (N_3) to the predicted life (N_3') is compared to the basecase database and to the full in-air database, for each loadcase. It can be seen that in both cases there is statistically no significant difference between the loading modes, although in both databases the OPB test specimens appear to have slightly longer lives.

Loadcase	Basecase database		Full database	
	No.	$\log(N_3)/\log(N_3')$	No.	$\log(N_3)/\log(N_3')$
Axial load	17	0.991	70	1.030
OPB	15	1.021	40	1.068
IPB	4	0.976	47	1.039
All loadcases	36	1.002	157	1.043

Table 6.1 Comparison of loading modes



6.1.2 Single loading applied to brace with compressive chord end loading

In the UKOSRP I project, a series of tests were performed on tubular T joints with compressive axial load of 77 N/mm² applied to the ends of the chord member (UKOSRP I 1988).

In Table 6.2, the ratio of the measured life (N3) to the predicted life (N3'), based on the basecase data, is compared to the full in-air database for test specimens both with and without compressive chord end loading. It can be seen that the fifteen joints under axial load and IPB with compressive chord end loading of 77 N/mm² have log(lives) around 10% larger than the remainder of the database, this roughly equates to a four-fold increase in life for N = 10⁶ cycles.

In reviewing the UKOSRP I data, no test reports recorded compressive chord end loading applied under the OPB loadcase (UKOSRP I 1989), although some of the summary tables in the final report do indicate this occurrence (UKOSRP I 1988). In this Guide, test reports take precedence over summary reports and so it has been assumed that no tests were performed under OPB with compressive chord end loading.

The increase in fatigue life that is noted when compressive chord end loading is applied to the specimen is probably due to the fact that cracks will not open to such an extent particularly if they run in the radial direction (eg. at the crown location). Therefore, leg nodes where the chord member is generally in compression and the predominant loadcases are axial and IPB, are likely to benefit from this effect. Conversely, although there is no supporting data, a reduction in fatigue life may be envisaged for joints where the chord member is predominantly in tension, for example the conductor framing.

Loadcase	No chord loading		Inc chord loading	
	No.	log(N3)/ log(N3')	No.	log(N3)/ log(N3')
Axial load	60	1.016	10	1.119
OPB	40	1.068	0	-
IPB	42	1.027	5	1.132
All loadcases	142	1.034	15	1.123

Table 6.2 The effect of compressive chord end loading of 77 N/mm²

6.1.3 Combined loading applied to brace

To date, most tubular joint tests have been performed under one loading mode, ie. either axial load, IPB or OPB. However, some work has been undertaken into the effect upon fatigue and fracture behaviour of applying combined or mixed mode loading.



Most of this work considers the effect of applying loading representative of in-service conditions such as the WASH Spectrum (Pook and Dover 1989), etc. with variation in both loading mode and amplitude. This type of loading is discussed further in Section 6.3.2. However, a few studies have considered varying the loadcase under constant amplitude loading.

Mshana (1992a, 1992b) in a pilot study for the Multiple Axis Loading and Environmental Testing (MALET) programme considered the so called 'crack in the wrong place' concept, where a tubular joint would be loaded under loadcase 'A' for N cycles and then under loadcase 'B' to the end of the test. This study was initiated following data reported by Rhee (1988) that suggested that cracks under multiple axes loading may grow faster than those calculated by the linear damage summation of stress ranges in different axes.

It was concluded by Mshana (1992a, 1992b) that under OPB followed by IPB and IPB followed by OPB loading, fatigue crack growth in the secondary location was consistent with single mode loading. At the primary crack location under the second loadcase, crack depth largely arrested, but the crack length did grow to some degree. Therefore, the presence of a crack away from the hot-spot location did not appear to adversely affect the joint fatigue life. However, it was noted that this conclusion should not be assumed of loading where multiple axes loading is occurring concurrently.

6.2 Constant Amplitude Loading

6.2.1 Mean and maximum load

In most tubular joint tests the specimen is tested under constant amplitude loading at stress ratios of $R = -1$ or $R = 0$, which imply that the mean stress is zero or $\sigma_{\max}/2$ respectively. The S-N approach does not account for the level of the mean stress applied since it is not considered to be significant on fatigue life for most in-service situations.

For plate connections, Maddox (1991a) notes that reduced life is associated with high stress ratios ($R > 1$). In particular, Maddox stated that for a vibration type loading with a relatively small stress range at a high mean load, significant reductions in fatigue life can occur. Such a loading would not be common on an offshore structure. For most offshore tubular joints API (1993) state that stress ratios of $R = -0.50$ to $R = -0.15$ would be typical. However, care should be taken on a connection such as that on a TLP tether where the joints are subjected to high mean tensile loads, yet relatively small stress ranges.

6.2.2 Stress ratio (R)

Most fatigue tests are performed under either full reversal loading ($R = -1$) or loading from zero to maximum load ($R = 0$). Axial load with $R = 0$ generally implies that the specimen is loaded only in tension, since the tensile loadcase tends to give



slightly lower fatigue lives due to crack opening effects.

In Table 6.3, the ratio of the measured life (N_3) to the predicted life (N_3') is compared to the basecase database and to the full in-air database, for $R = -1$ and $R \approx 0$. It can be seen that there is a tendency for the stress ratio of $R = -1$ to give fatigue lives that are slightly longer than those obtained from $R \approx 0$, although for the smaller but more controlled basecase database this difference appears negligible.

Loadcase	Stress range	Basecase database		Full database	
		No.	$\log(N_3)/\log(N_3')$	No.	$\log(N_3)/\log(N_3')$
Axial	$R = -1$	11	0.996	46	1.049
	$R \approx 0$	6	0.981	24	0.996
OPB	$R = -1$	6	1.042	6	1.042
	$R \approx 0$	9	1.008	34	1.073
IPB	$R = -1$	4	0.976	39	1.058
	$R \approx 0$	-	-	8	0.945
All loadcases	$R = -1$	21	1.005	91	1.052
	$R \approx 0$	15	0.997	66	1.029

Table 6.3 Comparison of stress range

6.2.3 Capacity limit (high stress - low cycle)

Fatigue S-N curves are generally based on data in the range $N = 10^5$ to $N = 10^7$, with the assumption that the joint is always governed by elastic response. Stresses above this elastic limit cannot be treated in the same way and it is recognised that the S-N curve has an upper limit on the linear $\log(S):\log(N)$ relationship. If the mean S-N curves for tubular joints were extrapolated back to $N = 10^0$ (= one cycle) then the estimated stresses would be around $S = 2 \times 10^4$ N/mm². Clearly, this value does not correspond to the static strength of the tubular joint, and is well in excess of possible plastic capacity.

At present, most of the Codes of Practice specify a maximum allowable stress range which acts as an upper bound to the S-N curve. The API Code (API 1993) gives an allowable stress range based on the water depth, member location, design fatigue life and stress ratio; while AWS (1992) specifies a cut-off at the static design capacity. HSE Guidance (HSE 1993) allows a maximum stress range equal to twice the material yield stress (based on $R = -1$); while neither DnV (1992), CAN/CSA (1992) nor Lloyds (1989) specify a maximum allowable hot-spot stress range. In the tubular joint S-N database there is only one joint with a life below 10^5 cycles. This joint is Specimen G1 in the UKOSRP II study (UKOSRP II 1989b) with a life of 3.85×10^4 and a hot-spot stress range of 619 N/mm², which is 76% of the $2\sigma_y$ (= 812 N/mm²) HSE maximum stress limit (nb. $R = -1$ for this joint test).



elastic limit is represented and very optimistic estimates of remaining life may be obtained.

Beyond yield, SCFs will rapidly rise and residual stresses will be introduced that may significantly change the behaviour of the joint. Therefore, in such cases the load history will affect joint behaviour, making it impossible to accurately estimate behaviour at the design stage and difficult to estimate behaviour in a nodal reassessment.

The following approach appears to be reasonably conservative yet gives the designer the ability to approximate remaining life where no alternative method currently exists. However, there is a need for some tubular joint data in this region to appraise the validity of this approach.

The true hot-spot stress elastic limit can be calculated by

$$\sigma_{\text{range}} \text{ (Elastic limit)} = \sigma_y \cdot (1-R)$$

although, in general for offshore structures, σ_y will be given by the characteristic rather than actual yield stress, and R will be largely unknown (although API (1993) suggest the stress range $-0.15 \leq R \leq -0.50$ as typical).

The review by TWI (1991a) and measurements from test specimens suggest that this hot-spot elastic limit would not be too dissimilar from that estimated at $N = 10^4$ cycles. Therefore, it is recommended that elastic fatigue design assessments can only be carried out for stress ranges with equivalent estimated lives in excess of around 10^4 cycles. For stress ranges with equivalent estimated lives below 10^4 cycles it is recommended that the S-N relationship for reassessment be based on the linear extrapolation between $S(N=10^4)$ and $S(N=1)$, see Figure 6.2.

- $S(N=10^4)$ is determined from the appropriate design S-N curve.
- $S(N=1)$ is determined from the static design capacity of the specified joint, by:

- i) Assuming $R = -0.25$ and that $P_y = 0.8P_u$, then

$$(1-R)P_y = 1.25P_y = P_u$$

where P_u is the ultimate load for the joint

and P_y is the yield load for the joint (not to be confused with the elastic limit at the hot-spot location).

- ii) If the axial mean stress level is compressive or unknown P_u is the compressive design resistance, else, if the axial mean stress level is tensile, P_u is the tensile design resistance.



For bending stresses, M_u is the design maximum allowable moment.

(See Chapter 3 for recommended static strength formulae.)

- iii) Determine nominal stress $\sigma_{nom} = P_u/A$ or $\sigma_{nom} = M_u/Z$.
- iv) Estimate the hot-spot stress range at static failure $S(N=1)$ by:

$$S(N=1) = \sigma_{nom} \cdot SCF$$

(See Chapter 4 for recommended SCF formulae)

The mean and design S-N curves for a T joint under tensile axial load with $T = 50\text{mm}$, $r = 0.5$, $\beta = 0.5$, $\gamma = 15$, $\theta = 90^\circ$ and $\sigma_y = 400\text{N/mm}^2$ are given on Figure 6.2. The static strength is based on the recommendations of the DEn background document (DEn 1989) as described in Chapter 3, and the SCF is based on the Efthymiou equations as proposed in Chapter 4. The S-N curve is the basecase curve proposed in Section 4.4.

High stress - Low cycle fatigue

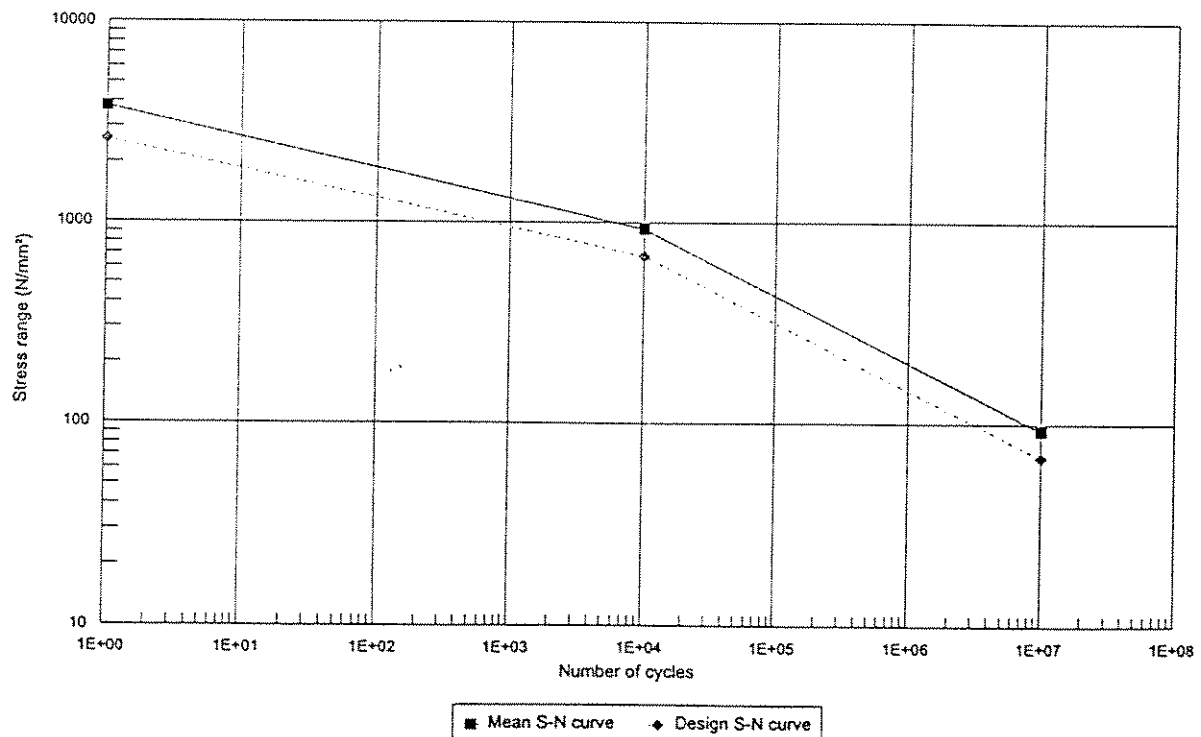


Figure 6.2 Example of mean and design S-N curves ($N < 10^7$) for the reassessment of a T joint



6.2.4 Endurance limit (low stress - high cycle)

In practice, the S-N curves under constant amplitude (CA) loading cut-off at an endurance limit S_o , which for all joint classes in-air, corresponds around to $N = 10^7$ cycles (Maddox 1991a).

Maddox (1991a) further states that:

'In cumulative damage calculations using Miner's rule stress ranges below the constant amplitude fatigue limit S_o , are assumed to be non-damaging. However in practice they become damaging as crack growth occurs under higher stress ranges in the spectrum. The omission of the damaging effect of these low stresses can lead to serious underestimates of resulting fatigue life, as there are many practical load spectra in which the majority of cycles produce relatively low stresses. Possible ways of dealing with this problem are as follows:

- a) The simplest approach is to assume that there is no fatigue limit and to extend the S-N curve downwards ad infinitum. Depending upon the stress spectrum this may be practical, but often the damaging effect of low stresses is excessively overestimated.*
- b) Independently of the design rules, fracture mechanics could be used to calculate the life on the basis that stresses will be damaging if the corresponding stress intensity factor range, ΔK exceeds the threshold value.*
- c) Use a modified S-N curve at low stress range which, when used with Miner's rule, predicts the same fatigue damage as b). For joints in air it has been found that extrapolation of the S-N curve below S_o (that is beyond 10^7 cycles) with a slope of $m+2$ would be suitable for a wide range of spectra [eg. as employed by the HSE, DnV and Canadian codes]. Alternatively, the slope could be extrapolated at the same slope to a lower effective fatigue limit, S'_o , corresponding to an endurance of 2×10^7 cycles [similar to the approach in API and AWS].'*

In Figure 6.3, the 'runners' from the UKOSRP I (1989) project (generally at 2×10^7 cycles) with $T = 32\text{mm}$, are compared to the remainder of the in-air database under CA loading.

It would be expected that under CA loading these runners would, on the whole, tend to fall below a given stress range. However, in nearly all cases, these data have end-of-test lives well in excess of other data which failed at similar stress ranges. This pattern is repeated for other chord thicknesses and, therefore, little evidence of a strict endurance limit for tubular joints under CA loading can be obtained from this data.

To resolve the problem of low stress variable amplitude loading, several authors have employed fracture mechanics models calibrated against the few plate data at long lives ($> 10^7$ cycles). Mohr (1995) reports the results of work by Tilly and



Nunn which considered tension loaded longitudinal attachment plates of thicknesses less than those typical of offshore structures. Their conclusion that a change of slope from m to $m+2$ at high endurance should be introduced to account for variable amplitude loading was widely adopted in international fatigue standards. Mohr (1995) reviewed the work of several authors and developed a new variable amplitude fatigue modelling program.

The program gives estimates of fatigue life including effects of weld toe geometry, plate thickness, distribution of stress ranges and sequence of stress ranges, for transverse welded plate attachments. The program assumes that all cracks are initiated by an initial cycle of the largest stress range and follows the propagation of each crack using fracture mechanics.

Mohr (1995) considered a variety of transverse attachments with differing thickness, width and weld size under tension loading, bending loading and combined tension and bending to simulate a typical tubular joint degree of bending of 0.82 with local shedding effects. The preliminary results are given in Table 6.4 for the HSE T' S-N curve with slope of $m=3$, $m=4$ and $m=5$ beyond 10^7 cycles.

Plate thickness	Damage summation		
	$m=3$	$m=4$	$m=5$
Tension load			
10mm	1.78	-	1.17
25mm	1.61	1.14	0.96
50mm	1.14	0.98	0.87
100mm	1.09	0.96	0.88
Bending load			
25mm	1.37	0.94	0.70
50mm	1.11	0.92	0.80
Combined loading (DOB = 0.82)			
25mm COLAS (cf. N Sea)	1.42	0.98	0.76
25mm Wirsching (cf. GoM)	1.15	0.97	0.87

Table 6.4 Comparison of Miner's damage summation for $m = 3, 4$ and 5 beyond $N = 10^7$ cycles

It can be seen in Table 6.4 that the change of slope from $m = 3$ to $m = 5$ at $N = 10^7$ cycles appears reasonable for tension loaded joints with $T \leq 25\text{mm}$. However in all other cases considered, particularly those more equivalent to tubular joints, a more rigorous S-N curve with a change of slope from $m = 3$ to $m = 4$ at $N = 10^7$ cycles appears necessary.



Therefore, this study shows consistency with the current basis for the change of slope employed in the T-S-N curve (ie. Tilly and Nunn tension plate data), but importantly highlights the limitations in this data for more typical loading and member thickness.

Further consideration of the endurance limit and behaviour of joints at low stress is dealt with consideration of variable amplitude loading and Miner's rule in Section 6.3.

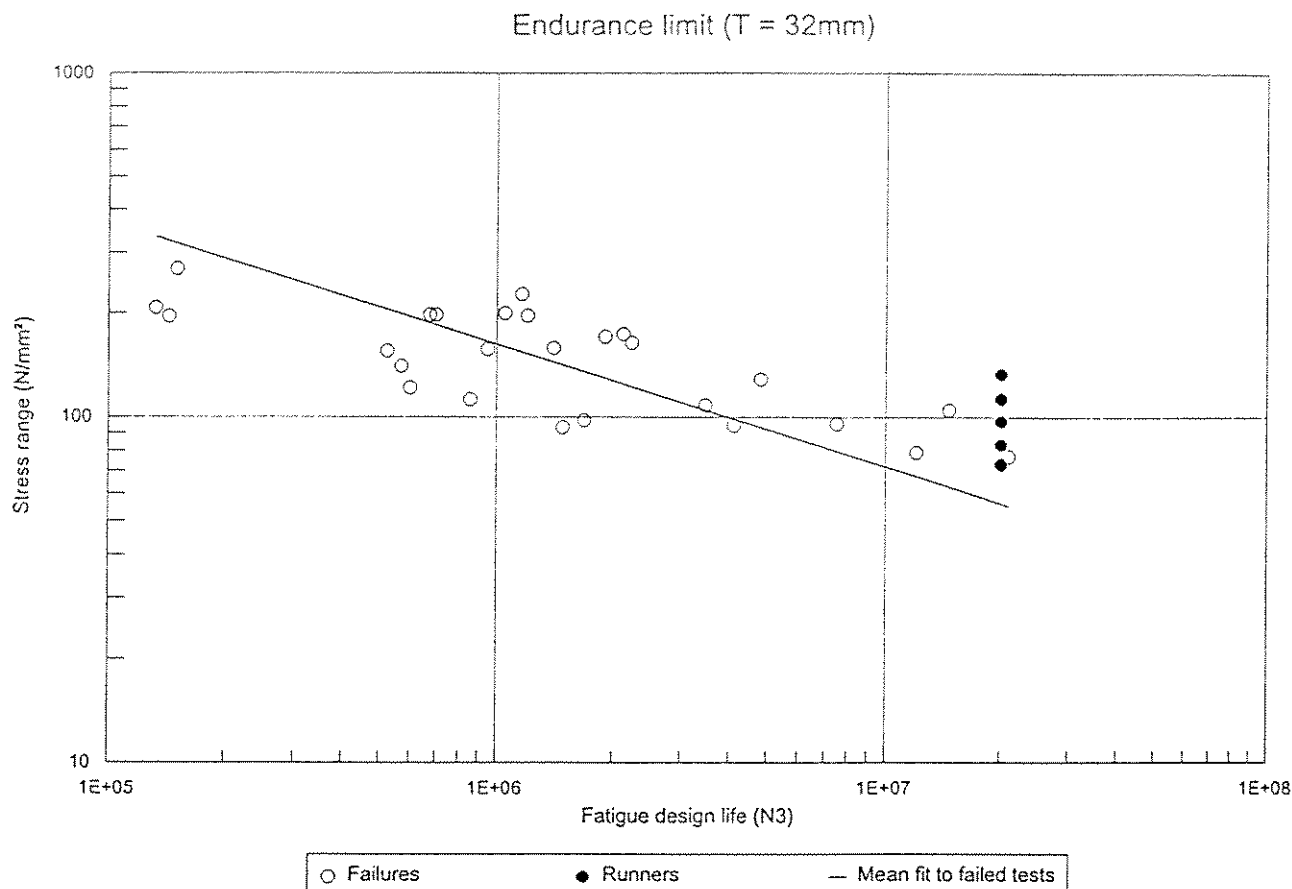


Figure 6.3 Comparison of failed and unfailed specimens with T = 32mm

6.2.5 Cyclic frequency

In UKOSRP I, all in-air plate and tubular joint tests were carried out at the loading frequencies between 0.5-15.0 Hz. It was reported that there was no influence on the fatigue life of variations in loading frequency (UKOSRP I 1988).

In Figure 6.4, the goodness of fit of the base case S-N curve to the test data is plotted against the average load frequency reported. Although there is some trend suggesting enhanced life with increased loading frequency it should be noted that the four low frequency test specimens all have T = 76mm while the highest frequency tests have T = 6mm. Therefore, once again there appears a strong correlation between member size and other variables, in this case loading frequency.



In seawater under free corrosion the loading frequency was varied between 0.01 - 10.0 Hz ($R = 0.2$ and $R = 0.5$). It was found that the rate of growth of cracks decreased as the loading frequency increased. At the limits of loading frequency there appeared to be a 'saturation' in this effect, while at intermediate frequency the crack propagation rate could vary by a factor of up to four with each factor of ten change in loading frequency.

A similar effect was noted for initial tests in-seawater with CP and consequently all subsequent tests in seawater were loaded at 0.1 - 0.2 Hz. This effect was also reported by Maahn (1981) for a series of plate tests in-seawater with CP.

It was explained that the most likely explanation for the effect of frequency on corrosion fatigue is the time dependent nature of the various electrochemical and physical processes which can occur under corrosion and corrosion protection.

Therefore, it is recommended that all tests in seawater be performed at realistic loading frequencies, ie. 0.1 - 0.2 Hz.

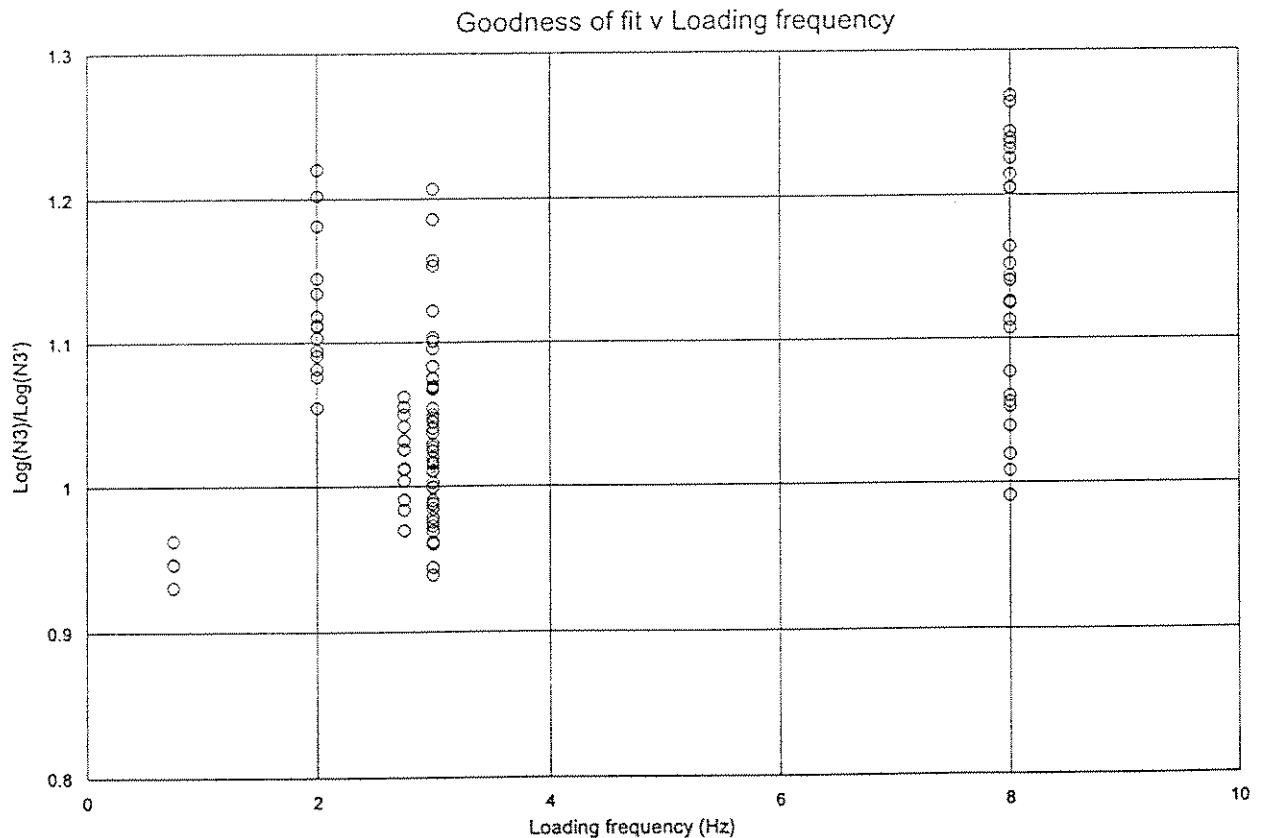


Figure 6.4 Goodness of fit of basecase S-N curve with variation in loading frequency



6.3 Variable Amplitude Loading

In-service, joints will experience variable amplitude (VA) loading under mixed loading modes, while to-date the S-N approach has only been appraised with regard to the large database of CA loaded tubular joints.

In this section the validity of the S-N approach is appraised for more complex loading modes. The simplest form of VA loading is a retest on a runner whereby only two regular cyclic stress ranges are applied. This is then extended to a single loading mode under narrow band loading with a high irregularity factor, where the variable loading pattern can be directly related to CA loading. More complex are the broad band loading spectra with lower irregularity factors and more numerous cycles that do not cross the mean stress line. The implications of these single loading modes on mixed mode loading and damage summation rules are discussed.

6.3.1 Runners retested at increased load range (single loading mode)

In Section 6.2.4, several runners were referenced with regard to their usefulness in determining an endurance limit for CA test specimens. It was reported that, in general, these tests lie above the expected life based on the mean fit S-N curve to the remainder of the database. Therefore, relating these data to the mean fit S-N curve will yield Miner's sums in excess of one for the initial loading level, irrespective of the secondary loading level.

In Table 6.5 the runner data is assessed on the basis that the Miner's sum equals one and that all data is above an endurance cut-off.

S-N curves both with a constant slope of $m = 3$ and also with a change of slope to $m = 5$ at $N = 10^7$ are assumed. From these suppositions two S-N curves can be proposed for each specimen with the only variable in the S-N curve being the constant K , adjusted to give $D_s = 1$ for each joint, ie.

$$\log(N) = K - 3.\log(S_B) \quad (\text{for all } N)$$

$$\begin{array}{ll} \text{or} & \log(N) = K - 3.\log(S_B) \quad (\text{for } N \leq 10^7) \\ & \log(N) = K - 5.\log(S_B) \quad (\text{for } N > 10^7) \end{array}$$

In accordance with the results of the single CA loading mode data there is evidence of a scale effect, such that, on average, the smaller scale joints have longer lives for the same stress range. Furthermore, the three joints with compressive chord end loading ($T \approx 6\text{mm}$) exhibit longer lives than the specimens with no chord end loading, although for this data the advantage of compressive chord end loading appears reduced.

It can be seen that the value of the S-N curve constant, K , is lower in the case of an S-N curve with a change of slope at $N = 10^7$, as would be expected. The value of K for the basecase $T = 16\text{mm}$ data is around $K = 14$, which is significantly higher than



found for the database of single CA loaded specimens in Section 4.4 where $K = 12.9$. This implies a factor of 2.3 increase in stress or a factor over ten increase in life.

This trend is not unexpected, given that most runners in the database exceeded the mean S-N curve based on the through thickness failure data. While this data should not be included in any curve fitting exercise, due to uncertainties over endurance limits, it should be borne in mind that the mean fit S-N curve is erring on the side of conservativeness due to the exclusion of this data.

Joint Ref.	T (mm)	S1 N/mm ²	n1	S2 N/mm ²	n2	K _{m = 3}	K _{m = 3:5}
T01/2 C	6.3	249.3	6.1E6	402.7	4.0E5	14.08	14.08
T18/5 C	5.7	190.0	2.0E7	319.0	1.4E6	14.26	14.13
T18/6 C	5.9	231.1	6.1E6	381.3	1.9E6	14.25	14.25
T18/8 C	5.9	161.3	1.5E7	376.3	3.9E5	13.92	13.82
T19/3 C	5.7	311.5	2.0E7	778.6	7.8E4	14.81	14.68
T20/2 C	5.9	243.3	2.0E7	486.6	2.4E5	14.50	14.37
T20/4 C	5.9	196.8	2.0E7	488.5	2.4E5	14.26	14.12
Average of 7 No. T = 6mm						14.30	14.21
T17/2 C	5.7c	178.7	2.0E7	306.4	3.2E5	14.09	13.96
T17/10 C	5.6c	264.0	2.0E7	443.5	1.5E6	14.70	14.56
T20/1 C	5.9c	329.1	2.0E7	482.7	2.7E6	15.01	14.87
Average of 3 No. T = 6mm (chord load)						14.60	14.46
T40/3 B	16.7	178.2	2.0E7	534.7	9.7E4	14.11	13.98
Average of 1 No. T = 16mm						14.11	13.98
T41/2 C	32.0	112.7	2.0E7	262.5	7.6E5	13.63	13.49
T42/1 C	31.9	52.3	2.0E7	122.1	5.3E5	12.58	12.45
T43/1 C	32.0	73.1	2.0E7	276.2	2.1E5	13.09	12.95
T43/2 C	32.0	83.1	2.0E7	142.1	2.4E6	13.26	13.13
T43/3 C	32.0	69.1	2.0E7	279.7	1.7E5	13.02	12.88
T44/4 B	32.0	132.8	2.0E7	398.3	1.5E5	13.75	13.62
Average of 6 No. T = 32mm						13.22	13.08

Notes:

C Chordside failure.
 B Braceside failure.
 c Compressive chord end loading.
 K Constant always relates to the $m = 3$ portion of the S-N curve.
 $m = 3:5$ Change of slope at $N = 10^7$.

Table 6.5 Best fit S-N curves to retest data



6.3.2 Narrow band random load history

The complex random loading experienced by joints in offshore platforms can be better approximated by performing tests under VA loading spectra. The simplest form of VA loading is termed narrow band loading and consists of a regular cyclic pattern that largely lies about the mean stress, see Figure 1.3. Thus this type of loading is associated with a high irregularity factor which is defined as the number of positive-going zero crossing points divided by the number of maxima.

To equate fatigue data performed under narrow band VA loading to CA data, the stress range needs to be adjusted in accordance to the root mean square (rms) approach. The rms approach is simple and is independent of both the outcome of the experiment and the slope of the S-N curve. Only the rms value of the cyclic part of the curve is taken and thus independent of the mean stress, S_m . Two definitions of rms are quoted in UKOSRP I (1988):

- i) S_2 , the rms of the peaks, where $S_2^2 =$ the average (amplitude)² of each cycle taken over a large number of cycles, ie, $S_2^2 = \text{average } [X(t)]^2$.
- ii) S^* , the rms of the process, where $S^{*2} =$ the average (stress)² of each part of each cycle taken over a large number of cycles, ie, $S^{*2} = \text{average } [S(t)]^2$.

where, for narrow band VA loading:

$$S(t) = S_m + X(t) \cdot \sin(2\pi f t) \quad \text{and} \quad S_2 = (2)^{0.5} S^*$$

$S(t)$ is the stress at time, t . $X(t)$ is the cyclic stress amplitude and is a (slowly) varying function of time, and f is the testing frequency.

The rms stress for the process S^* is the stress quoted in this Guide. It should be noted that for CA loading the rms of the process is $\sigma_{\text{range}}/2^{1.5}$ and rms of the peaks is $\sigma_{\text{range}}/2$.

For example under CA loading with $R = -1$, $S_m = 0$ and amplitude $X = \pm 100 \text{ N/mm}^2$, $S_2 = 100 \text{ N/mm}^2$ and $S^* = 70.71 \text{ N/mm}^2$.

In the UKOSRP I study three narrow band pseudo-random load spectra were employed (UKOSRP I 1988). A Rayleigh distribution represented the surface loading, a Laplace distribution for deepwater (in excess of 18m) and a C/12/20 distribution representing a 12ft (3.66m) diameter member immersed in 20ft (6.1m) of water, see Figure 6.5. To obtain reproducibility, each distribution has a limited block length of 100,000 cycles, with specified stress level variation in each block, eg. C/12/20 has 4% of stresses at $1.96\sigma_{LT}$, 30% @ $1.366\sigma_{LT}$, 40% @ $0.799\sigma_{LT}$, and 26% @ $0.347\sigma_{LT}$. nb.

$$\sigma_{LT} = [0.04(1.96\sigma_{LT})^2 + 0.30(1.366\sigma_{LT})^2 + 0.40(0.799\sigma_{LT})^2 + 0.26(0.347\sigma_{LT})^2]^{0.5}$$

where σ_{LT} = the long term (full block length) rms stress

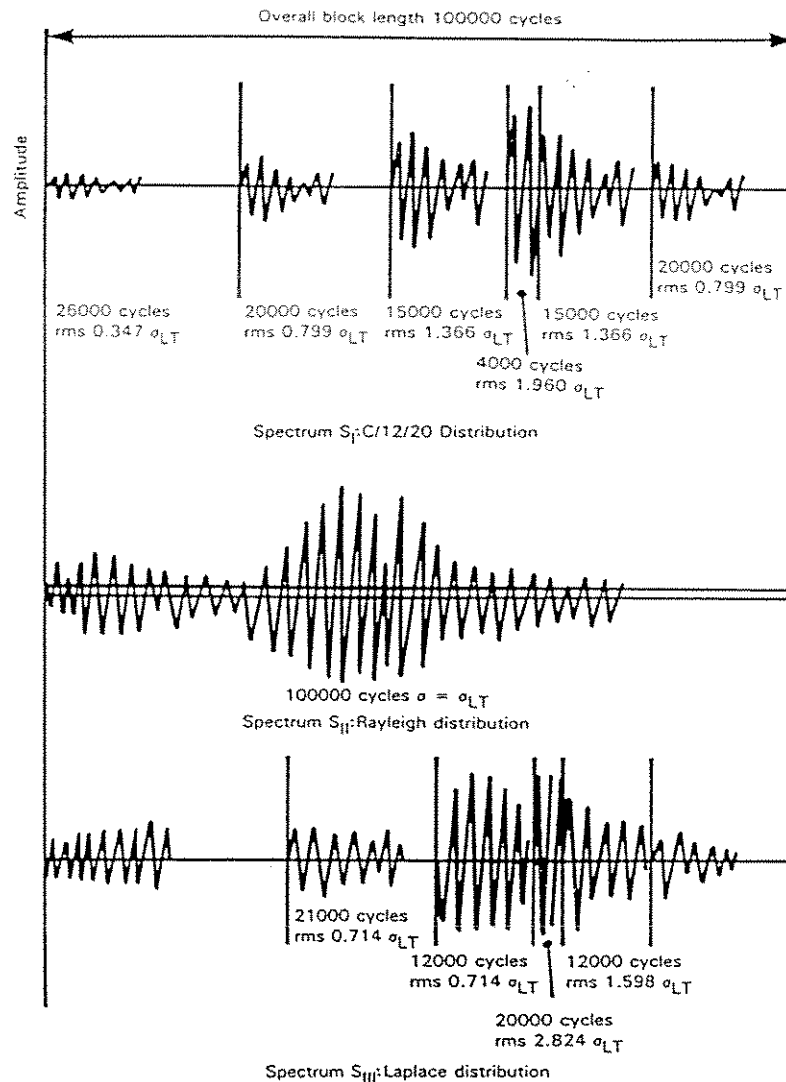


Figure 6.5 Non-stationary narrow band random load histories (UKOSRP I 1988)

The results from these three spectra gave similar results for plate connections, although spectra S_{III} tended to give slightly shorter lives on average. In UKOSRP I (1988) Spectra S_I , C/12/20, alone was applied to all tubular joint tests under VA load in-air and to the plate tests in-seawater. For comparison to these data the same spectra was applied to the narrow band VA tests in UKOSRP II (1989a).

In Figure 6.6, the VA data for simple tubular joints is compared to the CA database ($T = 16\text{mm}$). The VA data has been increased by a factor of $2^{1.5}$ to equate the results to CA loading with the assumption that each cycle crosses the mean line (ie. irregularity factor equals 1.0). It can be seen that there is good correlation between the CA and modified VA data, although the value of $\log(N_3)/\log(N_3')$ is around 3% less in the modified VA data. This difference is insignificant given the other potential variables in this database.

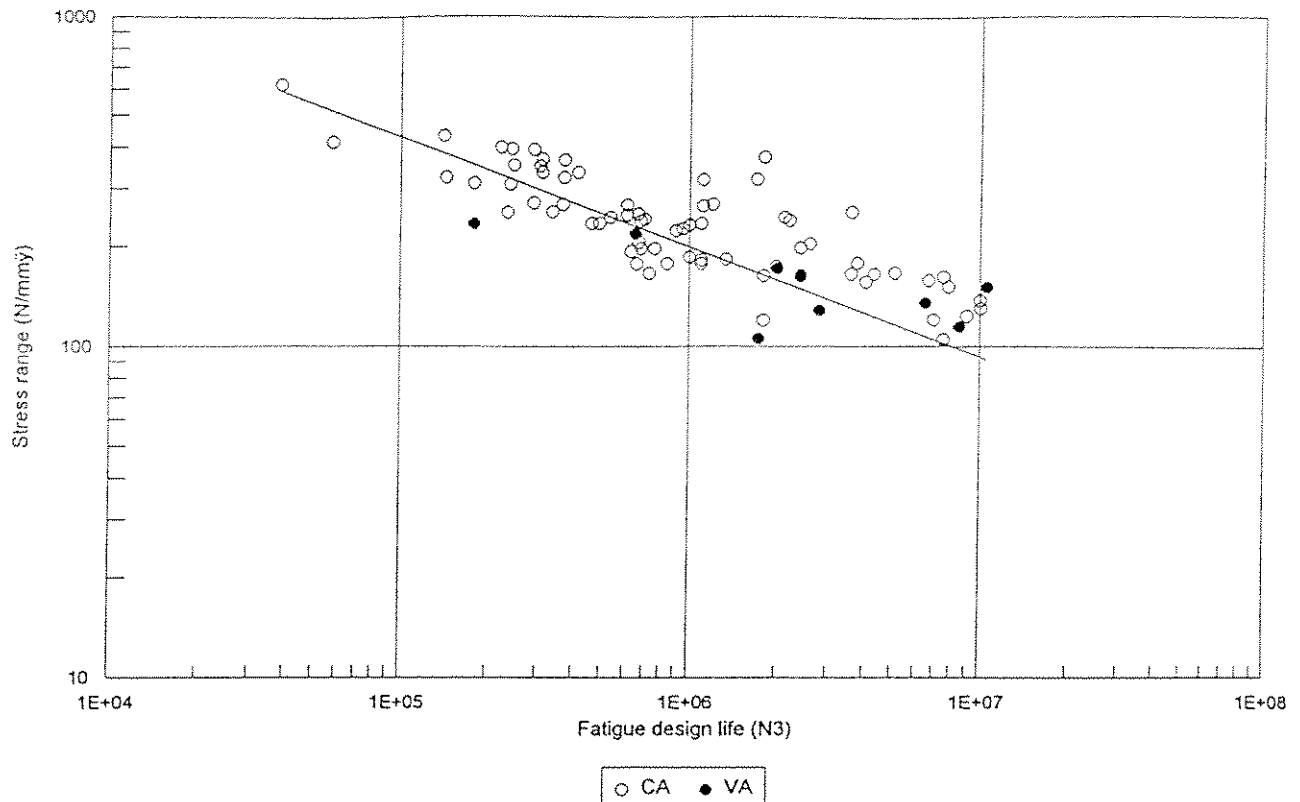


Figure 6.6 Comparison of CA and VA S-N data

6.3.3 Broad band random load history

A more complex and more representative variable amplitude loading pattern is generated under a broad band spectrum. This type of loading is associated with a lower irregularity factor than narrow band loading as illustrated in Figure 1.3, and is far more random in nature.

For narrow band loading the counting of cycles consists simply of the number of consecutive peaks and troughs experienced, and their associated ranges being simply the difference between these two values. For broad band loading the cycle counting and range estimation is less simple. Several techniques have been suggested, for example:

- i) Rainflow
- ii) Reservoir
- iii) Peak/trough
- iv) Positive peaks
- v) Zero crossing
- vi) Range-pair

Details of these methods are given in UKOSRP II (1989b) and Maddox (1991a). It should be noted that the most commonly referenced methods namely the rainflow and reservoir methods, 'give the same result if the waveform is considered in the form used to carry out the reservoir count', Maddox (1991a). While the methods themselves appear complex they may be easily automated by computer.



In the UKOSRP II project (1989a) cycle counting methods (i) to (v) were compared for a single plate connection in-air with no fatigue limit. The following damage summations were reported:

Cycle counting method	Damage summation
Rainflow	1.158
Reservoir	1.011
Peak/trough	0.664
Positive peaks	1.004
Zero crossing	0.951

It can be seen that there is reasonable correlation between all these cycle counting methods with the exception of the peak/trough method.

Overall, it was reported that the eight plate broad band loading tests in-air were in-line with the mean S-N curve, although slightly less, on average, than the mean fit to the in-air data under constant amplitude loading tested in this project (UKOSRP II 1989a).

6.3.4 Palmgren-Miner rule (Palmgren 1924 and Miner 1945)

The Palmgren-Miner rule (or more simply Miner's rule) relates the fatigue life under various loading ranges to that under constant load range by breaking down the random loading patterns into a series of stress range blocks (S_i) each containing n_i cycles of loading, such that:

$$\sum n_i/N_i = n_1/N_1 + n_2/N_2 + \dots + n_r/N_r = D_s$$

In current offshore design codes the Miner's sum of one (ie $D_s = 1$) is specified as failure (excluding reductions in D_s due to difficulty in inspection, criticality of joint, etc).

In the studies referenced in Sections 6.3.1 and 6.3.2 on both plates and tubular joints, under narrow and broad band loading, it was concluded that the behaviour of joints under VA loading was similar to CA loading, if correctly interpreted (UKOSRP I 1988 and UKOSRP II 1989a). TWI (1991b) in a summary of VA fatigue data for welded plate joints in-air conclude that Miner's rule is generally satisfactory for offshore fatigue design of welded plates in-air. In both programmes it was noted that there was increased scatter in life from VA data.

Alternatively, several researchers (Ibso and Agerskov (1993), Eide (1993) and Tubby (1994)) have reported Miner's sums in the range $D_s = 0.5 - 0.8$ in-air. Although all these test programmes investigated TT joints, which appear to give fatigue lives in-air under CA loading that are around one-third to one-half that seen in other joint types, see Section 5.2, Eide (1993) or Tubby (1994).

The conclusions for tubular joints in the Ibso and Agerskov (1993) study were largely based on runners, with $D_s = 0.75 - 0.85$ for the cracked tubular TT joints.



Eide (1993) recognised the inconsistencies in the TT joint data and corrected the data for the low degree of bending reported by Berge (1994). In-air the lives from one TT joint (two data points) appeared low once adjusted for the low degree of bending. In-seawater with CP the three adjusted TT joints tested gave lives around half the in-air curve, but in-line with the reduction factor of two on life suggested in the proposed HSE guidance (HSE 1995) for high stress ranges and the CSA codes (CAN/CSA 1992) for joints in-seawater protected by CP.

There are, however, several problems with the Miner linear cumulative damage rule which will lead to differences between CA and VA loading results in some cases:

- Sequence effects have been shown by Din (1994) to be significant with stress blocks stepping up to a peak value yielding longer lives than stress blocks which have a peak value followed by stepped stress ranges reducing to zero.
- Compressive stresses may cause less damage than the tensile loading spectrum and therefore compressive portions of the spectra may need to be factored accordingly.
- Din (1994) reports that while Miner tested sheet metal in-air at $R = -0.5$, $R = -0.2$ and $R = +0.2$ with no significant difference in fatigue behaviour, a series of S-N curves may be required for plate joints with larger stress ratios. However, it should be remembered that for offshore tubular joints fatigue life appears less sensitive to stress range and as noted in API (1993) typical values of R would be $R = -0.15$ to -0.50 .
- Different cycle counting methods yield different damage summation values, implying that care needs to be taken in selecting a cycle counting method. UKOSRP II (1989a) suggests that all methods be employed and the minimum damage estimate employed.
- Random loading generally includes many low stress cycles and therefore the way that the endurance limit is represented in the S-N curve may have a significant effect upon the damage summation derived. In several assessments of VA data the change in slope or endurance limit at low stress ranges is ignored.

6.4 Summary of Loading Effects

Under CA single mode loading, OPB tests tended to exhibit longer lives, on average, than those under axial load or IPB, although the difference was too small and inconsistent to draw any firm conclusions. However, the application of a compressive axial load of 77 N/mm^2 to the chord ends clearly gives a significant increase in fatigue life, irrespective of the load applied to the brace. This raises the prospect of lower lives being associated with members where the chord is in tension.



Stress ratio, R , has been identified as being significant for large values of R , ie. the fatigue life reduces as R increases. However, API specify that the stress ratio is likely to lie between $R = -0.15$ and $R = -0.50$ for most joints in offshore structures and, given that the fatigue lives noted for $R = -1$ and $R = 0$ are not dissimilar, it would appear reasonable to ignore stress ratio effects in most cases. Similarly, high mean stresses are likely to reduce fatigue life but are not likely to occur in offshore tubular joints in fixed steel platforms.

The cyclic frequency allied appears to have little effect in-air but is reported to be significant in-seawater either with or without corrosion protection. Consequently, joints tested in seawater should be loaded at frequencies representative of in-service joints (ie. 0.1 - 0.2 Hz). It was found that the rate of crack growth decreases as the loading frequency increases.

At high stress, most codes limit the stress range to either the capacity of the joint or to a function of steel yield strength, eg. $2\sigma_y$. However, platforms have experienced stresses in excess of this value and yet appeared to be undamaged. Therefore in reassessing such joints the designer is currently left with either no guidance in the case of a strict upper limit, or if the static capacity is adopted a potentially optimistic S-N curve for high stress-low cycle joints. An alternative method, based on the static design, but more conservative in the high stress-low cycle regime ($1 < N < 10^4$), has been proposed for joint reassessment in these cases.

At low stress, endurance limits have been identified in plate tests in-air under constant amplitude loading, with the limit tending to occur at a given number of cycles rather than at a given stress range. Few data exist on long life tubular joints with $N > 2 \times 10^7$. There is even less data in seawater where loading frequency must be realistic of offshore loading, ie 0.1 - 0.2 Hz. Furthermore, the scatter in retest and VA loaded joints is such that this data can give little aid in determining whether an endurance limit, change of slope or no change of slope should be employed.

Work at EWI, which is ongoing, included a review of crack growth models and long life plate tests. This review led to a new fracture mechanics model that can simulate crack growth in plates under tension and bending variable amplitude loadcases. This study showed that relatively thin specimens under tension load are best represented by a change in the S-N curve at 10^7 cycles from $m=3$ to $m=5$. However, for thicker plates under tensile load, and for more realistic degree of bending values of around 0.8 representing tubular intersections, a change in S-N curve from $m=3$ to $m=4$ at 10^7 cycles appears more valid.

Under both narrow band and broad band variable amplitude loading, the Miner's summation appears to give a reasonable representation of constant amplitude fatigue behaviour. However, there remain several cycle counting methods available for broad band loading, with the rainflow and reservoir methods appearing most reliable.



In conclusion, while it is clear that there are limitations in the Miner's damage accumulation model, this simple method does not appear to consistently overestimate fatigue life for typical tubular joints. However, clearly more investigation of tubular joint behaviour is required under broad band variable amplitude loading, in particular.



7. FATIGUE LIFE OF SIMPLE, AS-WELDED TUBULAR JOINTS IN-AIR

In Sections 5 and 6 of this Chapter, the influence of both geometric and loading variables upon tubular joint fatigue life have been considered in detail.

It has been observed that there is a very high degree of correlation (positive or negative) between the chord thickness, chord diameter, chord length, brace thickness, brace diameter, attachment leg length and cyclic loading frequency. Therefore, it has proved difficult to identify the cause and degree of effect that each of these parameters has on joint fatigue life. However, following the review of geometric and loading variables the following appear to be of particular significance:

- Thickness of the tubular connection
- Poor weld profile
- Chord axial loading
- High and low stress ranges
- Variable loading and damage summation.

Therefore, the database employed in Sections 5 and 6 required further refinement to isolate each of these factors.

The initial database outlined in Section 4 consists of 157 joints. These have been subdivided as follows:

- 103 joints with satisfactory weld fillets.
- 46 joints with unsatisfactory weld fillets.
- 8 TT joints.

The 103 joints with satisfactory weld fillets are primarily discussed in Section 7.1 and have led to the recommended S-N curve in this Guide.

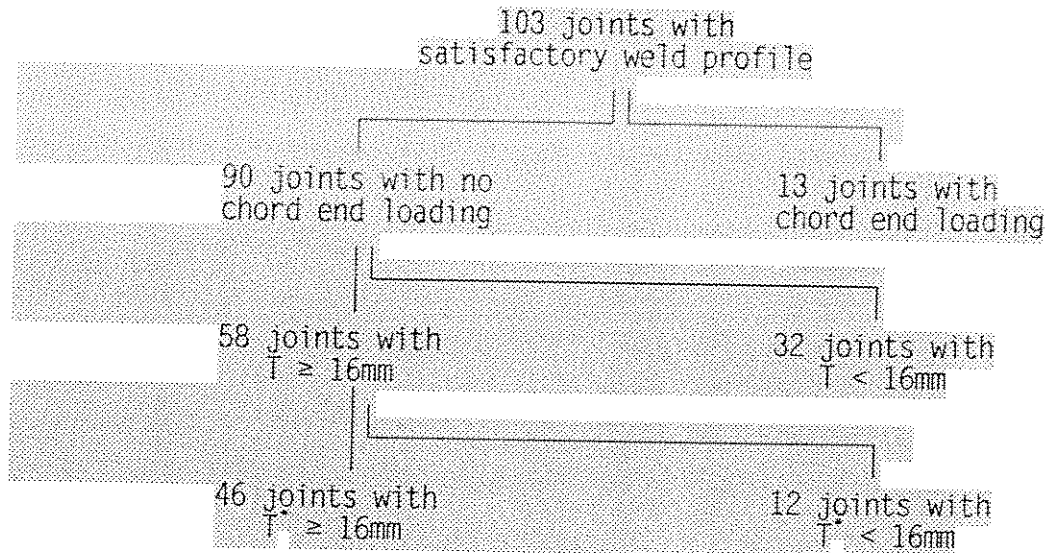
The 46 joints with unsatisfactory weld fillets are primarily discussed in Section 7.2. The definition of unsatisfactory weld fillet was presented in Section 5.5.2. This definition is in-part factual (eg. the steepness of the weld is in excess of 60°) and in-part subjective (eg. the transition between the plate and the weld being particularly poor). The reason for describing the weld fillets as unsatisfactory for each of these 46 specimens is given in Section 7.2.

The unusual results from the TT joint configurations were described in Section 5.2. These joints clearly exhibit untypical stress distributions and, since no other reliable data currently exists for these joints, it was felt that these eight joints should be excluded from the final database.



7.1 In-Air S-N Curve and Thickness Exponent

The final screened database with satisfactory weld profile contains 103 joints with $5.1\text{mm} \leq T \leq 76.0\text{mm}$. These joints can be further subdivided as follows:



T = Chord thickness

T^* = Failed member thickness

All data relate to joints tested under constant amplitude loading. No screening of data at high and low stress ranges was made since these cut-off values are less easily classified (see Sections 7.3 and 7.4).

Previous assessments have shown that tubular joints with very thin members ($\leq 6\text{mm}$) tend to behave in a different manner to the more representative test data with regard to the scale effect. It has been noted that data from tubular joints with a member thickness less than 16mm require a more substantial scale effect correction factor than data from tubular joints with members in excess of 16mm . However, it should be remembered that the bulk of the data relate to members that are nominally 6mm , 16mm , 32mm or 76mm thick, and that members between 6mm and 16mm may yield results more consistent with data from members with thicknesses around 16mm .

The following analyses have been performed both including and excluding data below the nominal thickness of 16mm (a 5% variation from this nominal value has been allowed and therefore the lower thickness limit was taken to be $T = 15.2\text{mm}$).

A summary database of the 46 acceptable tubular joints, with nominal failed member thicknesses of $T^* \geq 16\text{mm}$, is given in Table 7.1, while the twelve joints with $T \geq 16\text{mm}$ but $T^* < 16\text{mm}$ are presented in Table 7.2.



Paper Ref.	Joint Ref.	T mm	t mm	Weld leg length mm	Stress range N/mm ²		Failed Member	Fatigue life (N3) x10 ⁶
					Chord	Brace		
UKOSRP I	T25/3	15.8	15.5	70.0	111.6	156.0	C & W	4.050
Dijkstra	28	15.9	15.9	-	176.9	-	Chord	0.660
Dijkstra	29	15.9	15.9	-	119.8	-	Chord	1.800
TWI repair	1	16.0	12.0	50.0	235.3	109.8	Chord	0.492
TWI repair	2	16.0	12.0	-	352.6	164.5	Chord	0.247
TWI repair	3	16.0	12.0	-	268.0	125.0	Chord	0.366
TWI repair	4	16.0	12.0	55.0	335.3	156.4	Chord	0.414
TWI repair	6	16.0	12.0	-	335.5	156.5	Chord	0.310
TWI repair	7	16.0	12.0	40.0	350.5	163.5	Chord	0.305
TWI repair	13	16.0	12.0	37.0	164.8	76.9	Chord	4.326
TWI repair	15	16.0	12.0	55.0	399.6	186.4	Chord	0.223
TWI repair	19	16.0	12.0	50.0	239.0	111.5	Chord	0.679
UKOSRP II	G1	16.0	8.0	-	618.6	-	C & B	0.039
UKOSRP II	G2	16.0	8.0	-	432.2	-	Chord	0.141
UKOSRP II	G3	16.0	8.0	-	368.3	-	Chord	0.310
UKOSRP I	K30/1	16.0	8.6	24.0	180.3	182.2	Chord	1.100
UKOSRP I	T22/1	16.1	10.0	60.0	306.8	393.3	Chord	0.290
UKOSRP I	T22/2	16.1	9.2	60.0	177.5	227.0	Chord	0.950
UKOSRP I	T38/3	16.2	9.5	68.0	222.1	249.8	Brace	0.610
UKOSRP I	T25/2	16.3	16.3	70.0	310.5	261.5	Chord	0.180
UKOSRP I	T38/6	16.3	9.3	68.0	145.1	163.2	Chord	1.800
UKOSRP I	T38/5	16.4	9.4	68.0	148.3	174.7	Chord	1.980
UKOSRP I	T38/4	16.4	9.3	68.0	208.4	245.4	Chord	0.535
UKOSRP I	T39/1	16.4	6.5	59.0	163.7	240.0	Chord	2.200
UKOSRP I	T22/3	16.5	9.4	60.0	131.3	165.2	Chord	3.600
UKOSRP I	T21/3	17.5	17.3	70.0	132.3	161.7	Chord	7.500
UKOSRP I	T21/1	17.7	17.5	70.0	173.9	235.3	C & W	1.100
UKOSRP I	T21/2	17.7	17.1	70.0	267.1	264.1	C & W	0.610
COSRP	TA1	19.0	19.0	-	251.0	-	Chord	0.665
COSRP	TB1	19.0	19.0	-	254.1	-	Chord	0.235
Dijkstra	13	31.7	15.9	-	94.3	-	Chord	4.100
Dijkstra	14	31.7	15.9	-	269.0	-	Chord	0.150
Dijkstra	15	31.7	15.9	-	157.2	-	Chord	0.950
Dijkstra	34	31.7	15.9	-	79.1	-	Chord	12.000
Dijkstra	35	31.7	15.9	46.0	197.8	-	Chord	0.700
UKOSRP I	T42/4	31.9	9.6	50.0	88.6	164.4	Chord	2.230
UKOSRP I	T41/1	32.0	31.9	100.0	77.0	40.8	Chord	21.000
UKOSRP I	T41/3	32.0	31.9	100.0	158.6	100.2	Chord	1.400
UKOSRP I	T41/4	32.0	31.9	100.0	108.1	57.3	Chord	3.460
UKOSRP I	T43/4	32.0	15.0	60.0	90.9	95.7	Chord	7.500
UKOSRP II	T210	32.0	16.2	37.7	140.5	171.1	Chord	1.900
UKOSRP II	T215	32.0	15.8	33.1	197.9	173.2	Chord	0.673
UKOSRP II	T216	76.0	38.4	65.1	114.8	108.0	Chord	2.950
UKOSRP II	T217	76.0	38.0	63.2	204.1	228.5	Chord	0.324
UKOSRP II	T218	76.0	38.0	62.4	156.1	159.2	Chord	0.910
UKOSRP II	T219	76.0	37.7	65.1	287.7	306.1	Chord	0.116

Table 7.1 Fatigue S-N database for satisfactory weld profile, in-air, under CA loading with no chord end load ($T \geq 16\text{mm}$)



Paper Ref.	Joint Ref.	T mm	t mm	Weld leg length mm	Stress range N/mm ²		Failed Member	Fatigue life (N3) x10 ⁶
					Chord	Brace		
Dijkstra	30	15.9	8.7	-	-	232.6	Brace	1.000
Dijkstra	33	15.9	8.7	-	-	198.3	Brace	2.400
Dijkstra	37	15.9	8.7	-	-	157.8	Brace	6.700
Dijkstra	38	15.9	8.7	-	-	150.9	Brace	7.800
UKOSRP I	T38/3	16.2	9.5	68.0	222.1	249.8	Brace	0.610
UKOSRP I	T40/5	16.2	4.5	55.0	-	319.9	Brace	1.700
UKOSRP I	T38/8	16.3	9.3	68.0	275.2	324.2	B & C	0.369
UKOSRP I	T39/4	17.3	6.4	57.0	254.2	265.6	Brace	1.110
UKOSRP I	T39/5	17.6	6.4	57.0	175.1	183.0	Brace	1.340
UKOSRP I	T44/1	32.0	8.1	50.0	112.5	227.3	Brace	1.160
UKOSRP I	T44/2	32.0	8.1	50.0	86.2	174.1	Brace	2.120
UKOSRP I	T44/3	32.0	8.1	47.0	137.1	196.7	Brace	1.200

Table 7.2 Fatigue S-N database for satisfactory weld profile, in-air, under CA loading with no chord end load ($T^* < 16\text{mm}$)

The databases given in tables 7.1 and 7.2 are similar to that employed by the HSE to derive the new T^* S-N curve, although they do exclude some of the large scale test data in the ECSC project, see Section 4.2.2. The HSE derived a T^* curve $\log(N) = 12.942 - 3\log(S_e) - 0.233d$ ($d=0$ mean, $d=2$ design), with scale effect exponent $n = 0.30$. This was proposed following a comprehensive review of the 93 joint database reported in MaTSU (1992), summarised as follows:

'Since the publication of [DEn 1984a], more data have been accumulated on tubular joints. However, there are only two thicknesses, (16 and 32mm), for which a substantial body of data exists. These data have been plotted and show a deleterious effect of increasing chord wall thickness on fatigue endurance, with some of the data falling close to or below the design curve of 16mm. The best fit S-N curves to the data at each thickness have been calculated assuming a value of m of 3. The ratio of the fatigue strengths at a given endurance at these two thicknesses would correspond to a thickness correction exponent of 0.29. This is somewhat larger than the existing value of 0.25 and shows an effect of chord wall thickness below the previous limiting thickness of 22mm.

However, to allow for effects not readily manifest within the limited database a conservative thickness correction exponent of 0.3 is proposed. Additionally the base line thickness for thickness correction was extended to 16mm for tubular joints. This correction factor was applied to the tubular joint data. These proposals resulted in only one of the thickness corrected S-N data falling below the design line.

A slightly greater thickness correction exponent of 0.32 is obtained if a multi-regression analysis is carried out on all the data. However, the data responsible for this increase come from one national programme, as can be seen from the below average performance of tests from [Lieurade 1981a, 1981b]. This



would indicate that the results listed fall into two separate data sets. When the thickness effect is evaluated for individual datasets, lower values of thickness correction exponent are obtained, (0.304 for [Lieurade 1981a and 1981b], 0.239 for data from the rest). These would indicate that a thickness correction exponent of 0.3 is not too conservative. Thus a thickness correction exponent of 0.3 was proposed, which maintained consistency with that proposed for welded plates.

To determine the most appropriate S-N curve for in-air data under constant amplitude loading with acceptable weld profile, the database was appraised with the scale factor based on: the chord thickness (T), brace thickness (t), attachment length (l) and failed member thickness (T*). In all cases the base thickness was taken to be 16mm, with the values of the scale effect exponent (n) and coefficients K and m in the expressions:

$$\log(N) = K - m \cdot \log(S_B) \pm S_E$$

and $S_B = S \cdot (t_x/16)^n$

determined to give a minimum standard error (S_E). This expression was also optimised for the coefficients n and K for fixed m = 3. (nb. $t_x = T, t, l$ or T^* as specified).

The results of this assessment are given in Table 7.3a for all joints and in Table 7.3b excluding very small scale joints.

For the cases where the scale correction is based on the chord or brace thickness the database is assessed both for all joints and for joints with members greater than the nominal 16mm alone. For the case where the scale correction is based on the attachment thickness the database is assessed both for all joints and for joints with attachments greater than 25mm, which roughly excludes the same small scale joints as for the other scenarios.

Thickness effect		All thicknesses	
		Variable m	m = 3
$S_B = S \cdot (T/16)^n$ (90 tests)	$\log(N)$ n S_E	12.20-2.63.log(S) 0.39 0.2835	13.07-3.log(S) 0.39 0.2902
$S_B = S \cdot (t/16)^n$ (90 tests)	$\log(N)$ n S_E	11.87-2.58.log(S) 0.46 0.2857	12.82-3.log(S) 0.46 0.2944
$S_B = S \cdot (l/16)^n$ (71 tests)	$\log(N)$ n S_E	12.17-2.42.log(S) 0.42 0.2971	13.64-3.log(S) 0.44 0.3098
$S_B = S \cdot (T^*/16)^n$ (90 tests)	$\log(N)$ n S_E	12.06-2.60.log(S) 0.40 0.2686	13.00-3.log(S) 0.39 0.2773

Table 7.3a Appraisal of scale effect (full screened database)



Thickness effect		Excluding very small scale joints	
		Variable m	m = 3
$S_B = S.(T/16)^n$ (58 tests)	$\log(N)$ n S_E	12.25-2.68.log(S) 0.25 0.2425	12.99-3.log(S) 0.26 0.2494
$S_B = S.(t/16)^n$ (25 tests)	$\log(N)$ n S_E	13.05-3.14.log(S) 0.10 0.1990	12.74-3.log(S) 0.10 0.2006
$S_B = S.(l/16)^n$ (41 tests)	$\log(N)$ n S_E	11.95-2.37.log(S) 0.35 0.2887	13.55-3.log(S) 0.38 0.3077
$S_B = S.(T^*/16)^n$ (46 tests)	$\log(N)$ n S_E	12.25-2.72.log(S) 0.21 0.1931	12.90-3.log(S) 0.22 0.2011

Table 7.3b Appraisal of scale effect
(excluding very small scale joints)

It can be seen in both Tables 7.3a and 7.3b that basing the scale factor on the thickness of the appropriate member gives the least scatter ($S_E = 0.193 - 0.201$ for $T^* \geq 16\text{mm}$, and $S_E = 0.269 - 0.277$ for all joints). For this scale effect approach, an exponent of $n \approx 0.40$ would be required if all data were included or $n \approx 0.22$ if only member thicknesses in excess of 16mm were considered.

Since tubular joints with member thicknesses less than 16mm are particularly unrepresentative of offshore structures and have tended to be disregarded in the past, the scale effect correction of $n = 0.22$ for this database of 46 joints $T^* \geq 16\text{mm}$ appears most representative. It should also be noted that the standard error is relatively insensitive to changes in this scale effect exponent. Therefore, while it would appear reasonable to adopt the scale effect exponent of $n = 0.25$ currently employed in the API (1993), DnV (1992) and HSE (1993a) codes ($S_E = 0.2019$, $K = 12.92$), increasing this exponent to $n = 0.30$, as currently proposed by the HSE (1993b), does not appear justified from this tubular joint data.

Furthermore, the difference in standard error between the optimal slope S-N curve and the curve with $m = 3$ is small and therefore the fixing of the slope at $m = 3$ appears justified.

Therefore the recommended mean S-N curve for tubular joints in-air with no chord end loading is:

$$\log(N) = 12.90 - 3.\log(S_B) \quad S_E = 0.20$$

where $S_B = S.(T^*/16)^{0.25}$

and T^* is the thickness of the member under consideration.



The mean minus two standard deviation design S-N curve would therefore be given by:

$$\log(N) = 12.50 - 3.1 \log(S_B)$$

ie. The design fatigue life is 40% of the mean fatigue life.

These S-N curves and the 46 datapoints used to determine these S-N curves are illustrated in Figure 7.1.

This S-N curve is most similar to the proposed HSE T' curve (MaTSU 1992) with

$$T' \text{ mean: } \log(N) = 12.942 - 3.1 \log(S_B)$$

$$T' \text{ design: } \log(N) = 12.476 - 3.1 \log(S_B)$$

ie. $S_E = 0.233$.

Furthermore, by chance, this curve is identical to the base case S-N curve from the less well screened database defined in Section 4.4 and employed in Sections 5 and 6 of this Chapter. Therefore, the goodness of fit assessments made against the basecase S-N curve made in these sections remain valid.

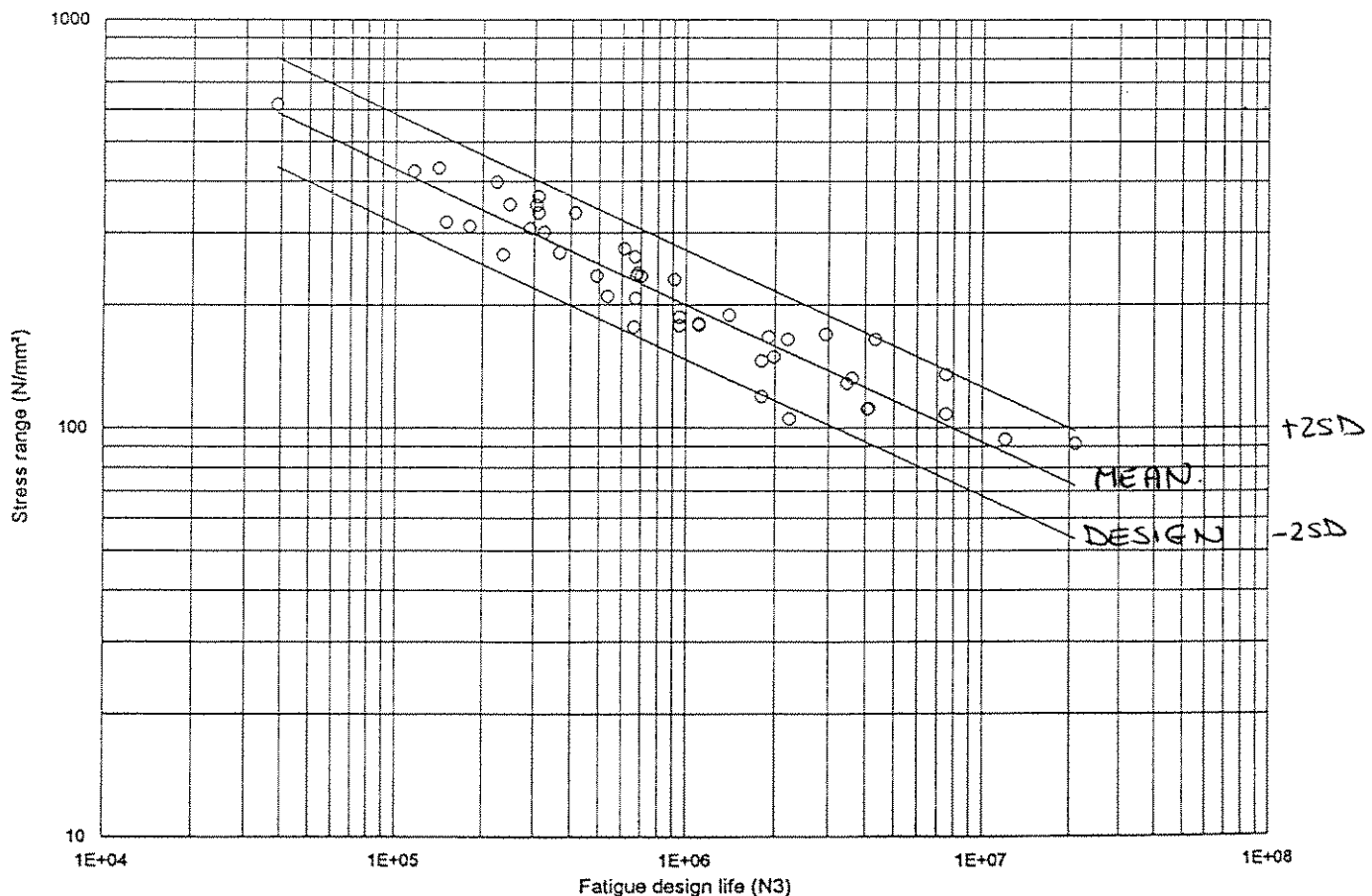


Figure 7.1 Mean and design S-N curves for acceptable profile, in-air, under CA loading (no chord end load)



7.2 Poor Weld Profile

The final screened database of 46 joints with unsatisfactory weld profile under constant amplitude is given in Table 7.4a for the 29 joints with the failed member thickness $T^* \geq 16\text{mm}$ and in Table 7.4b for the 17 joints with the failed member thickness $T^* < 16\text{mm}$. In the light of the findings in Section 7.1, only the 29 joints with $T^* \geq 16\text{mm}$, presented in Table 7.4a, have been assessed against the specimens with satisfactory profile. The data for specimens with $T^* < 16\text{mm}$ have been provided for completeness.

The best-fit S-N curve through the data given in Table 7.4a, for a fixed slope of $m = 3$, is given by:

$$\log(N) = 13.025 - 3.1 \log(S \cdot (T^*/16)^{0.50}) \quad S_E = 0.280$$

ie. $n = 0.50$

Therefore, there appears to be a significantly larger thickness exponent required on joints with poor welds than those with more acceptable or smooth ground welds. This finding is in accordance with the summary on scale effects given in Section 5.1.5. Furthermore, it is also consistent with the reported thickness exponent of $n = 0.30$ proposed by the HSE (1995) which is based on data from both satisfactory and unsatisfactory weld profiles, as defined for this Guide.

It is also worth noting that for this thickness exponent of $n = 0.50$, the mean S-N curve predicts longer lives for joints with $T = 16\text{mm}$ ($K = 13.03$, cf. $K = 12.90$ for satisfactory profiles), although the scatter associated with these joints is somewhat larger ($S_B = 0.28$, cf. $S_B = 0.20$ for satisfactory profiles).

Minimising the standard error for this dataset for fixed values of $n = 0.25$ and $m = 3$, in accordance with the acceptable weld profile S-N curve gives:

$$\log(N) = 12.91 - 3.1 \log(S_B) \quad S_E = 0.336$$

Therefore, the mean acceptable and poor weld profile S-N curves are almost identical, except for the degree of uncertainty in fatigue life estimates.

It is clearly anomalous that joints with $T = 16\text{mm}$ and a poor weld have longer lives than those with satisfactory welds, however, it does appear to be important to note the fact that the thickness exponent appears significantly more severe for these joints with poor welds.

Therefore, it is suggested that these types of joint be covered using the same basecase mean S-N as for the satisfactory profiles, given in Section 7.1, that a larger margin of safety be employed to recognise the increased scatter and that a larger thickness exponent of be taken for these joints - $n = 0.35$ is proposed.



Paper Ref.	Joint Ref.	T mm	t mm	Weld leg length mm	Stress range N/mm ²		Failed Member	Fatigue life (N3) x10 ⁶	Reason for poor weld class
					Chord	Brace			
UKOSRP I	T37/13	15.4	17.6	95.0	165.5	103.7	Chord	0.729	Poor profile
UKOSRP I	T37/3	15.7	17.9	95.0	323.5	206.3	Chord	0.144	Poor profile
UKOSRP I	T37/5	15.8	17.4	95.0	185.8	118.4	Chord	1.000	Poor profile
UKOSRP I	T23/2	15.9	6.6	20.0	366.0	292.1	Chord	0.370	Poor profile
Dijkstra	5	15.9	8.2	-	197.3	-	Chord	0.680	Poor profile
Dijkstra	6	15.9	8.2	-	177.6	-	Chord	1.100	Poor profile
Dijkstra	7	15.9	8.2	-	177.6	-	Chord	0.840	Poor profile
Dijkstra	8	15.9	8.2	-	104.8	-	Chord	7.500	Poor profile
Dijkstra	9	15.9	8.2	-	197.3	-	Chord	0.760	Poor profile
Dijkstra	11	15.9	6.3	-	123.1	-	Chord	9.000	Poor profile
Dijkstra	12	15.9	6.3	-	241.9	-	Chord	0.700	Poor profile
UKOSRP I	T37/7	16.0	17.6	95.0	129.8	81.3	Chord	10.010	Poor profile
UKOSRP I	T37/9	16.1	16.9	95.0	120.1	76.6	Chord	6.950	Poor profile
UKOSRP I	T37/8	16.5	17.8	95.0	269.2	168.7	Chord	1.200	Poor profile
UKOSRP I	T37/12	16.5	17.0	95.0	395.3	247.7	Chord	0.243	Poor profile
UKOSRP I	T37/1	16.6	17.8	95.0	271.1	169.8	Chord	0.290	Poor profile
UKOSRP I	T37/10	16.8	16.3	95.0	178.0	111.5	Chord	3.790	Poor profile
UKOSRP I	T24/1	17.2	5.0	20.0	204.1	187.4	C & B	2.600	Poor profile
<hr/>									
UKOSRP I	T23/1	18.3	6.6	20.0	166.3	147.4	Chord	5.100	Poor profile
Lieurade	A	22.8	21.5	31.5	235.7	162.4	Chord	0.462	Profile >60°
<hr/>									
UKOSRP I	T42/2	31.9	9.6	38.0	94.4	128.4	Chord	4.790	Poor profile
UKOSRP I	T42/3	31.9	9.6	38.0	76.3	104.8	Chord	14.600	Poor profile
UKOSRP II	T211	32.0	16.5	37.7	199.8	181.4	Chord	1.050	Poor profile
Lieurade	BB	40.0	22.0	32.0	152.8	150.7	Chord	0.649	Profile >60°
Lieurade	D	41.6	41.4	51.4	222.1	150.2	Chord	0.333	Profile >60°
Lieurade	DD	44.0	43.5	53.5	131.9	-	Chord	0.471	Profile >60°
<hr/>									
Lieurade	CC	75.0	22.8	32.8	86.0	177.4	Chord	0.650	Profile >60°
Lieurade	E	75.0	40.0	50.0	126.0	100.2	Chord	0.655	Profile >60°
Lieurade	EE	76.7	43.5	53.5	131.6	144.3	Chord	0.464	Profile >60°

Table 7.4a Fatigue S-N database for poor weld profile, in-air, under CA loading with no chord end load ($T^* \geq 16\text{mm}$)

Paper Ref.	Joint Ref.	T mm	t mm	Weld leg length mm	Stress range N/mm ²		Failed Member	Fatigue life (N3) x10 ⁶	Reason for poor weld class
					Chord	Brace			
UKOSRP I	T4/1	6.2	3.3	15.0	333.7	-	Chord	0.580	Convex weld
UKOSRP I	T4/2	6.2	3.3	15.0	276.7	-	Chord	2.100	Convex weld
UKOSRP I	T4/3	6.2	3.3	15.0	314.5	-	Chord	3.960	Convex weld
UKOSRP I	T18/1	5.9	4.0	14.0	322.6	287.7	Chord	0.498	Convex weld
UKOSRP I	T18/9	6.0	4.0	14.0	358.4	319.7	Chord	0.218	Convex weld
UKOSRP I	T18/11	5.9	4.0	14.0	250.9	223.8	Chord	1.000	Convex weld
UKOSRP I	T18/12	6.0	4.0	14.0	412.2	367.6	Chord	0.217	Convex weld
UKOSRP I	T18/15	5.5	3.9	14.0	257.2	229.4	Chord	0.415	Convex weld
Dijkstra	1	6.3	3.2	-	555.7	-	Chord	0.060	Poor profile
Dijkstra	2	6.3	3.2	-	185.2	-	Chord	12.000	Poor profile
Dijkstra	3	6.3	3.2	-	330.8	-	Chord	3.000	Poor profile
Dijkstra	24	6.3	3.2	-	246.9	-	Chord	0.330	Poor profile
Dijkstra	25	6.3	3.2	-	277.8	-	Chord	0.470	Poor profile
Dijkstra	26	6.3	3.2	-	194.5	-	Chord	1.500	Poor profile
<hr/>									
UKOSRP I	T23/3	16.1	6.6	20.0	223.4	173.1	Brace	0.900	Poor profile
UKOSRP I	T24/2	17.1	4.9	18.0	392.3	414.8	Brace	0.058	Poor profile
UKOSRP I	T24/3	17.5	4.9	18.0	299.9	308.7	Brace	0.240	Poor profile

Table 7.4b Fatigue S-N database for poor weld profile, in-air, under CA loading with no chord end load ($T^* < 16\text{mm}$)



For joints with poor weld profile it is recommended that the mean S-N curve employed is also:

$$\log(N) = 12.90 - 3.\log(S_B)$$

while the design S-N curve is:

$$\log(N) = 12.20 - 3.\log(S_B)$$

ie. The design fatigue life of uncontrolled weld profiles is 20% of the mean life or half the design life of joints with acceptable weld profiles.

Furthermore, the thickness exponent is taken to be:

$$S_B = S.(T^*/16)^{0.35}$$

The 29 datapoints representing the poor weld profiles are plotted, along with the satisfactory weld profile data, against the mean and design S-N curves in Figure 7.2 ($T = 16\text{mm}$).

It should be emphasised that joints should not be designed to this S-N curve with poor quality welds specified. This S-N curve should only be used to reassess joints where, on inspection, the weld is considered to be below the acceptable profile.

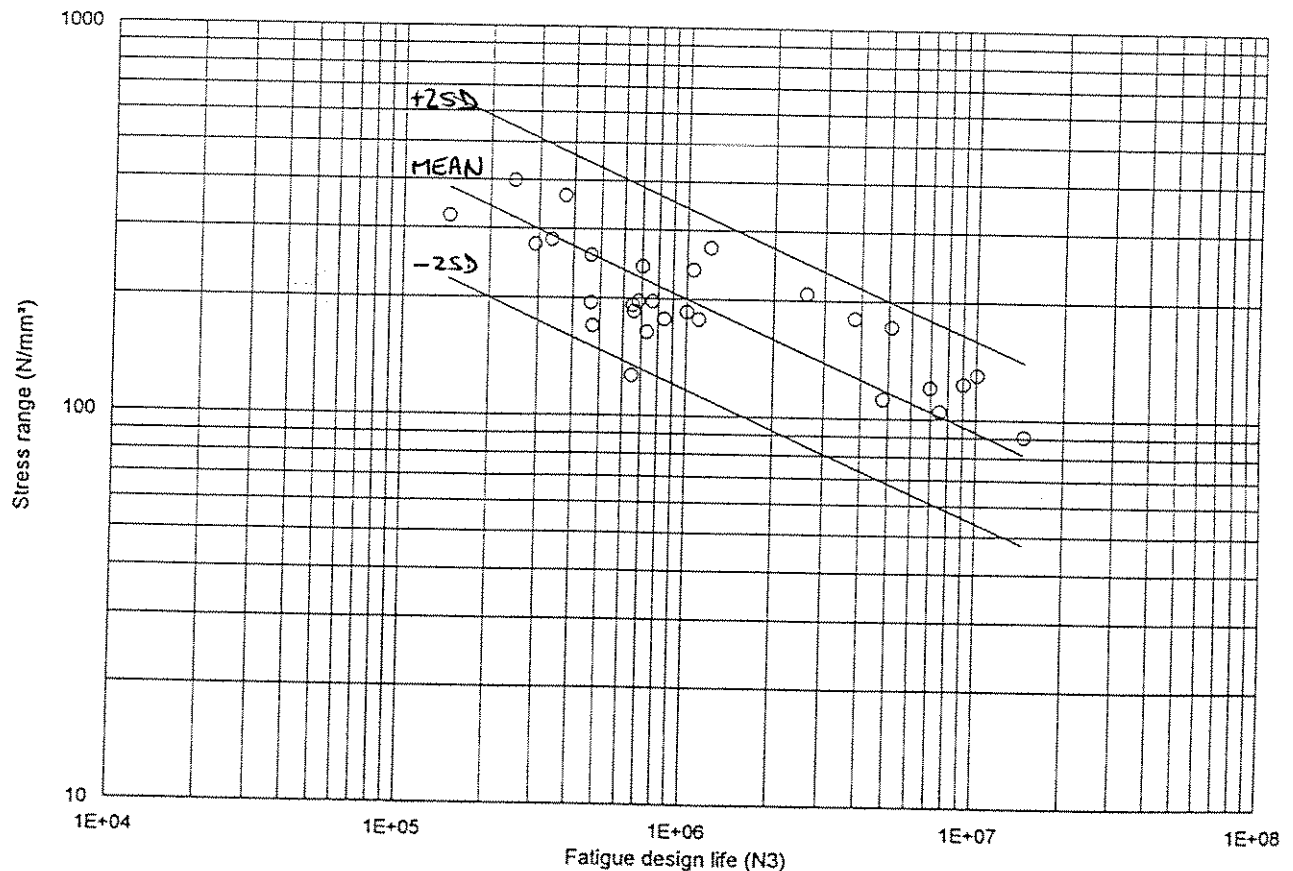


Figure 7.2 Mean and design S-N curves for poor and satisfactory weld profile data, in-air under CA loading (no chord end load)



7.3 Endurance Limits and Variable Amplitude Loading

In Section 6.3 test results from specimens that did not fail under a single constant amplitude load range were discussed. Runners retested at higher load ranges, narrow band random loading and broad band narrow loading were considered, along with the Palmgren-Miner damage summation rule (Palmgren 1924 and Miner 1945).

In Sections 6.2.4 and 6.3.1, the specification of an endurance limit was considered with reference to the 'runners' data. However, this review was inconclusive with runners (generally specimens that reached 20 million cycles) in line with, rather than below, stress ranges associated with typical fatigue failures.

This data is reproduced in Table 7.5 with the damage estimated under the assumption that the S-N curve has no change of slope at long life.

It can be seen that at the extremes, joint T42/1 failed below expectations ($D_s = 0.81$) although only 20% of the damage can be attributed to a stress range well in excess of a typical endurance limit of around 80-100 N/mm². Alternatively, specimen T43/3 failed well above expectations ($D_s = 2.19$) suggesting that little damage occurred at the stress range of 69.1 N/mm².

Of the variable amplitude loaded tubular joints considered in Section 6.3, only five joints in the UKOSRP I (1989) and UKOSRP II (1989b) programmes under narrow band (C/12/20) random loading pass the screening criteria specified in Section 7.1.

Joint Ref.	T mm	S N/mm ²	S _B N/mm ²	Meas. cycles x10 ⁶	Est. life x10 ⁶	Est. damage	Total damage
T41/2	32.0	112.7 262.5	134.0 312.2	20.00 0.76	3.30 0.26	6.06 2.91	8.97
T42/1	31.9	52.3 122.1	62.2 145.1	20.00 0.53	33.05 2.60	0.61 0.20	0.81
T43/1	32.0	73.1 276.2	86.9 328.5	20.00 0.21	12.16 0.22	1.65 0.94	2.59
T43/2	32.0	83.1 142.1	98.8 169.0	20.00 2.40	8.24 1.65	2.43 1.46	3.88
T43/3	32.0	69.1 279.7	82.1 332.6	20.00 0.17	14.34 0.22	1.39 0.80	2.19

Table 7.5 Runners retested at a higher stress range that pass the final screening criteria, from UKOSRP I (1989)



In this variable amplitude loading distribution, the irregularity factor exceeds 0.99 (ie over 99% of cycles cross the mean stress level, and the long term root mean squared stress range of the process $\sigma_{LTrms} (= \sigma_{range}/(2\sqrt{2}))$ comprises four average stress levels:

- i) 4% @ $1.960\sigma_{LTrms}$
- ii) 30% @ $1.366\sigma_{LTrms}$
- iii) 40% @ $0.799\sigma_{LTrms}$
- iv) 26% @ $0.347\sigma_{LTrms}$

For each of these stress levels there are variations in the magnitude of each individual stress cycle, however, these four levels do give an indication of the relative damage that can be attributed to each stress range.

In Table 7.6, the damage attributable to each stress range level is estimated (assuming no change in the slope of the S-N curve at low stress levels). It can be seen that for these specimens, the 26% of cycles at the lowest stress range contribute to less than 2% of the damage. Therefore, the difference in fatigue life between no change in slope and a cut-off endurance limit at around 90 N/mm² is inconsequential for these specimens.

Joint Ref.	T mm	S N/mm ²	S _B N/mm ²	Meas. cycles x10 ⁶	Est. life x10 ⁶	Est. damage	Total damage D _s
T39/8	16.0	162.1	317.7	0.096	0.248	0.388	1.65
			221.4	0.720	0.732	0.984	
			129.5	0.960	3.656	0.263	
			56.2	0.624	44.633	0.014	
T205	32.0	173.0	339.1	0.042	0.204	0.208	0.89
			236.3	0.318	0.602	0.529	
			138.2	0.424	3.007	0.141	
			60.0	0.276	36.704	0.008	
T207	32.0	231.9	454.5	0.092	0.085	1.092	4.65
			316.8	0.693	0.250	2.773	
			185.3	0.924	1.249	0.740	
			80.5	0.601	15.245	0.039	
T212	32.0	248.7	487.4	0.015	0.069	0.222	0.94
			339.7	0.114	0.203	0.563	
			198.7	0.152	1.013	0.150	
			86.3	0.099	12.362	0.008	
T213	32.0	98.2	192.4	0.344	1.115	0.309	1.31
			134.1	2.580	3.293	0.784	
			78.4	3.440	16.455	0.209	
			34.1	2.236	200.883	0.011	

Table 7.6 Variable amplitude tests that pass the final screening criteria, from UKOSRP I (1989) and UKOSRP II (1989b)



Comparing the data from runners retested to failure and narrow band variable amplitude, for joints with both acceptable and poor weld profile, to the mean and design S-N curves specified in Sections 7.1 and 7.2, indicates that the fatigue lives of acceptable weld profile joint are in-line with constant amplitude results, while the specimens with poor weld profile tend to fall below the mean S-N curve but above the appropriate design S-N curves, as illustrated in Figure 7.3.

While there is evidence from tests on plate connections, in particular, that an endurance limit occurs in-air under constant amplitude loading at around $N = 10^7$, the results from connections under variable amplitude loading are more uncertain. The point at which any endurance limit or reduced slope may be applied must be somewhat arbitrary due to the lack of data and inconsistencies in cycle counting methods and Miner's sum. Basing such an endurance transition on fatigue life rather than stress appears justified since a lower endurance limit could be anticipated for thicker joints due to the larger, coarser grain size with more unfavourably shaped inclusions and the higher probability of having a significant initial defect.

The work of Mohr (1995) at EWI has shown, from a fracture mechanics model, that fatigue damage at low stresses under variable amplitude loading is a function of the loading mode and the specimen thickness. Most work to date has concentrated on tensile load on relatively thin attachments, leading to the commonly applied change of slope from m to $m+2$ at 10^7 cycles. However, Mohr has found that for thicker plates and for loadcases more typical of those in tubular connections a change in slope of the S-N curve from m to $m+1$ is more suitable. Despite the current lack of independent tests or FE data these findings are recommended in this Guide, being more conservative than those of the current T or X S-N curves in-air.

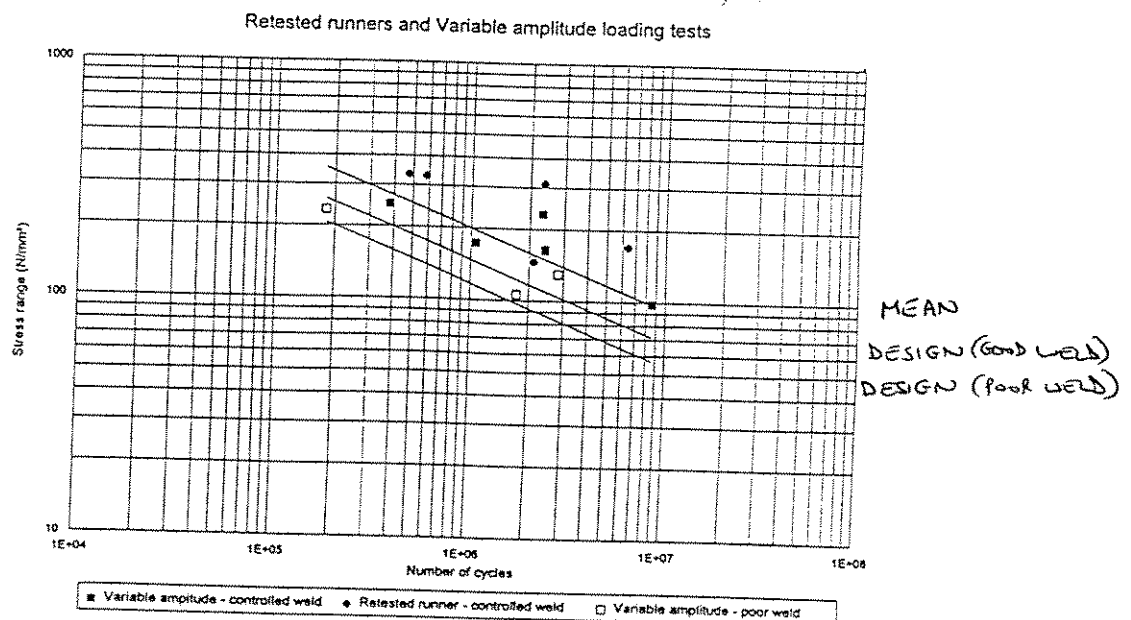


Figure 7.3 Mean S-N curves for runners retested and for narrow band variable amplitude loading



7.4 Highly Stressed Tubular Joints

The S-N approach assumes that stresses do not exceed the elastic limit. However, given that stress concentrations are generally very localised around hot-spot locations, offshore tubular joints may experience stresses that exceed local yield but do not cause significant plastic deformation.

In Section 6.2.3, the different approaches employed in the codes for specifying a maximum allowable stress range were presented. While designers are given guidance on the behaviour of joints under one extreme load and for many lesser loading cycles where the magnitude of the peak hot-spot stress does not exceed the material yield stress, there is little guidance on the treatment of stresses between these values. Therefore, under the current codes, reassessment of joints subjected to several high stress cycles implies that there is no remaining life on these joints, even though no visible cracking may be evident.

In Section 6.2.3 an alternative approach was suggested. This approach is summarised below. While load history affects the joint behaviour beyond local yield, this approach does appear to be relatively conservative in the assumption of SCF and stress ratio and consequently, despite the aforementioned limitations, gives the designer the ability to approximate remaining life where no suitable alternative method currently exists.

For stress ranges with equivalent estimated lives below 10^4 cycles it is recommended that the S-N relationship for reassessment be based on the linear extrapolation between $S(N=10^4)$ and $S(N=1)$.

- $S(N=10^4)$ is determined from the appropriate design S-N curve.
- $S(N=1)$ is determined from the static design capacity of the specified joint, by:

i) Assuming $R = -0.25$ and that $P_y = 0.8P_u$, then

$$(1-R)P_y = 1.25P_y = P_u$$

where P_u is the ultimate load for the joint
and P_y is the yield load for the joint (not to be confused with the elastic limit at the hot-spot location).

- ii) If the axial mean stress level is compressive or unknown P_u is the compressive design resistance, else, if the axial mean stress level is tensile, P_u is the tensile design resistance.

For bending stresses, M_u is the design maximum allowable moment.

(See Chapter 3 for recommended static strength formulae.)



- iii) Determine nominal stress $\sigma_{nom} = P_u/A$ or $\sigma_{nom} = M_u/Z$.
- iv) Estimate the hot-spot stress range at static failure $S(N=1)$ by:

$$S(N=1) = \sigma_{nom} \cdot SCF$$

(See Chapter 4 for recommended SCF formulae)

7.5 Chord Axial Loading

In Section 6.1.2, the application of a compressive chord loading of 77 N/mm² to the chord ends during the fatigue tests led to a significantly enhanced fatigue life under axial brace load or IPB. Screening this data in the manner described in Section 7.1, reduces the database to only one joint with an acceptable weld profile, while there are a further three joints with poor weld profiles.

In Figure 7.4, these four data points are compared to the mean S-N curve proposed for tubular joints. It can be seen that all four specimens exhibit lives in excess of those estimated for joints with no chord end loading. The three joints with poor welds have an average damage of $D_s = 2.58$, while the one joint with an acceptable weld profile has a damage summation of $D_s = 10.71$.

It should be noted that no tests have been performed with a significant tensile axial load or a bending moment applied to the chord ends and, therefore, it may be that these loadcases significantly reduce the fatigue life of the joint. This is an area worthy of further consideration, however, at present, no account of chord end loading is made in determining either SCFs or fatigue life.

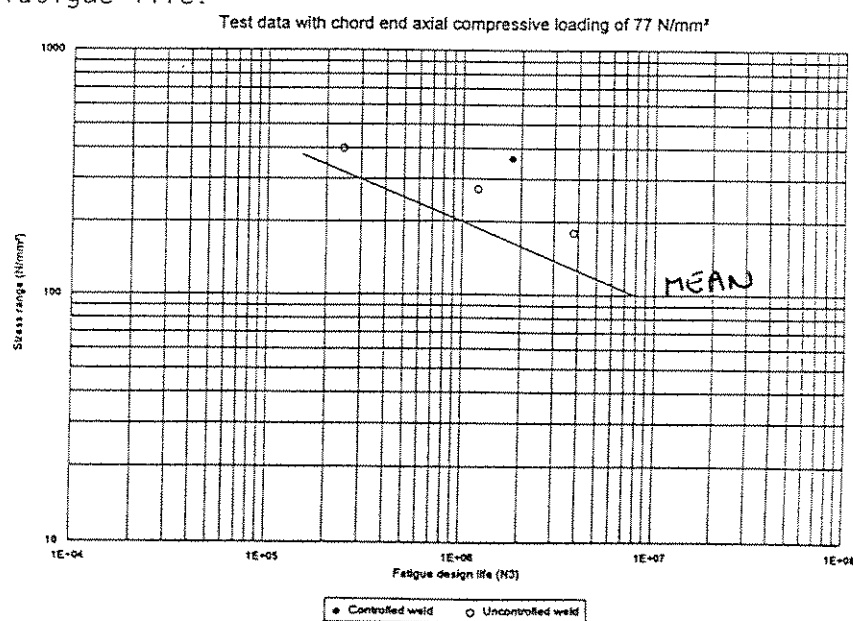


Figure 7.4 Mean S-N curves for joints tested with compressive chord axial loading of 77 N/mm²



7.6 Summary

For joints tested in-air the following S-N curves have been found to best represent the test data collated in this Guide and thoroughly screened. These S-N curves are illustrated in Figure 7.5.

The mean S-N curve for tubular joints in-air with no chord end loading is:

$$\log(N) = 12.900 - 3.\log(S_B) \quad 10^4 \leq N \leq 10^7$$

$$\log(N) = 14.867 - 4.\log(S_B) \quad N \geq 10^7$$

The design S-N curve is given by:

$$\log(N) = 12.500 - 3.\log(S_B) \quad 10^4 \leq N \leq 10^7$$

$$\log(N) = 14.333 - 4.\log(S_B) \quad N \geq 10^7$$

where $S_B = S.(T^*/16)^{0.25}$

and T^* is the thickness of the member under consideration ($T^* \geq 16\text{mm}$).

ie. The design fatigue life is 40% of the mean fatigue life.

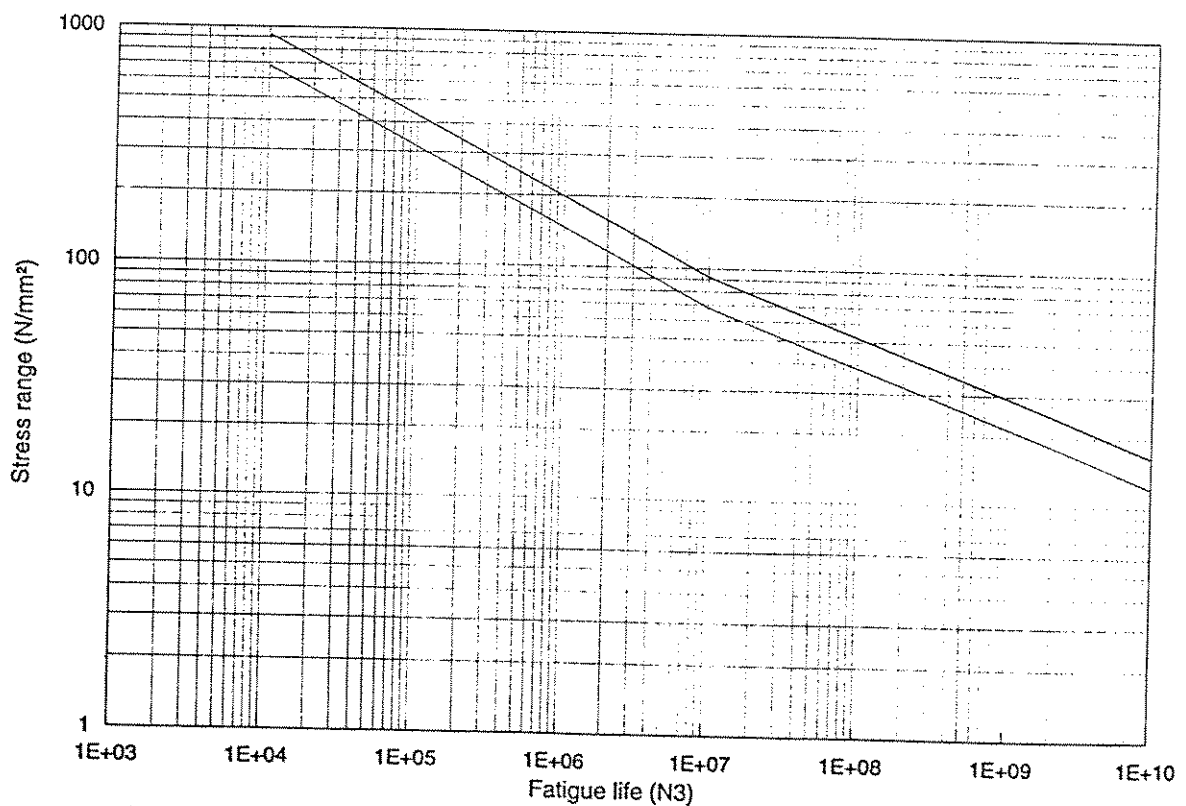


Figure 7.5 Mean and design S-N curves for joints tested in-air



For reassessment only, the remaining life for joints with poor weld profile should be based on the following design curve:

$$\log(N) = 12.200 - 3.\log(S_B) \quad 10^4 \leq N \leq 10^7$$

$$\log(N) = 13.933 - 4.\log(S_B) \quad N \geq 10^7$$

where $S_B = S \cdot (T^*/16)^{0.35}$

and T^* is the thickness of the member under consideration ($T^* \geq 16\text{mm}$).

ie. The design fatigue life of uncontrolled weld profiles is 20% of the mean life, or half the design life, of joints with acceptable weld profiles for the basecase of $T = 16\text{mm}$.

To estimate remaining life in joints that have experienced significant stress ranges, beyond the elastic limit, the S-N curve should be interpolated between the S-N value at $N = 10^4$ and at $N = 10^0$

The stress range at $N = 10^0 = 1$ can be based on the static design capacity of the specified joint, as follows:

$$\sigma_{\text{range}} (N=1) = \sigma_{\text{nom}} \cdot \text{SCF}$$

where $\sigma_{\text{nom}} = P_u/A$ or $\sigma_{\text{nom}} = M_u/Z$.

If the axial mean stress level is compressive or unknown P_u is the compressive design resistance; else, if the axial mean stress level is tensile, P_u is the tensile design resistance. For bending stresses, M_u is the design maximum allowable moment. See Chapter 3 for recommended static strength formulae and Chapter 4 for relevant SCF formulae.



8. INFLUENCE OF ENVIRONMENT

Most fatigue damage on fixed steel jacket structures tends to be associated with either the first level beneath the waterline or near to the base of the jacket. At both these regions of the jacket the tubular joints are continually subjected to the corrosive effects of seawater. In this Section the effect of seawater on tubular joint fatigue life is appraised in both the free corrosion (FC) condition and with varying levels of corrosive protection (CP) applied.

Due to the relatively few data from tubular joints tested in-seawater emphasis will be placed on the behaviour of the joints in-seawater relative to the behaviour of joints in-air, in accordance with the approach adopted in most design codes.

8.1 Design Codes

The API and AWS X and X' curves are presented as lower bound S-N curves to a database of test results covering all available data, irrespective of the loading, geometry, joint complexity and environment. It has been recognised in a review of the API approach by Marshall (1993) that the results from tests in-seawater lie, on average, below those from tests in-air. However, although the seawater data is nearer to the design curve and therefore 'less safe' no modification to these lower bound S-N curves was needed to account for seawater effects.

The Lloyd's Register Q curve (Lloyds 1989) assumes that CP and PWHT have been applied in the approved manner. No change of slope or endurance limit is specified with this curve, unless it can be justified by the designer.

The effect of seawater on fatigue life as described by the T S-N curve is treated differently by the current HSE (1993a), DnV (1992) and Canadian (CAN/CSA 1992) codes.

In previous UK HSE code (1993a), the fatigue life of a tubular joint in-seawater with adequate CP is treated in the same way as a joint in-air (ie. the T curve was applied). With inadequate, or no, CP the S-N curve is reduced by a factor of two on life and no relaxation in the slope of the S-N curve at $N = 10^7$ specified.

DnV (1992) follow the same approach as the UK HSE except for an additional reduction factor on the allowable damage sum, which is 1.0 above the splash zone, 0.5 below or in the splash zone, and 0.33 if there is no access for inspection and repair (which is considered to be the case in the splash zone in harsh environments such as the North Sea).

The Canadian code (CAN/CSA 1992) follows the same approach as the UK HSE code except that the S-N curve for submerged joints protected by CP is reduced by a factor of two on life and therefore only differs from the unprotected joint S-N curve in-seawater for $N > 10^7$.



In the latest modifications to the HSE Guidance Notes (HSE 1995) more severe penalties are applied to joints in-seawater. The T' curve is reduced by a factor of two on life for joints with adequate CP subjected to stresses in excess of $S_B = 95 \text{ N/mm}^2$ for the basecase thickness of $T = 16\text{mm}$. Beneath $S_B = 95 \text{ N/mm}^2$ the T' curve changes slope to $m = 5$ and merges with the in-air T' curve. For joints in-seawater under free corrosion conditions a factor of three is recommended with no change of slope at low stress ranges.

8.2 Review of Published Data

The database of joints in-seawater is given in Appendix D.

The main programmes of work and their individual conclusions are summarised below.

I	Cole (1990, 1993)		42 X joints, CP = - 850mV
II	Tubby (1994)	CA VA	4 TT joints, CP = -1030mV 10 TT joints, CP = -1030mV
III	Ramachandra Murthy (1994)		2 T/Y joints, FC simple joints 9 T/Y joints, FC stiffened joints
IV	Dover (1987, MaTSU 1992)	VA PWHT + CA PWHT + VA	4 T joints, CP = -850mV 4 T joints, CP = -850mV 2 T joints, CP = -850mV
V	Hara (1986)		4 T joints, FC 4 T joints, FC (ground)
VI	Gerald (1987)		6 X joints, CP = - 800mV
VII	Wylde (1988)		2 T joints, FC 3 T joints, FC (ground)
VII	UKOSRP II (1989a, 1989b)		4 T joints, CP = - 850mV
IX	Dijkstra and de Back (1981)		1 T joints, CP = - 850mV 3 T joints, FC
X	COSRP (1989)		2 T joints, CP = -850mV stiffened joints

8.2.1 Cole (1990 and 1993)

Cole (1990, 1993) reported comparisons of over 70 T-butt joints and over 45 X nodes both in-air and in-seawater with CP.

In Cole (1990), 25 X joint tests in-seawater with CP were discussed. These X joint tests comprised nine joints under IPB with normalised steel, eight joints under IPB with controlled rolled steel, four joints under IPB with accelerated cooled steel, two joints under tensile axial load with normalised steel



and two joints under tensile axial load with controlled rolled steel. In all cases the chord thickness was $T = 32\text{mm}$. No test results were tabulated in this Reference, although S-N plots were reproduced. It was found that neither the steel treatment nor the loading mode appeared to significantly affect fatigue life. It was reported that the fatigue life at low stress ranges was similar to, or even in excess of, that for in-air, while at high stress the life was around half that for in-air.

In Cole (1993), the results from a further seventeen X joints in seawater with CP and three X joints in-air were reported, under IPB loading, with $T = 50\text{mm}$. This enabled the authors to make conclusions about the thickness effect and the effect of seawater on joints with corrosion protection. Again the results were only presented as an S-N curve. It was concluded that the thickness effect in plate tests in-air differed from that in-seawater and with that for tubular joints. Again a consistent reduction in fatigue life was observed in joints in seawater with CP of -850mV . The authors suggested that this reduction in life was around two and argued that this reduction should be applied at all stress ranges.

For simple tubular joints in-air this data would have failed the screening criteria. However since this dataset represents nearly two-thirds of the data for tubular joints in-seawater with CP waiving the screening criteria appears justified. Consequently, data values have been estimated from the S-N plots.

The accuracy of this method could be checked for the 25 X joints in Cole (1990) where a best fit expression was reported for this data as:

$$\log(N3) = 13.4 - 3.43\log(S) \quad S_E = 0.128$$

The stress:fatigue life data based on the S-N plot in Cole (1990) is given in Appendix D and yields:

$$\log(N3) = 13.15 - 3.31\log(S) \quad S_E = 0.135$$

which is not significantly different. Attempts will be made to obtain the exact stress-life values and further details concerning the test programme.

8.2.2 Tubby (1994)

In this programme four TT joints were tested under CA loading and ten TT joints were tested under broad band VA loading in-seawater with CP of -1030mV . The TT joint configuration was discussed in Section 5.2 and was found to give inconsistent results in-air, with measured lives around half those typical of simple tubular joints. Consequently these configurations had to be screened out of the in-air database.

Therefore, in this Section the data are compared to the in-air database from the same study, but the seawater results are not included in the assessment in Section 8.3.



In comparison with the relatively low life in-air TT joints, Tubby (1994) concluded that the average reduction in life for the seawater tests with CP = -1030mV was a factor of 0.6, although there was considerable scatter in these results. At low stress, the data appeared to be less affected by seawater and the measured lives were similar to, if not greater than, those in-air at the same stress range.

8.2.3 Ramachandra Murthy (1994)

Ramachandra Murthy (1994) within the Indian SERC programme examined the free corrosion behaviour of nine stiffened T/Y joints and two unstiffened T/Y joints under axial load in warm seawater (25°C). Due to complex cracking near the ring-stiffeners the average free corrosion reduction factor on life of around four may be larger than expected, see Section 10.3. However, the two joints without stiffening also exhibited lives around one-quarter of those in-air.

8.3.4 Dover (1987, MaTSU 1992)

Within the scope of the 'Cohesive programme of research and development into fatigue of offshore structures', Dover (1987) reported results from eight T joints tested in-seawater with CP of -850mV. Four tests were tested under CA loading with PWHT applied (T = 19mm) while four were tested under broad band VA loading without PWHT. In MaTSU (1992) a further two tests under CA loading with PWHT in-seawater with CP applied (T = 16mm) were reported, although these have yet to be formally published.

Overall it was concluded (Dover 1987) that PWHT had no effect on these joint lives and that the reduction in life compared to in-air tests led to Miner's sums between 0.5 at high stress to 1.0 at lower stress ranges of around 110 N/mm². The VA data was modelled using the rainflow and range-pair cycle counting methods and it was found that the Miner's summation was on average 28% larger using the rainflow method. Cycle counting methods for broad band loading are discussed in Section 6.3.3.

8.3.5 Hara (1986)

Hara (1986) reported the results of 490 MPa class steels produced by both normal and thermo-mechanical control processes under free corrosion conditions. The eight T joint tests (T = 20mm) under axial load considered differences in these two steel processes and the effect of weld toe grinding on fatigue life. The results were inconsistently reported in terms of load range, nominal strain range and hot-spot strain range. It would appear that the most reliable data is the hot-spot 'stress' range plotted in this paper, with the hot-spot stress = hot-spot strain x E ($\approx 200,000$ N/mm²). In this assessment the stress has been increased by a further 20% to account for differences between SCFs and SNCFs.

Overall, it appears that the different steel processes have no effect on fatigue life. Grinding enhanced fatigue life in-seawater under free corrosion, particularly in the low endurance region where fewer corrosion pits formed.



8.2.6 Gerald (1987)

Within the French scope of the ECSC project, Gerald (1987) reported the results from six X joints with improved welds in-air and in-seawater with CP of -850mV.

As-welded the seawater test had a life around half that in-air. However, following TIG dressing the reverse effect was recorded with the life of the seawater test at least twice that for in-air (nb the seawater test was a runner at $N = 10^7$). The two tests with shot peening were both runners and therefore no conclusions could be made.

8.2.7 Wylde (1988)

Wylde (1988) considered the effect of FC on simple T joints both with and without grinding of the weld toe. Two joints were investigated with no grinding and three with grinding of the weld toe. Grinding the weld toe enhanced fatigue life.

The fatigue lives in-seawater were consistently less than the equivalent in-air lives, although the reduction in life was by less than a factor of two.

8.2.8 UKOSRP II (1989a, 1989b)

As part of the second phase of the UKOSRP study, four T joints were tested in seawater with CP of -850mV. All four joints were tested under axial load with a chord thickness of $T = 32\text{mm}$.

Overall it was noted that fatigue lives from these tests in-seawater were significantly less than for the equivalent in-air joints, and a reduction factor of two on life was recommended.

8.2.9 Dijkstra and de Back (1981)

In the ECSC project, Dijkstra and de Back (1981) in the Netherlands tested one T joint in-seawater with CP of -850mV and three T joints under free corrosion. The T joint with CP and one of the T joints under free corrosion had $T = 32\text{mm}$ while the other two T joints under free corrosion had $T = 16\text{mm}$.

It was concluded from these tests that the fatigue life in-seawater was 0.4 times the lifetime in-air. Although differences in crack initiation and growth were reported, no difference in life between the tests in-seawater with and without CP was noted.

8.2.10 COSRP (1989)

Within the scope of the COSRP (1989) two internally ring-stiffened T joints were tested under axial load in seawater with CP of -850mV applied. These were compared to a further eight stiffened joints in-air, of which two were tested under pure axial load. In addition, six pipe to plate joints were tested in-seawater (two with CP = -850mV, two with CP = -1100mV and two under free corrosion) and a further two pipe to plate joints were tested in-air.



The two tubular joints in-seawater exhibited lives slightly below half those in-air, with the in-air data correlating well with the simple joint mean S-N curve.

The two pipe to plate tests in-air also gave good correlation to the tubular T mean S-N curve. By comparison, the two pipe to plate tests with optimum CP exhibited lives around 1.8 below in-air, while the overprotected CP pipe to plates gave lives around 2.8 below the in-air curve. Under free corrosion, these pipe to plate connections gave even lower lives with an average reduction factor of around 5.0 on in-air life.

8.3 Appraisal of Test Data

8.3.1 In-seawater with corrosion protection

Figure 8.1 illustrates the S-N behaviour of tubular joints in seawater with cathodic protection (CP). The data has been obtained from the work by Cole (1990, 1993), Dover (1987, MaTSU 1992), UKOSRP II (1989b) and Dijkstra and de Back (1981). All these tests have CP levels of around -850mV.

It can be seen that the data from the seawater tests consistently lies below that for in-air (nb. the S-N curve in-air has been modified to $T = 32\text{mm}$, since most in-seawater data is from joints with $T = 32\text{mm}$). The average damage sum for these joints is $D_s = 0.65$ compared to the in-air S-N curve. For each data set the average damage sums are: Cole $D_s = 0.67$ from 42 tests, Dover $D_s = 0.62$ from ten tests, UKOSRP II $D_s = 0.59$ from four tests, and Dijkstra and de Back $D_s = 0.48$ from one test.

Fatigue behaviour of tubular joints in-seawater with CP

(All data normalised to $T = 32\text{mm}$)

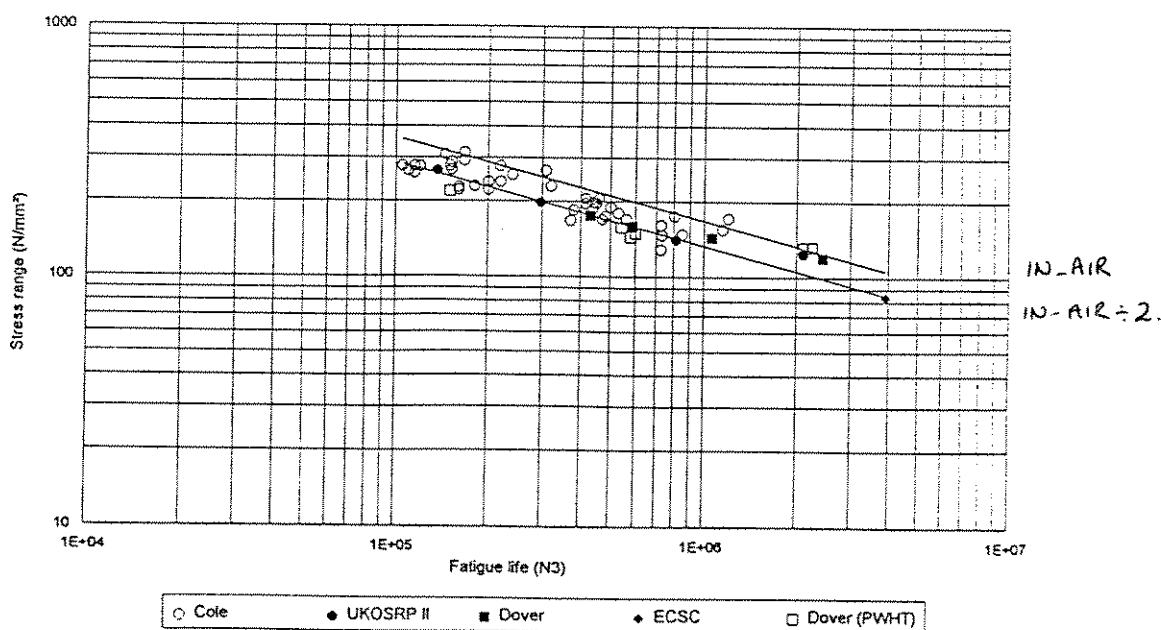


Figure 8.1 Mean T and 0.5T S-N curves for tubular joints in seawater with CP



The trend for a reduced slope in the S-N curve, particularly at low stress levels has been noted in several papers, with the lives of joints in-seawater with CP approaching and often exceeding those in-air at low stress ranges. This possible trend may be due to the build-up of calcareous scale deposits within cracks, although their reactions and effects upon fatigue life are very complex. UKOSRP II (1989a).

It should be noted that, with the exception of six tests by Dover ((1987) and referenced within MaTSU (1992)), all specimens were tested under constant amplitude loading. Therefore, the increase in life at low stress ranges may be due to an increased endurance limit for joints in-seawater with CP. It should also be noted that two of the three joints with long lives at low stress range tested by Dover were PWHHT which has more effect at low stress ranges (see Section 9.2.1).

In UKOSRP II (1989a) the effect of differing levels of CP was investigated with regard to plate connections under CA loading, while in COSRP (1989) CP level on pipe to plate joints under CA loading was assessed. In the UKOSRP II study it was concluded that lower lives were generally associated with high CP levels, although most data, including joints under free corrosion, fell near to the mean F plate curve, and therefore did not exhibit a significant reduction in life when compared to in-air tests. In the COSRP pipe to plate tests, reduction factors of 1.8 and 2.8 were reported for CP levels of -850mV and -1100mV respectively.

In conclusion, an average factor of around 0.65 on life was noted for joints with CP = -800mV to -850mV when compared to the in-air S-N curve. This is in-line with the findings by the HSE for joints subjected to stress ranges of around 95 N/mm² or more. Little data exists for welded joints in seawater at lower stress ranges under constant amplitude loading.

Therefore, it is recommended that the HSE proposals are adopted with a reduction factor of two on life in-seawater with adequate CP. Optimum CP (Ag/AgCl) is considered to be in the range -750mV to -1000mV otherwise the joint should be considered to be under free corrosion conditions (see Section 8.3.2).

This modification may be applied to the S-N curve in accordance with the guidance given by the HSE. Alternatively a reduction factor of two on life may be taken following the fatigue life calculation - in-line with the approach favoured in the Canadian code or in the DnV code inspectability criteria for all joints below the splash zone.

8.3.2 In-seawater under free corrosion

Figure 8.2 illustrates the S-N behaviour of tubular joints in seawater under free corrosion (FC). It can be seen that little data is available on tubular joints under FC, with most of this data failing to meet the strict screening criteria applied to the in-air database.



Data in the as-welded state has been obtained from Hara (1986), Wylde (1988), Dijkstra and de Back (1981) and Ramachandra Murthy (1994). It can be seen that, with one exception, this data lies below the mean in-air S-N curve.

The average damage sum for these joints is $D_s = 0.52$ compared to the in-air S-N curve. For each data set the average damage sums are: Hara $D_s = 0.67$ from four tests at 5°C, Wylde $D_s = 0.80$ from two tests at 10°C, Dijkstra and de Back $D_s = 0.37$ from three tests at 20°C and Ramachandra Murthy $D_s = 0.15$ from two tests at 25°C. Therefore, there is a significant degree of variation between these test data, with some apparent correlation to water temperature. However, it should also be noted that the two pipe to plate tests in the COSRP (1989) gave low damage sums around $D_s = 0.2$ in seawater of 5°C.

Fatigue behaviour of as-welded tubular joints in-seawater under free corrosion
(All data normalised to $T = 16\text{mm}$)

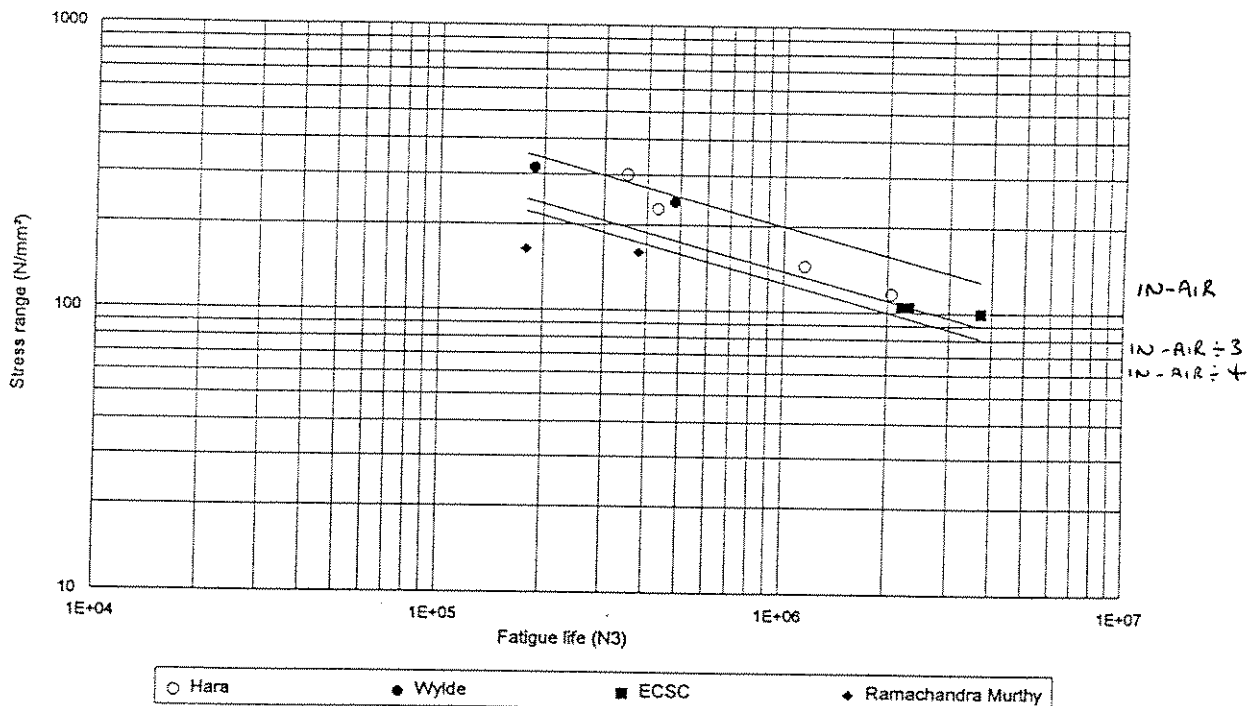


Figure 8.2 Mean T, 0.33T and 0.25T S-N curves for tubular joints in seawater under FC

In UKOSRP II (1989a) the effect of seawater temperature on fatigue life under free corrosion was investigated with regard to plate specimens. It was concluded that the life could be reduced by a factor of two between tests at 5° and tests at 20°C, although caution was expressed due to the lack of data.

In conclusion, it has generally been noted in tests on both tubular and plate connections that the fatigue life under free corrosion conditions is less than with optimum CP levels applied. However, there is considerable scatter and a lack of good quality data, particularly for tubular joints under FC conditions.



Due to the lack of quality data it is recommended that a reduction factor of three be applied for joints under free corrosion in cool waters ($\leq 10^\circ\text{C}$), and of four be applied for joints under free corrosion in warm waters ($> 10^\circ\text{C}$), against the in-air life. While the reduction in life due to temperature effects is less than two, it is recognised that based on this dataset the factor of three for FC in cool waters is a lower bound and therefore potentially conservative.

At low stress ranges, there is no tubular joint data and few plate data. Under variable amplitude loading it has been suggested that no change in slope of the S-N curve should be taken since crack-growth can occur at relatively low stresses due to the corrosive effects of seawater. This proposal has been adopted in this Guide and no change of slope is recommended for $N > 10^7$ cycles.

8.3.3 In-splash zone with coating

In addition to joints fully submerged in-seawater, it is important to protect joints in the splash zone against fatigue corrosion, where the corrosion protection system is deemed inoperative. To this effect fatigue tests were performed on plate connections in UKOSRP I (1989) under free corrosion conditions with intermittent immersion in seawater (six hours wet, six hours dry). However no difference was noted in comparison with the fully immersed joints under free corrosion conditions.

In UKOSRP II (1989a) the effect of applying paint coatings was assessed. Three types of coating were investigated on plate connections:

1. Polyamide adduct cured epoxy coal tar system
2. High build epoxy system
3. Isocyanate cured epoxy coal tar system

All coatings had beneficial effect in comparison to the unprotected data, particularly at low stress ranges. At $N = 10^6$ the average benefit in terms of increased strength was:

- | | |
|-----------------------------|-------|
| 1. Polyamide cured coating | = 38% |
| 2. Epoxy coating | = 17% |
| 3. Isocyanate cured coating | = 26% |

These average strength benefits are equivalent to increased lives over free corrosion of 2.6, 1.6, 2.0 (for $m=3$) and 3.6, 1.9, 2.5 (for $m=4$). The gain in life comes from before the crack initiation and crack growth phases of the fatigue life. Therefore, for typical offshore joints under relatively low stress ranges, where the gain in strength appears particularly effective, either of the cured coatings (Polyamide or Isocyanate) would be sufficiently effective to allow the in-air S-N curve to be used. However, it is important to note that there needs to be an effective coating (and therefore quality control) and overstressing these regions during installation needs to be avoided.



9. INFLUENCE OF MATERIALS AND POST-FABRICATION TREATMENTS

9.1 High Strength Steels

The influence of seawater on the fatigue behaviour of higher strength steels is thought to be possibly more severe than for medium strength steels because of their greater susceptibility to hydrogen induced cracking. This problem was addressed by the HSE (1993) in Section A21.3 of their Guidance Notes, and states that 'Since early 1988, the HSE and Department of Energy have been investigating a widespread problem of hydrogen-assisted cracking of high strength steels, particularly those used in the leg chords and spudcans of many self-elevating Offshore Installations.'

The findings of the investigations and of several meetings with owners, operators, Certifying Authorities and relevant Industry Associations, are set out below as conclusions and guidance to ensure awareness of the problem and of how it may be dealt with.

This information should be read in conjunction with Sections 4, 12 and 33.

The conclusions of the research may be summarised as follows:

- a) Some high strength steels can be susceptible to embrittlement by hydrogen which can arise from the cathodic protection (CP) system, particularly in the absence of oxygen, or from the generation of hydrogen sulphide in anaerobic conditions (eg. in spud cans).
- b) The susceptibility of the steel to hydrogen-assisted cracking is influenced by residual stresses which can be high in the case of high strength steels with no post weld heat treatment.
- c) The susceptibility of steels to hydrogen embrittlement can be established by tests.
- d) Commonly used CP systems are likely to give excessive negative voltages which may render high strength steels susceptible to hydrogen embrittlement. However, CP systems are now available which can offer controlled voltages with a predetermined limit to the negative value, and it is recommended that this type of system be used.
- e) The potential susceptibility of high strength steels to hydrogen embrittlement should be fully evaluated at the design stage as part of the material selection process, as should the design of the CP system. Internal volumes which can be sealed, such as the interior of spud cans on jack-up installations, may be protected by a corrosion inhibitor with an approved biocide.
- f) Surveys should take account of the possibility of the occurrence of hydrogen-assisted cracking.



- g) The finding and characterisation of hydrogen-assisted cracks required high quality non-destructive testing. Where paint coatings are removed (eg. in dry dock) to facilitate inspection of areas which would normally be submerged and thus protected by CP, the coating must be fully reinstated. If underwater inspections are necessary, paint coatings should not be removed, but NDT methods which can give adequate levels of detection through paint coatings should be used.

The lack of data on the effects of environment on the fatigue behaviour of high strength steel welds resulted in the HSE (1993a) including a caution for the application of the treatment of environmental effects for steels with yield strengths greater than 400 N/mm².

More recently, MaTSU (1992) have reported a limited number of tests on welded plates with yield stresses up to 540 N/mm². The range of environmental reduction factors in both freely corroding and cathodically protected environments were generally similar to those found for medium strength steels. This led to the recommendation that the high strength steel limit be increased to 500 N/mm² for plate specimens, but since only two tubular joints with stresses significantly in excess of 400 N/mm² have been tested in seawater, no increase in this limit was recommended for tubular joints.

In the modified HSE Guidance Notes (1995) the recommendations of the background document were summarised into a new Section (21.2.15). This states that:

The basic design S-N curves presented in this section should only be applied to steels with minimum guaranteed yield strengths less than 400 N/mm².

However, for welded plate details there is evidence that all the design S-N curves for class P are appropriate for steels with yield strengths up to 500 N/mm².

For higher yield strength steel (ie. for nodal joints, greater than 400 N/mm² and for welded plate details, greater than 500 N/mm²) data from an approved test programme or fracture mechanics analysis method which includes the effects of environment, cathodic protection level and temperature, should be used to establish the fatigue design parameters'.

Recent work at Cranfield, summarised by MTD (1995), suggests that fatigue growth in higher strength steels (up to 550 N/mm²) are in-line with steels of yield strength 350-450 N/mm². Therefore, it would appear reasonable to allow the use of higher strength steels in tubular joints up to 500 N/mm² with caution. Reference to test data should be made wherever possible.



9.2 Post Fabrication Treatment

In this Section, the effect of post fabrication joint improvement methods are considered in terms of improved fatigue behaviour. The following methods are considered:

- Post-Weld Heat Treatment (PWHT)
- Weld toe grinding
- Hammer peening
- Shot peening
- TIG dressing

In all of these cases the improvement noted tends to be illustrated by a rotation in the S-N curve such that the slope is more shallow, and the endurance limit under constant amplitude loading appears to become effective at higher stress levels.

In this Section, since there is a tendency for the S-N curve to be increased relative to the stress axis, fatigue benefit is generally expressed in terms of an improvement in fatigue strength as well as in fatigue life.

Reference should also be made to Chapter 7 where the use of these techniques in repair are assessed.

9.2.1 Post-weld heat treatment (PWHT)

9.2.1.1 Design Codes

Section 21.8.10 of the HSE Guidance Notes (HSE 1993) covers the effects of PWHT and circumstances in which PWHT is required.

'PWHT brings about a beneficial reduction in the level of tensile residual stress. It will also affect the mechanical properties of weldments but not always in a beneficial manner. The net effect on defect tolerance with regard to brittle fracture is usually beneficial, but each case should be treated on its merits.' Reference should be made to Chapter 2 for more details on PWHT application and guidance requirements.

In the proposed modifications to the HSE Fatigue Guidance Notes (HSE 1995) a new addition has been made to the section 'Stresses to be Considered' to cover the effect of PWHT.

'For PWHT joints the fatigue performance may improve as the load applied becomes more compressive. However, under purely tensile loading the fatigue performance should be regarded as that for as-welded joints. It is recommended that for PWHT joints, no advantage in terms of fatigue performance should be taken at the design stage.'



In addition to the clause stating that the stress range for PWHT should be the same as the as-welded case, HSE (1993b) states: *'However, in the event that it can be demonstrated using validated techniques that a compressive component of the combined applied and residual stresses exists and can be quantified, it would be permissible to assume a stress range for fatigue of the tensile component plus 60% of the compressive component. To ensure the effectiveness of post-weld heat treatment, the process should be carried out in accordance with accepted standards (eg. BS 5500).'*

This is the first quantitative recognition in codes of the beneficial effect of PWHT. In previous editions and alternative codes, PWHT is a safeguard against brittle fracture, through the guarantee of satisfactory standards of fracture toughness in the weld metal and heat affected zone. This treatment may also relieve the weld residual stresses which would otherwise be present at levels which can locally attain yield stress magnitude.

9.2.1.2 Review of published data

The database of joints with PWHT applied is given in Appendix E.

The main programmes of work and their individual conclusions are summarised below.

I	Lieurade (1981)	10 X joints, in-air
II	UKOSRP I (1988)	8 T joints, in-air
III	Dover (1987, MaTSU 1992)	4 T joints, seawater (CA) 2 T joints, seawater (VA)
IV	UKOSRP II (1989a, 1989b)	4 T joints, in-air

Lieurade (1981)

In the French programme of the ECSC funded project, Lieurade (1981) reported ten X joint tests. These tests, in-air, had one brace as-welded and one brace PWHT. Five joints were tested under axial load and five under IPB, with chord thicknesses in the range $T = 22\text{mm} - 78\text{mm}$ ($R = 0.1$).

In four tests failures were recorded in both the as-welded and PWHT braces, while a further three tests had failures in the PWHT brace but runners in the as-welded brace. These joints are summarised in Table 9.2.1. It can be seen that in most cases crack initiation occurs on the as-welded side prior to the PWHT side. This is in-line with expectations as most benefit of PWHT would be expected to be gained at the crack initiation and early crack growth stage, since the residual stresses involved are localised in nature. For the four joints with cracking on both sides, three fail on the as-welded side first, with the average benefit in life for these four joints only 5%. It should also be noted that the joints with the shortest life (ref. D) and longest life (ref. C') had the worst and best performance due to PWHT respectively.



Joint	AW or HT	Number of Cycles (R = 0.1)			
		N1	N2	N3	N4
A	AW	48000	140000	462000	750000
	HT	225000	350000	-	750000
B	AW	-	210000	-	580000
	HT	55000	174000	401000	580000
C	AW	260000	295000	-	1270000
	HT	130000	234000	1135000	1270000
D	AW	-	60000	333000	435000
	HT	40000	60000	300000	435000
E	AW	78000	128000	655000	911000
	HT	280000	420000	-	911000
A'	AW	55000	91000	-	191000
	HT	36000	82000	158000	191000
B'	AW	105000	130000	649000	760000
	HT	340000	395000	-	760000
C'	AW	25000	155000	650000	661000
	HT	170000	205000	722000	723000
D'	AW	125000	160000	471000	650000
	HT	135000	175000	501000	650000
E'	AW	35000	89000	464000	551000
	HT	30000	89000	507000	551000

Table 9.2.1 Comparison of as-welded and PWHT connections

UKOSRP I (1988) and UKOSRP II (1989a)

In UKOSRP I (1988) tubular joints were tested at nominal chord thicknesses of T = 6mm, 16mm, 32mm and 76mm. The HSE guidance at that time DEn (1984a) required PWHT to be applied to joints with member thicknesses in excess of 50mm. Consequently, to represent offshore practice the eight joints with T = 76mm were tested with PWHT applied. However, in assessing the results of the UKOSRP I programme it became clear that these data were affected by PWHT and consequently the scale effect was difficult to quantify for thick joints.

To determine the effects of both scale and PWHT, the second phase of the UKOSRP project (UKOSRP II 1989a) included four as-welded H joints with T = 76mm and four PWHT T joints with T = 32mm.

Overall, it was concluded that PWHT can increase the fatigue life by factors between 1.1 and 2.5 in tubular joints under axial load (R = -1) in the range $N = 10^5$ and 10^7 . Because crack initiation and early crack growth forms a larger proportion of the overall life at lower stresses the benefit of PWHT is considerably larger at low stresses (factor greater than two on life at 70MPa) than at high stresses (negligible benefit at 300 MPa). Furthermore, thick joints spend relatively less time in the crack initiation phase and therefore receive less benefit from PWHT.



Dover (1987, MaTSU 1992)

In Section 8 of this Chapter, the effect of seawater on fatigue life was considered. In this assessment, six tests by Dover (1987, MaTSU 1992) were reported with PWHT applied to the joints. It was reported that PWHT of the joints had negligible effect in the seawater environment with corrosion protection under either constant or variable amplitude loading ($R \geq 0$).

However, in Figure 8.1, it can be seen that the joints at very low stress range with PWHT do have longer lives, although it cannot be determined whether this is due to PWHT effects or seawater effects.

9.2.1.3 Assessment of PWHT effects

In Figure 9.2.1, the Lieurade (1981) and UKOSRP (UKOSRP I 1988, UKOSRP II 1989a) datasets have been reproduced.

It can be seen that the Lieurade data lies below the mean in-air S-N curve based on as-welded joints. However, as can be seen in Table 9.2.1 all the data from this Reference have lives lower than expected. Potential reasons for the low life reported in these tests are the fairly steep weld and possible inaccuracy in the SCF measurement near the weld toe.

The UKOSRP data shows a clear rotation in the S-N curve, with significant enhancement in life at stress ranges normalised to around 200 N/mm^2 for $T = 16\text{mm}$. The three joints with failures below the in-air curve are brace failures and consequently have had the brace stress adjusted for the brace thickness.

In the UKOSRP II (1989a) project, the effect of PWHT was also assessed for plate connections in-air and in-seawater with CP. It was noted that the stress ratio had a significant effect on the benefit of PWHT. For $R = -1$ there was maximum benefit (factors on life of 1.2 to 2.2), at $R = -0.5$ factors on life of 1.2 to 1.5, while at tensile $R = 0$, negligible benefit was observed.

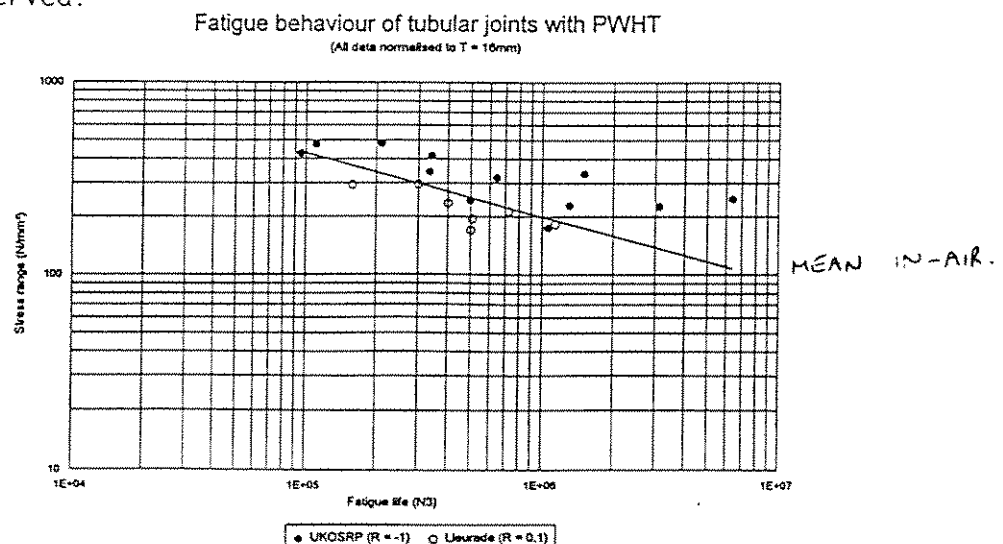


Figure 9.2.1 Effect of PWHT on tubular joints in-air



9.2.1.4 Summary

PWHT of tubular joints can improve the fatigue behaviour of tubular joints at stress ranges of $R < 0$ (ie. some compressive component), although this benefit may only be significant at relatively low stress ranges.

Therefore, it is recommended that the proposed HSE (1993b) modification be adopted, as given in Section 9.2.1.1, ie.

'For PWHT joints the fatigue performance may improve as the load applied becomes more compressive. However, under purely tensile loading the fatigue performance should be regarded as that for as-welded joints. It is recommended that for PWHT joints, no advantage in terms of fatigue performance should be taken at the design stage.'

'However, in the event that it can be demonstrated using validated techniques that a compressive component of the combined applied and residual stresses exists and can be quantified, it would be permissible to assume a stress range for fatigue of the tensile component plus 60% of the compressive component. To ensure the effectiveness of post-weld heat treatment, the process should be carried out in accordance with accepted standards (eg. BS 5500).'

9.2.2 Grinding

9.2.2.1 Design Codes

In the design codes reviewed in Section 3, improvements in fatigue due to weld toe grinding are allowed for in most codes.

API (1993) state that *'For branch thicknesses greater than 1 in. (25mm), the X-curve may be used without scale effect provided the profile is ground smooth to a radius greater than or equal to half the branch thickness. Final grinding marks should be transverse to the weld axis and the entire finished profile should pass magnetic particle inspection.'*

AWS (1992) gives guidance on obtaining the required weld profile to allow use of the curves X_1 and K_1 . The recommended weld profile is similar to that given in API (1993). AWS state that *'For the purpose of enhanced fatigue behaviour, and where specified in contract documents, the following profile improvements [wrt grinding] may be undertaken:*

- 1. A capping layer may be applied so that the as-welded surface merges smoothly with the adjoining base metal, and approximates the profile specified. Notches in the profile shall be no deeper than 1.0mm relative to a disc having a diameter equal to or greater than the brace member thickness.*
- 2. The weld surface may be ground to the profile specified. Final grinding marks shall be transverse to the weld axis.'*



AWS also state that the smooth surface profile of fully ground welds exhibit no size effects.

The current HSE (1993a) and proposed HSE (1993b) codes are essentially similar with respect to grinding benefit. The current HSE code states that *'For welded joints involving potential fatigue cracking from the weld toe an improvement in strength by at least 30%, equivalent to a factor of 2.2 on life, can be obtained by controlled local machining or grinding of the weld toe. However, it is recommended that no advantage for toe grinding should be taken at the initial design stage and only joints adequately protected from corrosion can receive this benefit.'*

'This is normally carried out either with a rotary burr or by disc grinding. The treatment should produce a smooth concave profile at the weld toe with the depth of the depression penetrating into the plate surface to at least 0.5mm below the bottom of any visible undercut and ensuring that no exposed defects remain. The maximum depth of local machining or grinding should not exceed 2mm or 5% of the plate thickness.', see Figure 9.2.2.

The proposed modification allows the same benefit of grinding in reassessment but *'It is recommended that the final grinding operation should be carried out using a rotary burr to provide a generous radius to blend with the surrounding material.'*, ie, disc grinding is no longer recommended. Furthermore, *'An appropriate NDE technique eg. BS 6072 should be used to ensure that no significant defects remain after grinding. Where appropriate, the final ground surface should be suitably protected in order to avoid local corrosion pitting prior to the application of cathodic protection.'*

DnV (1992) note that the effect of weld profiling giving the weld a smooth concave profile compared to the typical triangular or convex shape may increase the fatigue properties. Thus, provided weld profiling is carried out, an X curve in line with API RP2A (API 1993) may be accepted instead of the T curve.

For joints in seawater with adequate CP grinding may be used, once in-service, to enhance the joint life. A factor of two on life can be obtained by controlled local machining or grinding of the weld toe. This is normally carried out by a rotary burr. The treatment should produce a smooth concave profile at the weld toe with the depth of depression penetrating into the plate surface to at least 0.5mm below the bottom of any visible undercut. The maximum grinding depth should not exceed 2mm or 5% of the plate thickness, whichever is smaller.

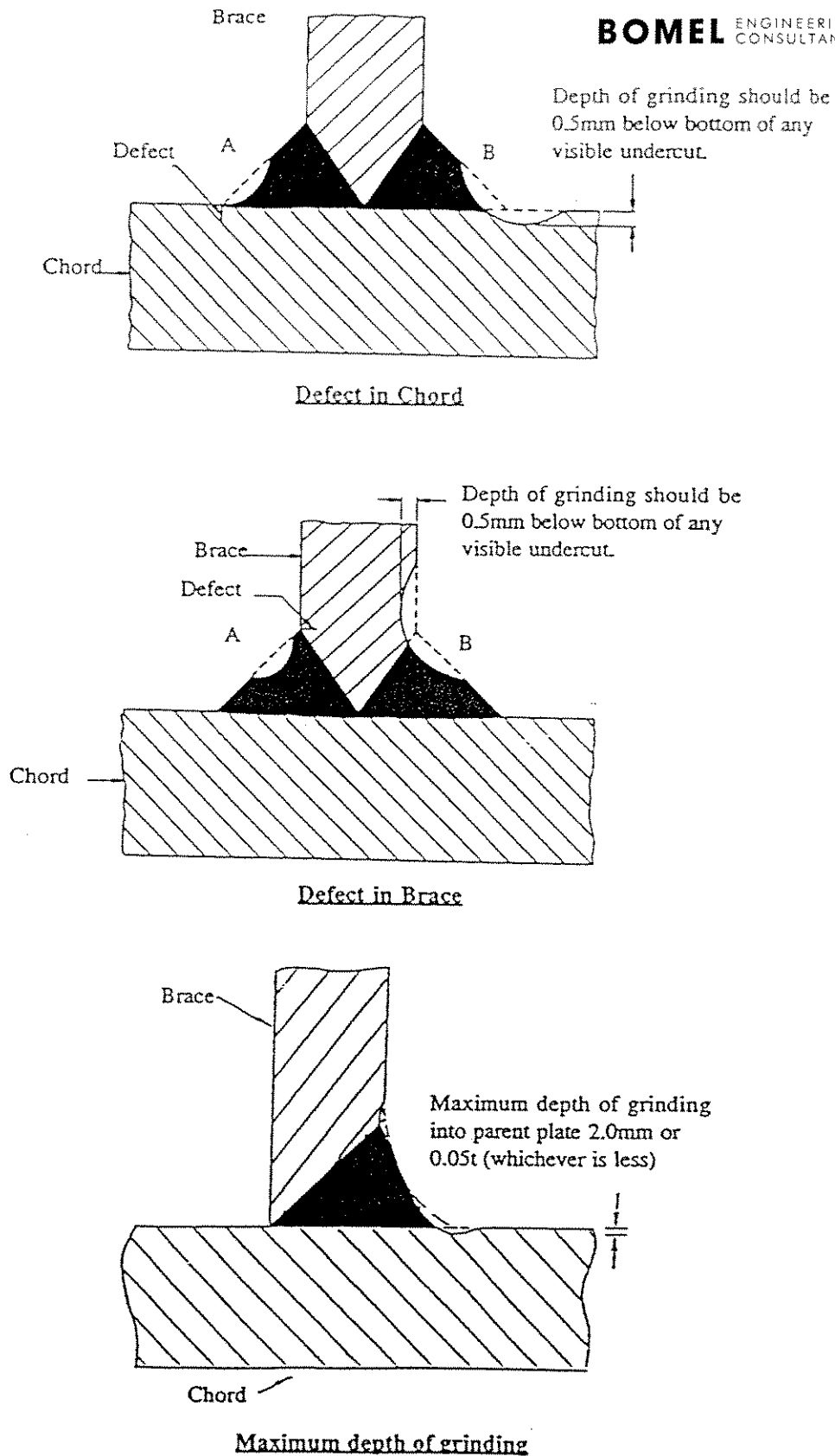


Figure 9.2.2 Weld toe grinding (HSE 1995)



9.2.2.2 Review of published data

Since the effect of grinding is local to the weld, the vast majority of studies concerned with the effects of grinding have been carried out on plate connections rather than more expensive tubular joints. In UKOSRP II (1989b) one brace of the four large H joints tested with $T = 76\text{mm}$ under axial load was ground. However, in all cases the test was terminated soon after the as-welded end of the cross-brace failed and thus no valid data on ground joints was obtained on through thickness failures. Comparing crack initiation (N2), the ground weld toes exhibited cracking 1.9 to 4.3 times later (on average over three times later) than the as-welded braces.

In Section 8 of this Chapter, seven joints were reported in seawater under free corrosion with ground welds, four by Hara (1986) and three by Wylde (1988). In comparison with the other six as-welded tests in seawater examined in these studies the benefit of grinding was equivalent to a factor of 1.7 on life. Despite being in-seawater under free corrosion the average life of these joints is around 20% greater than the mean in-air S-N curve, although there is considerable scatter in these results.

In UKOSRP I (1988) and UKOSRP II (1989a) several tests on plate connections with ground welds were also investigated.

In UKOSRP I (1988) tests were carried out on 25mm and 38mm plates under axial and bending loads ($R = 0$). It was reported that at an endurance of $N = 2 \times 10^6$, a 100% increase in strength (factor of eight on life) in-air and a 30% increase in strength (factor of 2.2 on life) in-seawater under free corrosion resulted from grinding the weld. It was also stated that comparable tests within the ECSC project, as reported by Haagensen (1981) and Van Leevwen (1981), gave improved strengths of 40% in-air (2.7 on life) and 45% in-seawater (3.0 on life).

In UKOSRP II (1989a) the effects of grinding on welds in-seawater and on welds in-air with PWHT were investigated using cruciform and T-butt specimens. In-seawater, on plate tests with $CP = -850\text{mV}$ and $CP = -1100\text{mV}$ (following pre-corrosion) it was concluded that the benefit of grinding was the same in-seawater with optimum CP as in-air. Tests in-seawater with cathodic overprotection following a period of free corrosion suggested that the benefit of grinding was less at around a factor of 1.7 on life (cf. Hara (1986) and Wylde (1988) tubular joint tests). In-air with PWHT, the fatigue behaviour was in-line with that noted for tubular joints and ground plate tests, with increased life due to grinding and additional increases in life on joints with $R < 0$ under low stress ranges due to the effect of PWHT.

Pang (1993) has modelled fillet welded joints using the MARC FE program with differing weld toe radii in-line with those produced by grinding (0.5mm, 1.0mm, 2.5mm and 5.0mm). Pang recommended a weld toe radius of 5.0mm as giving the lowest stress concentration factor. The FE analysis showed that weld toe treatment by grinding could enhance the fatigue strength by up to 53%.



Haagensen (1987, 1994) has given consideration to the improvement in fatigue life due to several techniques, including grinding, on plate specimens. In 1987, Haagensen noted a fairly consistent improvement of 50% in the fatigue strength due to grinding, and 156% in both grinding and shot peening was performed on the joint. In an extension to this study Haagensen (1994) reported fatigue strength improvements of 50% - 60% at $N = 2 \times 10^6$ cycles due to grinding and a 154% - 216% improvement when grinding was performed prior to hammer peening.

9.2.2.3 Summary

An improvement in strength of around 30% was adopted in the HSE (1993a) and DnV (1992) Guidance Notes in-air or in-seawater with adequate CP largely based on this plate data, although this benefit cannot be taken at the design stage. It appears reasonable that similar effects will result on tubular joints.

Increases in fatigue lives tend to be more significant at lower stress ranges, but even so, improvements in fatigue strength in excess of 30% are typical in-air and in-seawater with CP. In-seawater under free corrosion conditions, grinding is less effective, yet improvements in strength by a factor of 20% are common.

Due to the lack of data, it is recommended that the largest factor on life currently allowed for in guidance notes be adopted. This allowance is an increase of 30% on fatigue strength (ie. 2.2 on life) in-air or in seawater with adequate CP, as specified in the HSE (1993a) Guidance Notes.

9.2.3 Hammer peening

9.2.3.1 Design Codes

AWS (1992) gives the most comprehensive guidance on peening. The Code states that *'For the purpose of enhanced fatigue behaviour, and where specified in contract documents, the following profile improvements [wrt peening] may be undertaken:*

'The toe of the weld may be peened with a blunt instrument, so as to produce local plastic deformation which smooths the transition between weld and base metal, while inducing a compressive residual stress. Such peening shall always be done after visual inspection, and be followed by magnetic particle inspection' (as described).

Consideration should be given to the possibility of locally degraded notch toughness due to peening.

In order to qualify for fatigue categories X_1 and K_1 , representative welds (all welds for non-redundant structures or where peening has been applied) shall receive magnetic particle inspection for surface and near-surface discontinuities. Any indications which cannot be resolved by light grinding shall be repaired.



Since peening only improves a relatively limited volume of welded joint, the size effect would be expected to show up fairly soon if peening is the only measure taken; however, peening should not incur a size effect penalty where it is done in addition to profile control.'

Other design codes have not yet included detailed provisions on hammer peening and its application to offshore structures.

9.2.3.2 Review of published data

In UKOSRP I (1988) a few plate specimens of $T = 25\text{mm}$ and $T = 38\text{mm}$ were hammer peened and tested in-air under axial and bending loading modes. The data showed a substantial improvement in fatigue life, particularly at low stress ranges. There was some uncertainty in the data as thinner plates tended to fail at lower lives than the thicker plates, with all failures occurring well away from the peened region in the parent plate.

In UKOSRP II (1989a), further plate tests were undertaken in-seawater with CP. In accordance with the results in Phase 1, all tests failed away from the peened area in the parent plate at very long fatigue lives. It was concluded that the hot-spot location was no longer associated with the weld toe due to the substantial benefit of hammer peening. Therefore, the S-N curve applicable to the parent plate (Class B) determined the fatigue lives of these specimens, although caution was expressed due to the lack of data in these studies.

Hammer peening combined with grinding was appraised by Haagensen (1994) who reported strength improvements of 154% - 216%.

9.2.3.3 Summary

Hammer peening improves the fatigue life of joints by introducing compressive residual stresses. All test data on hammer peening comes from plate specimens and consistently shows a very significant increase in fatigue behaviour, particularly at the lower stress ranges. For lives of around $N = 2 \times 10^6$ an increase in fatigue strength in excess of 150% is typical (ie. a factor of over 15 on life), which diminishes at lower lives so that at $N = 10^4$ there would be little, if any, benefit. In most tests reported the base plate fails prior to the weld toe suggesting that the Class B S-N curve should be applied to determine the joint fatigue life in these cases.

Clearly codes should encourage the use of hammer peening provided it is applied in the correct manner. To prevent possible overestimation of strength that could occur at high stress ranges, it is recommended that an S-N curve with shallower slope (eg. Class B) be adopted. However, it should be remembered that in the proposed HSE (1993b) guidance all S-N curves will have a slope of $m = 3$ below $N = 10^7$ cycles.



9.2.4 Shot peening

9.2.4.1 Design Codes

The effect of shot peening is covered in AWS (1992) as described in Section 9.3.3.1. Other codes do not discuss the effect of shot peening.

9.2.4.2 Review of published data

The effect of shot peening is mainly to compress the surface layers of the specimens and create residual compressive stresses in the weld toe region.

In UKOSRP II (1989a) the effect of light and heavy shot was considered for plate specimens in-air and in-seawater with CP. It was reported that both methods gave improvement in strength of around 50% in-air and 30% in-seawater with CP at $N = 2 \times 10^6$. The use of heavy shot peening resulted in a marginally greater increase in the fatigue strength in-air, but the results were more widely scattered. Since the effect of shot peening is restricted to the introduction of surface compressive stresses, it was considered that the benefits of this method are limited to the crack initiation and early crack growth phases.

Haagensen (1987) in a study of several weld improvement techniques stated that hammer peening has little, or no, effect at $N = 10^4$ but increased strength by 58% at $N = 2 \times 10^6$.

Bignonnet (1987) also considered shot peening on plate specimens of two steel grades, E460 and E550. The fatigue strength enhancement for these two steel types was similar, increasing the strength by around 80% at $N = 10^6$. Extrapolating the mean fit S-N curves would also indicate that there would be no benefit of shot peening at $N = 10^4$.

9.2.4.3 Summary

Shot peening, in a similar manner to hammer peening, improves the fatigue life of joints by introducing compressive residual stresses. All test data on shot peening comes from plate specimens and consistently shows a significant increase in fatigue behaviour, particularly at the lower stress ranges. For lives of around 2×10^6 an increase in fatigue strength in excess of 50% is typical (ie. a factor of over three on life), which diminishes at lower lives so that at $N = 10^4$ there would be little, if any, benefit.

Like hammer peening, it is recommended that an S-N curve with shallower slope be adopted and good practice established in the codes.



9.2.5 TIG dressing

9.2.5.1 Design Codes

The effect of TIG dressing is not discussed in the current design codes

9.2.5.2 Review of published data

In UKOSRP I (1988) some plate tests were performed on $T = 25\text{mm}$ and 38mm specimens under axial load and bending in-air with TIG dressing. The weld toe region was remelted using a tungsten electrode. No filler material was used and the fusion area was surrounded by an inert gas to reduce oxidation. The results of these tests suggest that TIG dressing gave an insignificant benefit above 200 N/mm^2 , but did give a more consistent benefit below this stress level.

Within the ECSC project Haagensen (1981) and Van Leeuwen (1981) also considered the effects of TIG dressing on fatigue life in-seawater. In these tests the effect of TIG dressing was considered to be superior to that observed in the UKOSRP I programme, with Haagensen reporting an increase of 44% in strength over that in the as-welded condition.

9.2.5.3 Summary

TIG dressing does give some improvement in fatigue life, although it appears to be the least effective method for enhancing fatigue behaviour considered in this Chapter.

Improvements in fatigue strength of 20% - 40% have been reported at $N = 2 \times 10^6$, although this benefit appears to diminish until around $N = 10^5$, below which no significant difference is reported between as-welded and TIG dressed specimens.



10. FATIGUE BEHAVIOUR OF COMPLEX TUBULAR JOINTS AND GIRTH WELDS

10.1 Overlapping Braces

10.1.1 Design codes

In the fatigue S-N design codes, the effect upon joint life of overlapping braces is not considered to be significant, although it is recognised that the maximum stress and failure location may differ considerably from those associated with non-overlapping braces.

In the proposed modifications to the HSE Guidance Notes (HSE 1995), overlapped joints are referenced under 'Stresses to be Considered'. In this Section it states that *'The hot-spot stress approach should also be used for overlapped joints except that the joint intersection includes the common weld between the two braces.'*

10.1.2 Review of published data

The database of joints with overlapping braces is given in Appendix F. The data have been obtained from the two phases of the UKOSRP programme:

I	UKOSRP I (1988, 1989)	10	K joints, in-air
		4	KT joints, in air
II	UKOSRP II (1989a, 1989b)	18	K joints, in-air

10.1.2.1 UKOSRP I (1988, 1989)

In the first phase of the UKOSRP programme a total of fourteen overlapped K and KT joints were tested in-air under balanced axial load and unbalanced out-of-plane bending. Five K joints with $T = 6\text{mm}$ are screened out in accordance with the criteria specified for non-overlapping braces in Section 7. The remaining nine joints have a nominal chord thickness of $T = 16\text{mm}$. Eight of these specimens failed in the chord member (or in the weld itself) under unbalanced OPB loading, while the ninth test under balanced axial loading was a runner at 8.2×10^6 cycles.

In the UKOSRP I final summary report the data from the overlapping joint tests were not differentiated from the remainder of the database.

10.1.2.2 UKOSRP II (1989a, 1989b)

In the second phase of the UKOSRP programme a total of eighteen K joints were tested with overlapping braces - six under Task 5.2 at Wimpey Laboratories and twelve under Task 5.6 of the project. While most joints had nominal chord thicknesses of $T = 16\text{mm}$ two tests examined joints with $T = 12\text{mm}$ and two tests considered joints with $T = 9\text{mm}$. With the exception of two tests with brace thicknesses of $t = 12.5\text{mm}$, these specimens had brace thicknesses of $t = 8\text{mm}$.



All joints were tested under balanced axial load. Two specimens failed prematurely at the attachment flanges, five joints failed in the chord member while eleven joints failed in the brace member.

Overall it was reported that the fatigue results from these tests with overlapping braces are in-line with the data for simple tubular joint tests.

10.1.3 Appraisal of test data

In the database, there are eight tests with chordside failures and $T = 16\text{mm}$ thus meeting the screening criteria for simple tubular joints. (In the UKOSRP II project there are two further results meeting this specification, although no N3 values were reported. One additional test only had strain gauge results on the chordside yet experienced failure on the braceside.) These data are plotted on Figure 10.1.1 and it can be seen that in comparison with the mean fit S-N curve for simple tubular joints these specimens generally exhibit lives in excess of those predicted. For the eight joints with $T = 16\text{mm}$ that passed the screening criteria the average damage summation is $D_s = 1.53$.

For the six joints that failed on the chordside with $T < 16\text{mm}$, the average damage summation is considerably higher at $D_s = 3.21$, with significantly longer lives measured on joints with $T = 6\text{mm}$ than on joints with $T = 9\text{-}12\text{mm}$. This reinforces the findings from the simple joint database that the limit of $T = 16\text{mm}$ on the scale effect gives a conservative estimate of life for very small scale tubular joints.

The data relating to failures on the braceside ($t < 16\text{mm}$) also has an average damage sum in excess of that for the chordside with $T = 16\text{mm}$ ($D_s = 1.69$). However, the results from these braceside failures are considerably more scattered with more specimens failing prior to expectation than in excess of expectation. This increase in scatter is primarily due to the failures along the common weld between the overlapping braces where both the weld and stress distribution are more complex.

10.1.4 Recommendations

From the database collated in this Guide, the average fatigue life on overlapped tubular joints appears longer than for the equivalent gapped joints, provided the hot-spot location is away from the common weld region. However, there is insufficient evidence to suggest that an alternative classification detail should be specified for the common weld.

Given the limited data on overlapping braces in tubular joints it is recommended that overlapped joints be assessed in an identical manner to simple gapped tubular joints. Designers should attempt to design the connection so that the maximum stress is on the brace/chord intersection rather than on the common weld between overlapping braces. Alternatively, it may be advisable to grind the common weld to minimise the risk of premature failure in this region.

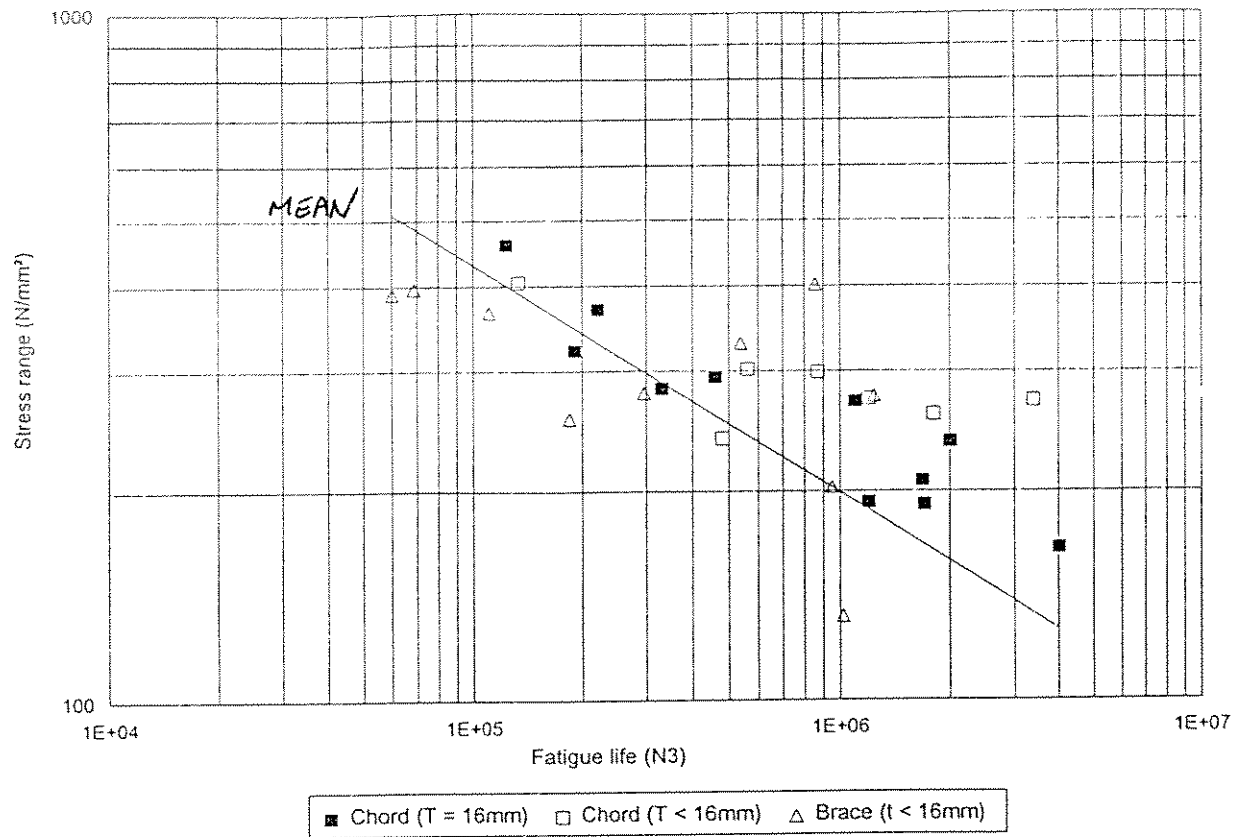


Figure 10.1.1 S-N data for overlapped tubular joints



10.2 Multipplanar Tubular Joints

10.2.1 Design codes

At present, while some Design Codes for tubular joints recognise different SCFs for multipplanar rather than uniplanar joints, no differentiation is made with regard to the S-N approach.

10.2.2 Review of published data

The fatigue database of multipplanar tubular joints is given in Appendix F. This database only covers two test programmes with all tests performed in-air. The main programmes of work and their individual conclusions are summarised below.

I	Romeijn (1993)	16	KK joints, in-air
II	Dijkstra and de Back (1981)	4	T(T) joints, in-air
		2	T(X) joints, in-air
		2	X(T) joints, in-air

(nb. X(T) represents a loaded X joint with an unloaded T brace out-of-plane, etc.)

10.2.2.1 Romeijn (1993)

TNO Building and Construction Research in conjunction with Delft University, Mannesmannröhren-Werke AG and Universität Karlsruhe performed a number of experimental and theoretic model tests on circular and rectangular hollow truss frames, with triangular cross-section.

Four tubular girders were tested at TNO with $\tau = 0.5$, $\beta = 0.4$ and 0.6 , and $\gamma = 6$ and 12 (ie. $T = 8\text{mm}$ and 16mm). The braces were inclined at 45° in-plane and 60° out-of-plane forming the triangular truss. Each girder contained four joints, two gap joints and two overlapped joints. Load was applied at the mid-span location and stresses in each joint measured accordingly. Thus in the fatigue tests four failures were sought, one associated with each joint. In this paper no consideration was given to the effect of one joint failing on the other intact joints within the girder. However, some increase in stress range may be expected following the first joint failure.

Overall, the data lay about the mean proposed HSE (1993b) S-N curve for uniplanar joints with an average $D_s = 0.82$ reported. It was, therefore, recommended that multipplanar joints be assessed against uniplanar S-N curves although the authors cautioned that no thickness correction should be taken for plate thicknesses if less than 16mm .

10.2.2.2 Dijkstra and de Back (1981)

In addition to the large UKOSRP I (1988) study, the ECSC funded several complementary test programmes throughout Europe. Eight multipplanar fatigue tests were performed at TNO : two T joints with an additional brace at 90° ($T = 6.3\text{mm}$), two T joints with two additional braces at 90° and 270° ($T = 6.3\text{mm}$), two T joints



with one additional brace at 90° (T = 31.7mm) and two X joints with one additional brace at 90° (T = 31.7mm). In all cases the β ratio was near $\beta = 0.5$ and consequently there was no out-of-plane overlap of braces. The additional braces in all tests remained unloaded throughout the test and so these tests were more useful in gauging the stiffening effect of additional braces upon SCF rather than the effect upon fatigue behaviour of complex multiplanar braced tubular joints.

Overall, these data exhibited fatigue lives in accordance with the uniplanar data tested by TNO and mean S-N curves based on uniplanar test results.

10.2.3 Appraisal of test data

Few fatigue tests have been performed on multiplanar tubular joints. Early tests in the ECSC funded programme included out-of-plane braces but these were incorporated primarily to gauge the effect upon SCFs of non-planar braces and as such these braces were not loaded during the cyclic tests. Data from these tests is in accordance with that from uniplanar tests and is not considered further in this chapter.

In Figure 10.2.1 the fatigue N3 results from the TNO girder tests are reproduced. The 16mm chord failures are emphasised since these would pass the screening criteria specified for uniplanar joints, while the remaining data for failures in members of 8mm or 4mm thickness is included to enhance the database (nb. no thickness correction is applied to this data).

It can be seen in Figure 10.2.1 that four of the five data from the 16mm chord thickness joints lie below the mean in-air S-N curve with the average $D_s = 0.72$. However, if the two runners with T = 16mm were included then the average damage summation would be $D_s > 0.90$.

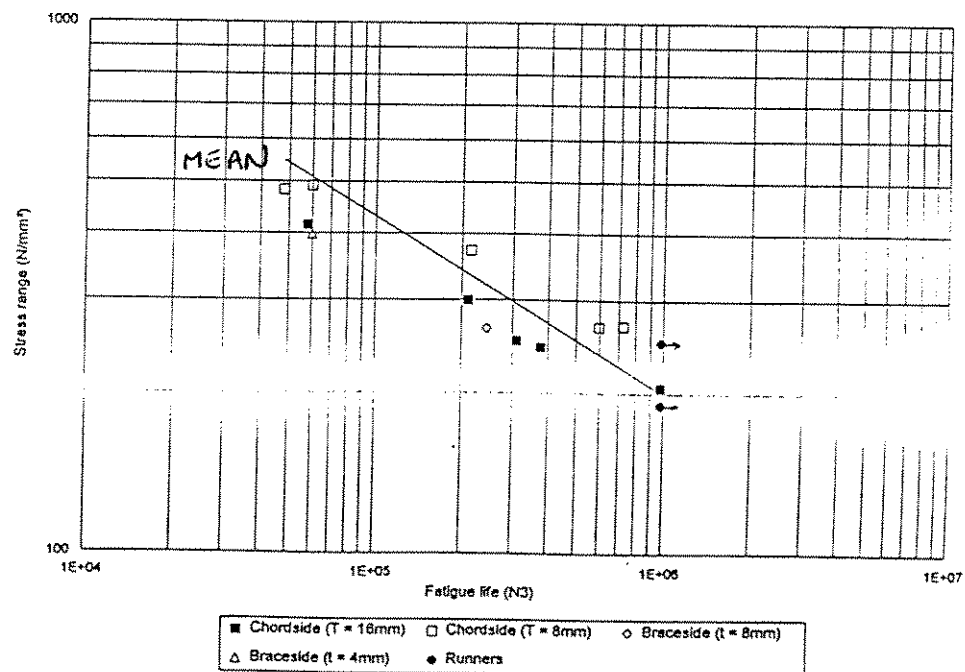


Figure 10.2.1 S-N data for multiplanar tubular joints



10.2.4 Recommendations

There is a very small database of multiplanar tubular joints where the out-of-plane braces are loaded. This data suggests a slight reduction in fatigue life compared to equivalent uniplanar tubular joints. However, given the paucity of data it is recommended that multiplanar joints be assessed in an identical manner to uniplanar tubular joints.



10.3 Internally Ring-Stiffened Tubular Joints

10.3.1 Design codes

Current design codes do not specifically address ring-stiffened joints, except in specifying classification details.

Current HSE (1993a), DnV (1984, 1992) and CAN/CSA (1992) codes specify a Class F curve for the ring web to inner chord wall joint, while the ring inner edge would have a classification depending upon the edge finish.

In the proposed modifications to the HSE Guidance Notes (1993b) ring-stiffened joints are specifically addressed under the Section 'Stresses to be Considered'. It is stated that 'For ring-stiffened joints, the maximum stress may not be at the saddle or crown locations on the brace-chord intersection. Care should be taken to identify stress elsewhere in the joint, eg. at the locations where a brace crosses a ring-stiffener {ie. the brace/ring intersection (BRI) or the ring inner edge}. The design S-N curves appropriate to these locations are given [see below]. Since cracking of the ring-stiffeners is extremely difficult to detect in service ring-stiffeners should be designed with minimum lives of at least ten times the service life.'

In the proposed joint classifications, the brace-chord intersection is classed with the T' curve away from the BRI and 1.34P (cf. Class F) curve at the BRI (internal and external). The internal edge of a flat bar or flanged internal ring-stiffener is classed as 1.00P (cf. Class D).

10.3.2 Review of published data

The fatigue database for ring-stiffened tubular joints is given in Appendix F.

This database covers tests in-air, in-seawater with cathodic protection (CP) and in-seawater under free corrosion (FC). The main programmes of work and their individual conclusions are summarised below.

I	Ramachandra Murthy (1994a, 1994b)	4 T joints, in-air 3 Y joints, in-air 6 T joints, in-seawater FC 3 Y joints, in-seawater FC
II	COSRP (1989, 1991)	8 T joints, in-air 2 T joints, in-seawater CP
III	UKOSRP II (1989a, 1989b)	6 T joints, in-air
IV	Haugland and Thuestad (1990)	1 K joint, in-seawater CP
V	Sawada (1979)	3 T joints, in-air
VI	TWI (1992) (confidential)	5 T joints, in-air 5 K joints, in-air



10.3.2.1 Ramachandra Murthy (1994a, 1994b)

There have been a number of papers presented by the Structural Engineering Centre (SERC) in Madras, with the best summaries of their work to date contained in Ramachandra Murthy (1994b) for the in-air tests and Ramachandra Murthy (1994a) for the corrosion fatigue tests.

In-air, Ramachandra Murthy (1994b), a total of seven tests have been reported with chord thickness $T = 12\text{mm}$: four T joints (axial load) and three Y joints (axial, IPB and OPB loading). Three plate type stiffeners were employed in the 'optimum arrangement' of one stiffener beneath the saddle and one stiffener beneath each of the crown positions. Five joints failed with cracks forming at the hot-spot location on the chordside, while two joints failed on the braceside where no strain gauges were employed. Furthermore, no strain gauges were placed on the ring stiffeners themselves. Overall, it was reported that the results were conservative relative to the current HSE design S-N curve (HSE 1993).

In-seawater under free corrosion, Ramachandra Murthy (1994a), a total of nine stiffened joint tests and two unstiffened joint tests were reported with dimensions similar to the in-air test programme. All tests were performed under axial loading. One stiffened joint failed by brace separation from the chord, while all other joints failed on the chordside at, or near, the location of maximum stress concentration, ie. near the saddle. Again, no strain gauges were placed on either the brace or stiffeners. Overall, it was reported that the results were in-line with the HSE design S-N curve for free corrosion (HSE 1993), ie. below the in-air data but generally in accordance with the results of the two unstiffened joint tests in seawater with no CP.

10.3.2.2 COSRP (1989, 1991)

The COSRP gave thorough consideration to the effect of ring-stiffening tubular joints in-air and in-seawater with adequate CP. The tests themselves were performed at the University of Waterloo, Ontario (five under axial load and one under combined axial and IPB loading giving equal stresses at the two saddles and one crown position) and at the Memorial University, Newfoundland (four under IPB and two under OPB). In addition tests were performed on plate to pipe connections.

A total of ten ring-stiffened joint tests and two unstiffened joint tests were reported with dimensions similar to the UKOSRP II test series, see 10.3.2.3. One joint failed prematurely due to accidental overload, while all others failed on the chordside. The specimens were comprehensively strain gauged and it was reported that the maximum stresses were often found on the stiffeners although no primary cracking occurred at this location since the stiffeners were machined rather than flame cut (see UKOSRP II (1989a)).



Overall, the stiffened in-air tests gave reasonable correlation with the unstiffened joints and the current mean HSE (1993) S-N curve, although the IPB tests often gave shorter fatigue lives. In-seawater with CP, the data lay on the HSE free corrosion line (ie. a factor of two reduction on life) rather than on the HSE in-air curve which is also applicable to in-seawater with adequate CP.

10.3.2.3 UKOSRP II (1989a, 1989b)

The second phase of UKOSRP included six tests on ring-stiffened tubular T joints in-air. Two configurations were studied, one with two plate stiffeners and one with two flanged stiffeners. Although the specimens were thoroughly strain gauged, the flanged specimens failed at a location around 10° from the nearest strain gauges, on the chordside over the ring location, ie. at the BRI. The plate stiffener specimens failed with cracking occurring on the flame cut ring inner edge and at the chord saddle.

Overall, the plate stiffener specimens failed in-line with the current HSE (1993) mean S-N curves for an unstiffened tubular joint and flame cut plate edge. However, the flanged stiffeners exhibited lower lives, nearer the current HSE S-N design T curve, particularly at higher stress ranges.

10.3.2.4 Haugland and Thuestad (1990)

In 1987, a fatigue test was performed on a ring-stiffened K joint in-seawater at a depth of 20m.

The joint formed a non-symmetric K node with two flanged ring-stiffeners located beneath each brace footprint. In-plane bending was applied via a self-reacting hydraulic actuator. The external weld toes were ground and the node was equipped with sacrificial anodes giving a CP level of -1030mV. Internally, the node was dry and the welds unground. This configuration represented the conditions on the Oseberg B jacket.

A total of thirteen loading periods were reported ($\sigma_{nom} = 15 - 173 \text{ N/mm}^2$) each lasting between 3,580 cycles and over one million cycles.

Cracks initiated on the ring web to inner chord attachment (SCF = 1.4) but were not considered to be critical with regard to joint behaviour. No crack depth measurements could be made at this location due to inaccessibility.

The maximum stress (SCF = 2.3) was measured at the ground weld toe of the smaller inclined brace member initiating at $D_s = 5.3$ and produced a through thickness crack at $D_s = 6.0$, based on the DnV (1992) mean S-N T curve corrected for both the member thickness ($T = 25\text{mm}$) and weld toe grinding - ie. a factor of 2.2 on estimated fatigue life.



10.3.2.5 Sawada (1979)

Sawada (1979) reported static and fatigue tests on ring-stiffened joints under axial load. These joints had a single plate stiffener ($t_w \approx 8\text{mm}$) beneath the saddle, a chord thickness of $T = 9.6\text{mm}$ and a brace thickness of $t = 6.9\text{mm}$.

SNCFs were estimated on the chord and the brace, based on single strain gauges close to the weld. The maximum SNCF was reported at the brace saddle, however, in two cases the rings failed prior to the joint.

Given the method of SNCF derivation, the thickness of the failed members and the lack of strain gauging at the location of failure, these data are not considered further.

10.3.2.6 TWI (1992)

A joint industry funded project was carried out by TWI, NEL and LR to consider the fatigue behaviour of ring-stiffened joints in-air.

Ten ring-stiffened joints were tested, five T joints at NEL under axial loading and five K joints at TWI under unbalanced OPB.

The results of this project are currently confidential to sponsors, although the specimen geometries were presented in the SCF Chapter 4.

10.3.3 Appraisal of test data

It has been recognised in the proposed HSE (1995) guidance that the ring-stiffened joint is a complex connection that can fail in many ways:

- i) On the brace/chord junction well away from the influence of the internal stiffeners.
- ii) On the brace/chord junction in the vicinity of the internal stiffeners, the so called brace/ring intersection (BRI) location.
- iii) At the ring stiffener inner edge.
- iv) At the ring web to inner chord connection.

Since each of these locations may be subject to a different joint classification, care is needed in assessing the collective results from ring-stiffened joints.

In the following sections the measured data is compared to the mean in-air S-N curve derived from simple tubular joint tests in Section 7.6. Since the chord thicknesses lie in a narrow range between $T = 12\text{mm}$ and $T = 19\text{mm}$ no thickness correction is made to the stress range, and the S-N curve is based on $T = 16\text{mm}$.



10.3.3.1 In-air

Of the 21 ring-stiffened joint in-air tests reported in the Ramachandra Murthy (1994b), COSRP (1989, 1991) and UKOSRP II (1989a) studies, a further three have been screened out. Specimen TB3 in the COSRP due to accidental overload between crack initiation and through thickness failure, and Specimens SP5 and SP11 in Ramachandra Murthy which failed in the brace member.

The remaining eighteen specimens are illustrated in Figure 10.3.1, and represent three of the four potential failure modes. These data are also compared to the mean S-N curve proposed in Section 7.6 for simple tubular joints in-air. The other mean S-N curves specified in the current HSE (1993), DnV (1992) and Canadian (CAN/CSA 1992) codes (T curve modified to 16mm) and the new proposed HSE (1995) fatigue guidance (T' curve) are too close to this S-N curve to warrant reproducing on this figure.

It can be seen in Figure 10.3.1 that the two specimens failing from the flame cut ring inner edge (Type III) lie above the mean S-N curve for the unstiffened data, with the through thickness fatigue life on average 40% larger than this mean S-N curve and a factor of 2.8 on life above the mean 1.00P curve recommended in HSE (1995).

For the specimens with failures on the brace/chord junction well away from the BRI (Type I), two data lie above and five data lie below the mean S-N curve, although, due to one of the UKOSRP II specimens having a measured fatigue life over five times that predicted, the average Miner's sum exceeds unity, $D_s = 1.42$.

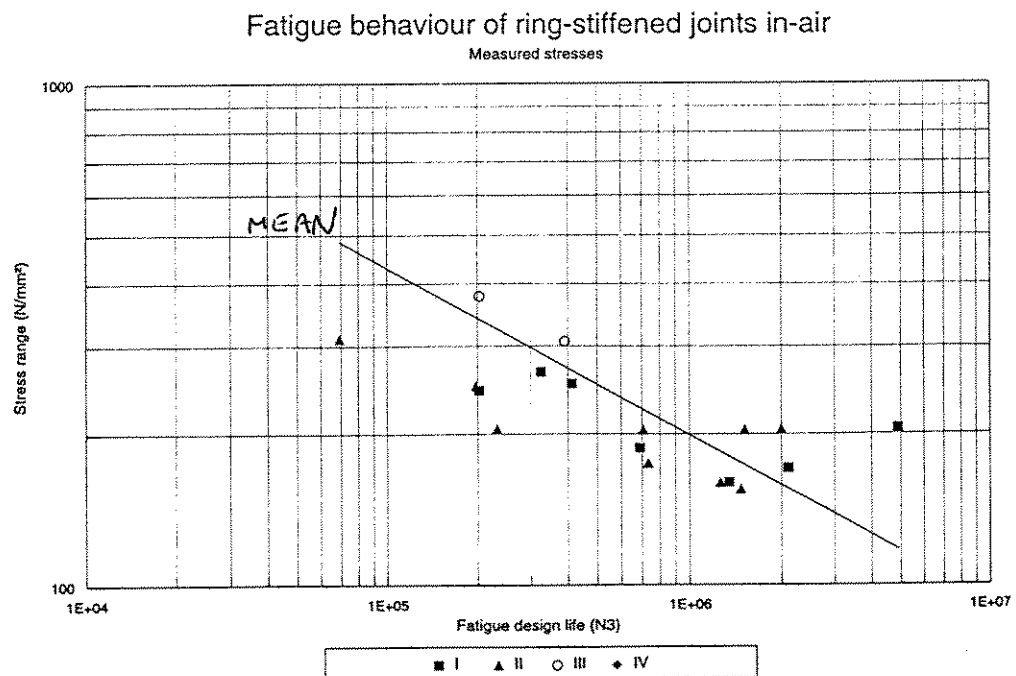


Figure 10.3.1 Comparison of mean S-N curve with in-air data based on measured stress range



It should be noted that the two specimens with the lowest damage sum ratios are the two specimens that were tested under IPB loading. This trend is potentially reinforced by the fact that two of the three tests screened out were tested under IPB and also had reported lives less than expected.

For the specimens with failures on the brace/chord junction near the BRI (Type II), two data lie above and seven data lie below the mean S-N curve. For this case, the average Miner's sum is less than unity, $D_s = 0.81$, and is therefore around 60% of the average Type I failure life. In comparison to the 1.34P curve proposed in HSE (1995) most data lie well in excess of this curve with an average D_s of around five. Two joints (UKOSRP II 1989a) lie below this mean curve, although for the three UKOSRP II joints it should be remembered that stresses were measured around 10° from the hot-spot locations.

The crack growth mechanisms for all modes of loading are discussed in the COSRP final report (COSRP 1989). It was noted that the ring-stiffeners tend to act as crack length stops, with the stiffeners causing the cracks to turn when the crack depth exceeds 80% of through thickness. The authors report that the crack growth rate in stiffened joints under axial load and OPB appears to slow by an order of magnitude as the crack depth approaches through thickness. Under IPB, the crack aspect ratio (crack depth/crack length) appears smaller than under axial load and OPB. This is perhaps due to the very even stress distribution around the brace/chord junction and the longer distance from the hot-spot location to the stiffeners. In a fracture mechanics assessment of a ring-stiffened joint under axial load or OPB, COSRP recommends that the crack shape should be taken as crack depth/stiffener spacing when the crack is a few millimetres deep (eg. 4mm or less), thus yielding a lower bound solution if the crack turning is not included in the model, see Chapter 6.

10.3.3.2 In-seawater

Of the ten ring-stiffened joint in-seawater tests reported in the Ramachandra Murthy (1994b), COSRP (1989, 1991) and UKOSRP II (1989a) studies, only two had adequate CP while eight were unprotected. The CP was applied at -850mV in-seawater of around 5°C . In the unprotected cases the seawater was representative of the Indian Ocean with a temperature of 25°C . These specimens are illustrated in Figure 10.3.2. These data are also compared to the mean S-N curve proposed for unstiffened tubular joints in-seawater, ie. 50% life in-air for joints with adequate CP, and 25% life in-air for free corrosion in warm water.

It can be seen in Figure 10.3.2 that the two specimens failing in-seawater with CP exhibited fatigue cracking on the brace/chord junction well away from the BRI (Type I). These joints fall below the mean in-seawater with CP = -850mV S-N curve. The average Miner's sum for these two specimens is $D_s = 0.50$. This represents a life 20% of the average in-air tests, although perhaps more representatively represents 40% of the average life of the in-air axial load tests within the same test programme.



The single Haugland and Thuestad (1990) specimen with CP applied at -1030mV was tested in-seawater under VA loading. Appraising this data indicates that the crack initiation on the ring web to chord weld (Type IV) occurred between $N1 = 4.4 \times 10^5$ and $N1 = 7.5 \times 10^5$ cycles of constant amplitude loading against the mean in-air curve (1.34P) estimate of $N'3 = 5.6 \times 10^5$ (SCF = 1.4), ie $N1/N3 > 78\%$ which appears high. However, while crack depth measurements were not made at this location, crack length and through thickness stress distributions suggest that this crack did not grow through thickness until well in excess of the estimated fatigue life $N'3$.

Fatigue behaviour of ring-stiffened joints in-seawater

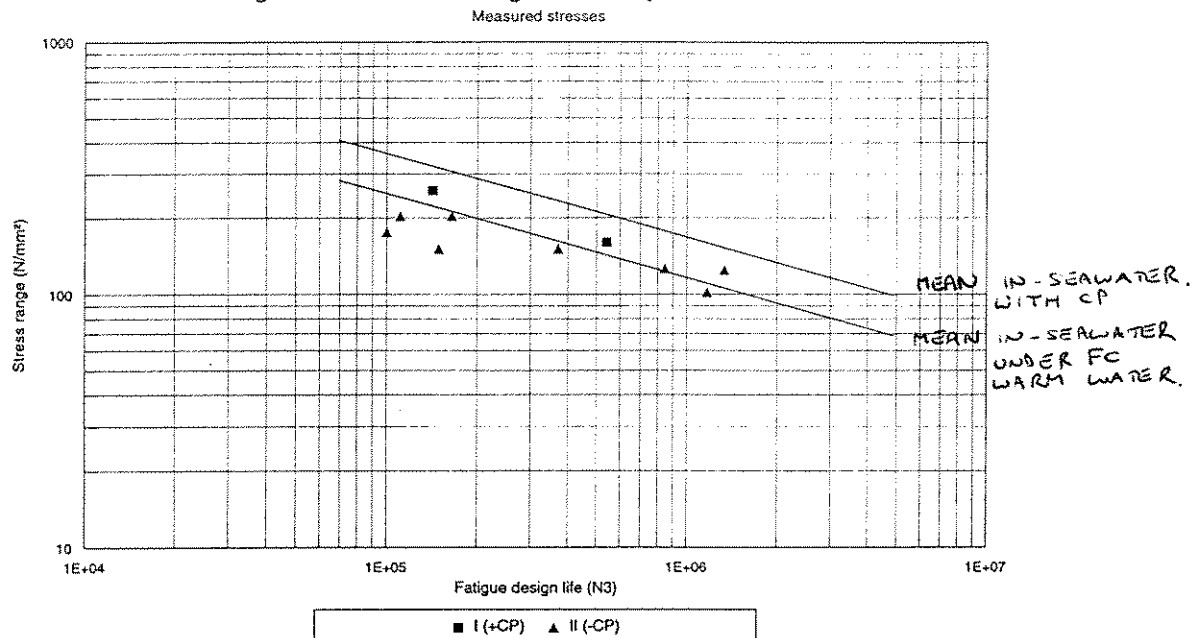


Figure 10.3.2 Comparison of mean S-N curve with in-seawater data based on measured stress range

At the external location on the chord (Type I) cracking initiated after $N1 = 2.8 \times 10^7$ cycles and became a through thickness crack N3 after 3.3×10^7 cycles of varying amplitude loading. Compared to the mean in-seawater S-N curve (0.5 in-air), with no allowance for grinding, these lives represent damage sums of $D_s(N1) \approx 29$ and $D_s(N3) = 32$. (nb. $T = 25\text{mm}$, $\text{SCF} = 2.3$, no change of slope at low stress ranges). Therefore, for this configuration and loading a very long life has been obtained for this joint, if the Type IV cracking is considered to have insignificant effect on joint behaviour.

For the eight specimens failing in seawater without CP, cracking occurs on the brace/chord junction near the BRI (Type II). In this case the data lie near but below the mean in-seawater FC curve for warm water and generally below the data from the two specimens that have CP. For this case, the average Miner's sum is $D_s = 0.80$, and is around 20% of the average Type II failure life in-air, in accordance with the FC findings in Section 8.3.2.



10.3.4 Recommendations

The proposed HSE (1995) guidance notes require that the various components within a ring-stiffened joint be classified in different ways. The database of ring-stiffened joints collated in this study support the need for several joint classifications.

Data for fatigue failures on the brace/chord junction well away from the influence of the internal stiffeners suggest that similar S-N behaviour to unstiffened joints may be anticipated. It should be remembered that the SCFs will generally be significantly less in a stiffened joint so that the joint life will be substantially improved if this region is the location of initial cracking.

On the brace/chord junction at the BRI location a lower bound S-N curve appears to be required, with around 60%-80% the simple joint fatigue life both in-air and in-seawater. In the proposed HSE (1995) notes a 1.34P curve is specified which appears to be too conservative for joints with cracking above a stiffener at the crown location, in particular.

The two failures at the ring stiffener inner edge were associated with an edge that had been flame-cut, for which a 1.0P curve is specified in the proposed HSE (1995) guidance. It was found that this curve was very conservative for these two specimens. In the COSRP it was noted that once the ring edge was machined no significant cracking occurred on the rings even though this was the location of maximum stress.

There was insufficient stress or fatigue data on the ring web to inner chord wall location to comment on a suitable fatigue classification.

In-seawater with cathodic protection and under free corrosion the reduction factors on in-air life appear suitable for these joints when applied to the simple joint curve. However, when applied to the BRI curve (1.34P) very conservative values are obtained for the joints with cracking beneath the crown.

The one complex ring-stiffened joint in-seawater with ground welds under variable amplitude loading gave reasonable lives in relation to the ring web crack initiation but a damage sum in excess of 30 for the ground welds on the exterior of the joint.

Overall, without more data, it is recommended that the proposed HSE (1995) guidance on ring-stiffened joints be applied where the following classifications are specified:

- 1.00T on the brace/chord junction well away from the influence of the internal stiffeners.
- 1.34P on the brace/chord junction at the BRI location.
- 1.00P at the ring stiffener inner edge.
- 1.34P at the ring web to inner chord connection.



The 1.00P and 1.34P factors appear high, particularly for joints where the stiffeners are directly beneath the crown.

It should also be remembered that factors for non-inspectable connections are required for the ring inner edge and ring to chord weld. These vary from reduction factors of three in the DnV (1992) code to ten in the proposed HSE (1995) code.



10.4 Internally Grouted Tubular Joints

10.4.1 Design codes

Only the proposed HSE (1995) Guidance Notes specifically address composite joints within the section 'Stresses to be considered'. This Section states that 'The introduction of grout into simple tubular joints results in a reduction of the hot-spot stress at the brace/chord intersection. However, for some joint configurations and loading modes this reduction in stress is insignificant. A conservative approach should therefore be taken by considering the joint as being ungrouted and treating it as a simple nodal joint.'

10.4.2 Review of published data

Little work has been published covering the fatigue behaviour of grouted tubular joints, although there is a substantial database of both fully grouted chord members and double-skinned chord members outside the public domain. The main programmes of work and their individual conclusions are summarised below:

I	le Meur (1994)	4 X joints, in-air 5 T joints, in-air
II	Veritec (1984)	3 X joints, in-air 1 K joint, in-air
III	Brown (1988)	2 T joints, in-air
IV	Tebbett (1979, 1982) (confidential)	11 T/Y joints, in-air 3 X joints, in-air

10.4.2.1 le Meur (1994)

In 1994, the initial results of a joint industry funded and managed project concerned with the static and fatigue behaviour of grouted tubular joints (SMAB) were published. Four shear tests, five static strength tubular joint tests and nine fatigue loaded tubular joint tests were examined. Four X joints (three under tensile and one under compressive axial loading) and five T joints (two under IPB and three under OPB) were tested under cyclic loading, $R > 0$. The results from one IPB and one OPB specimen have yet to be reported.

The difficulty in determining through thickness cracking was noted by the authors and consequently both strain measurements and deflection measurements were monitored to identify when through thickness cracking was most likely to have occurred. In these papers no details of the load range or fatigue lives are reported. However, it can be seen from a summary S-N curve that the tensile axial load data and results from the tensile hot-spot location in the bending tests are in-line with estimated lives for ungrouted joints. The compressive axial load test and the lack of crack initiation on the compression side of the specimens in bending imply that the fatigue life of grouted joints is significantly enhanced under compression loading.



10.4.2.2 Veritec (1984)

Veritec fatigue tested four double-skin grouted tubular joints in 1984. The method of strain gauging these specimens differed from the approach recommended in this Guide and consequently two of the specimens were screened out of the SCF review in Chapter 4. Furthermore, these specimens were subjected to both tensile and compressive preloads prior to the reversing cyclic load ($R = -1$). In all cases fatigue lives were well in excess of expectation and compressive residual stresses were considered to be affecting the fatigue performance of these joints.

Two X specimens did not fail while the third X joint, which failed after 10.5 million cycles at ± 4 tonnes, was subjected to 500,000 cycles of load at a lower stress range of ± 3 tonnes and an alternating load sequence reducing from +40T, -40T, +35T, -35T,, +5T, -5T, 0T. The fourth specimen, a K joint, was tested in a more consistent manner and at a higher load range to encourage failure prior to the cyclic limit. Overall, all four results gave fatigue lives in excess of those from a database of ungrouted tubular joints.

10.4.2.3 Brown (1988)

Two specimens, originally fatigue tested in the UKOSRP II project (1989a), were repaired by gouging out fatigue damaged areas, filling with weld material to the original plate thickness ($T = 32\text{mm}$) and finally re-welding to API (1993) RP2A specifications. The specimens were then reinforced by injecting cement into two spherical bags through 50mm holes in the chord wall. This operation was carried out in 1.5m of water and the specimen was left in this condition for twelve days to allow the cement to cure. Thus the chord was fully grouted either side of the brace member while a void existed beneath the hot-spot stress location.

The two tests at $R = -1$ yielded fatigue lives less than the mean ungrouted joint S-N curve (irrespective of thickness correction factor chosen). The authors report that the large extent of repair welding and the fact that balanced welding could not be achieved may not have restored the joint to its virgin condition. Furthermore, the extent of the welding may have induced high residual stresses in the joints.

10.4.2.4 Tebbett (1979, 1982)

The results of this project, with the exception of the ungrouted SCF value, remain confidential to the new owners of the data SLP Engineering. However, some trends in the SCFs measured were reported in Chapter 4.



The fatigue test programme comprised:

Fatigue tests	Joint type	Single skin	Double skin
Axial loading (10 tests)	7 T/Y	3	4
	3 X	1	2
OPB (3 tests)	3 T	0	3
IPB (1 test)	1 T	0	1

In addition 71 joints were tested to determine the static strength of single and double skinned tubular joints.

10.4.3 Appraisal of test data

The thirteen grouted joints from the le Meur (1994), Veritec (1984) and Brown (1988) studies are illustrated in Figure 10.4.1. None of these data were sufficiently well reported and tested in the manner recommended in this Guide to pass the screening criteria normally applied. Consequently, the results of these tests can only be considered to identify trends in grouted joint behaviour. The measured data is also compared to the mean S-N curve recommended for ungrouted tubular joints in-air.

It can be seen that the recent le Meur data gives very good agreement with the ungrouted mean S-N curve for crack locations in tension. In compression, the fatigue life is significantly enhanced. The results from the two test series under $R = -1$ axial load are significantly different with the Veritec data showing substantially enhanced fatigue life, probably due to the high preload on these joints, while the Brown data shows a reduced fatigue life, probably due to the repair welding and incomplete grouting of the chord member.

10.4.4 Recommendations

At present, chord members that are either fully grouted or which have a double-skin section with a grout sandwich are treated in a similar manner to simple ungrouted tubular joints.

There is a very small S-N database of grout filled tubular joints in the public domain. However, the available data does show that a significant improvement in fatigue life can be achieved by the introduction of grout into the chord member. This benefit is primarily obtained by reducing the level of hot-spot stress, particularly in compression. From a fatigue S-N point of view, the joint life appears to be in accordance with the in-air S-N curve for tubular joints, where the thickness correction is based on the outer chord member thickness. Although, again under compressive axial load there appears to be a significant enhancement in joint life.

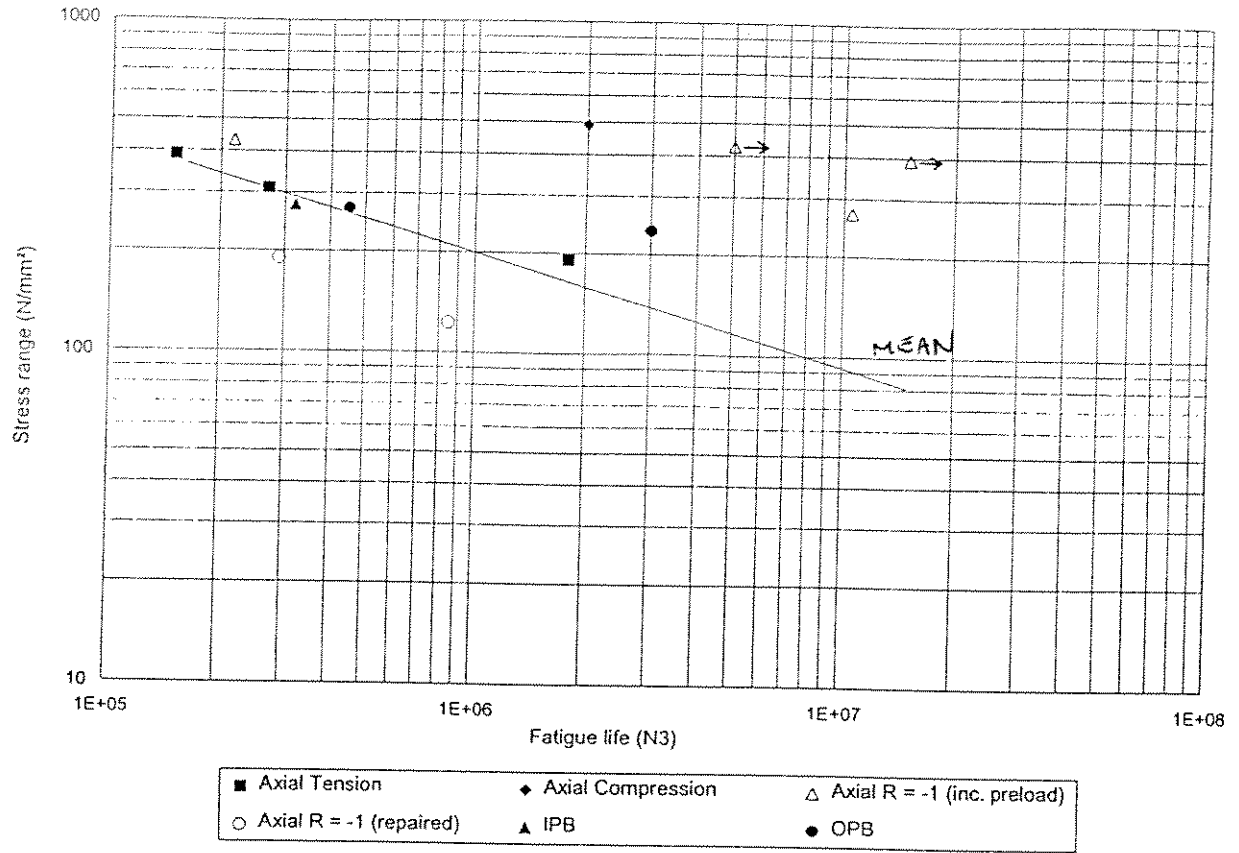


Figure 10.4.1 Comparison of mean S-N curve with in-air grouted joint data based on measured stress range



10.5 Cast and Forged Steel Joints

With the advent of modern foundry techniques steel manufacturers have been able to produce sound castings of suitable quality and composition for use in offshore environments. The use of castings for tubular joints offers obvious advantages. They offer a homogeneous integral component, with significantly lower residual stresses and free from the stress raisers associated with welded joints. In addition, the thickness of the casting can be varied to accommodate any areas of high stress. Castings also offer the opportunity to place padears or launch rails as an integral part of the joint.

10.5.1 Design codes

Until recently, the design codes have given scant reference to the fatigue design of cast or forged nodes. In the previous HSE (1993) Guidance Notes a qualitative statement is given in Section 21.2.15:

'In designs incorporating cast or forged steel components the fatigue life of which is important to the safety of the structure, the data submitted to the Certifying Authority with the calculations should include the fatigue endurance for the material taking account of the particular environment, mean stress and the existence of casting defects, and the derivation of any stress concentration factors. Alternatively, where such components are designed to the requirements of a recognised code or standard specification (or the rules of a classification society) details of the references are to be clearly stated.'

The need for more comprehensive guidance has been recognised in the proposed modifications to HSE (1995) Guidance Notes where Section 21.2.15 has been substantially altered for cast steel components.

The proposed Guidance on cast steel components states that *'cast steel joints may be used in primary or secondary structures subject to long term fatigue loading provided the castings are fabricated to accepted standards.'*

S-N curves are proposed in-air under the classification code CS:

mean: $\log(N) = 16.121 - 4.1 \log(S_B)$ ($S_E = 0.238$)

design: $\log(N) = 15.169 - 4.1 \log(S_B)$

The HSE state that *'this curve should only be used for castings which satisfy agreed defect acceptance criteria'.....* which should be validated by the use of the fracture mechanics approach recommended. The mean and design S-N curve in-air is illustrated in Figure 10.5.1.

It should be noted that the design curve in this case is based on the mean S-N curve minus four standard deviations. This more severe criteria is based on the possibility of small defects being present that would be missed during the normal inspection of the joint (MaTSU 1992).



The scale effect factor proposed differs from that for as-welded steel joints:

$$S = S_B (38/t)^{0.15}$$

although the corrections to this curve accounting for the effect of seawater are identical to those previously reported for as-welded tubular joints.

Alternatively, cast steel joints may be designed using theoretical S-N curves derived from fracture mechanics analysis methods. It is important that the following should be included in the assessment procedure:

- Crack growth data pertinent to the environment in which the particular grade of cast steel is to be used,
- Defect quality level consistent with the standard of inspection which will be applied to the casting, eg. the defect acceptance criteria given in BS6208,
- Validation of the fracture mechanics fatigue life calculations.

For the particular case of cast tubular nodal connections it is important to note that the brace to casting circumferential butt weld may become the most critical location for potential fatigue cracking. To verify the position of the maximum stress range in the casting it is therefore recommended that a finite element analysis should be undertaken for fatigue sensitive joints.

For forged components, the Guidance Notes remain unaltered from the earlier statement requiring full details of the component's behaviour to be submitted to the Certification Authority for approval.

In UEG (1985) reference was made to a design approach developed by Hoesch for optimised cast joints, which introduced variable thicknesses and diameters throughout the node.

The design criteria proposed by Hoesch have been established by the testing of small-scale specimens and large cast joints. The methods of manufacture have also been examined to determine what effect the manufacturing process has on the design philosophy for cast joints.

In the fatigue design process, the cast joint is initially subject to non-destructive testing. Defects are then classified according to ASTM (1993) E446. Test results, fracture mechanics techniques and ASTM defect groups (according to wall thickness) provide factors by which a basic S-N curve can be shifted to a higher or lower order to take account of defects. Thus the non-destructive testing of a cast joint becomes an integral part of the fatigue analysis. Where casting defects are of a sufficient size, such that a fatigue life cannot be accurately estimated, Hoesch recommend that these defects are removed. This can be done by gouging and repair welding techniques, see Chapter 7.



The basic S-N curve developed for Hoesch GS-ARK 10 material has been derived from tests on 32 specimens approximately 25mm thick taken from cast K joints, within which natural casting defects were allowed to occur.

Fatigue tests were carried out at stress ratios of $R = -1$ and $R = 0$, followed by radiographic examination to classify any defects. Figure 10.5.1 shows the proposed basic S-N curve for GS-ARK 10, with a stress ratio $R = 0$ and a probability of survival of 98%. This S-N curve can be described mathematically as:

$$\log_{10}(N) = 16.30 - 5.1 \log_{10}(S_{nom}) \quad (N < 2 \times 10^8)$$

It must be noted that this S-N curve is recommended only for

- (a) Stress ratio $R = 0$.
- (b) Probability of survival of 98%.
- (c) Wall thickness, $t = 25\text{mm}$.
- (d) Defect Group 4 according to ASTM (1993) E446 with defect types A4, B4, Ca4, Cb4 and Cc4.

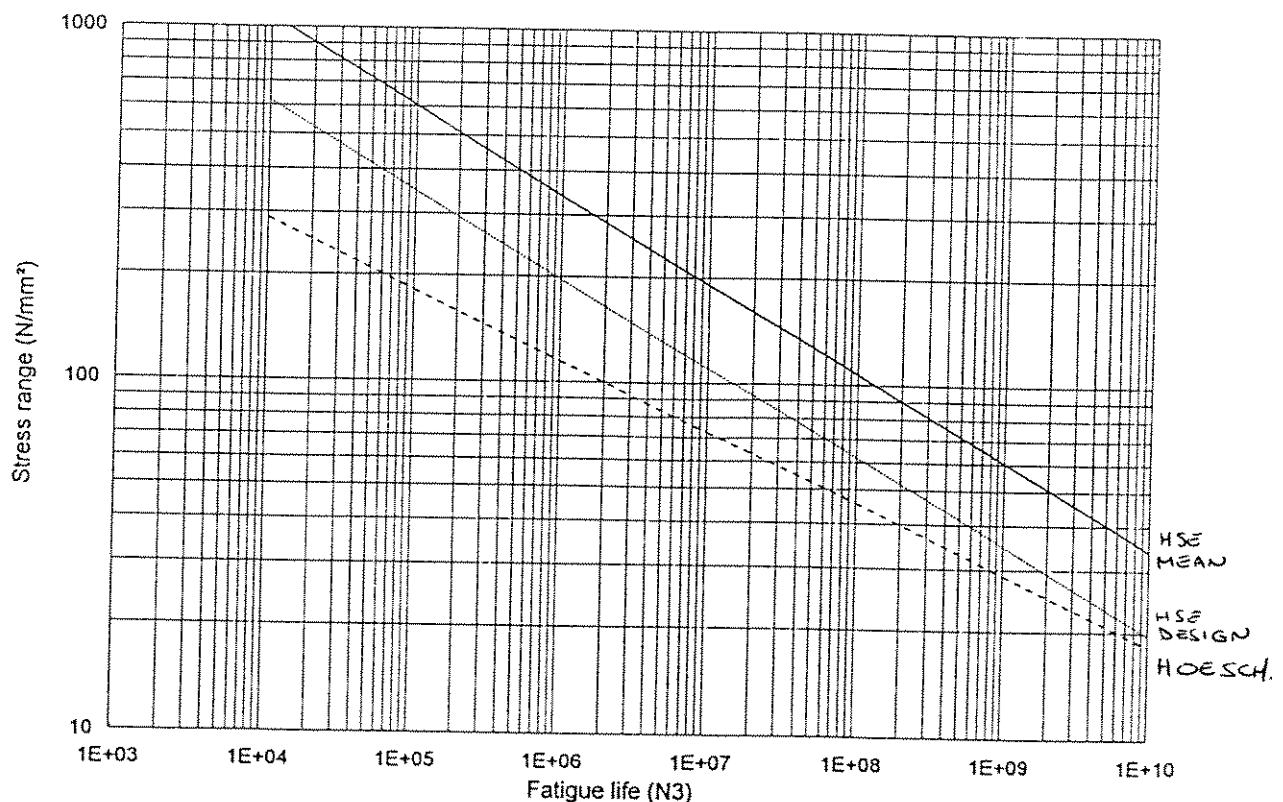


Figure 10.5.1 Proposed HSE (1993b) mean and design S-N curves for cast steel nodes and from Hoesch (UEG 1985)



Other stress ratios, wall thicknesses, defect groups etc. are accounted for by the use of influence factors which effectively displace the basic S-N curve towards a higher or lower number of cycles or stress range. The stress factors S and load cycle factors η are defined as

$$S = \bar{f}/f \quad \eta = \bar{N}/N$$

where f and N are the stresses and numbers of cycles respectively for the basic S-N curve, and \bar{f} and \bar{N} are those of the displaced curve with \bar{f}_0 defined as the stress range for $N = 2 \times 10^6$ cycles.

Derivation of influence factors

The following define the various influence factors proposed:

η_R : influence of mean stress (of the stress ratio R compared with $R = 0$)

η_d : influence of defect size

η_t : influence of wall thickness

η_i : accessibility for inspection and repair.

The interaction of these effects is given by $\eta = \eta_R \eta_d \eta_t \eta_i$

Influence of mean stress

In as-welded components the effect of mean stresses or stress ratio R is usually not taken into account. Cast steel joints are not influenced by residual stresses because of their stress-relieving heat treatment. Tests have been carried out on cast material, showing that the endurable stress ranges depend both on mean stress and on the stress ratio, R . From this and other results a lower limit of 85% of the stress value when $R = 0$ is assumed. The influence factors for mean stress can be summarised as:

$$\begin{aligned} \eta_R &= 0.444 & R > 0 \\ \eta_R &= 1.000 & R < 0 \end{aligned}$$

For each case with $R = 0$, it must be shown that stresses with $R < 0$ will occur.

Influence of defect size

The influence of defect size is based on the ASTM catalogues for the characterisation and classification of defects. From a fracture mechanics investigation it can be shown that the influence coefficients for defect size can be expressed by

$$\eta_d = 0.85^{5(j-4)}$$

where j denotes the defect group according to the ASTM defect catalogues.



A summary of these coefficients is given below.

	j				
	1	2	3	4	5
η_d	11.45	5.08	2.25	1.00	0.44

Influence of wall thickness

According to the ASTM catalogues the defect sizes in the same defect group will increase with increasing wall thickness. Here again a fracture mechanics approach has been used to determine the influence of wall thickness. These influence coefficients have been determined as:

$$S_t = (t/25)^{-0.15}$$

$$\text{ie. } \eta_t = (t/25)^{-0.75}$$

where t is in millimetres.

Accessibility for inspection and repair

The following influence coefficients relate to the accessibility of a cast joint for inspection and repair:

$$\eta_i = 10^{-Q_a/2}$$

where $Q_a = 2$, no accessibility
 $Q_a = 1$, splash zone and below
 $Q_a = 0$, above splash zone

These factors are similar to those recommended by DnV (1992) for welded offshore structures, although the safety factor for stresses is lower than that specified by DnV (for welded offshore structures). This is due to the shallower slope of the basic S-N curve for GS-ARK 10 steel.

10.5.2 Review of published data

A number of investigations into the S-N relationships for offshore steel castings have been reported during the past fifteen years. Due to cost restraints most of the test data were obtained from tests on small scale models, including cast pieces, V-shaped specimens and cruciforms. Those data relating to tubular joints are as follows:

I	Hoesch (Veritas 1982)	4 K joints, in-air
II	Webster and Walker (1985)	3 T joints, in-air
III	Nakamura (1986)	3 K joints, in-air
IV	Hurden (1986)	2 X joints, in-air
V	Wimpey (1990)	3 X joints, in-air



SLP Engineering have reviewed data from all types of cast components and generated a database of 234 tests (SLP 1995):

- 1) CA loading in-air:
 - 92 cast pieces under axial or bending loads
 - 61 cruciforms under 3 point or 4 point loading
 - 16 large scale nodes under axial brace loads or in-plane bending loads
- 2) CA loading in-seawater without CP unless otherwise stated:
 - 32 cast pieces under axial or bending loads
 - 8 V-shaped specimens under bending loads
 - 6 cruciforms under 4 point bending with and without corrosion protection
- (3) VA loading in-seawater without CP:
 - 19 V-shaped specimens under bending loads

10.5.2.1 Hoesch (Veritas 1982)

Four fatigue tests were completed on cast K nodes with chord diameters of 600mm and a general wall thickness of 18mm. However, at the location of the through wall thickness cracking the local thickness was 35mm. The specimens were heavily strain gauged and the location of the maximum stresses determined as well as the value of the SCF. Five different crack patterns were observed of which two were dominant. These were:

- (a) The crack initiated at the interior surface on the reaction side in the transition zone between chord and brace.
- (b) This crack was located at the position of maximum stress range on the exterior surface in the transition zone between chord and reaction brace. In general this crack initiated earlier than the one in location (a).

10.5.2.2 Webster and Walker (1985)

Three cast T nodes were tested, but only one of these failed in the casting. This specimen (CTI) had a chord diameter of 914mm and a nominal wall thickness of 32mm. This node was subject to extensive weld repair in the fillet region. The node failed from a slightly sub-surface defect which was located close to an extensive weld repair, some 65° around the brace from the crown position. It is not clear from the report whether this location was the region of maximum stress range.

10.5.2.3 Nakamura (1986)

Three tests were undertaken on cast K nodes. One of these failed in the cast material, the other two tests were runners. Few details appear to be available on the location of the major cracks and the maximum stress range.



10.5.2.4 Hurden (1986)

These two nodes had chord diameters of 600mm and a wall thickness of 40mm. In both cases failure occurred by a fatigue crack growing from the inside of the specimen along the chord centreline offset from the brace centre. This was found to be the maximum stress location, with an estimated SCF of 6 on the first specimen and 4.3 on the second.

It should be noted that the nominal thickness range for these large scale nodes is smaller (20-40mm) than for cast cruciforms and hence it was not possible to establish any thickness effects for these nodes.

10.5.2.5 Wimpey (1990)

Wimpey reported three X joint tests under axial load with $T = 34\text{mm}$. In all three tests the brace and chord diameters were equal thus giving a smooth loadpath across the X braces. The maximum SCF on all three of these specimens was measured on the inside of the chord member.

10.5.2.6 Summary of all test data

Examination of the database reveals the following:

- The database consists of results from tests on 16 real sized cast nodal joints of either T, X or K configuration. All specimens were subjected to axial brace load except for two T joints which were tested under in-plane moment loads. All tests on large scale steel models were conducted in air under constant amplitude loading.
- A number of data points were obtained from retest of specimens which were unbroken at the end of the first tests at a lower stress level. Due to the difficulty in assessing the level of damage in the first tests, these data points were excluded from further analysis.
- A number of test results gave the life to initiation and end of test. In line with the practice for welded joints, this analysis has been based on life to through-thickness cracking.
- In many cases, SCFs for individual specimens were not measured. Instead, the SCFs for each group of nominally identical specimens were determined by tests on a small sample of specimens using either strain gauge measurement or finite element analysis.
- The majority of the tests were carried out on specimens in air under constant amplitude loading.
- Parameters which can be extracted from this database include section thickness, environment, variable amplitude loading and weld repairs.



10.5.3 Appraisal of test data

10.5.3.1 Test data in air under constant amplitude loading

Results of tests on large scale cast nodes tested under constant amplitude loading in-air are presented in Figure 10.5.2. The joint type, loading mode and joint dimensions for each data point are specified in the figure. In studying the figure, the following points should be noted:

- Hurden (1986) reported that the magnitude of residual stresses which exist within a cast node are of the order of 50% of the applied compressive stress. Nakamura (1986) indicate that maximum residual stresses of 20% of yield stress existed in their cast nodes. The total stress ranges for these specimens have then been reduced by the reported level of residual stresses accordingly.
- For the stress cases where premature failure at the welded end connections attaching the specimen and the rig occurred, the results have been omitted in the subsequent analysis.
- For the specimens with 'optimised' joint shape, the dominant fatigue crack for each of the specimens was initiated at the central point of the chord member. Accordingly, the thickness values of the specimens quoted in Figure 10.5.2 were measured from the central point of the chord members.

A mean fit to the nodal joint data alone, ignoring runners, gives:

$$\log(N) = 15.523 - 3.747\log(S)$$

By normalising the data in terms of a scale effect parameter an S-N curve in-line with those for as-welded joints can be derived. It was found (SLP 1995) that a scale exponent of 0.15 was more typical of these joints in accordance with the findings of Section 5.1.5. Adjusting the data to a basecase member thickness of 16mm gave a shallower slope than found for as-welded joints, with $m \approx 4$.

Overall the mean fit S-N curve with $m = 4$ is:

$$\log(N) = 16.121 - 4.\log(S_B) \quad (S_E = 0.238)$$

which is the new Class CS curve specified by the HSE (1993b). In accordance with the reported design curve, four standard deviations are taken to account for additional uncertainty in finding small initial defects. ie. the design S-N curve is:

$$\log(N) = 15.169 - 4.\log(S_B)$$

SLP (1995) reported fatigue results from tests on cast pieces that were carried out by Kobe, ARSEM and Lokomo. The tests with a stress ratio $R = -1$ resulted in a substantially greater fatigue life compared to $R = 0$ tests when the full stress range was used. This is primarily because of the almost negligible



residual stresses in these small scale cast pieces. The fatigue lives of ARSEM data were substantially higher than those of the Kobe and Lokomo data. SLP report that this was because of the compressive residual stress of up to 350 N/mm^2 which was introduced into the ARSEM specimens by shot blasting operations, see Section 9.2.4.

Results on tests on cruciforms were carried out by Hoesch, BSC and Kobe. The shape of fillet in these cruciforms has little effect on fatigue endurance once the appropriate SCF has been calculated. This implies that a specimen under a particular load case can be characterised by a maximum stress which can be used with a relevant S-N curve and confirms the maximum stress range design concept.

Figure 10.5.2 shows that the large scale test data generally follow the trend of the small scale specimens.

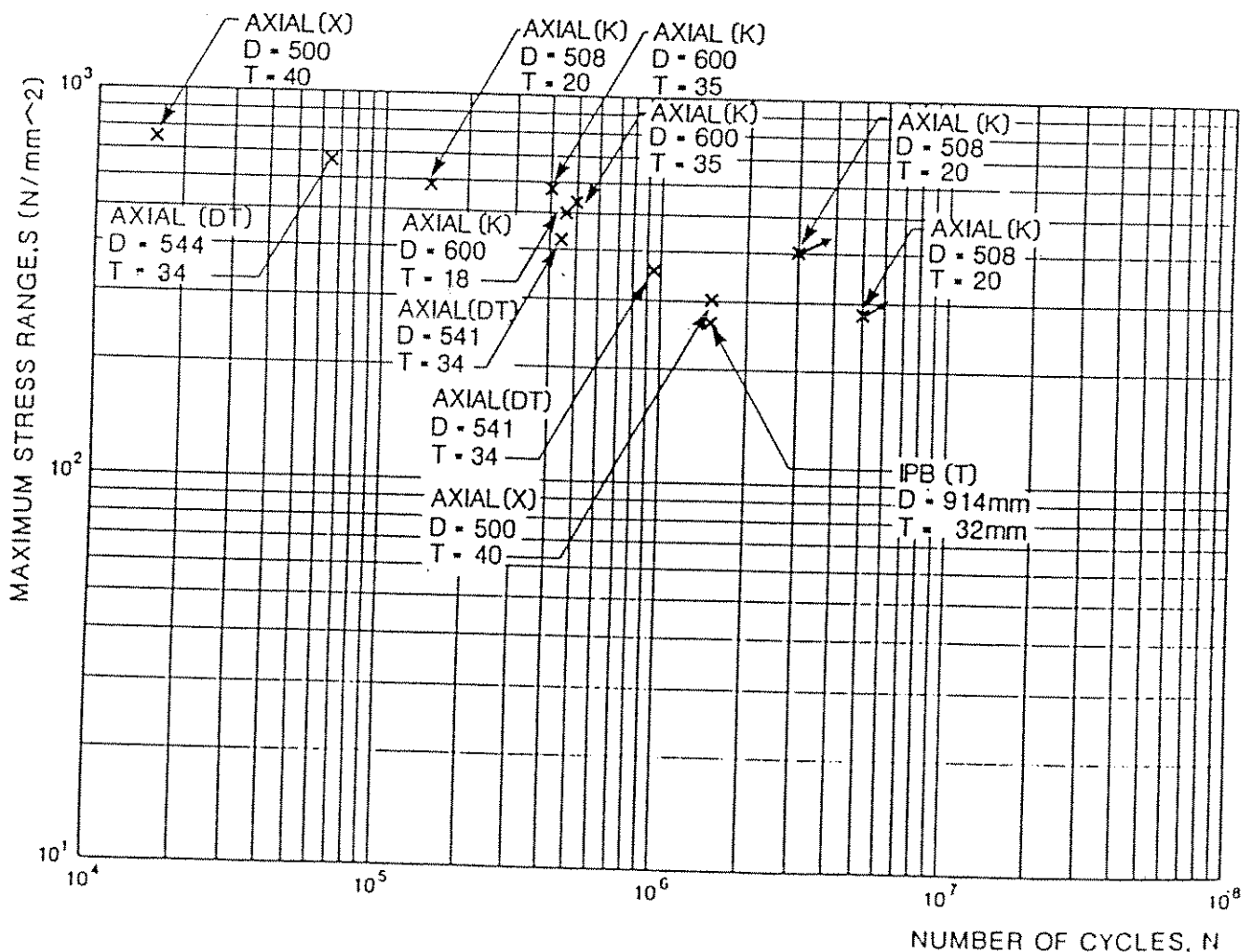


Figure 10.5.2 Cast joint tests in-air



10.5.3.2 Test data in-seawater

No test data exist for nodes in-seawater. However, SLP (1995) report test data in-seawater from castings by BSC (cruciforms tested under free corrosion conditions) and Glasgow University (cruciforms tested with and without CP).

It was reported by SLP (1995) that the seawater data points cover restrictive ranges (from 1.8×10^5 to 2×10^6 in terms of number of cycles and from 250 N/mm^2 to 320 N/mm^2 in terms of stress range). The fatigue lives of unprotected specimens in a seawater environment are lower than in air by a factor of 1.9.

Based on two data points at a stress range of 475 N/mm^2 , the benefits of cathodic protection with potential at -850mV are not being realised. The effect of CP for cast joints and the effect of cathodic over-protection cannot currently be quantified empirically without making conservative assumptions due to lack of adequate data.

10.5.3.3 Test data under VA loading

No test data exist for VA load tests on large scale joints.

Only one set of data obtained from tests on V-shaped specimens are available (SLP 1995). SLP report that the effects of variable loading on cast specimens are the same as that on as-welded specimens. Analysis of data by SLP indicates that the use of the linear damage accumulation law of Palmgren-Miner with the damage sum of 1.0 gives a safe estimate of fatigue life.

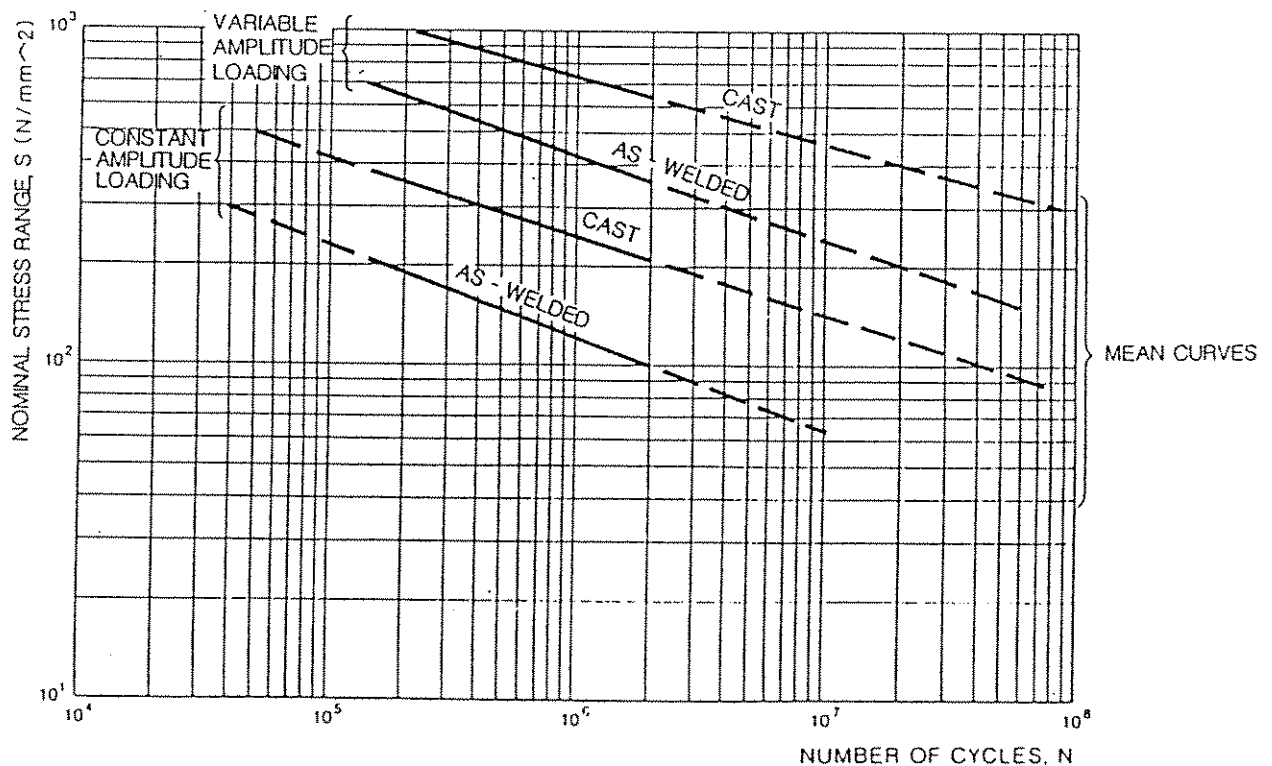


Figure 10.5.3 Cast joint data under VA loading



10.5.4 Recommendations

Most data on castings comes from cast pieces and cruciforms rather than nodal joints. However, it has been shown that in-air there is little difference, on average, between the data from the nodal joints and the remainder of the database.

In-air the S-N curve derived was based on the data used by the HSE to develop a new S-N curve for castings (HSE 1995). Therefore, the mean S-N curve is identical to that specified, and the design curve has been taken as the mean less four standard deviations in-line with the HSE's approach.

In-seawater most cast piece data is under free corrosion conditions and give a life, on average, a factor of 1.9 less than in-air, which is less than recommended for as-welded specimens. However, it is recommended that the seawater factors derived for as-welded joints be applied to castings.



10.6 Tubular Girth Welds

10.6.1 Design codes

The current HSE (1993), DnV (1992) and CAN/CSA (1992) codes classify girth welds as:

Class C if the weld is made from both sides with the weld dressed flush with the surface and free from significant defects by NDE

Class E if the weld is made from both sides

Class F if the weld is made from one side with a permanent backing strip

Class F2 if the weld is made from one side without a backing strip provided that full penetration is achieved.

These are replicated in the proposed HSE (1995) guidance with the new classification factors 0.76P, 1.14P, 1.34P and 1.52P.

10.6.2 Single sided closure welds

In 1990, TWI prepared a report for the UK Department of Energy on 'single sided welding of closure joints in large tubular fabrications', TWI (1991). In the introduction to this report it was noted that 'In the fabrication of tubular steel offshore structures using the 'node' principle, it is often necessary to make a large number of closure butt welds. Typical locations are, for example, brace to node stub connections. These welds must be made from the outside and normally without the assistance of any form of backing. Alternatively, provision can be made for access to the inside by means of a 'window', but in this case fitting of the plate which closes the window again calls for a butt weld to be made from the outside only. Both weld types may be subject to fatigue loading which is further exacerbated by the effect of the poor fit-up conditions often present in closure joints. The normal fabrication tolerances due for example, to out-of-roundness, together with misalignment of the tubulars gives rise to variable root preparations.'

'The fatigue performance of the closure welds will become increasingly important as the fatigue strength of the node itself is improved by, for example, the use of castings, forgings, or thickened tubulars for the chords.'

'The recent survey of offshore fabrication practice showed that root gaps of up to 20mm and joint misalignment of up to 6mm could be encountered in making single-sided closure welds (SSCW), although in the majority of cases the standard of fit-up was better. Under these conditions it is difficult to ensure that closure joints are free of root defects, such as incomplete penetration and lack of root fusion, which may impair the fatigue performance of the joint. Added to this is the effect of a thickness transition which is very often located on the inside edge of circumferential welds thus coinciding with the root.'



The difficulties of making sound closure welds are compounded by the fact that the potential root defects are hard to detect, characterise and size by conventional non-destructive testing (NDT) methods. For these reasons the fatigue performance of SSCW may be variable. Because of this uncertainty, they are not classified as a detail for fatigue design to BS5400 and they have been assigned a low class (F2) in the current UK Department of Energy Guidance Notes (1993). In addition, a number of recent fatigue failures in North Sea structures which have initiated either at circumferential closure welds or at window welds serve to highlight the critical nature of these problems.

TWI investigated the stress-fatigue behaviour of single sided closure welds via 44 small scale and one large scale joint test. The 44 small scale test pieces were cut from three complete closure welds in 25mm : 38mm tubular connections ($D = 1000\text{mm}$). Each test piece was nominally 125mm wide and welded using either the manual metal arc (MMA) or self-shielded flux-cored arc welding process. The connections also represented a range of axial and angular misalignment, each tested at $R = 0$ tensile axial loading. The one full scale test consisted of a complete closure joint ($D = 1800\text{mm}$) under four-point bending.

The mean S-N lines resulting from this analysis are shown in Figure 10.6.1. The mean of the present data is above the HSE Class F mean line, whilst the mean-2SD of the present data crosses the Class F design line at about 400,000 cycles. The present data has a slightly steeper slope, ($m = 2.83$ compared with $m = 3.0$) than the standard fatigue classes. However, similar slopes ranging from $m = 2.74$ to $m = 2.97$, were obtained in the original analysis from which the design classes were derived.

Current HSE (1993) design guidance for offshore structures recommends a fatigue Class of F2 for a single-sided girth weld made from one side without a backing strip. It is also stated that 'the stress should include the stress concentration factor to allow for any thickness change and for fabrication tolerances'.

Examination of this data suggests that the current test results would be compatible with a design classification of F provided the stress concentrating effects of misalignment are taken fully into account. If specimens showing defects on the fracture face are disregarded, the results come close to a classification of E. However, it must be noted that some of these defects were not rejected to ASME VIII by the fabricator's inspection. Thus it is possible that similar defects would exist in production welds. It should also be noted that the stresses acting at the weld root were accurately defined by strain gauge measurements. In practice the stress acting would be estimated and the misalignment would not be accurately known. Also, the mean-2 standard deviations fit to the data falls slightly below the Class F design line at low stresses. To allow for these uncertainties, it was recommended by TWI (1990) that the current recommendation in the Guidance Notes of Class F2 be maintained.

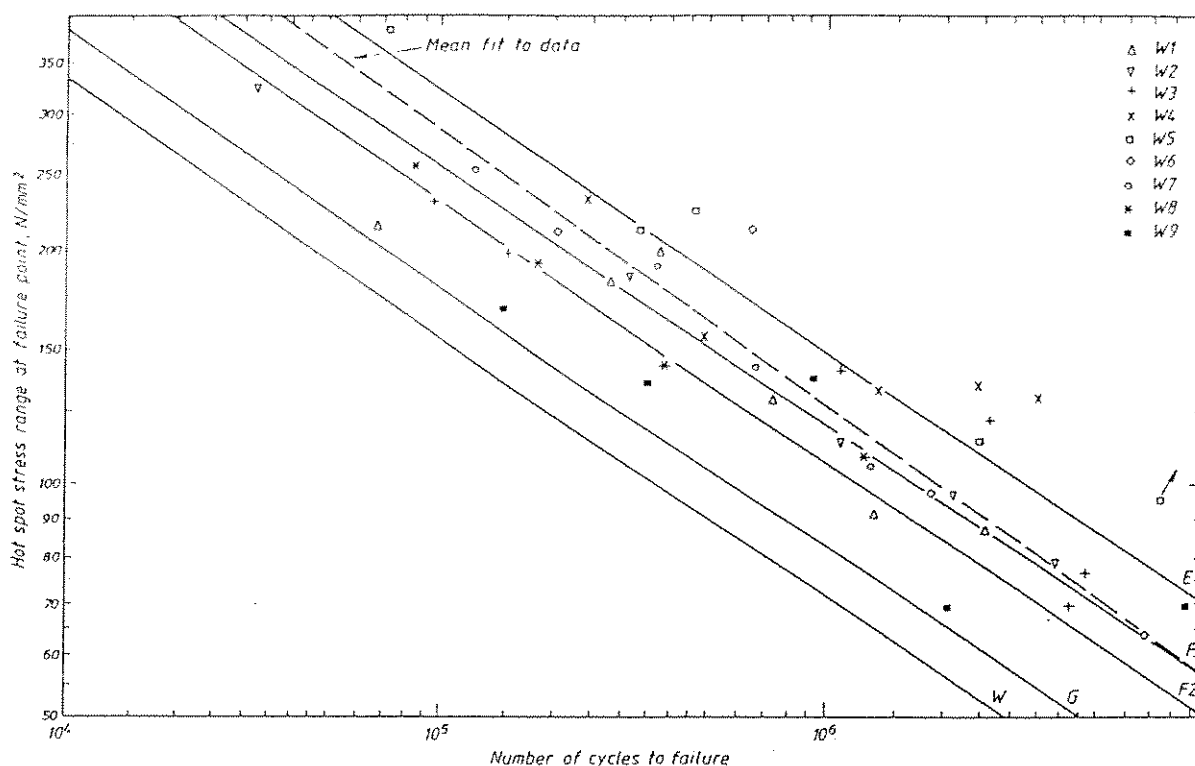


Figure 10.6.1 Girth weld tests against the mean and design weld classes and the mean fit regression line (TWI 1991)

10.6.3 Backing strips

The use of thin plate backing strips in girth welding is becoming increasingly accepted as a method for improving weld consistency and economy.

Marshall(1992) summarised a series of tests on transition pieces with a backing plate held in position during welding by a bolting arrangement. The backing strips were 4mm thick, 50mm wide and made from Grade 43C steel to BS4360.

Figure 10.6.2 illustrates the test results from thin specimens in 22mm, 30mm and 51mm plate. The test results were not published and therefore this figure is only a reproduction of the results published. In Figure 10.6.2, the data has been corrected to 22mm S-N curves. It can be seen that this approach gives fatigue lives that are at least as good as those from single sided closure welds, while giving a more consistent quality weld that can be made in a connection with less controlled fit-up and potentially would need less inspection and repair. However, as the author states, it is important for welding standards and limits to be developed and adhered to if reductions in weld defects are to be reduced.

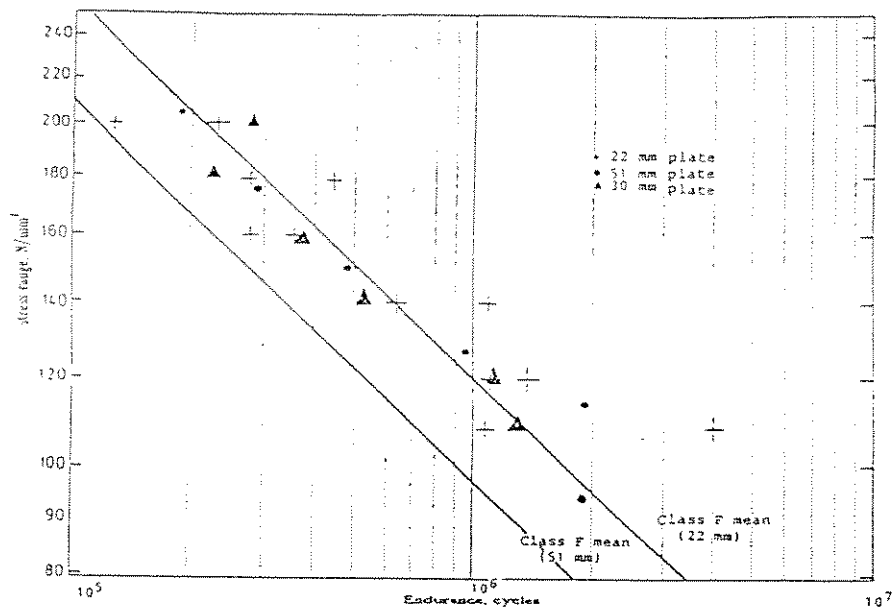


Figure 10.6.2 Fatigue test data of connections made using backing strips, by Marshall (1993)



11. SUMMARY OF MEAN AND DESIGN S-N CURVES FOR TUBULAR JOINTS

11.1 Mean Fit S-N Curves

For joints tested in-air the following S-N curves have been found to best represent the test data collated and screened in this Guide.

11.1.1 Tubular Joints

The mean S-N curve for tubular joints in-air with no chord end loading is given by:

$$\text{Basic curve } (10^4 \leq N \leq 10^7) \quad \log(N) = 12.900 - 3.\log(S_B)$$

$$\text{High endurance } (N > 10^7) \quad \log(N) = 14.867 - 4.\log(S_B)$$

Low endurance ($N < 10^4$):

Linear extrapolation between $\log(S_B\{N=0\})$ and $\log(S_B\{N=10^4\})$, as specified in Section 7.4.

11.1.2 Cast joints

$$\log(N) = 16.121 - 4.\log(S_B)$$

11.2 Design S-N Curves

11.2.1 Tubular Joints

The mean S-N curve for tubular joints in-air with no chord end loading is given by:

$$\text{Basic curve } (10^4 \leq N \leq 10^7) \quad \log(N) = 12.500 - 3.\log(S_B)$$

$$\text{High endurance } (N > 10^7) \quad \log(N) = 14.333 - 4.\log(S_B)$$

Low endurance ($N < 10^4$):

Linear extrapolation between $\log(S_B\{N=0\})$ and $\log(S_B\{N=10^4\})$, as specified in Section 7.4.

ie. The design fatigue life of the S-N curve is 0.4 times the mean life.

11.2.2 Cast joints

$$\log(N) = 15.169 - 4.\log(S_B)$$



11.3 Factors on Fatigue Life

11.3.1 Scale effect

Tubular joints with satisfactory weld profile:

$$S_B = S.(T^*/16)^{0.25} \quad \text{where } T^* \text{ is the thickness of the member under consideration } (T^* \geq 16\text{mm}).$$

Tubular joints with unsatisfactory weld profile:

$$S_B = S.(T^*/16)^{0.35} \quad \text{where } T^* \text{ is the thickness of the member under consideration } (T^* \geq 16\text{mm}).$$

Cast joints:

$$S_B = S.(T^*/38)^{0.15} \quad \text{where } T^* \text{ is the thickness of the member under consideration } (T^* \geq 38\text{mm}).$$

11.3.2 Other factors

<u>Reason for factor</u>	<u>Factor on life</u>
Seawater with CP (or HSE recommendations of 0.5 of high stressed joints only)	0.50
Epoxy coated in splash zone	0.50
Seawater under free corrosion	
Cool waters (roughly $\leq 10^\circ\text{C}$)	0.33
Warm waters (roughly $> 10^\circ\text{C}$)	0.25
Post-weld heat treatment	see proposed HSE
Inspectability: Account should be taken for accessibility and redundancy	
Overlapped joints	1.00
Multiplanar joints	1.00
Ring-stiffened joints	
at the brace/chord junction (not BRI)	1.00
at the brace/chord junction (near BRI)	1.34P
at the ring web to inner chord connection	1.34P
at the ring stiffener inner edge	1.00P
Grouted joints	1.00
Girth welds	
no backing strips	1.14P
with backing strips	1.34P



Reassessment only	
Poor weld profile	0.50
Grinding	2.20
Hammer peening	Class B curve (or alternatively 0.64P)
Slot peening	Class C curve (or alternatively 0.76P)
TIG dressing	1.50

nb. for weld improvement methods no benefit should be taken for
 $N < 10^5$ cycles.



12. REFERENCES FOR CHAPTER 5

1924

Palmgren, 1924.

Palmgren, A. L. 'Endurance of ball-bearings', VDI Zeitschrift, Volume 68, Pages 339-341, 1924.

1945

Miner, 1945.

Miner, M. A. 'Cumulative damage in fatigue', Journal of Applied Mechanics (ASME), Volume 1, Pages 159-164, September 1945.

1956

Kellogg, 1956.

Kellogg, M. W. 'Design of piping systems', Second Edition, Wiley, 1956.

1974

Marshall, 1974.

Marshall, P. W. 'General consideration for tubular joint design', Proc. of Welding Institute Conference on Welding in Offshore Construction, Newcastle, UK, 1974.

Marshall and Toprac, 1974.

Marshall, P. W. and Toprac, A. A. 'Basis for Tubular Joint Design', Welding Research Supplement, May 1974.

1975

Kuang, 1975.

Kuang, J. G., Potvin, A. B. and Leick, R. D. 'Stress concentrations in tubular joints', OTC 2205, Houston, Texas, USA, 1975.

1977

Kuang, 1977.

Kuang, J. G., Potvin, A. B., Leick, R. D. and Kahlick, J. L. 'Stress concentration in tubular joints', Society of Petroleum Engineers Journal, August 1977.

1978

Gibstein, 1978.

Gibstein, M. B. 'Parametric stress analysis of T joints', European Offshore Steels Research Seminar, Cambridge, UK, November 1978.

Lawrence, 1978.

Lawrence, F. V., Burk, J. D., et al. 'Estimating the fatigue crack initiation life of welds', ASTM STP 648, pp 134-145, 1978.

Wordsworth and Smedley, 1978.

Wordsworth, A. C. and Smedley, G. P. 'Stress concentrations at unstiffened tubular joints', European Offshore Steels Research Seminar, Cambridge, UK, November 1978.

1979

Gurney, 1979.

Gurney, T. R. 'Fatigue of welded structures', Second Edition, Cambridge University Press, 1979.

Sawada, 1979.

Sawada, Y., Idogaki, S and Sekita, K. 'Static and fatigue tests on T joints stiffened by an internal ring', Offshore Technology Conference, OTC 3422, Houston, USA, 1979.

Tebbett, I. E., Beckett, C. D. and Billington, C. J. 'The punching shear strength of tubular joints reinforced with a grouted pile', Offshore Technology Conference, OTC 3463, Houston, USA, 1979.

1981

Brandi, 1981.

Brandi, R. 'Behaviour of unstiffened and stiffened tubular joints'. Steel in Marine Structures, SIMS 6.1, Paris, France, 1981.

Damilano, 1981.

Damilano, G. F., Camisetti, C. and Negri, A. 'Fatigue behaviour of unstiffened and stiffened Y tubular joints'. Steel in Marine Structures, SIMS 10.1, Paris, France, 1981.

Dijkstra and de Back, 1981.

Dijkstra, O. D. and de Back, J. 'Fatigue strength of tubular X- and T- joints (Dutch) tests', Steels in Marine Structures, SIMS 8.4, Paris, France, 1981.

Gibstein, 1981.

Gibstein, M B. 'Fatigue strength of welded tubular joints', Steel in Marine Structures, SIMS 8.5, Paris, France, 1981.

Haagensen, 1981.

Haagensen, P. J. 'Improvement in the fatigue strength of welded joints', Steel in Marine Structures, SIMS PS6, Paris, France, 1981.

Lieurade, 1981a.

Lieurade, H-P. and Gerald, J. P. 'Results of static tests on ten full-scale X-joints', Steel in Marine Structures, SIMS 6.4, Paris, France, 1981.

Lieurade, 1981b.

Lieurade, H-P., Sanz, G. and Gerald, J. P. 'Fatigue tests on ten full-scale X-joints', Steel in Marine Structures, SIMS 8.1, Paris, France, 1981.

Maahn, 1981.

Maahn, E. 'The influence of cathodic protection on crack growth rate in fatigue of steel in seawater', Steel in Marine Structures, SIMS 5.3, Paris, France, 1981.

Van Leeuwen, 1981.

Van Leeuwen, J. L., de Back, J. and Vaessen, G. H. 'Constant amplitude fatigue tests on welded steel joints performed in air and seawater', Steel in Marine Structures, SIMS 2.1, Paris, France, 1981.



Wordsworth, 1981.

Wordsworth, A. C. 'Stress concentration factors at K and KT tubular joints', Conference on Fatigue in Offshore Structural Steel. Institute of Civil Engineers, London, UK, 1981.

1982

Hoesch, 1982.

'Stress analysis and fatigue testing of cast steel K-nodes manufactured by Hoesch', Veritas Report No. 82-1096, 1982.

Tebbett, I. E. 'The reappraisal of steel jacket structures allowing for the composite action of grouted piles', Offshore Technology Conference, OTC 4194, Houston, USA, 1982.

1983

Marshall, 1983.

Marshall P. W. 'Size effect in tubular welded joints', ASCE Structures Congress, Houston, USA, 1983.

1984

DEn, 1984a.

Department of Energy 'Offshore Installations: Guidance on Design and Construction', HMSO, London, April, 1984.

DEn, 1984b.

'Background to new fatigue design guidance for steel welded joints in offshore structures', HMSO, London, 1984.

DnV, 1984.

Det Norske Veritas Classification Note No. 30.2 'Fatigue Strength Analysis for Mobile Offshore Units', August 1984.

Veritec, 1984.

'Double-skin grout reinforced tubular joints', Final Report, Veritec report No.84-3564.

1985

Bainbridge, 1985.

Bainbridge, C. A. 'Fatigue analyses/Offshore structures', Institute of Marine Engineers, London, UK, October 1985.

Efthymiou and Durkin, 1985.

Efthymiou, M. and Durkin, S. 'Stress concentrations T/Y and gap/overlap K-joints', Behaviour of Offshore Structures, BOSS'85, Delft, The Netherlands, 1985.

UEG, 1985.

'Design of Offshore Tubular Joints for Offshore Structures', UEG Publication UR33, 1985.

Webster and Walker, 1985.

Webster, S. E. and Walker, E. F. 'Summary of research work undertaken on the development of node steel', BSC Report RSC/7436/-85, 1985.



1986

Hara, 1986.

Hara, M., Kawai, Y., Narumoto, A. and Matsumoto, S. 'Corrosion fatigue strength of 490 MPa class high-strength steels produced by thermo-mechanical control process', Offshore Technology Conference, OTC 5611, Houston, USA, 1986.

Hurden, 1986.

Hurden, D. C., Tebbett, I. E. and Wood, T. 'New data on the fatigue performance of cast steel tubular joints', Offshore Technology Conference, OTC 5310, Houston, USA, 1986.

Nakamura, 1986.

Nakamura, K. et al, 'Fatigue strength of cast steel node', International Meeting on Safety Criteria in Design of Tubular Structures, Tokyo, 1986.

1987

Bignonnet, 1987.

Bignonnet, A., Picouet, L., Lieurade, H-P. and Castex, L. 'The application of shot peening to improve the fatigue life of welded steel structures', Steel in Marine Structures, SIMS TS33, Delft, The Netherlands, 1987.

Gerald, 1987.

Gerald, J. P., Bignonnet, A., Lieurade, H-P. and Lecoq, H. 'Fatigue tests on ten full-scale X-joints', Steel in Marine Structures, SIMS TS15, Delft, The Netherlands, 1987.

Haagensen, 1987.

Haagensen, P. J., Dragen, A., Slind, S. and Orjasaeter, O. 'Prediction of the improvement in fatigue life of welded joints due to grinding, TIG dressing, weld shape control and shot peening', Steel in Marine Structures, SIMS TS35, Delft, The Netherlands, 1987.

Thomson and Tyson, 1987.

Thomson, R. and Tyson, W. 'An overview of the National Canadian Offshore Steels Research Programme', Steel in Marine Structures, SIMS RS4, Delft, The Netherlands, 1987.

UKOSRP II, 1987.

'United Kingdom Offshore Steels Research Project - Phase II Final Summary Report', HMSO, OTH 87 265, 1987.

1988

Brown, G. M., Holmes, R. and Kerr, J. 'Fatigue life enhancement of welded tubular joints by injection of grout', Behaviour of Offshore Structures Conference, BOSS'88, Trondheim, Norway, 1988.

Efthymiou, 1988.

Efthymiou, M. 'Development of SCF formulae and generalised influence functions for use in fatigue analysis', Offshore Tubular Joints Conference, OTJ'88, Egham, Surrey, UK, 1988.



Rhee, 1988.

Rhee, H. C. 'Fracture mechanics fatigue life for a multi-plane K-joint', Offshore Mechanics and Arctic Engineering Conference, OMAE 1988, Houston, USA, February 1988.

UKOSRP I, 1988.

'United Kingdom Offshore Steels Research Project - Phase I. Final report', HMSO, OTH 88 282, 1988.

Wylde, 1988.

Wylde, J. G. and Yamamoto, N. 'Seawater corrosion fatigue tests on steel tubular joints', Paper 7921.01/87/589.2, The Welding Institute, March 1988.

1989

COSRP, 1989.

Pates, M. J., Burns, D. J., Mohaupt, U. H., Forbes, J., Swamidas, A. S., Munaswamy, K. and Hopkins R. M. 'Fabrication and fatigue evaluation of welded joints for structures in marine environment - Phase II', Final Report, June 1989.

DEn, 1989.

'Background to new static strength guidance for tubular joints in steel offshore structures', HMSO, OTH 89 308, 1989.

Lloyds, 1989.

Lloyd's Register of Shipping 'Rules for the classification of fixed offshore installations', Part 4, Steel structures, December 1989.

Pook and Dover, 1989.

Pook, L. P. and Dover, W. D. 'Progress in the development of a wave action standard history (WASH) for fatigue testing relevant to tubular structures in the North Sea', Development of Fatigue loading Spectra, ASTM STP 1006, pp 99-120, 1989.

UKOSRP I, 1989.

'United Kingdom Offshore Steels Research Project - Phase I. Research contract reports' (in microfiche format), HMSO, OTI 89 540, 1989.

UKOSRP II, 1989a.

'United Kingdom Offshore Steels Research Project - Phase II. Summary of project task reports', HMSO, OTH 89 266, 1989.

UKOSRP II, 1989b.

'United Kingdom Offshore Steels Research Project - Phase II. Project task reports' (in microfiche format), HMSO, OTH 89 310, 1989.

1990

Cole, 1990

Cole, I., Pietrosanti, C., Vittori, O., Bufalini, P. and Rizzi, L. 'Welded joints in offshore structures: the significance of data derived from small and full scale tests', Offshore Mechanics and Arctic Engineering Conference, OMAE 1990, Houston, USA, February 1990.



Haagensen, 1990.

Haagensen, J., Slind, T and Oerjasaeter, O. 'Scale Effects in Fatigue Design data for Welded and Unwelded Components', Offshore Mechanics and Arctic Engineering Conference, OMAE 1990, Houston, USA, February 1990.

Haugland and Thuestad, 1990.

Haugland, H. and Thuestad, T. C. 'Fatigue and crack growth in a submerged ring-stiffened tubular joint', Integrity of Offshore Structures - 4, Glasgow, July 1990.

Ramachandra Murthy, 1990.

Ramachandra Murthy, D. S., Madhava Rao, A. G., Gandhi, P., Pant, P. K. and Sarkar, P. P. 'Stress concentration in internally ring-stiffened steel tubular joints used in offshore structures', Proc. 1st Pacific/Asia Offshore Mechanics Symposium, Seoul, Korea, June 1990.

TWI, 1990.

'Single-sided welding of closure joints in large tubular fabrications - Final Summary Report', HMSO, OTH 90 335, 1990.

Wimpey, 1990.

Wimpey Offshore, 'Joint Industry Cast Joints Research Project, Phases I and II', Final Report, 1990.

1991

COSRP, 1991.

Pates, M. J., Swamidas, A. S., Hopkins R. M. and Muggeridge, D. B. 'Final report of the project on fabrication and fatigue evaluation of welded tubular T-joints for structures in marine environments - Phase III. Combined axial and bending load fatigue test on tubular T-joint', April 1991.

Maddox, 1991.

Maddox, S. J. 'Fatigue strength of welded structures', Abington Publishing, Second Edition, 1991.

Smedley and Fisher, 1991a.

Smedley, P. A. and Fisher, P. J. 'Stress concentration factors for simple tubular joints', Offshore and Polar Engineering Conference, ISOPE-1, Edinburgh, UK, 1991.

Smedley and Fisher, 1991b.

Smedley, P. A. and Fisher, P. J. 'Stress concentration factors for ring-stiffened tubular joints', Fourth International Symposium on Tubular Structures, Delft, The Netherlands, 1991.

TWI, 1991a.

'A compilation of fatigue test results for welded joints subjected to high stress/low cycle conditions - Stage 1', HMSO, OTI 91 552, 1991.

TWI, 1991b.

'Summary of variable amplitude fatigue data for welded joints', HMSO, OTH 91 359, 1991.

1992

AWS, 1992.

American Welding Society. 'Structural welding code', AWS D1.1-92, 1992.

Bolt, H. M., Seyed-Kebari, H. and Ward, J. K. 'The Influence of Chord Length and Boundary Conditions on K Joint Capacity', Second International Offshore and Polar Engineering Conference, ISOPE, San Francisco, California, June 1992.

CAN/CSA, 1992.

CAN/CSA-S473-92, 'Steel structures, forming part of the Code for the Design, Construction and Installation of Fixed Offshore Structures', June 1992.

DnV, 1992.

Det norske Veritas. 'Rules for the classification of fixed offshore installations', July 1992.

MaTSU, 1992.

'Fatigue background guidance document', HMSO, OTH 92 390.

Marshall, 1992.

Marshall, V. G. 'Improvement in tubular jacket closure weld fatigue performance through alternative fabrication techniques', Offshore Technology Conference, OTC 6906, Houston, USA.

Mshana, 1992a.

Mshana, Y., Kam, J. C. and Pook L. P. 'On mixed mode fatigue crack growth in tubular welded joints', 11th International Conference on Offshore Mechanics & Arctic Engineering, OMAE, Calgary, Canada, June 1992.

Mshana, 1992b.

Mshana, Y., Kam, J. C. and McDiarmid, D. L. 'Fatigue crack growth of welded tubular joints under sequential multiple axis loading', 11th International Conference on Offshore Mechanics & Arctic Engineering, OMAE, Calgary, Canada, June 1992.

TWI, 1992.

'Fatigue behaviour of internally stiffened tubular joints', Final Report, TWI report 5592/15A/92, April 1992. Currently confidential to sponsors.

1993

API, 1993.

American Petroleum Institute. 'Recommended practice for planning, designing and constructing fixed offshore platforms', API RP 2A, Twentieth Edition, 1993.

ASTM, 1993.

American Society for Testing and Materials. 'Standard reference radiographs for steel castings up to 2 in. (51mm) in thickness', E446-93.

Cole, 1993.

Cole, I., Vittori, O. and Cerretti, G. 'Cathodic protection and the thickness effect: A final conclusion?', Proceedings of the Third International Offshore and Polar Engineering Conference, ISOPE-3, Singapore, June 1993.



Eide, 1993.

Eide, O. I., Skallerud, B. and Berge, S. 'Fatigue of large scale tubular joints - Effects of sea water and spectrum loading', Fatigue under Spectrum Loading and in Corrosive Environments, Lyngby, Denmark, August 1993.

HSE, 1993.

Health and Safety Executive. 'Offshore installations: Guidance on design, construction and certification', 4th (Consolidated) Edition, March 1993.

Ibso and Agerskov, 1993.

Ibso, J. B. and Agerskov, H. 'Fatigue life prediction of offshore tubular structures under stochastic loading', Fatigue under Spectrum Loading and in Corrosive Environments, Lyngby, Denmark, August 1993.

Marshall, 1993.

'API Provision for SCF S-N, and size profile effects', Offshore Technology Conference, OTC 7155, Houston, USA, 1993.

Pang, 1993.

Pang, H. L. 'Analysis of fatigue strength improvements by weld toe grinding', Proceedings of the Third International Offshore and Polar Engineering Conference, ISOPE-3, Singapore, June 1993.

Romeijn 1993.

Romeijn, A., Wardenier, J., de Koning, C. H., Puthli, R. S. and Dutta, D. 'Fatigue behaviour and influence of repair on multiplanar K-joints made of circular hollow sections', Proceedings of the Third International Offshore and Polar Engineering Conference, ISOPE-3, Singapore, June 1993.

1994

Berge, 1994.

Berge, S., Haswell, J. and Engesvik, K. 'Fracture mechanics analysis of tubular joint tests degree of bending effects', 13th International Conference on Offshore Mechanics and Arctic Engineering, OMAE, Houston, USA, March 1994.

Din, 1994.

Din, K. B. 'A preliminary investigation to assess the validity of Miner's cumulative damage rule', Seminar on Recent Developments in Steel Construction, Kuala Lumpur, January 1994.

Haagensen, 1994.

Haagensen, P. J. 'Effectiveness of grinding and peening techniques for fatigue life extension of welded joints', 13th International Conference on Offshore Mechanics and Arctic Engineering, OMAE, Houston, USA, March 1994.

le Meur, G., Falcinaigne, J. and Ozanne, P. 'Ultimate strength and fatigue resistance of grouted tubular joints', 13th International Conference on Offshore Mechanics and Arctic Engineering, OMAE, Houston, USA, March 1994.

Ramachandra Murthy, 1994a.

Ramachandra Murthy, D. S., Madhava Rao, A. G., Gandhi, P., Pant, P. K., Anto, P. F. and Samant, A. K. 'Corrosion fatigue of stiffened tubular T and Y joints', Proceedings of the Fourth International Offshore and Polar Engineering Conference, ISOPE-4, Osaka, Japan, April 1994.



Ramachandra Murthy, 1994b.

Ramachandra Murthy, D. S., Gandhi, P. and Madhava Rao, A. G. 'A model for fatigue life prediction of offshore welded stiffened steel tubular joints using FM approach', International Journal of Offshore and Polar Engineering, IJOPE, Volume 4, No. 3, September 1994.

Tubby, 1994.

Tubby, P. J., Eide, O. I., Skallerud, B. and Berge, S. 'Variable amplitude fatigue of steel tubular joints in sea water with cathodic protection', 13th International Conference on Offshore Mechanics and Arctic Engineering, OMAE, Houston, USA, March 1994.

1995

HSE, 1995.

Health and Safety Executive. 'Offshore installations: Guidance on design, construction and certification'. 4th Edition (1990). February 1995.

Mohr, W., 1995

To be published

MTD, 1995

'High strength steels in offshore engineering'. Publication 95/100

SLP (1995)

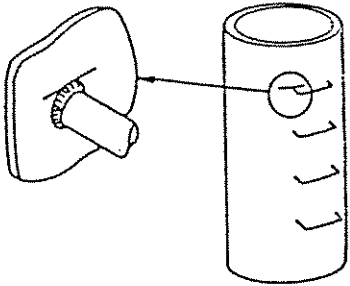
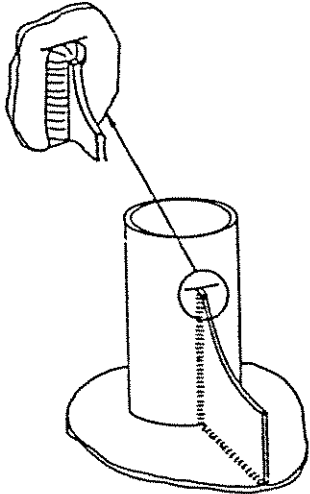
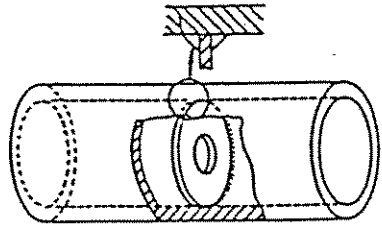
OTH report to be published




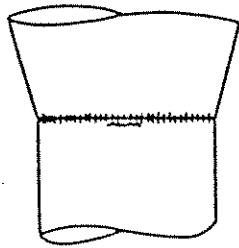
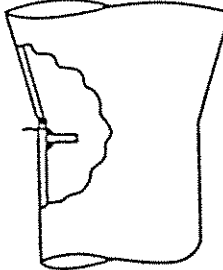
APPENDIX A
TUBULAR JOINT CLASSIFICATIONS



A1. CURRENT HSE

Type number, description and notes on mode of failure	Class Explanatory comments	Examples, including failure modes
TYPE 7 DETAILS RELATING TO TUBULAR MEMBERS		
7.1 Parent material adjacent to the toes of full penetration welded nodal joints.	T In this situation design should be based on the hot spot stress as defined in section 4.2.1.11.(a) (See this Section also for guidance on partial penetration welds).	
7.2 Parent metal at the toes of welds associated with small ($\leq 150\text{mm}$ in the direction parallel to the applied stress) attachments to the tubular member. Ditto, but with attachment length $> 150\text{mm}$.	F F2	
7.3 Gusseted connections made with full penetration or fillet welds. (But note that full penetration welds are normally required).	F Note that the design stress must include any local bending stress adjacent to the weld end. W For failure in the weld throat of fillet welded joints.	
7.4 Parent material at the toe of a weld attaching a diaphragm or stiffener to a tubular member.	F Stress should include the stress concentration factor due to overall shape of adjoining structure.	



Type number, description and notes on mode of failure	Class	Explanatory comments	Examples, including failure modes
<p>7.5 Parent material adjacent to the toes of circumferential butt welds between tubes.</p> <p>(a) Weld made from both sides with the weld overfill dressed flush with the surface and with the weld proved free from significant defects by non-destructive examination.</p> <p>(b) Weld made from both sides.</p> <p>(c) Weld made from one side on a permanent backing strip.</p> <p>(d) Weld made from one side without a backing strip provided that full penetration is achieved.</p>	<p>C</p> <p>E</p> <p>F</p> <p>F2</p>	<p>In this type of joint the stress should include the stress concentration factor to allow for any thickness change and for fabrication tolerances.</p> <p>The significance of defects should be determined with the aid of specialist advice and/or by the use of fracture mechanics analysis. The NDT technique should be selected with a view to ensuring the detection of such significant defects.</p> <p>Note that step changes in thickness are in general, not permitted under fatigue conditions, but that where the thickness of the thicker member is not greater than $1.15 \times$ the thickness of the thinner member, the change can be accommodated in the weld profile without any machining.</p>	
<p>7.6 Parent material at the toes of circumferential butt welds between tubular and conical sections.</p>	<p>C</p> <p>E</p> <p>F</p> <p>F2</p>	<p>Class and stress should be those corresponding to the joint type as indicated in 7.5, but the stress must also include the stress concentration factor due to overall form of the joint.</p>	
<p>7.7 Parent material (of the stressed member) adjacent to the toes of bevel butt or fillet welded attachments in a region of stress concentration.</p>	<p>F</p> <p>or</p> <p>F2</p>	<p>Class depends on attachment length (see Type 4.1) but stress should include the stress concentration factor due to overall shape of adjoining structure.</p>	



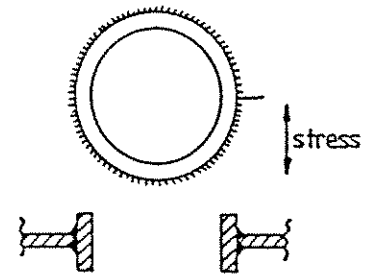
Type number, description and notes on mode of failure

Class Explanatory comments

Examples, including failure modes

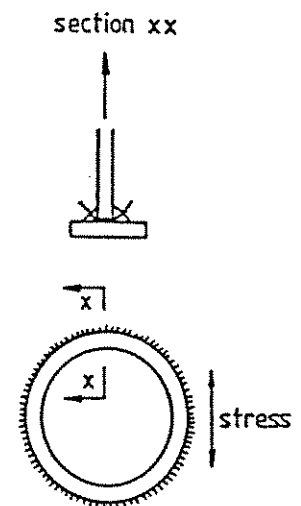
7.8 Parent metal adjacent to, or weld metal in, welds around a penetration through the wall of a member (on a plane essentially perpendicular to the direction of stress). Note that full penetration welds are normally required in this situation.

D In this situation the relevant stress should include the stress concentration factor due to the overall geometry of the detail.



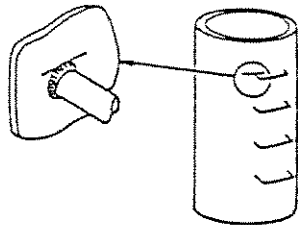
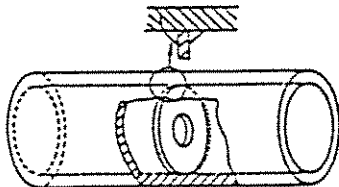
7.9 Weld metal in partial penetration or fillet welded joints around a penetration through the wall of a member (on a plane essentially parallel to the direction of stress).

W The stress in the weld should include an appropriate stress concentration factor to allow for the overall joint geometry.





A2. DnV

TYPE 7 DETAILS RELATING TO TUBULAR MEMBERS			
7.1	Parent material adjacent to the toes of full penetration welded nodal joints.	T	In this situation design should be based on the hot spot stress.
7.2		F2	
7.3 (a)	Gusseted connections made with full penetration welds.	F2	The design stress must include the stress concentration factor due to the overall form of the joint.
7.3 (b)	Gusseted connections made with fillet welds.	F2	The design stress must include the stress concentration factor due to the overall form of the joint for failure in parent metal.
		W	Ditto but for failure in weld throat
7.4	Parent material at the toe of a weld attaching a diaphragm to a tubular member	F	




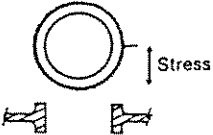
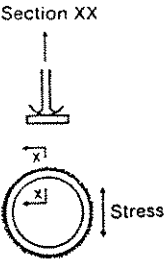
<p>7.5 Parent material at the toes of circumferential butt welds between tubes:</p> <p>(a) Weld made from both sides dressed flush</p> <p>(b) Weld made from both sides</p> <p>(c) Weld made from one side on a backing bar</p> <p>(d) Weld made from one side without a backing bar</p>	<p>C E F</p>	<p>In all cases stress must include the stress concentration factor to allow for any thickness change and for fabrication tolerances.</p>	
<p>7.6 Parent material at the toes of circumferential butt welds between tubular and conical sections.</p>	<p>E F F2</p>	<p>Class and stress are to be those corresponding to the joint type as indicated in 7.5, but the stress must also include the stress concentration factor due to overall form of the joint.</p>	
<p>7.7 Parent material (of the stressed member) adjacent to the toes of bevel butt or fillet welded attachments in a region of stress concentration.</p>	<p>F or F2</p>	<p>Class depends on attachment length (see Type 4.1) but stress must include the stress concentration factor due to overall shape of adjoining structure.</p>	
<p>7.8 Parent metal adjacent to, or weld metal in welds around a penetration through the wall of a member (on a plane essentially perpendicular to the direction of stress)</p>	<p>D</p>	<p>In this situation the relevant stress must include the stress concentration factor due to the overall geometry of the detail.</p>	
<p>7.9 Weld metal in partial penetration or fillet welded joints around a penetration through the wall of a member (on a plane essentially parallel to the direction of stress)</p>	<p>W</p>	<p>The stress in the weld should include an appropriate stress concentration factor to allow for the overall joint geometry.</p>	



A3. CAN/CSA

Type number, description, and notes on mode of failure	Class	Explanatory comments	Examples, including failure modes
Type 7: Details Relating to Tubular Members			
7.1 Parent material adjacent to the toes of complete joint penetration groove welded nodal joints.	T	In this situation, design should be based on the hot spot stress.	
7.2 Parent metal at the toes of welds associated with small (≤ 150 mm in the direction parallel to the applied stress) attachments to the tubular member.	F		
The same, but with attachment length > 150 mm.	F2		
7.3 Gussied connections made with complete joint penetration groove or fillet welds. Complete joint penetration groove welds are normally required.	F	The design stress must include any local bending stress adjacent to the weld end.	
	W	For failure in the weld throat of fillet welded joints.	
7.4 Parent material at the toe of a weld attaching a diaphragm or stiffener to a tubular member.	F	Stress should include the stress concentration factor due to overall shape of adjoining structure.	
7.5 Parent material adjacent to the toes of circumferential butt welds between tubes.		In this type of joint the stress should include the stress concentration factor to allow for any thickness change and for fabrication tolerances.	
(a) Weld made from both sides with the weld overfill dressed flush with the surface and with the weld proved free from significant defects by nondestructive examination.	C		
(b) Weld made from both sides.	E		
(c) Weld made from one side on a permanent backing strip.	F		
(d) Weld made from one side without a backing strip, provided that complete joint penetration groove weld is achieved.	F2	Step changes in thickness are in general not permitted under fatigue conditions, but that where the thickness of the thicker member is not greater than $1.15 \times$ the thickness of the thinner member, the change can be accommodated in the weld profile without any machining.	
7.6 Parent material at the toes of circumferential butt welds between tubular and conical sections.	C E F F2	Class and stress should be those corresponding to the joint type as indicated in type 7.5, but the stress must also include the stress concentration factor due to overall form of the joint.	



Type number, description, and notes on mode of failure	Class	Explanatory comments	Examples, including failure modes
7.7 Parent material (of the stressed member) adjacent to the toes of bevel groove or fillet welded attachments in a region of stress concentration.	F or F2	Class depends on attachment length (see type 4.1) but stress should include the stress concentration factor due to overall shape of adjoining structure.	
7.8 Parent metal adjacent to, or weld metal in, welds around a penetration through the wall of a member (on a plane essentially perpendicular to the direction of stress). Note that complete joint penetration groove welds are normally required in this situation.	D	In this situation the relevant stress should include the stress concentration factor due to the overall geometry of the detail.	
7.9 Weld metal in partial joint penetration or fillet welded joints around a penetration through the wall of a member (on a plane essentially parallel to the direction of stress).	W	The stress in the weld should include an appropriate stress concentration factor to allow for the overall joint geometry.	



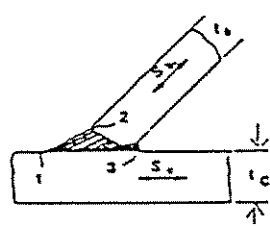
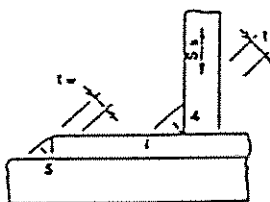
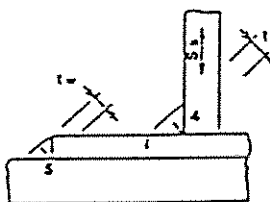
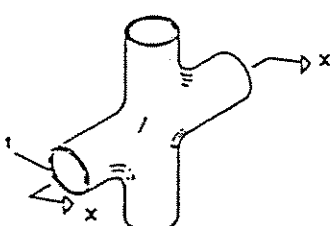
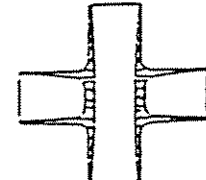
A4. PROPOSED HSE

General comments

Since fillet and partial penetration butt welds have poor fatigue performance, they should be avoided if at all possible for joints where fatigue is a significant consideration.

Notes on Thickness Correction Factor for S-N Curves

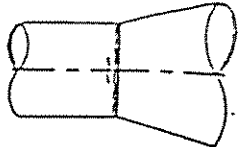
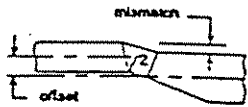
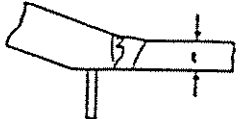
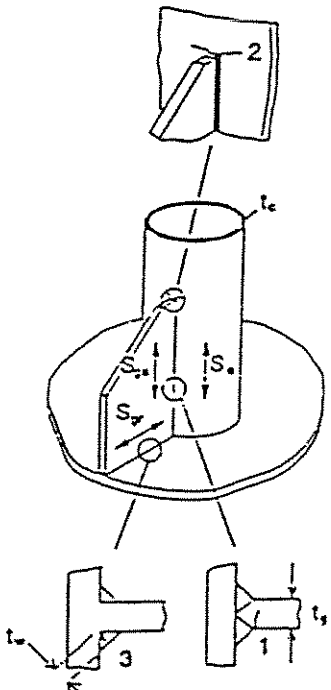
The reference thickness to be used in the calculation of the thickness correction is 16 mm for both the T* and P curve and 38 mm for the CS curve. Thickness correction is based on the local thickness at the predicted failure site.

Description and mode of failure	Classification Factor	Explanatory comments	Examples, including failure modes
7.1 Simple tubular and overlapped joints. Parent metal adjacent to, or weld metal in fillet, partial - or full penetration welds.			
(a) Parent metal adjacent to the toes of full penetration welded nodes - Locations 1 and 2.		Fatigue design using T* curve is based on the brace nominal stress range S_b and the appropriate hot-spot SCFs. For location 1 the chord SCF is used with a thickness correction based on t_c . For location 2 brace SCF with thickness correction based on t_b is used.	
(b) Parent metal adjacent to the root of a full-penetration stub to chord weld - Location 3.	1.34P	The nominal stress range (S_b) in the chord should be used with an appropriate SCF and with a thickness correction based on t_c .	
(c) Weld metal in fillet or partial penetration welded tubular joints and doubler plates e.g. anodes, pipe supports etc. - Locations 4 and 5.	2.54P	For Location 4, the nominal stress range across the weld should be multiplied by the brace SCF. For location 5, an assessment of the stress range in the weld throat should be made. In each case, the thickness correction should be based on the weld throat thickness t_w .	
7.2 Cast steel joints. Parent metal or weld repair metal in cast steel joints.			
(a) Locations within the body of the joint.	CS curve	The reference thickness for the S-N curve is 38 mm. Reference should be made to section 21.2.15 of Guidance for a general discussion on the fatigue design of cast steel joints. Stress distributions in the joint should be calculated using an appropriate method e.g. Finite Element. The thickness correction should be based on the actual thickness at the predicted failure site. Note: It is possible that the lowest life in the joint may not occur at the maximum stress location due to the influence of thickness.	 SECTION X-X 
(b) Parent metal or weld metal adjacent to the casting (Location 1).		These locations should be classified as tubular butt joints (see Type 7.5).	

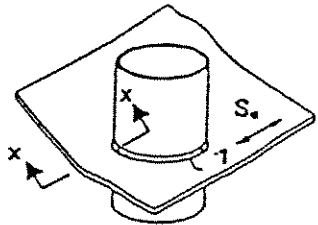
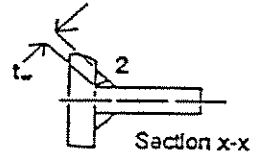
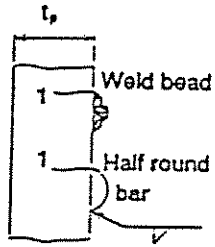


Description and mode of failure	Classification Factor	Explanatory comments	Examples, including failure modes
<p>7.3 Ring stiffened and fully backed up tubular joints. Parent metal or weld metal in tubular joints.</p>		<p>Ring stiffened joints should be initially classified as simple tubular joints (see Type 7.1) in unstiffened brace to chord intersection regions. SCF's for stiffened joints may be calculated using parametric equations, detailed finite element analyses, acrylic model tests or other appropriate techniques.</p>	
<p>(a) Parent and weld metal at the brace to ring intersection - Location 1.</p>	1.14P	<p>Stress ranges at this location should be calculated based on the brace nominal stress range with an appropriate SCF.</p>	
<p>(b) Parent or weld metal on the inside edge of a flat bar or flanged internal ring stiffener - Location 2.</p>	1.0P	<p>Stress ranges at this location should be calculated based on the brace nominal stress range with an appropriate SCF. The thickness effect should be based on web or flange thickness whichever is greater.</p>	
<p>(c) Parent metal adjacent to shear plate connection to shell, at cope hole position - Location 3.</p>	1.34P	<p>The nominal stress range in the chord (S_c) should be used with a thickness correction based on t_c.</p>	
<p>7.4 Attachments to tubular members. Parent metal of loaded tubular members adjacent to fillet, partial or full-penetration welded connections of attachments (loaded or unloaded).</p>		<p>The relevant stress range is based on stress range in the tubular member (S_c) at the attachment. The thickness correction should be based on the thickness (t_c) at the actual location of the attachment.</p>	
<p>(a) Dimensions of attachment (L) parallel to stress < 150 mm e.g. ring stiffeners.</p>	1.34P		
<p>(b) Dimensions of attachment (L) parallel to stress \geq 150 mm.</p>	1.52P	<p>Long load-carrying attachments may require special considerations (see Type 4.1).</p>	
<p>7.5 Tubular butt joints. Parent and weld metal at butt welds between tubular members e.g. stub to brace connections. Changes in thickness should be machined to a smooth transition not steeper than 1 in 4. Changes of less than 1.15 times the thinner member thickness may be accommodated in the weld profile without machining.</p>		<p>The stress range considered should be that at the actual crack location. It should include SCF's arising from any thickness change, fabrication tolerance (e.g. mismatch) or due to the overall form of the joint (e.g. butt joint at the end of a conical transition piece). The thickness correction should be based on the wall thickness (t).</p>	
<p>(a) Weld made from both sides with the weld cap ground flush and the surface and the weld proved to be free from significant defects by NDE.</p>	0.76P	<p>For significance of defects see explanatory comments for Type 3.1(a).</p>	



Description and mode of failure	Classification Factor	Explanatory comments	Examples, including failure modes
(b) Full penetration weld made from both sides e.g. piles, the large ends of conical transitions and the small end where a pup-piece is used. Generally, all circumferential welds other than those in (a) (e.g. legs) are considered in this group.	1.14P	Where the conditions of Type 3.1(b) apply a classification factor of 1.0P may be used.	
(c) Full penetration weld made from one side.	1.34P		
(d) Full penetration weld made from one side without permanent backing strip, e.g. small end of conical diameter transition (unless a pup-piece is specifically included in the node, in which case the remote end of the pup-piece will be considered in this way). All circumferential welds in tubulars of less than 650 mm diameter will be considered single-sided - Location 2.	1.52P		
7.6 Gusseted connections			
Parent and weld metal in gusseted connections.			
(a) Parent metal of gusset plate adjacent to or weld in full penetration welds connecting a gusset plate to a member - Location 1.	1.34P	The stress range should be that in the gusset plate (radial S_r or axial S_a), including any SCF which arises from the overall form of the joint. The thickness correction factor should be calculated using the gusset thickness (t_g).	
(b) Parent metal of a member adjacent fillet, full or partial penetration welded gusseted connections - Location 2. Full penetration welds are normally required in such joints.	1.34P	The nominal stress range (S_n) in the tubular member should be used including an appropriate stress concentration factor due to the overall form of the joint (e.g. SCF for end of gusset attachment).	
(c) Weld metal in fillet or partial penetration welds attaching a gusset plate to a member - Location 3.	2.54P	The shear stress range across the weld throat should be used, together with any SCF arising from the overall form of joint. The thickness correction should be based on the weld throat thickness (t_w).	



Description and mode of failure	Classification Factor	Explanatory comments	Examples, including failure modes
<p>7.7 Penetrations. Parent metal adjacent to a penetration or hole in a member and the weld metal around a penetration. Full penetration welds are recommended in this situation.</p>			
(a) Parent metal of a tubular, adjacent to a penetration - Location 1. Crack is essentially perpendicular to the direction of applied stress (S_a).	1.0P	The stress range used should include a SCF arising from the detail taking full account of stiffening effect of the penetration. The thickness correction should be based on the plate thickness.	
(b) Weld metal in a fillet or partial - penetration welded joint around a penetration - Location 2.	2.54P	The shear stress across the weld throat should be used, including any SCF's due to the geometry of the detail. Full account should be taken of the stiffening effect of the penetration. The thickness correction factor should be based on the weld throat thickness (t_w).	
<p>7.8 Pile shear connectors. Parent metal adjacent to, or weld metal in pile shear connectors.</p>			
Parent metal adjacent to pile shear connectors inside or outside the grouted connection - Location 1.	1.34P	The maximum stress range in the section of the pile with shear connectors should be used in conjunction with a thickness correction factor based on the pile wall thickness (t_p).	



APPENDIX B

INITIAL SCREENED DATABASE OF SIMPLE TUBULAR JOINTS

Joint Type	Paper Ref.	Joint Ref.	T mm	Theta deg	C	Alpha spec.	Alpha supp.	Gamma	Tau	Beta	Pai deg	Zeta	Loading mode	R	Max SCF	Max SCF	Weld angle	Yield stress N/mm ²	Stress range N/mm ²	Max SCF	Max SCF	Weld angle	Yield stress N/mm ²	Stress range N/mm ²	Failed Member	N3
T	UKOSRP1	T01/1	6.3	90	0.5	17.0	17.0	13.4	1.00	1.00	20	-	OPB	0.0	10.34	4.50	35.0	465.0	414.4	4.50	saddle	10.0	465.0	180.4	Chord	270000
T	UKOSRP1	T01/3	6.3	90	0.5	17.0	17.0	13.4	1.00	1.00	20	-	OPB	0.0	9.92	3.80	35.0	465.0	281.0	3.80	saddle	10.0	465.0	124.6	Chord	1200000
T	UKOSRP1	T02/1	6.3	90	0.5	17.0	17.0	13.4	0.71	1.00	20	-	OPB	0.0	6.28	3.40	25.0	465.0	331.1	3.40	saddle	10.0	399.0	201.0	Chord	1300000
T	UKOSRP1	T02/3	6.3	90	0.5	17.0	17.0	13.4	0.71	1.00	20	-	OPB	0.0	6.14	3.40	25.0	465.0	297.8	3.40	saddle	10.0	389.0	184.9	Chord	600000
T	UKOSRP1	T03/1	6.3	90	0.5	17.0	17.0	13.4	0.87	0.54	-	-	OPB	0.0	6.73	3.80	25.0	465.0	306.1	3.80	saddle	10.0	399.0	208.4	Chord	470000
T	UKOSRP1	T05/2	6.3	90	0.5	17.0	17.0	13.4	0.97	0.53	-	-	OPB	0.0	8.04	-	40.0	465.0	239.1	-	-	25.0	437.0	-	Chord	4480000
T	UKOSRP1	T05/3	6.3	90	0.5	17.0	17.0	13.4	0.99	0.53	-	-	OPB	0.0	7.74	-	40.0	465.0	239.7	-	-	25.0	437.0	-	Chord	680000
T	UKOSRP1	T04/1	6.3	90	0.5	17.0	17.0	13.4	0.93	0.63	-	-	OPB	0.0	8.43	-	40.0	465.0	274.0	-	-	25.0	437.0	-	Chord	520000
T	UKOSRP1	T04/3	6.3	90	0.5	17.0	17.0	13.4	0.93	0.63	-	-	OPB	0.0	8.39	-	35.0	465.0	333.7	-	-	25.0	365.0	-	Chord	580000
T	UKOSRP1	T05/1	6.3	90	0.5	17.0	17.0	13.4	0.93	0.63	-	-	OPB	0.0	8.39	-	35.0	465.0	333.7	-	-	25.0	365.0	-	Chord	2100000
T	UKOSRP1	T05/2	6.3	90	0.5	17.0	17.0	14.8	1.02	1.00	20	-	OPB	0.0	9.35	3.90	35.0	465.0	314.5	3.90	saddle	10.0	465.0	135.2	Chord	5900000
T	UKOSRP1	T05/3	6.3	90	0.5	17.0	17.0	14.8	1.02	1.00	20	-	OPB	0.0	9.24	-	22.5	465.0	349.0	-	-	5.0	465.0	-	Chord	720000
K	UKOSRP1	K10/1	6.7	90/45	-	15.1	14.2	13.6	0.93	0.53	-	0.12	Axial	0.0	9.41	-	22.5	465.0	349.0	-	-	5.0	465.0	-	Chord	1150000
K	UKOSRP1	K11/1	6.7	90/45	-	15.1	14.2	13.6	0.93	0.53	-	0.12	Axial	0.0	9.41	-	22.5	465.0	349.0	-	-	5.0	465.0	-	Chord	310000
K	UKOSRP1	K11/2	6.7	90/45	-	15.1	14.2	13.6	0.93	0.53	-	0.12	OPB	0.0	7.64	-	40.0	465.0	204.8	-	-	20.0	437.0	0.0	Chord	2900000
K	UKOSRP1	K11/3	6.7	90/45	-	15.1	14.2	13.6	0.93	0.53	-	0.12	OPB	0.0	7.64	-	40.0	465.0	224.8	-	-	20.0	437.0	0.0	Chord	8500000
K	UKOSRP1	K11/4	6.7	90/45	-	15.1	14.2	13.6	0.93	0.53	-	0.12	Axial	0.0	7.64	-	40.0	465.0	224.8	-	-	20.0	437.0	0.0	Chord	9000000
T	UKOSRP1	T11/1	6.7	90	0.5	10.0	10.0	14.8	1.02	1.00	20	-	Axial	-1.0	4.16	-	80.0	465.0	242.8	4.50	saddle	40.0	399.0	173.5	Chord	260000
T	UKOSRP1	T11/3	6.7	90	0.5	10.0	10.0	15.0	1.00	1.00	20	-	Axial	-1.0	6.30	4.50	80.0	465.0	184.9	4.50	saddle	40.0	399.0	132.1	Chord	1520000
T	UKOSRP1	T11/4	6.7	90	0.5	10.0	10.0	15.0	1.02	1.00	20	-	Axial	-1.0	6.30	4.50	80.0	465.0	176.9	4.50	saddle	40.0	399.0	268.9	Chord	5970000
T	UKOSRP1	T11/5	6.7	90	0.5	10.0	10.0	14.8	1.02	1.00	20	-	IPB	-1.0	2.80	1.70	80.0	465.0	306.9	1.70	maximum	40.0	399.0	236.1	Chord	184000
T	UKOSRP1	T11/6	6.7	90	0.5	10.0	10.0	14.8	0.98	1.00	20	-	IPB	-1.0	2.80	1.70	80.0	465.0	306.9	1.70	maximum	40.0	399.0	236.1	Chord	1760000
T	UKOSRP1	T11/7	6.7	90	0.5	10.0	10.0	15.0	1.00	1.00	20	-	IPB	-1.0	2.80	1.70	80.0	465.0	228.4	1.70	maximum	40.0	399.0	160.3	Chord	2890000
T	UKOSRP1	T11/8	6.7	90	0.5	10.0	10.0	15.0	1.00	1.00	20	-	IPB	-1.0	2.80	1.70	80.0	465.0	401.3	1.70	maximum	40.0	399.0	243.6	Chord	3700000
T	UKOSRP1	T11/9	6.7	90	0.5	10.0	10.0	15.0	1.00	1.00	20	-	IPB	-1.0	2.80	1.70	80.0	465.0	430.5	1.70	maximum	40.0	399.0	265.0	Chord	1510000
T	UKOSRP1	T11/10	6.7	90	0.5	10.0	10.0	15.0	1.00	1.00	20	-	IPB	-1.0	2.80	1.70	80.0	465.0	430.5	1.70	maximum	40.0	399.0	265.0	Chord	1480000
T	UKOSRP1	T11/11	6.7	90	0.5	10.0	10.0	15.0	1.00	1.00	20	-	IPB	-1.0	2.80	1.70	80.0	465.0	322.8	1.70	maximum	40.0	399.0	179.2	Chord	838000
T	UKOSRP1	T11/12	6.7	90	0.5	10.0	10.0	14.3	0.88	1.00	15	-	Axial	-1.0	3.70	3.50	30.0	465.0	406.3	3.50	maximum	40.0	399.0	287.7	Chord	488000
T	UKOSRP1	T11/13	6.7	90	0.5	10.0	10.0	14.3	0.88	1.00	15	-	IPB	-1.0	2.20	3.30	30.0	465.0	358.4	3.30	maximum	40.0	399.0	314.0	Chord	1860000
T	UKOSRP1	T11/14	6.7	90	0.5	10.0	10.0	14.3	0.88	1.00	15	-	IPB	-1.0	2.20	3.30	30.0	465.0	358.4	3.30	maximum	40.0	399.0	314.0	Chord	2180000
T	UKOSRP1	T11/15	6.7	90	0.5	10.0	10.0	14.3	0.88	1.00	15	-	IPB	-1.0	2.20	3.30	30.0	465.0	426.9	3.30	maximum	40.0	399.0	331.4	Chord	2110000
T	UKOSRP1	T11/16	6.7	90	0.5	10.0	10.0	14.3	0.88	1.00	15	-	Axial	-1.0	3.70	3.30	30.0	465.0	250.9	3.30	maximum	5.0	399.0	223.8	Chord	1000000
T	UKOSRP1	T11/17	6.7	90	0.5	10.0	10.0	14.0	0.87	1.00	15	-	Axial	-1.0	3.70	3.30	30.0	465.0	412.2	3.30	maximum	5.0	399.0	387.8	Chord	2170000
T	UKOSRP1	T11/18	6.7	90	0.5	10.0	10.0	14.0	0.86	1.00	15	-	IPB	-1.0	2.20	3.30	30.0	465.0	603.0	3.30	maximum	40.0	399.0	512.3	Chord	222000
T	UKOSRP1	T11/19	6.7	90	0.5	10.0	10.0	15.0	0.70	1.00	15	-	IPB	-1.0	2.20	1.70	80.0	465.0	497.2	1.70	maximum	40.0	399.0	384.2	Chord	784000
T	UKOSRP1	T11/20	6.7	90	0.5	10.0	10.0	15.3	0.71	1.00	15	-	Axial	-1.0	3.70	3.30	30.0	465.0	257.2	3.30	maximum	5.0	399.0	229.4	Chord	416000
T	UKOSRP1	T11/21	6.7	90	0.5	9.9	9.9	14.8	0.86	0.53	-	-	Axial	-1.0	11.38	8.50	40.0	465.0	553.7	8.50	saddle	15.0	437.0	316.8	Chord	421000
T	UKOSRP1	T11/22	6.7	90	0.5	9.9	9.9	14.8	0.86	0.53	-	-	Axial	-1.0	11.38	8.50	40.0	465.0	553.7	8.50	saddle	15.0	437.0	262.4	Chord	1720000
T	UKOSRP1	T11/23	6.7	90	0.5	9.9	9.9	14.8	0.86	0.53	-	-	Axial	-1.0	11.38	8.50	40.0	465.0	553.7	8.50	saddle	15.0	437.0	316.8	Chord	4250000
T	UKOSRP1	T11/24	6.7	90	0.5	9.9	9.9	14.8	0.86	0.53	-	-	Axial	-1.0	11.38	8.50	40.0	465.0	553.7	8.50	saddle	15.0	437.0	316.8	Chord	980000
T	UKOSRP1	T11/25	6.7	90	0.5	9.9	9.9	14.8	0.86	0.53	-	-	IPB	-1.0	2.49	2.08	35.0	465.0	554.5	2.08	maximum	55.0	437.0	524.7	Chord	820000
T	UKOSRP1	T11/26	6.7	90	0.5	9.9	9.9	14.8	0.86	0.53	-	-	IPB	-1.0	2.49	2.08	35.0	465.0	282.9	2.08	maximum	55.0	437.0	293.3	Chord	1850000
T	UKOSRP1	T11/27	6.7	90	0.5	9.9	9.9	14.8	0.86	0.53	-	-	IPB	-1.0	2.49	2.08	35.0	465.0	478.0	2.08	maximum	55.0	437.0	217.5	Chord	1950000
T	UKOSRP1	T20/5	5.1	90	0.5	9.9	9.9	14.3	0.86	0.53	-	-	IPB	-1.0	1.88	2.41	45.0	465.0	309.0	2.41	maximum	45.0	365.0	396.4	Chord	362000
T	UKOSRP1	T20/6	5.1	90	0.5	9.9	9.9	14.3	0.86	0.53	-	-	IPB	-1.0	1.88	2.41	45.0	465.0	309.0	2.41	maximum	45.0	365.0	443.2	Chord	518000
T	UKOSRP1	T20/7	5.1	90	0.5	9.9	9.9	14.3	0.86	0.53	-	-	Axial	-1.0	1.88	4.90	45.0	465.0	177.7	4.90	saddle	25.0	365.0	254.8	Brace	1000000
T	UKOSRP1	T20/8	5.1	90	0.5	9.9	9.9	14.3	0.86	0.53	-	-	Axial	-1.0	1.88	4.90	45.0	465.0	177.7	4.90	saddle	25.0	365.0	254.8	Brace	450000
T	UKOSRP1	T20/9	5.1	90	0.5	9.9	9.9	14.3	0.86	0.53	-	-	Axial	-1.0	1.88	4.90	45.0	465.0	177.7	4.90	saddle	25.0	365.0	254.8	Brace	60000
T	UKOSRP1	T20/10	5.1	90	0.5	9.9	9.9	14.3	0.86	0.53	-	-	Axial	-1.0	1.88	4.90	45.0	465.0	177.7	4.90	saddle	25.0	365.0	254.8	Brace	1200000
T	UKOSRP1	T20/11	5.1	90	0.5	9.9	9.9	14.3	0.86	0.53	-	-	Axial	-1.0	1.88	4.90	45.0	465.0	177.7	4.90	saddle	25.0	365.0	254.8	Brace	3000000
T	UKOSRP1	T20/12	5.1	90	0.5	9.9	9.9	14.3	0.86	0.53	-	-	Axial	-1.0	1.88	4.90	45.0	465.0	177.7	4.90	saddle	25.0	365.0	254.8	Brace	350000
T	UKOSRP1	T20/13	5.1	90	0.5	9.9	9.9	14.3	0.86	0.53	-	-	Axial	-1.0	1.88	4.90	45.0	465.0	177.7	4.90	saddle	25.0	365.0	254.8	Brace	470000
T	UKOSRP1	T20/14	5.1	90	0.5	9.9	9.9	14.3	0.86	0.53	-	-	Axial	-1.0	1.88	4.90	45.0	465.0	177.7	4.90	saddle	25.0	365.0	254.8	Brace	1500000

Joint Type	Joint Ref.	Joint Ref.	T mm	Theta deg	C	Alpha spec.	Alpha supp.	Gamma	Tau	Beta	Psi deg	Zeta	Loading mode	R	Max. SCF	Max. SCF	Weld angle	Yield stress N/mm ²	Stress range N/mm ²	Max. SCF	Max. SCF	BRACE Weld angle	Yield stress N/mm ²	Stress range N/mm ²	Failed Member	N3	
T	UKOSRP1	T24/1	17.2	90	0.5	14.0	14.0	13.3	0.26	0.26	-	-	OPB	0.0	1.84	1.89	50.0	485.0	204.1	1.89	30.0	485.0	187.4	C & B	2600000		
T	UKOSRP1	T24/2	17.1	90	0.5	14.0	14.0	13.4	0.26	0.26	-	-	OPB	0.0	1.87	1.86	50.0	485.0	322.3	1.86	30.0	485.0	414.8	Brace	58000		
T	UKOSRP1	T24/3	17.3	90	0.5	14.0	14.0	13.1	0.26	0.26	-	-	OPB	0.0	1.71	1.76	50.0	485.0	209.9	1.76	30.0	485.0	308.7	Brace	240000		
T	UKOSRP1	T26/1	16.3	90	0.5	13.9	13.9	14.1	1.00	1.00	0	0	OPB	0.0	5.12	4.49	7.5	485.0	208.3	4.49	0.0	485.0	180.9	C & W	670000		
T	UKOSRP1	T25/2	16.3	90	0.5	13.9	13.9	14.1	1.00	1.00	0	0	OPB	0.0	5.02	5.02	7.5	485.0	310.5	5.02	0.0	485.0	281.5	Chord	180000		
K	UKOSRP1	T25/3	16.8	90	0.5	13.9	13.9	14.6	0.98	0.98	0	0	OPB	0.0	3.52	4.02	7.5	485.0	111.6	4.02	0.0	485.0	168.0	C & W	4050000		
K	UKOSRP1	K30/1	16.0	90/45	1.0	14.1	14.1	14.3	0.54	0.54	-	0.10	Axial	0.0	3.88	3.70	40.0	397.0	180.3	3.70	20.0	445.0	182.2	Chord	1100000		
T	UKOSRP1	KT36/1	18.0	45/90/45	1.0	14.1	14.1	14.3	0.54	0.54	-	-	Axial	0.0	-	2.37	50.0	397.0	-	2.37	maximum	30.0	445.0	182.2	Chord	630000	
T	UKOSRP1	T37/1	18.7	90	0.5	10.2	10.2	14.6	1.07	1.00	0	-	IPB	-1.0	3.40	2.13	45.0	397.0	271.1	2.13	maximum	45.0	380.0	189.3	C & W	290000	
T	UKOSRP1	T37/2	18.7	90	0.5	10.2	10.2	14.6	1.14	1.00	0	-	Axial	-1.0	8.00	5.10	45.0	397.0	323.5	5.10	maximum	45.0	380.0	189.3	Chord	144000	
T	UKOSRP1	T37/7	18.0	90	0.5	10.1	10.1	14.5	1.10	1.00	0	-	Axial	-1.0	8.00	5.10	45.0	397.0	185.8	5.10	maximum	45.0	380.0	208.3	Chord	1000000	
T	UKOSRP1	T37/8	18.5	90	0.5	10.2	10.2	14.3	1.10	1.00	0	-	IPB	-1.0	3.40	2.13	45.0	397.0	129.8	2.13	maximum	45.0	380.0	118.4	Chord	1000000	
T	UKOSRP1	T37/9	18.1	90	0.5	10.2	10.2	13.9	1.08	1.00	0	-	IPB	-1.0	3.40	2.13	45.0	397.0	269.2	2.13	maximum	45.0	380.0	81.3	Chord	1000000	
T	UKOSRP1	T37/10	18.6	90	0.5	10.2	10.2	14.2	1.05	1.00	0	-	Axial	-1.0	8.00	5.10	45.0	397.0	120.1	5.10	maximum	45.0	380.0	168.7	Chord	1200000	
T	UKOSRP1	T37/11	18.5	90	0.5	10.2	10.2	13.8	0.97	1.00	0	-	IPB	-1.0	3.40	2.13	45.0	397.0	178.0	2.13	maximum	45.0	380.0	78.6	Chord	690000	
T	UKOSRP1	T37/12	18.5	90	0.5	10.2	10.2	13.9	1.03	1.00	0	-	IPB	-1.0	3.40	2.13	45.0	397.0	395.3	2.13	maximum	45.0	380.0	111.5	Chord	3790000	
T	UKOSRP1	T37/13	18.4	90	0.5	10.2	10.2	14.3	1.14	1.00	0	-	IPB	-1.0	3.40	2.13	45.0	397.0	165.5	2.13	maximum	45.0	380.0	103.7	Chord	243000	
T	UKOSRP1	T38/1	17.1	90	0.5	10.2	10.2	14.3	0.84	1.00	0	-	Axial	-1.0	3.77	4.44	60.0	411.0	208.4	4.44	30.0	485.0	360.0	Chord	729000		
T	UKOSRP1	T38/3	18.2	90	0.5	10.2	10.2	14.1	0.59	1.00	0	-	IPB	-1.0	2.00	2.25	60.0	411.0	222.1	2.25	30.0	485.0	245.4	Brace	2110000		
T	UKOSRP1	T38/4	18.4	90	0.5	10.2	10.2	13.9	0.57	1.00	0	-	Axial	-1.0	3.77	4.44	60.0	411.0	208.4	4.44	30.0	485.0	245.4	Brace	610000		
T	UKOSRP1	T38/5	18.4	90	0.5	10.2	10.2	13.9	0.57	1.00	0	-	Axial	-1.0	3.77	4.44	60.0	411.0	148.3	4.44	30.0	485.0	245.4	Chord	835000		
T	UKOSRP1	T38/6	18.3	90	0.5	10.2	10.2	14.0	0.57	1.00	0	-	IPB	-1.0	2.00	2.25	60.0	411.0	148.3	2.25	30.0	485.0	174.7	Chord	1980000		
T	UKOSRP1	T38/7	18.0	90	0.5	10.2	10.2	14.3	0.59	1.00	0	-	Axial	-1.0	3.77	4.44	60.0	411.0	275.2	4.44	30.0	485.0	319.4	Chord	1800000		
T	UKOSRP1	T38/8	18.3	90	0.5	10.2	10.2	13.9	0.57	1.01	0	-	Axial	-1.0	3.77	4.44	60.0	411.0	163.7	4.44	30.0	485.0	324.2	Brace	3890000		
T	UKOSRP1	T39/1	18.4	90	0.5	10.1	10.1	14.0	0.40	0.25	-	-	IPB	-1.0	1.03	1.51	42.5	409.0	254.2	1.51	30.0	485.0	240.0	Chord	2200000		
T	UKOSRP1	T39/4	17.3	90	0.5	10.1	10.1	13.3	0.37	0.25	-	-	IPB	-1.0	4.21	4.40	42.5	409.0	175.1	4.40	maximum	47.5	448.0	265.6	Brace	1110000	
T	UKOSRP1	T39/5	17.8	90	0.5	10.1	10.1	13.1	0.36	0.25	-	-	Axial	-1.0	4.21	4.40	42.5	409.0	347.6	4.40	maximum	47.5	448.0	183.0	Brace	1340000	
T	UKOSRP1	T39/6	18.8	90	0.5	10.2	10.2	13.8	0.36	0.25	-	-	Axial	-1.0	4.21	4.40	42.5	409.0	253.6	4.40	maximum	47.5	448.0	373.3	Chord	1800000	
T	UKOSRP1	T40/2	18.2	90	0.5	10.1	10.1	14.4	0.40	0.25	-	-	Axial	-1.0	4.21	4.40	42.5	409.0	347.6	4.40	maximum	47.5	448.0	254.2	Brace	3360000	
T	UKOSRP1	T40/3	18.2	90	0.5	10.1	10.1	14.2	0.40	0.25	-	-	IPB	-1.0	4.21	1.82	42.5	409.0	-	1.82	maximum	47.5	455.0	319.9	Chord	9600000	
K	UKOSRP1	G1(5.5)	18.0	90/45	1.0	12.7	16.0	14.3	0.50	0.53	-	0.11	IPB	-1.0	-	4.05	42.5	409.0	618.6	-	-	-	-	-	Brace	1700000	
K	UKOSRP1	G2(5.5)	18.0	90/45	1.0	12.7	16.0	14.3	0.50	0.53	-	0.11	Axial	-1.0	2.92	4.05	42.5	409.0	432.2	4.05	-	-	-	-	-	C & B	385000
K	UKOSRP1	G3(5.5)	18.0	90/45	1.0	12.7	16.0	14.3	0.50	0.53	-	0.11	Axial	-1.0	2.79	4.05	42.5	409.0	366.3	2.79	-	-	-	-	-	Chord	141000
T	Dijeta	5	15.9	90	0.5	10.0	10.0	14.4	0.52	0.48	-	-	Axial	0.0	6.70	6.70	maximum	-	197.3	6.70	-	-	-	-	-	Chord	310000
T	Dijeta	6	15.9	90	0.5	10.0	10.0	14.4	0.52	0.48	-	-	Axial	0.0	6.70	6.70	maximum	-	177.6	6.70	-	-	-	-	-	Chord	880000
T	Dijeta	7	15.9	90	0.5	10.0	10.0	14.4	0.52	0.48	-	-	Axial	0.0	6.70	6.70	maximum	-	177.6	6.70	-	-	-	-	-	Chord	1100000
T	Dijeta	8	15.9	90	0.5	10.0	10.0	14.4	0.52	0.48	-	-	Axial	0.0	6.70	6.70	maximum	-	177.6	6.70	-	-	-	-	-	Chord	840000
T	Dijeta	9	15.9	90	0.5	10.0	10.0	14.4	0.52	0.48	-	-	Axial	0.0	6.70	6.70	maximum	-	177.6	6.70	-	-	-	-	-	Chord	7500000
T	Dijeta	11	15.9	90	0.5	10.0	10.0	14.4	0.40	0.25	-	-	Axial	-1.0	4.70	4.70	maximum	-	123.1	4.70	-	-	-	-	-	Chord	780000
T	Dijeta	12	15.9	90	0.5	10.0	10.0	14.4	0.40	0.25	-	-	Axial	-1.0	4.70	4.70	maximum	-	123.1	4.70	-	-	-	-	-	Chord	9000000
T	Dijeta	28	15.9	90	0.5	10.0	10.0	14.4	0.40	0.25	-	-	Axial	-1.0	4.70	4.70	maximum	-	241.9	4.70	-	-	-	-	-	Chord	700000
X	Dijeta	29	15.9	90	0.5	10.0	10.0	14.4	1.00	1.00	10	-	Axial	-1.0	3.00	3.00	maximum	-	176.9	3.00	-	-	-	-	-	Chord	1600000
X	Dijeta	30	15.9	90	0.5	10.0	10.0	14.4	1.00	1.00	10	-	Axial	-1.0	3.00	3.00	maximum	-	176.9	3.00	-	-	-	-	-	Chord	1600000
X	Dijeta	33	15.9	90	0.5	10.0	10.0	14.4	0.55	1.00	10	-	Axial	-1.0	-	-	maximum	-	119.8	-	-	-	-	-	-	Chord	1600000
X	Dijeta	36	15.9	90	0.5	10.0	10.0	14.4	0.55	1.00	10	-	Axial	-1.0	-	-	maximum	-	119.8	-	-	-	-	-	-	Chord	1600000
X	Dijeta	37	15.9	90	0.5	10.0	10.0	14.4	0.55	1.00	10	-	Axial	-1.0	-	-	maximum	-	119.8	-	-	-	-	-	-	Chord	1600000
X	Dijeta	38	15.9	90	0.5	10.0	10.0	14.4	0.55	1.00	10	-	Axial	-1.0	-	-	maximum	-	119.8	-	-	-	-	-	-	Chord	1600000
X	Dijeta	39	15.9	90	0.5	10.0	10.0	14.4	0.55	1.00	10	-	Axial	-1.0	-	-	maximum	-	119.8	-	-	-	-	-	-	Chord	1600000
X	Dijeta	40	15.9	90	0.5	10.0	10.0	14.4	0.55	1.00	10	-	Axial	-1.0	-	-	maximum	-	119.8	-	-	-	-	-	-	Chord	1600000
X	Dijeta	41	15.9	90	0.5	10.0	10.0	14.4	0.55	1.00	10	-	Axial	-1.0	-	-	maximum	-	119.8	-	-	-	-	-	-	Chord	1600000
X	Dijeta	42	15.9	90	0.5	10.0	10.0	14.4	0.55	1.00	10	-	Axial	-1.0	-	-	maximum	-	119.8	-	-	-	-	-	-	Chord	1600000
X	Dijeta	43	15.9	90	0.5	10.0	10.0	14.4	0.55	1.00	10	-	Axial	-1.0	-	-	maximum	-	119.8	-	-	-	-	-	-	Chord	1600000
X	Dijeta	44	15.9	90	0.5	10.0	10.0	14.4	0.55	1.00	10	-	Axial	-1.0	-	-	maximum	-	119.8	-	-	-	-	-	-	Chord	1600000
X	Dijeta	45	15.9	90	0.5	10.0	10.0	14.4	0.55	1.00	10	-	Axial	-1.0	-	-	maximum	-	119.8	-	-	-	-	-	-	Chord	1600000
X	Dijeta	46	15.9	90	0.5	10.0	10.0	14.4	0.55	1.00	10	-	Axial	-1.0	-	-	maximum	-	119.8	-	-	-	-	-	-	Chord	1600000
X	Dijeta																										

Joint Type	Joint Ref.	Paper Ref.	C	Alpha spec.	Alpha supp.	Gamma	Tau	Beta	Rel deg	Zeta	Loading mode	R	Max SCF	Max SCF	CHORD Weld angle	Yield stress N/mm ²	Stress range N/mm ²	BRACE Weld angle	Yield stress N/mm ²	Stress range N/mm ²	Failed Member	N3
T	T	COSRP	TA1	18.0	90	0.5	8.3	8.3	24.1	1.00	0.50	0.2	24.60	24.60	saddle	405.0	251.0	-	-	-	Chord	665000
T	T	COSRP	T81	18.0	90	0.5	6.3	6.3	24.1	1.00	0.50	0.1	4.90	4.90	crown	405.0	254.1	-	-	-	Chord	235000
X	X	Leurade	A	32.0	90	-	6.5	6.5	10.4	0.94	0.72	0.1	13.08	13.08	saddle	-	235.7	-	-	-	Chord	482000
T	T	UKOSRP	T41/1	32.0	90	0.5	6.0	6.0	14.3	1.00	0.50	-1.0	4.85	4.85	maximum	80.0	158.6	30.0	494.0	162.4	Chord	21000000
T	T	UKOSRP	T41/3	32.0	90	0.5	6.0	6.0	14.3	1.00	0.50	-1.0	4.85	4.85	maximum	80.0	158.6	30.0	494.0	162.4	Chord	14000000
T	T	UKOSRP	T41/4	32.0	90	0.5	6.0	6.0	14.3	1.00	0.50	-1.0	4.85	4.85	maximum	80.0	158.6	30.0	494.0	162.4	Chord	34000000
T	T	UKOSRP	T42/2	31.9	90	0.5	6.0	6.0	14.3	0.90	0.50	-1.0	3.32	3.32	saddle	35.0	94.4	25.0	392.0	87.3	Chord	47000000
T	T	UKOSRP	T42/3	31.9	90	0.5	6.0	6.0	14.3	0.90	0.50	-1.0	3.32	3.32	saddle	35.0	94.4	25.0	392.0	87.3	Chord	14800000
T	T	UKOSRP	T42/4	31.9	90	0.5	6.0	6.0	14.3	0.90	0.50	-1.0	3.32	3.32	saddle	35.0	94.4	25.0	392.0	87.3	Chord	22300000
T	T	UKOSRP	T43/4	32.0	90	0.5	6.0	6.0	14.3	0.90	0.50	-1.0	1.51	1.51	crown	45.0	90.9	35.0	494.0	95.7	Chord	75000000
T	T	UKOSRP	T44/1	32.0	90	0.5	6.0	6.0	14.3	0.25	0.24	-1.0	0.99	0.99	crown	40.0	112.5	35.0	494.0	95.7	Chord	11800000
T	T	UKOSRP	T44/2	32.0	90	0.5	6.0	6.0	14.3	0.25	0.24	-1.0	0.99	0.99	crown	40.0	112.5	35.0	494.0	95.7	Chord	21200000
T	T	UKOSRP	T210(2.1)	32.0	90	0.5	6.3	6.3	14.3	0.51	0.50	-1.0	2.80	2.80	saddle	40.0	137.1	40.0	494.0	174.1	Brace	12000000
T	T	UKOSRP	T211(2.1)	32.0	90	0.5	6.3	6.3	14.3	0.52	0.50	-1.0	5.50	5.50	saddle	35.0	140.5	20.0	494.0	171.1	Chord	19000000
T	T	UKOSRP	T215(2.1)	32.0	90	0.5	6.3	6.3	14.3	0.49	0.50	-1.0	6.60	6.60	saddle	40.0	199.8	23.0	400.0	181.4	Chord	10500000
T	T	Dikura	13	31.7	90	1.0	8.7	8.5	14.4	0.50	0.50	-	7.70	7.70	saddle	-	94.3	-	-	-	Chord	8730000
T	T	Dikura	14	31.7	90	1.0	8.7	8.5	14.4	0.50	0.50	-	7.70	7.70	saddle	-	289.0	-	-	-	Chord	41000000
T	T	Dikura	15	31.7	90	1.0	8.7	8.5	14.4	0.50	0.50	-	7.70	7.70	saddle	-	137.2	-	-	-	Chord	1500000
X	X	Dikura	34	31.7	90	1.0	8.7	8.5	14.4	0.50	0.50	-	10.90	10.90	saddle	-	79.1	-	-	-	Chord	9500000
X	X	Dikura	35	31.7	90	1.0	8.7	8.5	14.4	0.50	0.50	-	10.90	10.90	saddle	-	197.8	-	-	-	Chord	12000000
TT	TT	SINTEF	S1A	32.0	90	-	8.6	8.3	14.3	0.50	0.50	-1.0	2.30	2.30	crown	-	207.6	-	-	-	Chord	7000000
TT	TT	SINTEF	S1B	32.0	90	-	8.6	8.3	14.3	0.50	0.50	-1.0	2.30	2.30	crown	-	185.6	-	-	-	Chord	1320000
TT	TT	SINTEF	S2A	32.0	90	-	8.6	8.3	14.3	0.50	0.50	-1.0	2.30	2.30	crown	-	121.3	-	-	-	Chord	1430000
TT	TT	SINTEF	S2B	32.0	90	-	8.6	8.3	14.3	0.50	0.50	-1.0	2.30	2.30	crown	-	112.5	-	-	-	Chord	8000000
TT	TT	SINTEF	S3A	32.0	90	-	8.6	8.3	14.3	0.50	0.50	-1.0	2.30	2.30	crown	-	97.9	-	-	-	Chord	8590000
TT	TT	SINTEF	S3B	32.0	90	-	8.6	8.3	14.3	0.50	0.50	-1.0	2.30	2.30	crown	-	93.5	-	-	-	Chord	18600000
TT	TT	TW	T2A	32.0	90	-	8.6	8.3	14.3	0.50	0.50	-1.0	2.30	2.30	crown	-	144.8	-	-	-	Chord	1430000
TT	TT	TW	T2B	32.0	90	-	8.6	8.3	14.3	0.50	0.50	-1.0	2.30	2.30	crown	-	140.3	-	-	-	Chord	5220000
X	X	Leurade	BB	40.0	90	-	4.2	-	11.4	1.00	0.72	0.1	1.78	1.78	crown	-	142.6	-	-	-	Chord	597000
X	X	Leurade	DD	44.0	90	-	4.2	-	10.8	0.99	0.72	0.1	12.42	12.42	saddle	-	222.1	-	-	-	Chord	8490000
X	X	UKOSRP	T210(1.1)	76.0	90	0.5	4.2	4.2	12.0	0.51	0.50	-1.0	3.28	3.28	crown	-	123.1	-	-	-	Chord	3330000
H	H	UKOSRP	T217(1.1)	76.0	90	0.5	4.2	4.2	12.0	0.50	0.50	-1.0	5.10	5.10	saddle	40.0	387.0	17.5	400.0	108.0	Chord	4710000
H	H	UKOSRP	T218(1.1)	76.0	90	0.5	4.2	4.2	12.0	0.50	0.50	-1.0	5.00	5.00	saddle	40.0	397.0	22.5	400.0	228.5	Chord	28500000
H	H	UKOSRP	T219(1.1)	76.0	90	0.5	4.2	4.2	12.0	0.50	0.50	-1.0	5.10	5.10	saddle	40.0	397.0	20.0	400.0	199.2	Chord	3240000
X	X	Leurade	CC	75.0	90	-	3.1	-	8.5	0.30	0.27	-	4.70	4.70	saddle	40.0	287.7	20.0	400.0	306.1	Chord	9100000
X	X	Leurade	E	75.0	90	-	3.1	-	8.5	0.53	0.53	0.1	4.82	4.82	saddle	-	80.2	-	-	-	Chord	1180000
X	X	Leurade	EE	75.7	90	-	3.1	-	8.3	0.57	0.54	0.1	1.87	1.87	crown	-	120.0	-	-	-	Chord	850000
X	X	Leurade				-									crown	-	122.6	-	-	-	Chord	555000
X	X	Leurade				-									crown	-	134.7	-	-	-	Chord	444000



APPENDIX C
BASECASE DATABASE OF SIMPLE TUBULAR JOINTS

Joint Type	Paper Ref.	Joint Ref.	T mm	theta deg	C	Alpha spec.	Alpha supp.	Gamma	Tau	Beta	Psi deg	Zeta	Weld length mm	Loading mode	R	Max. SCF	Max. SCF loc'n	Yield stress N/mm²	Stress range N/mm²	Failed Member	N3
T	UKOSRP I	T21/3	17.5	90	0.5	14.0	14.0	13.1	0.99	1.00	0	-	70	OPB	0.0	5.09	saddle	465	132.3	Chord	7500000
T	UKOSRP I	T22/1	16.1	90	0.5	14.0	14.0	14.2	0.62	1.00	0	-	60	OPB	0.0	3.26	saddle	465	306.8	Chord	2900000
T	UKOSRP I	T22/2	16.1	90	0.5	14.0	14.0	14.2	0.57	1.00	0	-	60	OPB	0.0	2.80	saddle	465	177.5	Chord	9500000
T	UKOSRP I	T22/3	16.5	90	0.5	14.0	14.0	13.8	0.57	1.00	0	-	60	OPB	0.0	2.83	saddle	465	131.3	Chord	3600000
T	UKOSRP I	T23/2	15.9	90	0.5	14.0	14.0	14.4	0.42	0.25	-	-	20	OPB	0.0	2.82	saddle	465	366.0	Chord	3700000
T	UKOSRP I	T25/2	16.3	90	0.5	13.9	13.9	14.1	1.00	1.00	0	-	70	OPB	0.0	5.96	nr saddle	465	310.5	Chord	1800000
K	UKOSRP I	K30/1	16.0	90/45	1.0	14.1	14.1	14.3	0.54	0.54	-	0.10	24	Axial	0.0	3.66	saddle	397	180.3	Chord	11000000
T	UKOSRP I	T37/1	16.6	90	0.5	10.2	10.2	13.8	1.07	1.00	0	-	95	IPB	-1.0	3.40	maximum	397	271.1	Chord	2900000
T	UKOSRP I	T37/3	15.7	90	0.5	10.2	10.2	14.6	1.14	1.00	0	-	95	Axial	-1.0	8.00	nr crown	397	323.5	Chord	1440000
T	UKOSRP I	T37/5	15.8	90	0.5	10.1	10.1	14.5	1.10	1.00	0	-	95	Axial	-1.0	8.00	nr crown	397	185.8	Chord	10000000
T	UKOSRP I	T37/9	16.1	90	0.5	10.2	10.2	14.2	1.05	1.00	0	-	95	Axial	-1.0	8.00	nr crown	397	120.1	Chord	6950000
T	UKOSRP I	T37/13	15.4	90	0.5	10.2	10.2	14.9	1.14	1.00	0	-	95	IPB	-1.0	3.40	maximum	397	165.5	Chord	7290000
T	UKOSRP I	T38/4	16.4	90	0.5	10.2	10.2	13.9	0.57	1.00	0	-	68	Axial	-1.0	3.77	crown	411	208.4	Chord	5350000
T	UKOSRP I	T38/5	16.4	90	0.5	10.2	10.2	13.9	0.57	1.00	0	-	68	Axial	-1.0	3.77	crown	411	148.3	Chord	19800000
T	UKOSRP I	T38/6	16.3	90	0.5	10.2	10.2	14.0	0.57	1.00	0	-	68	IPB	-1.0	2.00	crown	411	145.1	Chord	18000000
T	UKOSRP I	T39/1	16.4	90	0.5	10.1	10.1	14.0	0.40	0.25	-	-	59	IPB	-1.0	1.03	nr crown	409	163.7	Chord	2200000
T	Dijkstra	5	15.9	90	0.5	10.0	10.0	14.4	0.52	0.48	-	-	-	Axial	0.0	6.70	saddle	-	197.3	Chord	6800000
T	Dijkstra	6	15.9	90	0.5	10.0	10.0	14.4	0.52	0.48	-	-	-	Axial	0.0	6.70	saddle	-	177.6	Chord	11000000
T	Dijkstra	7	15.9	90	0.5	10.0	10.0	14.4	0.52	0.48	-	-	-	Axial	0.0	6.70	saddle	-	177.6	Chord	8400000
T	Dijkstra	8	15.9	90	0.5	10.0	10.0	14.4	0.52	0.48	-	-	-	Axial	0.0	6.70	saddle	-	104.8	Chord	75000000
T	Dijkstra	9	15.9	90	0.5	10.0	10.0	14.4	0.52	0.48	-	-	-	Axial	0.0	6.70	saddle	-	197.3	Chord	7600000
T	Dijkstra	11	15.9	90	0.5	10.0	10.0	14.4	0.40	0.25	-	-	-	Axial	-1.0	4.70	saddle	-	123.1	Chord	90000000
T	Dijkstra	12	15.9	90	0.5	10.0	10.0	14.4	0.40	0.25	-	-	-	Axial	-1.0	4.70	saddle	-	241.9	Chord	7000000
X	Dijkstra	28	15.9	90	0.5	10.0	10.0	14.4	1.00	1.00	10	-	-	Axial	-1.0	3.00	maximum	-	176.9	Chord	6800000
X	Dijkstra	29	15.9	90	0.5	10.0	10.0	14.4	1.00	1.00	10	-	-	Axial	-1.0	3.00	maximum	-	119.8	Chord	18000000
T	TWI repairs	1	16.0	90	0.5	14.0	14.4	14.3	0.75	0.50	-	-	-	OPB	0.0	7.78	saddle	380	235.3	Chord	491642
T	TWI repairs	2	16.0	90	0.5	14.0	14.4	14.3	0.75	0.50	-	-	-	OPB	0.0	7.78	saddle	380	352.6	Chord	247044
T	TWI repairs	3	16.0	90	0.5	14.0	14.4	14.3	0.75	0.50	-	-	-	OPB	0.0	7.78	saddle	380	268.0	Chord	366050
T	TWI repairs	4	16.0	90	0.5	14.0	14.4	14.3	0.75	0.50	-	-	-	OPB	-1.0	7.78	saddle	380	335.3	Chord	413590
T	TWI repairs	6	16.0	90	0.5	14.0	14.4	14.3	0.75	0.50	-	-	-	OPB	-1.0	7.78	saddle	380	335.5	Chord	309840
T	TWI repairs	7	16.0	90	0.5	14.0	14.4	14.3	0.75	0.50	-	-	-	OPB	-1.0	7.78	saddle	380	350.5	Chord	304885
T	TWI repairs	13	16.0	90	0.5	14.0	14.4	14.3	0.75	0.50	-	-	-	OPB	-1.0	7.78	saddle	380	164.8	Chord	4326250
T	TWI repairs	15	16.0	90	0.5	14.0	14.4	14.3	0.75	0.50	-	-	-	OPB	-1.0	7.78	saddle	380	399.6	Chord	223050
T	TWI repairs	19	16.0	90	0.5	14.0	14.4	14.3	0.75	0.50	-	-	-	OPB	-1.0	7.78	saddle	380	239.0	Chord	678783
K	UKOSRP II	G2(5.5)	16.0	90/45	1.0	12.7	16.0	14.3	0.50	0.53	-	0.11	-	Axial	-1.0	2.92	saddle max 45	-	432	Chord	141000
K	UKOSRP II	G3(5.5)	16.0	90/45	1.0	12.7	16.0	14.3	0.50	0.53	-	0.11	-	Axial	-1.0	2.79	saddle max 45	-	368	Chord	310000



APPENDIX D
DATABASE OF TUBULAR JOINTS IN-SEAWATER

Joint Type	Rebar Ref.	Joint Ref.	T mm	Angle deg	Alpha spec	Alpha supp	Gamma	Tau	Bolt	Loading mode	R	Load Req. Hz	Max SCF	CHORD Max SCF Yield stress N/mm ² Stress range N/mm ²	BRACE Max SCF Yield stress N/mm ² Stress range N/mm ²	Failed Member	N3	N4	CP	pH	°C
X	SIMS17	B'	40.0	90	0.6	4.4	4.7	8.0	0.55	0.54	0.10	0.75	1.89	540.0	540.0	Chord	640000	-	-	-	-
X	SIMS17	B3	40.0	90	0.6	4.4	4.7	8.0	0.55	0.54	0.10	0.50	1.86	540.0	540.0	Chord	640000	-	-	-	-
X	SIMS17	B3	40.0	90	0.6	4.4	4.7	8.0	0.55	0.54	0.10	0.50	2.04	540.0	540.0	Chord	640000	-	-	-	-
X	SIMS17	B1	40.0	90	0.6	4.4	4.7	8.0	0.55	0.54	0.10	0.50	1.86	540.0	540.0	Chord	640000	-	-	-	-
X	SIMS17	B1	40.0	90	0.6	4.4	4.7	8.0	0.55	0.54	0.10	0.50	1.86	540.0	540.0	Chord	640000	-	-	-	-
X	SIMS17	B4	40.0	90	0.6	4.4	4.7	8.0	0.55	0.54	0.10	0.30	1.56	540.0	540.0	Chord	640000	-	-	-	-
X	SIMS17	B4	40.0	90	0.6	4.4	4.7	8.0	0.55	0.54	0.10	0.30	1.56	540.0	540.0	Chord	640000	-	-	-	-
T	UKOSRP H T200(2.1)	SW & CP	32.0	90	0.5	5.3	5.3	14.3	0.52	0.50	0.0	0.187	6.70	387.0	400.0	Chord	2100000	2370000	-850 mV	8.0	8.5
T	UKOSRP H T200(2.1)	SW & CP	32.0	90	0.5	5.3	5.3	14.3	0.51	0.50	0.0	0.187	5.90	387.0	400.0	Chord	2100000	2370000	-850 mV	8.0	8.5
T	UKOSRP H T200(2.1)	SW & CP	32.0	90	0.5	5.3	5.3	14.3	0.40	0.50	0.0	0.187	5.50	387.0	400.0	Chord	2100000	2370000	-850 mV	8.0	8.5
T	UKOSRP H T214(2.1)	SW & CP	32.0	90	0.5	5.3	5.3	14.3	0.50	0.50	0.0	0.187	5.90	387.0	400.0	Chord	1300000	1300000	-850 mV	8.0	8.5
T	Dijkstra	16	SW&CP	31.7	90	1.0	6.7	8.5	14.4	0.50	0.50	0.20	7.70	saddle	-	Chord	3900000	4300000	-	-	-
TT	TW1	T1A	SW & CP	32.0	90	0.5	6.6	3.3	14.3	0.50	0.50	0.50	2.30	crown	-	Chord	650000	-	-1050 mV	8.4	5.0
TT	TW1	T1B	SW & CP	32.0	90	0.5	6.6	3.3	14.3	0.50	0.50	0.50	2.30	crown	-	Chord	650000	-	-1050 mV	8.4	5.0
TT	TW1	T4A	SW & CP	32.0	90	0.5	6.6	3.3	14.3	0.50	0.50	0.50	2.30	crown	-	Chord	650000	-	-1050 mV	8.4	5.0
TT	TW1	T4B	SW & CP	32.0	90	0.5	6.6	3.3	14.3	0.50	0.50	0.50	2.30	crown	-	Chord	650000	-	-1050 mV	8.4	5.0
T8	COSRP	T4A	Stiffened	18.0	90	0.5	6.3	6.3	24.1	1.00	0.50	0.1	6.30	nr saddle	405.0	Chord	147300	147300	-850 mV	8.4	5.0
T8	COSRP	T4A	Stiffened	18.0	90	0.5	6.3	6.3	24.1	1.00	0.50	0.1	6.70	saddle	405.0	Chord	540000	652000	-850 mV	8.4	5.0
X	Cole	1	Normalised	32.0	90	0.5	7.2	7.2	14.3	0.50	0.50	0.35	276.0	276.0	150000	Chord	150000	-	-850mV	10.0	10.0
X	Cole	2	Normalised	32.0	90	0.5	7.2	7.2	14.3	0.50	0.50	0.35	276.0	276.0	120000	Chord	120000	-	-850mV	10.0	10.0
X	Cole	3	Normalised	32.0	90	0.5	7.2	7.2	14.3	0.50	0.50	0.35	265.0	265.0	110000	Chord	110000	-	-850mV	10.0	10.0
X	Cole	4	Normalised	32.0	90	0.5	7.2	7.2	14.3	0.50	0.50	0.35	260.0	260.0	110000	Chord	110000	-	-850mV	10.0	10.0
X	Cole	5	Normalised	32.0	90	0.5	7.2	7.2	14.3	0.50	0.50	0.35	226.0	226.0	180000	Chord	180000	-	-850mV	10.0	10.0
X	Cole	6	Normalised	32.0	90	0.5	7.2	7.2	14.3	0.50	0.50	0.35	222.0	222.0	180000	Chord	180000	-	-850mV	10.0	10.0
X	Cole	7	Normalised	32.0	90	0.5	7.2	7.2	14.3	0.50	0.50	0.35	175.0	175.0	800000	Chord	800000	-	-850mV	10.0	10.0
X	Cole	8	Normalised	32.0	90	0.5	7.2	7.2	14.3	0.50	0.50	0.35	172.0	172.0	1200000	Chord	1200000	-	-850mV	10.0	10.0
X	Cole	9	Normalised	32.0	90	0.5	7.2	7.2	14.3	0.50	0.50	0.35	155.0	155.0	1150000	Chord	1150000	-	-850mV	10.0	10.0
X	Cole	10	Cont. rolled	32.0	90	0.5	7.2	7.2	14.3	0.50	0.50	0.35	276.0	276.0	115000	Chord	115000	-	-850mV	10.0	10.0
X	Cole	11	Cont. rolled	32.0	90	0.5	7.2	7.2	14.3	0.50	0.50	0.35	276.0	276.0	180000	Chord	180000	-	-850mV	10.0	10.0
X	Cole	12	Cont. rolled	32.0	90	0.5	7.2	7.2	14.3	0.50	0.50	0.35	230.0	230.0	200000	Chord	200000	-	-850mV	10.0	10.0
X	Cole	13	Cont. rolled	32.0	90	0.5	7.2	7.2	14.3	0.50	0.50	0.35	222.0	222.0	200000	Chord	200000	-	-850mV	10.0	10.0
X	Cole	14	Cont. rolled	32.0	90	0.5	7.2	7.2	14.3	0.50	0.50	0.35	180.0	180.0	530000	Chord	530000	-	-850mV	10.0	10.0
X	Cole	15	Cont. rolled	32.0	90	0.5	7.2	7.2	14.3	0.50	0.50	0.35	175.0	175.0	460000	Chord	460000	-	-850mV	10.0	10.0
X	Cole	16	Cont. rolled	32.0	90	0.5	7.2	7.2	14.3	0.50	0.50	0.35	148.0	148.0	650000	Chord	650000	-	-850mV	10.0	10.0
X	Cole	17	Cont. rolled	32.0	90	0.5	7.2	7.2	14.3	0.50	0.50	0.35	240.0	240.0	730000	Chord	730000	-	-850mV	10.0	10.0
X	Cole	18	Acc. cooled	32.0	90	0.5	7.2	7.2	14.3	0.50	0.50	0.35	185.0	185.0	320000	Chord	320000	-	-850mV	10.0	10.0
X	Cole	19	Acc. cooled	32.0	90	0.5	7.2	7.2	14.3	0.50	0.50	0.35	185.0	185.0	320000	Chord	320000	-	-850mV	10.0	10.0
X	Cole	20	Acc. cooled	32.0	90	0.5	7.2	7.2	14.3	0.50	0.50	0.35	185.0	185.0	320000	Chord	320000	-	-850mV	10.0	10.0
X	Cole	21	Acc. cooled	32.0	90	0.5	7.2	7.2	14.3	0.50	0.50	0.35	185.0	185.0	320000	Chord	320000	-	-850mV	10.0	10.0
X	Cole	22	Normalised	32.0	90	0.5	7.2	7.2	14.3	0.50	0.50	0.35	240.0	240.0	240000	Chord	240000	-	-850mV	10.0	10.0
X	Cole	23	Normalised	32.0	90	0.5	7.2	7.2	14.3	0.50	0.50	0.35	190.0	190.0	220000	Chord	220000	-	-850mV	10.0	10.0
X	Cole	24	Cont. rolled	32.0	90	0.5	7.2	7.2	14.3	0.50	0.50	0.35	170.0	170.0	470000	Chord	470000	-	-850mV	10.0	10.0
X	Cole	25	Cont. rolled	32.0	90	0.5	7.2	7.2	14.3	0.50	0.50	0.35	170.0	170.0	470000	Chord	470000	-	-850mV	10.0	10.0

Joint Type	Joint Ref.	Joint Ref.	T mm	T deg	C	Alpha spec.	Alpha supp.	Gamma	Tau	Beta	Loading mode	R	Load Req. Hz	Max. BCF	Max. BCF	Yield stress N/mm²	Stress range N/mm²	Max. BCF	Max. BCF	BRACE Yield stress N/mm²	Stress range N/mm²	Filled Member	N3	N4	CP	pH	°C
X	X	Cole	50.0	90	0.5	5.9	5.9	10.2	0.50	0.30	IPB	0.10	0.35			403.0	261.0			403.0			167000		-850mV		10.0
X	X	Cole	50.0	90	0.5	5.9	5.9	10.2	0.50	0.30	IPB	0.10	0.35			403.0	278.0			403.0			144500		-850mV		10.0
X	X	Cole	50.0	90	0.5	5.9	5.9	10.2	0.50	0.30	IPB	0.10	0.35			403.0	281.0			403.0			167000		-850mV		10.0
X	X	Cole	50.0	90	0.5	5.9	5.9	10.2	0.50	0.30	IPB	0.10	0.35			403.0	297.0			403.0			152000		-850mV		10.0
X	X	Cole	50.0	90	0.5	5.9	5.9	10.2	0.50	0.30	IPB	0.10	0.35			403.0	246.0			403.0			105000		-850mV		10.0
X	X	Cole	50.0	90	0.5	5.9	5.9	10.2	0.50	0.30	IPB	0.10	0.35			403.0	246.0			403.0			219000		-850mV		10.0
X	X	Cole	50.0	90	0.5	5.9	5.9	10.2	0.50	0.30	IPB	0.10	0.35			403.0	240.0			403.0			152000		-850mV		10.0
X	X	Cole	50.0	90	0.5	5.9	5.9	10.2	0.50	0.30	IPB	0.10	0.35			403.0	238.0			403.0			306000		-850mV		10.0
X	X	Cole	50.0	90	0.5	5.9	5.9	10.2	0.50	0.30	IPB	0.10	0.35			403.0	184.0			403.0			415000		-850mV		10.0
X	X	Cole	50.0	90	0.5	5.9	5.9	10.2	0.50	0.30	IPB	0.10	0.35			403.0	177.0			403.0			457000		-850mV		10.0
X	X	Cole	50.0	90	0.5	5.9	5.9	10.2	0.50	0.30	IPB	0.10	0.35			403.0	176.0			403.0			438500		-850mV		10.0
X	X	Cole	50.0	90	0.5	5.9	5.9	10.2	0.50	0.30	IPB	0.10	0.35			403.0	176.0			403.0			415000		-850mV		10.0
X	X	Cole	50.0	90	0.5	5.9	5.9	10.2	0.50	0.30	IPB	0.10	0.35			403.0	176.0			403.0			450000		-850mV		10.0
X	X	Cole	50.0	90	0.5	5.9	5.9	10.2	0.50	0.30	IPB	0.10	0.35			403.0	167.0			403.0			455500		-850mV		10.0
X	X	Cole	50.0	90	0.5	5.9	5.9	10.2	0.50	0.30	IPB	0.10	0.35			403.0	152.0			403.0			562000		-850mV		10.0
X	X	Cole	50.0	90	0.5	5.9	5.9	10.2	0.50	0.30	IPB	0.10	0.35			403.0	144.0			403.0			729000		-850mV		10.0
X	X	Cole	50.0	90	0.5	5.9	5.9	10.2	0.50	0.30	IPB	0.10	0.35			403.0	115.0			403.0			729000		-850mV		10.0
T	T	Dover	19.0								Asid	0.1	0.167			250							150000				
T	T	Dover	19.0								Asid	0.1	0.167			150							2100000				
T	T	Dover	19.0								Asid	0.3	0.167			180							540000				
T	T	Dover	13.5	90		7.3	0.0	14.7	1.00	0.71	Asid	0.1	0.167	13.4		378	143					Chord	600000		-850mV	8.0	9.0
T	T	Dover	15.5	90		7.3	0.0	14.7	1.00	0.71	Asid	0.1	0.167	13.6		378	172					Chord	2430000		-850mV	8.0	9.0
T	T	Dover	15.5	90		7.3	0.0	14.7	1.00	0.71	Asid	0.1	0.167	13.1		378	191					Chord	1060000		-850mV	8.0	9.0
T	T	Dover	16.0								Asid	0.1	0.167	13.1		378	210					Chord	580000		-850mV	8.0	9.0
T	T	Dover	16.0								Asid	0	0.167			157						Chord	429000		-850mV	8.0	9.0
T	T	Dover	16.0								Asid	0	0.167			171						Chord	2215000		-850mV	8.0	9.0
TT	TT	SINTEF	32.0	90	0.5	8.8	8.8	14.3	0.50	0.50	IPB(VA)	-1.0		2.30			0.0						574000		-1030mV		
TT	TT	SINTEF	32.0	90	0.5	8.8	8.8	14.3	0.50	0.50	IPB(VA)	-1.0		2.30			0.0						574000		-1030mV		
TT	TT	SINTEF	32.0	90	0.5	8.8	8.8	14.3	0.50	0.50	IPB(VA)	-1.0		2.30			0.0						2240000		-1030mV		
TT	TT	SINTEF	32.0	90	0.5	8.8	8.8	14.3	0.50	0.50	IPB(VA)	-1.0		2.30			0.0						1990000		-1030mV		
TT	TT	SINTEF	32.0	90	0.5	8.8	8.8	14.3	0.50	0.50	IPB(VA)	-1.0		2.30			0.0						2420000		-1030mV		
TT	TT	THI	32.0	90	0.5	8.8	8.8	14.3	0.50	0.50	IPB(VA)	-1.0		2.30			0.0						1420000		-1030mV		
TT	TT	THI	32.0	90	0.5	8.8	8.8	14.3	0.50	0.50	IPB(VA)	-1.0		2.30			0.0						1190000		-1030mV		
TT	TT	THI	32.0	90	0.5	8.8	8.8	14.3	0.50	0.50	IPB(VA)	-1.0		2.30			0.0						960000		-1030mV		
TT	TT	THI	32.0	90	0.5	8.8	8.8	14.3	0.50	0.50	IPB(VA)	-1.0		2.30			0.0						4200000		-1030mV		
TT	TT	THI	32.0	90	0.5	8.8	8.8	14.3	0.50	0.50	IPB(VA)	-1.0		2.30			0.0						6610000		-1030mV		

Part Ref.	Joint Ref.	T	mm	°	C	Alpha spec.	Alpha supp.	Gamm	Tau	Beta	Loading mode	R	Load freq. Hz	Max SCF	Yield stress N/mm²	Stress range N/mm²	Max SCF	Yield stress N/mm²	Stress range N/mm²	Failed Member	N3	N4	CP	pH	°C
Machine	YUS2	SW	12.0	60	0.5	11.1	11.5	13.5	0.65	0.85	Adial	0.00	0.20	-	240.00	178.24	-	240	-	Chord	178500	212700	FC	8.0	25.0
Machine	CFTUS3	SW	12.0	90	0.5	11.3	11.7	13.3	0.87	0.80	Adial	-1.00	0.20	-	250.00	172.18	-	250	-	Chord	378000	400000	FC	8.0	25.0
Dikreta	4	SW	15.0	90	0.5	10.0	10.0	14.4	0.52	0.48	Adial	0.0	0.20	-	-	104.8	-	-	-	Chord	2200000	2700000	FC	20.0	20.0
Dikreta	10	SW	15.0	90	0.5	10.0	10.0	14.4	0.52	0.48	Adial	-1.0	0.20	-	-	104.8	-	-	-	Chord	2300000	2800000	FC	20.0	20.0
Dikreta	17	SW	31.7	90	1.0	8.7	8.5	14.4	0.50	0.50	Adial	0.0	0.20	-	-	83.8	-	-	-	Chord	3700000	4300000	FC	20.0	20.0
Wylde		SW	20.0			0.0	0.0	11.4				0.00	0.17	-	345.0	228.0	-	-	-	Chord	480000		FC	10.0	10.0
Wylde		SW + Grind	20.0			0.0	0.0	11.4				0.00	0.17	-	370.0	300.0	-	-	-	Chord	187000		FC	10.0	10.0
Wylde		SW + Grind	20.0			0.0	0.0	11.4				0.00	0.17	-	385.0	212.0	-	-	-	Chord	487000		FC	10.0	10.0
Wylde		SW + Grind	20.0			0.0	0.0	11.4				0.00	0.17	-	399.0	293.0	-	-	-	Chord	294000		FC	10.0	10.0
Hara	1	SW	20.0	90	0.5	11.4	11.8	12.7	0.45	0.53	Adial	-1.00	0.30	6.84	451.0	284.4	-	-	-	Chord	470000		FC	10.0	10.0
Hara	2	SW	20.0	90	0.5	11.4	11.8	12.7	0.45	0.53	Adial	-1.00	0.30	5.40	451.0	194.8	-	-	-	Chord	350000	380000	FC	8.0	8.0
Hara	3	SW + Grind	20.0	90	0.5	11.4	11.8	12.7	0.45	0.53	Adial	-1.00	0.30	5.40	451.0	194.8	-	-	-	Chord	1150000	1540000	FC	8.0	8.0
Hara	4	SW + Grind	20.0	90	0.5	11.4	11.8	12.7	0.45	0.53	Adial	-1.00	0.30	5.40	451.0	226.0	-	-	-	Chord	1010000	1080000	FC	8.0	8.0
Hara	5	SW	20.0	90	0.5	11.4	11.8	12.7	0.45	0.53	Adial	-1.00	0.30	5.52	451.0	144.0	-	-	-	Chord	1680000	1770000	FC	8.0	8.0
Hara	6	SW	20.0	90	0.5	11.4	11.8	12.7	0.80	0.53	Adial	-1.00	0.30	10.44	451.0	216.0	-	-	-	Chord	430000	480000	FC	8.0	8.0
Hara	7	SW + Grind	20.0	90	0.5	11.4	11.8	12.7	0.80	0.53	Adial	-1.00	0.30	10.56	451.0	106.0	-	-	-	Chord	2050000	2230000	FC	8.0	8.0
Hara	8	SW + Grind	20.0	90	0.5	11.4	11.8	12.7	0.80	0.53	Adial	-1.00	0.30	10.56	451.0	222.0	-	-	-	Chord	1380000	1430000	FC	8.0	8.0
Hara	8	SW + Grind	20.0	90	0.5	11.4	11.8	12.7	0.80	0.53	Adial	-1.00	0.30	10.20	451.0	134.8	-	-	-	Chord	2950000	3400000	FC	8.0	8.0



APPENDIX E
DATABASE OF TUBULAR JOINTS WITH POST FABRICATION TREATMENT

Joint Type	Paper Ref.	Joint Ref.	T mm	theta deg	C	Alpha spec.	Alpha supp.	Gamma	Tau	Beta	Loading mode	R	Max SCF	CHORD Max SCF bo'n	Yield stress N/mm ²	Stress range N/mm ²	Max SCF	BRACE Max SCF bo'n	Yield stress N/mm ²	Stress range N/mm ²	Failed Member	N3	N4
H	UKOSRP I	H45	PWHT	76.2	90	0.5	2.8	2.8	12.0	0.25	Axial	-1.0	-	-	380.0	-	2.87	saddle	380.0	167.5	Brace	1080000	1250000
H	UKOSRP I	H46	PWHT	76.2	90	0.5	2.8	2.8	12.0	0.25	Axial	-1.0	-	-	380.0	-	2.81	saddle	380.0	232.4	Brace	497000	666000
H	UKOSRP I	H47	PWHT	76.2	90	0.5	4.2	4.2	12.0	0.51	Axial	-1.0	4.09	nr saddle	380.0	218.4	-	-	380.0	-	Chord	840000	740000
H	UKOSRP I	H48	PWHT	76.2	90	0.5	4.2	4.2	12.0	0.51	Axial	-1.0	4.48	saddle	380.0	153.0	-	-	380.0	-	Chord	3110000	4340000
H	UKOSRP I	H49	PWHT	76.2	90	0.5	2.9	2.9	12.0	0.25	IPB	-1.0	-	-	380.0	-	1.77	crown	380.0	409.4	Brace	96000	110000
H	UKOSRP I	H51	PWHT	76.0	90	0.5	4.2	4.2	12.0	0.50	IPB	-1.0	1.68	nr crown	380.0	329.9	-	-	352.0	-	Chord	110000	148000
T	UKOSRP II	T201(3.1)	PWHT	32.0	90	0.5	5.3	5.3	14.3	0.49	Axial	-1.0	6.00	saddle	387.0	350.6	-	-	400.0	-	Chord	340000	478000
T	UKOSRP II	T202(3.1)	PWHT	32.0	90	0.5	5.3	5.3	14.3	0.50	Axial	-1.0	6.10	saddle	387.0	281.6	-	-	400.0	-	Chord	1500000	1750000
T	UKOSRP II	T203(3.1)	PWHT	32.0	90	0.5	5.3	5.3	14.3	0.51	Axial	-1.0	8.10	saddle	387.0	207.4	-	-	400.0	-	Chord	6370000	7780000
T	UKOSRP II	T204(3.1)	PWHT	32.0	90	0.5	5.3	5.3	14.3	0.50	Axial	-1.0	5.70	saddle	387.0	403.4	6.70	saddle	400.0	403.4	Chord	210000	279000
X	Lieurade	AA	HT	22.3	90	-	8.5	-	10.6	0.99	IPB	0.1	3.80	maximum	-	270.0	2.21	maximum	-	158.7	Chord	158000	191000
X	Lieurade	B	HT211	40.0	90	-	5.8	-	8.6	0.56	Axial	0.1	5.74	saddle	-	186.9	5.28	saddle	-	172.0	Chord	401000	590000
X	Lieurade	C	*HT215	77.6	90	-	3.1	-	8.3	0.29	Axial	0.1	2.32	saddle	-	123.0	2.04	saddle	-	108.4	Chord	1135000	1270000
X	Lieurade	CC	*HT	75.0	90	-	4.1	-	8.5	0.30	IPB	0.1	0.74	crown	-	86.0	1.69	crown	-	195.5	Brace	722000	723000
X	Lieurade	D	*HT213	41.8	90	-	3.1	-	11.4	1.00	Axial	0.1	12.98	saddle	-	232.3	7.80	saddle	-	139.5	Chord	300000	435000
X	Lieurade	DD	*HT214	44.0	90	-	4.2	-	10.8	0.99	IPB	0.1	3.29	crown	-	131.9	-	-	-	-	Chord	501000	850000
X	Lieurade	EE	*HT218	76.7	90	-	3.1	-	8.3	0.57	IPB	0.1	1.87	crown	-	131.6	2.05	crown	-	144.3	Chord	507000	551000
H	UKOSRP I	H50	PWHT	76.2	90	0.5	2.9	2.9	12.0	0.25	IPB	-1.0	1.56	-	380.0	96.7	1.70	crown	380.0	106.3	Run out	-	20000000
H	UKOSRP I	H50	PWHT(R)	76.2	90	0.5	2.9	2.9	12.0	0.25	IPB	-1.0	1.70	-	380.0	330.0	1.70	crown	380.0	330.0	Brace	334000	360000
H	UKOSRP I	H52	PWHT	78.0	90	0.5	4.2	4.2	12.0	0.50	IPB	-1.0	1.68	nr crown	382.0	101.6	-	-	382.0	-	Run out	-	20000000
H	UKOSRP I	H52	PWHT(R)	78.0	90	0.5	4.2	4.2	12.0	0.50	IPB	-1.0	1.68	nr crown	382.0	155.1	-	-	382.0	-	Chord	1302000	1580000



APPENDIX F
COMPLEX TUBULAR JOINTS

OVERLAPPED JOINTS

Joint Type	Joint Ref.	Joint Ref.	T mm	theta deg	C	Alpha spec	Alpha supp	Gamma	Tau	Beta	Psi deg	Zeta	Loading mode	R	Max SCF	CHORD Max SCF	Yield stress N/mm ²	Stress range N/mm ²	Max SCF	BRACE Max SCF	Yield stress N/mm ²	Stress range N/mm ²	Failed Member	N3	N4
OK	UKOSRP I	K08/1	8.1	90/45	0.5	15.1	14.2	13.9	0.92	0.53	-	-0.41	Axial	0.0	1.10	maximum	465.0	47.9	-	-	437.0	-	Run out	-	8100000
OK	UKOSRP I	K07/1	8.2	90/45	0.5	17.1	17.1	13.8	0.88	0.54	-	-0.42	OPB	0.0	9.58	saddle	465.0	273.3	-	-	437.0	-	Chord	1200000	1800000
OK	UKOSRP I	K07/2	8.1	90/45	0.5	17.1	17.1	13.8	0.90	0.53	-	-0.40	OPB	0.0	9.81	saddle	465.0	272.0	-	-	437.0	-	Chord	3400000	4000000
OK	UKOSRP I	K08/1	8.2	90/45	0.5	17.0	17.0	13.6	0.83	0.53	-	-0.40	OPB	0.0	8.01	maximum	465.0	299.1	-	-	365.0	-	Chord	870000	1300000
OK	UKOSRP I	K08/2	8.0	90/45	0.5	17.0	17.0	14.1	0.83	0.53	-	-0.41	OPB	0.0	8.09	maximum	465.0	259.8	-	-	365.0	-	Chord	1800000	2300000
OK	UKOSRP I	K28/1	18.0	90/45	1.0	14.1	14.1	14.3	0.80	0.53	-	-0.39	Axial	0.0	-	-	397.0	-	1.87	maximum	445.0	80.1	Runner	-	8200000
OK	UKOSRP I	K27/1	18.0	90/45	1.0	14.0	14.0	14.3	0.80	0.54	-	-0.40	OPB	0.0	7.26	saddle	410.0	368.5	-	-	445.0	-	Chord	220000	3400000
OK	UKOSRP I	K27/2	18.3	90/45	1.0	14.0	14.0	14.0	0.80	0.54	-	-0.40	OPB	0.0	8.59	saddle	410.0	185.4	-	-	445.0	-	C & W	4000000	5300000
OK	UKOSRP I	K29/1	18.1	90/45	1.0	14.0	14.0	12.6	0.87	0.54	-	-0.40	OPB	0.0	8.72	saddle	410.0	271.2	-	-	445.0	-	Chord	1100000	1800000
OK	UKOSRP I	K29/2	18.2	90/45	1.0	14.0	14.0	12.6	0.86	0.54	-	-0.40	OPB	0.0	7.72	saddle	410.0	321.9	-	-	445.0	-	Chord	190000	320000
OK	UKOSRP I	K33/1	18.4	45/90/45	1.0	14.1	14.1	14.0	0.83	0.53	-	-0.39	OPB	0.0	7.14	saddle	410.0	192.8	-	-	445.0	-	Chord	1200000	2100000
OK	UKOSRP I	K33/2	15.9	45/90/45	1.0	14.1	14.1	14.1	0.83	0.54	-	-0.40	OPB	0.0	8.78	saddle	410.0	294.1	-	-	445.0	-	Chord	480000	590000
OK	UKOSRP I	K35/1	18.7	45/90/45	1.0	14.1	14.1	13.7	0.74	0.54	-	-0.40	OPB	0.0	10.81	saddle	410.0	191.3	-	-	445.0	-	Chord	1700000	2700000
OK	UKOSRP I	K35/2	18.8	45/90/45	1.0	14.1	14.1	13.7	0.74	0.54	-	-0.40	OPB	0.0	9.21	saddle	410.0	282.7	-	-	445.0	-	Chord	330000	590000
OK	UKOSRP I	K15/1	18.0	90/45	-	13.0	13.3	13.3	0.70	0.53	-	-0.39	Axial	0.0	1.80	rr heel	398.0	368.4	2.25	com. weld	445.0	560.2	Flange	639000	728000
OK	UKOSRP I	K15/2	18.0	90/45	-	13.0	13.3	14.3	0.50	0.53	-	-0.39	Axial	0.0	1.80	rr heel	398.0	368.4	2.25	com. weld	445.0	560.2	Flange	112000	112000
OK	UKOSRP I	K15/2	18.0	90/45	-	13.0	13.3	14.3	0.50	0.53	-	-0.39	Axial	0.0	1.80	rr heel	398.0	368.4	2.25	com. weld	445.0	560.2	Flange	219000	219000
OK	UKOSRP I	K15/2	18.0	90/45	-	13.0	13.3	14.3	0.50	0.53	-	-0.39	Axial	0.0	1.80	rr heel	398.0	368.4	2.25	com. weld	445.0	560.2	Flange	859000	1290000
OK	UKOSRP I	K15/2	18.0	90/45	-	13.0	13.3	14.3	0.50	0.53	-	-0.39	Axial	0.0	1.80	rr heel	398.0	368.4	2.25	com. weld	445.0	560.2	Flange	1020000	1290000
OK	UKOSRP I	K15/2	18.0	90/45	-	13.0	13.3	14.3	0.50	0.53	-	-0.39	Axial	0.0	1.80	rr heel	398.0	368.4	2.25	com. weld	445.0	560.2	Flange	1890000	2740000
OK	UKOSRP I	K15/2	18.0	90/45	-	13.0	13.3	14.3	0.50	0.53	-	-0.39	Axial	0.0	1.80	rr heel	398.0	368.4	2.25	com. weld	445.0	560.2	Flange	1890000	2740000
OK	UKOSRP I	K15/2	18.0	90/45	-	13.0	13.3	14.3	0.50	0.53	-	-0.39	Axial	0.0	1.80	rr heel	398.0	368.4	2.25	com. weld	445.0	560.2	Flange	1890000	2740000
OK	UKOSRP I	K15/2	18.0	90/45	-	13.0	13.3	14.3	0.50	0.53	-	-0.39	Axial	0.0	1.80	rr heel	398.0	368.4	2.25	com. weld	445.0	560.2	Flange	1890000	2740000
OK	UKOSRP I	K15/2	18.0	90/45	-	13.0	13.3	14.3	0.50	0.53	-	-0.39	Axial	0.0	1.80	rr heel	398.0	368.4	2.25	com. weld	445.0	560.2	Flange	1890000	2740000
OK	UKOSRP I	K15/2	18.0	90/45	-	13.0	13.3	14.3	0.50	0.53	-	-0.39	Axial	0.0	1.80	rr heel	398.0	368.4	2.25	com. weld	445.0	560.2	Flange	1890000	2740000
OK	UKOSRP I	K15/2	18.0	90/45	-	13.0	13.3	14.3	0.50	0.53	-	-0.39	Axial	0.0	1.80	rr heel	398.0	368.4	2.25	com. weld	445.0	560.2	Flange	1890000	2740000
OK	UKOSRP I	K15/2	18.0	90/45	-	13.0	13.3	14.3	0.50	0.53	-	-0.39	Axial	0.0	1.80	rr heel	398.0	368.4	2.25	com. weld	445.0	560.2	Flange	1890000	2740000
OK	UKOSRP I	K15/2	18.0	90/45	-	13.0	13.3	14.3	0.50	0.53	-	-0.39	Axial	0.0	1.80	rr heel	398.0	368.4	2.25	com. weld	445.0	560.2	Flange	1890000	2740000
OK	UKOSRP I	K15/2	18.0	90/45	-	13.0	13.3	14.3	0.50	0.53	-	-0.39	Axial	0.0	1.80	rr heel	398.0	368.4	2.25	com. weld	445.0	560.2	Flange	1890000	2740000
OK	UKOSRP I	K15/2	18.0	90/45	-	13.0	13.3	14.3	0.50	0.53	-	-0.39	Axial	0.0	1.80	rr heel	398.0	368.4	2.25	com. weld	445.0	560.2	Flange	1890000	2740000
OK	UKOSRP I	K15/2	18.0	90/45	-	13.0	13.3	14.3	0.50	0.53	-	-0.39	Axial	0.0	1.80	rr heel	398.0	368.4	2.25	com. weld	445.0	560.2	Flange	1890000	2740000
OK	UKOSRP I	K15/2	18.0	90/45	-	13.0	13.3	14.3	0.50	0.53	-	-0.39	Axial	0.0	1.80	rr heel	398.0	368.4	2.25	com. weld	445.0	560.2	Flange	1890000	2740000
OK	UKOSRP I	K15/2	18.0	90/45	-	13.0	13.3	14.3	0.50	0.53	-	-0.39	Axial	0.0	1.80	rr heel	398.0	368.4	2.25	com. weld	445.0	560.2	Flange	1890000	2740000
OK	UKOSRP I	K15/2	18.0	90/45	-	13.0	13.3	14.3	0.50	0.53	-	-0.39	Axial	0.0	1.80	rr heel	398.0	368.4	2.25	com. weld	445.0	560.2	Flange	1890000	2740000
OK	UKOSRP I	K15/2	18.0	90/45	-	13.0	13.3	14.3	0.50	0.53	-	-0.39	Axial	0.0	1.80	rr heel	398.0	368.4	2.25	com. weld	445.0	560.2	Flange	1890000	2740000
OK	UKOSRP I	K15/2	18.0	90/45	-	13.0	13.3	14.3	0.50	0.53	-	-0.39	Axial	0.0	1.80	rr heel	398.0	368.4	2.25	com. weld	445.0	560.2	Flange	1890000	2740000
OK	UKOSRP I	K15/2	18.0	90/45	-	13.0	13.3	14.3	0.50	0.53	-	-0.39	Axial	0.0	1.80	rr heel	398.0	368.4	2.25	com. weld	445.0	560.2	Flange	1890000	2740000
OK	UKOSRP I	K15/2	18.0	90/45	-	13.0	13.3	14.3	0.50	0.53	-	-0.39	Axial	0.0	1.80	rr heel	398.0	368.4	2.25	com. weld	445.0	560.2	Flange	1890000	2740000
OK	UKOSRP I	K15/2	18.0	90/45	-	13.0	13.3	14.3	0.50	0.53	-	-0.39	Axial	0.0	1.80	rr heel	398.0	368.4	2.25	com. weld	445.0	560.2	Flange	1890000	2740000
OK	UKOSRP I	K15/2	18.0	90/45	-	13.0	13.3	14.3	0.50	0.53	-	-0.39	Axial	0.0	1.80	rr heel	398.0	368.4	2.25	com. weld	445.0	560.2	Flange	1890000	2740000
OK	UKOSRP I	K15/2	18.0	90/45	-	13.0	13.3	14.3	0.50	0.53	-	-0.39	Axial	0.0	1.80	rr heel	398.0	368.4	2.25	com. weld	445.0	560.2	Flange	1890000	2740000
OK	UKOSRP I	K15/2	18.0	90/45	-	13.0	13.3	14.3	0.50	0.53	-	-0.39	Axial	0.0	1.80	rr heel	398.0	368.4	2.25	com. weld	445.0	560.2	Flange	1890000	2740000
OK	UKOSRP I	K15/2	18.0	90/45	-	13.0	13.3	14.3	0.50	0.53	-	-0.39	Axial	0.0	1.80	rr heel	398.0	368.4	2.25	com. weld	445.0	560.2	Flange	1890000	2740000
OK	UKOSRP I	K15/2	18.0	90/45	-	13.0	13.3	14.3	0.50	0.53	-	-0.39	Axial	0.0	1.80	rr heel	398.0	368.4	2.25	com. weld	445.0	560.2	Flange	1890000	2740000
OK	UKOSRP I	K15/2	18.0	90/45	-	13.0	13.3	14.3	0.50	0.53	-	-0.39	Axial	0.0	1.80	rr heel	398.0	368.4	2.25	com. weld	445.0	560.2	Flange	1890000	2740000
OK	UKOSRP I	K15/2	18.0	90/45	-	13.0	13.3	14.3	0.50	0.53	-	-0.39	Axial	0.0	1.80	rr heel	398.0	368.4	2.25	com. weld	445.0	560.2	Flange	1890000	2740000
OK	UKOSRP I	K15/2	18.0	90/45	-	13.0	13.3	14.3	0.50	0.53	-	-0.39	Axial	0.0	1.80	rr heel	398.0	368.4	2.25	com. weld	445.0	560.2	Flange	1890000	2740000
OK	UKOSRP I	K15/2	18.0	90/45	-	13.0	13.3	14.3	0.50	0.53	-	-0.39	Axial	0.0	1.80	rr heel	398.0	368.4	2.25	com. weld	445.0	560.2	Flange	1890000	2740000
OK	UKOSRP I	K15/2	18.0	90/45	-	13.0	13.3	14.3	0.50	0.53	-	-0.39	Axial	0.0	1.80	rr heel	398.0	368.4	2.25	com. weld	445.0	560.2	Flange	1890000	2740000
OK	UKOSRP I	K15/2	18.0	90/45	-	13.0	13.3	14.3	0.50	0.53	-	-0.39	Axial	0.0	1.80	rr heel	398.0	368.4	2.25	com. weld	445.0	560.2	Flange	1890000	2740000
OK	UKOSRP I	K15/2	18.0	90/45	-	13.0	13.3	14.3	0.50	0.53	-	-0.39	Axial	0.0	1.80	rr heel	398.0	368.4	2.25	com. weld	445.0	560.2	Flange	1890000	2740000
OK	UKOSRP I	K15/2	18.0	90/45	-	13.0	13.3	14.3	0.50	0.53	-	-0.39	Axial	0.0	1.80	rr heel	398.0	368.4	2.25	com. weld	445.0	560.2	Flange	1890000	2740000
OK	UKOSRP I	K15/2	18.0	90/45	-	13.0	13.3	14.3	0.50	0.53	-	-0.39	Axial	0.0	1.80	rr heel	398.0	368.4	2.25	com. weld	445.0	5			

MULTIPLANAR JOINTS

Joint Type	Paper Ref.	Joint Ref.	T mm	theta deg	C	Alpha spec.	Alpha spec.	Gamma	Tau	Beta	Psi deg	Zeta	Loading mode	R	Max SCF	CHORD Max SCF Yield stress N/mm² Stress range N/mm²	BRACE Max SCF Yield stress N/mm² Stress range N/mm²	Failed Member	N3	N4	
T (MP)	Dijkstra	18	6.3	90	0.5	10.0	10.0	13.4	0.51	0.53	-	-	Axial	0.0	5.40	-	219.4	-	Chord	3000000	3900000
T (MP)	Dijkstra	19	6.3	90	0.5	10.0	10.0	13.4	0.51	0.53	-	-	Axial	0.0	5.40	-	501.4	-	Chord	80000	74000
T (MP)	Dijkstra	22	6.3	90	0.5	10.0	10.0	13.4	0.51	0.53	-	-	Axial	0.0	5.10	-	268.4	-	Chord	880000	960000
T (MP)	Dijkstra	23	6.3	90	0.5	10.0	10.0	13.4	0.51	0.53	-	-	Axial	0.0	5.10	-	189.4	-	Chord	2000000	2400000
T (MP)	Dijkstra	20	31.7	90	1.0	8.7	8.5	14.4	0.50	0.50	-	-	Axial	0.0	8.00	-	217.8	-	Chord	410000	880000
T (MP)	Dijkstra	21	31.7	90	1.0	8.7	8.5	14.4	0.50	0.50	-	-	Axial	0.0	8.00	-	79.8	-	Chord	8100000	1800000
X (MP)	Dijkstra	39	31.7	90	1.0	8.7	8.5	14.4	0.50	0.50	-	-	Axial	0.0	11.20	-	76.2	-	Chord	20000000	28000000
X (MP)	Dijkstra	40	31.7	90	1.0	8.7	8.5	14.4	0.50	0.50	-	-	Axial	0.0	11.20	-	198.2	-	Chord	500000	730000
KK (MP)	TNO	5 Gap 1	8.0	45	20.7	20.7	20.7	12.1	0.50	0.39	-	0.44	Axial	0.1	1.81	-	287.9	-	Chord	723000	-
KK (MP)	TNO	6 Gap 2	8.0	45	18.6	18.6	18.6	12.1	0.50	0.39	-	0.44	Axial	0.1	1.58	-	268.8	-	Chord	598000	-
KK (MP)	TNO	5 Lap 1	8.0	45	17.2	17.2	17.2	12.1	0.50	0.39	-	-0.28	Axial	0.1	2.95	-	371.7	-	Chord	214000	-
KK (MP)	TNO	5 Lap 2	8.0	45	18.5	18.5	18.5	12.1	0.50	0.39	-	-0.28	Axial	0.1	2.18	-	481.8	-	Chord	48000	-
KK (MP)	TNO	6 Gap 1	18.0	45	20.7	20.7	20.7	12.1	0.50	0.39	-	0.44	Axial	0.1	1.83	-	243.4	-	Chord	375000	-
KK (MP)	TNO	6 Gap 2	18.0	45	18.6	18.6	18.6	12.1	0.50	0.39	-	0.44	Axial	0.1	1.74	-	298.3	-	Brace	244000	-
KK (MP)	TNO	8 Lap 1	18.0	45	17.2	17.2	17.2	12.1	0.50	0.39	-	-0.28	Axial	0.1	2.25	-	413.7	-	Chord	210000	-
KK (MP)	TNO	8 Lap 2	18.0	45	16.5	16.5	16.5	12.1	0.50	0.39	-	-0.28	Axial	0.1	1.97	-	490.5	-	Chord	58000	-
KK (MP)	TNO	7 Gap 1	8.0	45	20.7	20.7	20.7	12.1	0.50	0.59	-	0.17	Axial	0.1	2.71	-	490.5	-	Chord	80000	-
KK (MP)	TNO	7 Gap 2	8.0	45	18.6	18.6	18.6	12.1	0.50	0.59	-	0.17	Axial	0.1	2.19	-	219	-	Brace	80000	-
KK (MP)	TNO	7 Lap 1	8.0	45	19.3	19.3	19.3	12.1	0.50	0.59	-	-0.56	Axial	0.1	-	-	219	-	Runner	-	220000
KK (MP)	TNO	7 Lap 2	8.0	45	18.8	18.8	18.8	12.1	0.50	0.59	-	-0.56	Axial	0.1	-	-	-	-	Chord	93000	-
KK (MP)	TNO	8 Gap 1	18.0	45	20.7	20.7	20.7	12.1	0.50	0.59	-	0.17	Axial	0.1	2.32	-	250.6	-	Chord	310000	-
KK (MP)	TNO	8 Gap 2	18.0	45	18.6	18.6	18.6	12.1	0.50	0.59	-	0.17	Axial	0.1	1.97	-	204.9	-	Chord	978000	-
KK (MP)	TNO	8 Lap 1	18.0	45	19.3	19.3	19.3	12.1	0.50	0.59	-	-0.56	Axial	0.1	2.80	-	249.6	-	Runner	-	978000
KK (MP)	TNO	8 Lap 2	18.0	45	18.8	18.8	18.8	12.1	0.50	0.59	-	-0.56	Axial	0.1	1.81	-	190.1	-	Runner	-	978000

RING-STIFFENED JOINTS																														
Joint Type	Paper Ref.	Joint Ref.	T mm	W mm	W mm	H mm	E mm	n	p	d mm	θ deg	C	Alpha spec.	Alpha supp.	Gamma	Tau	Basis	Loading mode	R	Max. SCF	CHORD Max. SCF	Stress range N/mm²	Max. SCF	BRACE Max. SCF	Stress range N/mm²	Max. SCF	RING Max. SCF	Stress range N/mm²	Failed Member	N3
TS	Sewada	F-1-1	9.6	100.0	8.3	-	-	1	0.0	318.5	90	1.0	11.0	10.1	37.1	0.72	0.45	Axial	-1.0	4.80	saddle	304.2	6.90	saddle	546.3	-	-	-	Ring	35500
TS	Sewada	F-1-2	9.6	100.0	8.0	-	-	1	0.0	318.5	90	1.0	11.0	10.1	37.1	0.72	0.45	Axial	-1.0	3.70	saddle	728.3	6.90	saddle	728.3	-	-	-	Brace	16000
TS	Sewada	F-1-3	9.6	100.0	8.0	-	-	1	0.0	318.5	90	1.0	11.0	10.1	37.1	0.72	0.45	Axial	-1.0	3.90	saddle	205.8	7.10	saddle	374.7	-	-	-	Ring	20000
TS	UKOSRP # T220(5.1)	T220(5.1)	16.0	100.0	16.0	-	-	2	266.0	457.0	90	0.5	6.3	5.3	28.6	1.03	0.50	Axial	0.0	7.60	nr saddle	205.6	4.84	maximum	130.9	-	-	-	Chord/Ring	4900000
TS	UKOSRP # T221(6.1)	T221(6.1)	16.0	100.0	16.0	-	-	2	266.0	457.0	90	0.5	6.3	5.3	28.6	1.03	0.50	Axial	0.0	7.00	saddle	306.6	4.60	saddle	210.2	-	-	-	Ring	390000
TS	UKOSRP # T223(5.1)	T223(5.1)	16.0	100.0	16.0	-	-	2	266.0	457.0	90	0.5	6.3	5.3	28.6	1.02	0.50	Axial	0.0	6.20	saddle	377.5	4.20	saddle	263.7	-	-	-	Ring	203000
TS	UKOSRP # T224(6.1)	T224(6.1)	16.0	200.0	16.0	120.0	30.0	2	316.0	457.0	90	0.5	6.3	5.3	28.6	1.04	0.50	Axial	0.0	4.00	saddle	155.2	2.10	BRI	81.5	-	-	-	Chord	1470000
TS	UKOSRP # T224(6.1)	T224(6.1)	16.0	200.0	16.0	120.0	30.0	2	316.0	457.0	90	0.5	6.3	5.3	28.6	1.01	0.50	Axial	0.0	3.20	saddle	311.1	3.40	BRI	330.5	-	-	-	Chord	69200
TS	UKOSRP # T224(6.1)	T224(6.1)	19.0	200.0	16.0	120.0	30.0	2	316.0	457.0	90	0.5	6.3	5.3	28.6	1.04	0.50	Axial	0.0	3.60	saddle	249.3	1.50	BRI	104.0	-	-	-	Chord	197000
TS	COSRP	TA2	19.0	100.0	19.0	-	-	2	250.0	457.0	90	0.5	6.3	6.3	24.1	1.00	0.50	Axial	0.1	6.40	nr saddle	232.3	-	-	-	8.30	60°	-	Chord	411600
TS	COSRP	TA3	19.0	100.0	19.0	-	-	2	250.0	457.0	90	0.5	6.3	6.3	24.1	1.00	0.50	Axial	0.1	7.00	saddle	160.2	-	-	-	6.40	90°	-	Chord	134800
TS	COSRP	TA4	19.0	100.0	19.0	-	-	2	250.0	457.0	90	0.5	6.3	6.3	24.1	1.00	0.50	Axial	0.1	6.90	nr saddle	237.5	-	-	-	7.50	70°	-	Chord	142600
TS	COSRP	TA5	19.0	100.0	19.0	-	-	2	250.0	457.0	90	0.5	6.3	6.3	24.1	1.00	0.50	Axial	0.1	6.70	nr saddle	160.7	-	-	-	6.70	80°	-	Chord	540000
TS	COSRP	TA6	19.0	100.0	19.0	-	-	2	250.0	457.0	90	0.5	6.3	6.3	24.1	1.00	0.50	Combined	-	6.70	BRI	160.0	4.35	BRI	161.7	-	-	-	Chord	1260000
TS	COSRP	TB2	19.0	100.0	19.0	-	-	2	250.0	457.0	90	0.5	6.3	6.3	24.1	1.00	0.50	IPB	0.1	3.00	nr crown	244.7	-	-	-	2.00	55°	-	Chord	163.1
TS	COSRP	TB3	19.0	100.0	19.0	-	-	2	250.0	457.0	90	0.5	6.3	6.3	24.1	1.00	0.50	IPB	0.1	3.10	nr crown	159.6	-	-	-	2.13	55°	-	Chord	202000
TS	COSRP	TB4	19.0	100.0	19.0	-	-	2	250.0	457.0	90	0.5	6.3	6.3	24.1	1.00	0.50	OPB	0.1	4.70	nr saddle	296.4	-	-	-	5.33	25°	-	Chord	470000
TS	COSRP	TB5	19.0	100.0	19.0	-	-	2	250.0	457.0	90	0.5	6.3	6.3	24.1	1.00	0.50	OPB	0.1	4.50	nr saddle	171.1	-	-	-	5.33	25°	-	Chord	325000
TS	COSRP	TB6	19.0	100.0	19.0	-	-	2	250.0	457.0	90	0.5	6.3	6.3	24.1	1.00	0.50	IPB	0.1	3.70	nr crown	188.0	-	-	-	6.16	25°	-	Chord	211000
TS	Madras	TS1	12.0	64.0	10.0	-	-	3	100.0	220.0	90	0.5	11.3	11.7	13.3	0.67	0.69	Axial	-1.0	2.93	saddle	233.7	-	-	-	-	-	-	Separation	660000
TS	Madras	TS2	12.0	64.0	10.0	-	-	3	100.0	220.0	90	0.5	11.3	11.7	13.3	0.67	0.69	Axial	0.0	2.93	saddle	101.7	-	-	-	-	-	-	Chord	1165000
TS	Madras	TS3	12.0	64.0	10.0	-	-	3	100.0	220.0	90	0.5	11.3	11.7	13.3	0.67	0.69	Axial	0.0	2.93	saddle	151.2	-	-	-	-	-	-	Chord	142000
TS	Madras	TS4	12.0	64.0	10.0	-	-	3	100.0	220.0	90	0.5	11.3	11.7	13.3	0.67	0.69	Axial	-1.0	2.93	saddle	151.2	-	-	-	-	-	-	Chord	37000
YS	Madras	YS1	12.0	76.0	12.0	-	-	3	114.4	252.9	90	0.5	11.1	11.5	13.5	0.68	0.68	Axial	-1.0	3.73	saddle	203.1	-	-	-	-	-	-	Chord	110000
TS	Madras	CFTS1	12.0	64.0	10.0	-	-	3	100.0	220.0	90	0.5	11.3	11.7	13.3	0.67	0.69	Axial	-1.0	2.93	saddle	128.6	-	-	-	-	-	-	Chord	845000
TS	Madras	CFTS2	12.0	64.0	10.0	-	-	3	100.0	220.0	90	0.5	11.3	11.7	13.3	0.67	0.69	Axial	-1.0	2.93	saddle	176.0	-	-	-	-	-	-	Chord	100000
YS	Madras	CFYS1	12.0	64.0	10.0	-	-	3	115.0	254.0	60	0.5	11.3	11.7	13.3	0.67	0.69	Axial	0.0	3.50	saddle	203.6	-	-	-	-	-	-	Chord	164000
YS	Madras	CFYS2	12.0	64.0	10.0	-	-	3	115.0	254.0	60	0.5	11.3	11.7	13.3	0.67	0.69	Axial	0.0	3.50	saddle	124.6	-	-	-	-	-	-	Chord	1334000
TS	Madras	SP4	12.0	76.0	12.0	-	-	3	97.5	219.0	90	0.5	11.1	11.5	13.5	0.68	0.68	Axial	-1.0	3.16	maximum	175.0	-	-	-	-	-	-	Chord	735000
TS	Madras	SP6	12.0	76.0	12.0	-	-	3	97.5	219.0	90	0.5	11.1	11.5	13.5	0.68	0.68	Axial	-1.0	3.16	maximum	204.1	-	-	-	-	-	-	Chord	705000
TS	Madras	SP7	12.0	76.0	12.0	-	-	3	97.6	219.0	90	0.5	11.1	11.5	13.5	0.68	0.68	Axial	-1.0	3.16	maximum	233.3	-	-	-	-	-	-	Brace	584000
YS	Madras	SP10	12.0	76.0	12.0	-	-	3	150.0	324.0	90	0.5	11.1	11.5	13.5	0.68	1.00	Axial	-1.0	6.00	maximum	204.7	-	-	-	-	-	-	Chord	23000
YS	Madras	SP11	12.0	76.0	12.0	-	-	3	115.0	252.9	90	0.5	11.1	11.5	13.5	0.68	0.68	Axial	-1.0	3.73	maximum	204.1	-	-	-	-	-	-	Chord	1516000
YS	Madras	SP12	12.0	76.0	12.0	-	-	3	115.0	252.9	60	0.5	11.1	11.5	13.5	0.68	0.68	IPB	-1.0	1.88	maximum	204.3	-	-	-	-	-	-	Chord	600000
YS	Madras	SP12	12.0	76.0	12.0	-	-	3	115.0	252.9	60	0.5	11.1	11.5	13.5	0.68	0.68	OPB	-1.0	1.04	maximum	204.2	-	-	-	-	-	-	Brace	2000000

GRADED JOINTS

Joint Type	Joint Ref.	Joint Ref.	To mm	Do mm	Ti mm	Di mm	Tg mm	I _{su} N/mm ²	Beta deg	C	Alpha spec.	Alpha' supp.	Alpha' gout	Gamma	Tau	Beta	Zeta	Loading mode	R	Max. SCF	CHORD Max. SCF Yield stress N/mm ²	Stress range N/mm ²	Max. SCF	BRACE Max. SCF Yield stress N/mm ²	Stress range N/mm ²	Failed Member	N3	N4		
Verhoo	PP1-2	PP1-2	6.2	208.0	8.0	219.1	33.3	87.3	90.0	-	12.1	-	8.1	24.2	0.90	0.51	-	Adial	-1.0	7.87	saddle	355.0	202.2	7.12	saddle	398.0	187.8	-	-	500000
Verhoo	PP1-2 (R)	PP1-2 (R)	6.2	208.0	8.0	219.1	33.3	87.3	90.0	-	12.1	-	8.1	24.2	0.90	0.51	-	Adial	-1.0	7.87	saddle	355.0	202.2	7.12	saddle	398.0	187.8	-	-	500000
Verhoo	PP2-X1	PP2-X1	8.4	208.0	8.8	218.0	25.8	78.8	90.0	-	12.5	-	8.3	15.3	0.76	0.52	-	Adial	-1.0	9.87	saddle	378.0	382.6	7.21	saddle	385.0	250.1	-	1000000	-
Verhoo	PP2-X2	PP2-X2	8.4	208.0	8.8	218.0	26.1	72.8	90.0	-	12.4	-	8.3	22.5	0.71	0.25	-	Adial	-1.0	7.18	saddle	367.0	428.5	4.82	saddle	375.0	292.7	-	-	1500000
Verhoo	PP2-X1	PP2-X1	15.2	800.0	10.0	457.0	68.3	68.2	90.0	0.5	8.0	-	6.8	18.7	0.85	0.43	0.19	Adial	-1.0	5.13	maximum	377.0	430.4	3.72	maximum	368.0	298.3	-	-	5000000
T	NEL	T208	32.0	914.0	-	-	-	-	90.0	0.5	5.0	5.0	-	14.3	0.50	0.50	-	Adial	-1.0	3.40	saddle	387.0	122.0	3.30	saddle	400.0	118.4	-	217000	275000
T	NEL	T215	32.0	914.0	-	-	-	-	90.0	0.5	5.0	5.0	-	14.3	0.50	0.50	-	Adial	-1.0	3.30	saddle	387.0	190.1	2.85	saddle	400.0	108.8	-	800000	1150000
X	SHAB	A2	9.5	508.0	8.8	406.4	41.3	30.0	90.0	-	7.1	7.1	3.2	28.7	1.05	0.41	-	Tension	-	12.70	saddle	-	390.0	-	-	-	-	-	150000	-
X	SHAB	A3	9.5	508.0	8.8	406.4	41.3	30.0	90.0	-	7.1	7.1	3.2	28.7	1.05	0.41	-	Tension	-	12.70	saddle	-	310.0	-	-	-	-	-	170000	-
X	SHAB	A4	9.5	508.0	8.8	406.4	41.3	30.0	90.0	-	7.1	7.1	3.2	28.7	1.05	0.41	-	Tension	-	12.70	saddle	-	190.0	-	-	-	-	-	180000	-
X	SHAB	B2	9.5	508.0	8.8	406.4	41.3	30.0	90.0	-	7.1	7.1	3.2	28.7	1.05	0.41	-	Tension	-	12.70	saddle	-	490.0	-	-	-	-	-	2000000	-
T	SHAB	C2	9.5	508.0	8.8	406.4	41.3	30.0	90.0	0.5	7.1	7.1	3.2	28.7	1.05	0.41	-	Compression	-	4.00	crown	-	275.0	-	-	-	-	-	320000	-
T	SHAB	D2	9.5	508.0	8.8	406.4	41.3	30.0	90.0	0.5	7.1	7.1	3.2	28.7	1.05	0.41	-	Compression	-	0.40	saddle	-	270.0	-	-	-	-	-	450000	-
T	SHAB	D3	9.5	508.0	8.8	406.4	41.3	30.0	90.0	0.5	7.1	7.1	3.2	28.7	1.05	0.41	-	Compression	-	0.40	saddle	-	225.0	-	-	-	-	-	300000	-

CAST JOINTS

Joint Type	Paper Ref.	Joint Ref.	T mm	Phi °deg	C	Alpha spec.	Alpha supp.	Gamma	Tau	Beta	Phi °deg	Zeta	Loading mode	R	Load req. Hz	Stress range N/mm²	Max SCF	CHORD			BRACE			Failed Member	N3	N4
																		Max SCF	Yield stress N/mm²	Stress range N/mm²	Max SCF	Yield stress N/mm²				
K	Hoechst	1	35.0	90			8.8	1.00	0.70		-		Bel. axial	-1.0		574							Castling	402000	140000	
K	Hoechst	2	35.0	90			8.8	1.00	0.70		-		Bel. axial	-1.0		604							Premature	490000		
K	Hoechst	3	35.0	90			8.8	1.00	0.70		-		Bel. axial	-1.0		524							Castling	456000		
K	Hoechst	4	35.0	90			8.8	1.00	0.70		-		Bel. axial	-1.0		500							Castling	456000		
T	BSC	CT1	32.0	90			14.3	1.00	0.50		-	-	IPB	0.0		270							Castling	1450000	144000	
T	BSC	CT2	32.0	90			14.3	1.00	0.50		-	-	IPB	0.0		678							Premature	1450000	105000	
T	BSC	CT3	32.0	90			14.3	1.00	0.50		-	-	Adial	0.0		540							Premature	1450000	105000	
K	Kobe	1	20.0	45			12.7	1.00	0.80		-		Bel. axial	-1.0		600							Castling	150000	3000000	
K	Kobe	2	20.0	45			12.7	1.00	0.80		-		Bel. axial	-1.0		400							Runner	150000	5000000	
K	Kobe	3	20.0	45			12.7	1.00	0.80		-		Bel. axial	-1.0		280							Runner	150000	5000000	
X	Corroco	1	40.0	90			6.3	1.00	1.00		-	-	Adial	-1.0		753							Castling	18000		
X	Corroco	2	40.0	90			6.3	1.00	1.00		-	-	Adial	-1.0		300							Castling	1510000		
X	Winney	1	34.0	90			8.0	1.00	1.00		-	-	Adial	-1.0		424							Castling	440000		
X	Winney	2	34.0	90			8.0	1.00	1.00		-	-	Adial	-1.0		353							Castling	950000		
X	Winney	3	34.0	90			8.0	1.00	1.00		-	-	Adial	-1.0		650							Castling	84000		